NASA/TP-2003-212438

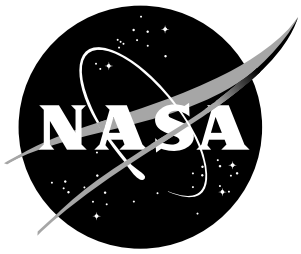

Portable Wireless LAN Device and Two-Way Radio Threat Assessment for Aircraft Navigation Radios

Truong X. Nguyen, Sandra V. Koppen, Jay J. Ely,
Reuben A. Williams and Laura J. Smith
Langley Research Center, Hampton, Virginia

Maria Theresa P. Salud
Lockheed Martin, Hampton, Virginia

July 2003

The NASA STI Program Office . . . in Profile

Since its founding, NASA has been dedicated to the advancement of aeronautics and space science. The NASA Scientific and Technical Information (STI) Program Office plays a key part in helping NASA maintain this important role.

The NASA STI Program Office is operated by Langley Research Center, the lead center for NASA's scientific and technical information. The NASA STI Program Office provides access to the NASA STI Database, the largest collection of aeronautical and space science STI in the world. The Program Office is also NASA's institutional mechanism for disseminating the results of its research and development activities. These results are published by NASA in the NASA STI Report Series, which includes the following report types:

- TECHNICAL PUBLICATION. Reports of completed research or a major significant phase of research that present the results of NASA programs and include extensive data or theoretical analysis. Includes compilations of significant scientific and technical data and information deemed to be of continuing reference value. NASA counterpart of peer-reviewed formal professional papers, but having less stringent limitations on manuscript length and extent of graphic presentations.

- TECHNICAL MEMORANDUM. Scientific and technical findings that are preliminary or of specialized interest, e.g., quick release reports, working papers, and bibliographies that contain minimal annotation. Does not contain extensive analysis.

- CONTRACTOR REPORT. Scientific and technical findings by NASA-sponsored contractors and grantees.

- CONFERENCE PUBLICATION. Collected papers from scientific and technical conferences, symposia, seminars, or other meetings sponsored or co-sponsored by NASA.

- SPECIAL PUBLICATION. Scientific, technical, or historical information from NASA programs, projects, and missions, often concerned with subjects having substantial public interest.

- TECHNICAL TRANSLATION. English-language translations of foreign scientific and technical material pertinent to NASA's mission.

Specialized services that complement the STI Program Office's diverse offerings include creating custom thesauri, building customized databases, organizing and publishing research results ... even providing videos.

For more information about the NASA STI Program Office, see the following:

- Access the NASA STI Program Home Page at ***http://www.sti.nasa.gov***

- E-mail your question via the Internet to help@sti.nasa.gov

- Fax your question to the NASA STI Help Desk at (301) 621-0134

- Phone the NASA STI Help Desk at (301) 621-0390

- Write to:
  NASA STI Help Desk
  NASA Center for AeroSpace Information
  7121 Standard Drive
  Hanover, MD 21076-1320

NASA/TP-2003-212438

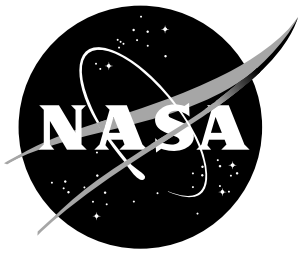

Portable Wireless LAN Device and Two-Way Radio Threat Assessment for Aircraft Navigation Radios

Truong X. Nguyen, Sandra V. Koppen, Jay J. Ely,
Reuben A. Williams and Laura J. Smith
Langley Research Center, Hampton, Virginia

Maria Theresa P. Salud
Lockheed Martin, Hampton, Virginia

National Aeronautics and
Space Administration

Langley Research Center
Hampton, Virginia 23681-2199

July 2003

Acknowledgments

Special thanks is extended to United Airlines and Eagle Wings Incorporated for their technical support and for providing access to operational Boeing 737-200 and 747-400 aircraft in support of aircraft interference pathloss measurements.

The authors wish to express their gratitude to Dave Walen, John Dimtroff, and Tony Wilson of the Federal Aviation Administration for their continuing support and technical direction.

The authors are also appreciative of Drs. John Beggs, Manohar Deshpande, Robin Cravey, and Mr. Bruce Fisher for their assistance in technical and editorial editing.

This work was funded by the Federal Aviation Administration as part of FAA/NASA Interagency Agreement DFTA03-96-X-90001, Revision 9, as well as the NASA Aviation Safety Program (Single Aircraft Accident Prevention Project)

Available from:

NASA Center for AeroSpace Information (CASI)
7121 Standard Drive
Hanover, MD 21076-1320
(301) 621-0390

National Technical Information Service (NTIS)
5285 Port Royal Road
Springfield, VA 22161-2171
(703) 605-6000

Table of Contents

Acronyms

AP	Access Point
ATC	Air Traffic Control
ATCRBS	Air Traffic Control Radar Beacon System
B737, B747	Boeing 737, 747 Aircraft
BPSK	Binary Phase Shift Keying
COTS	Commercial-Off-The-Shelf
CW	Continuous-wave
dBi	dB relative to isotropic reference pattern
dBm	dB relative to 1 milliwatt
dBμV/m	Field strength unit in dB relative to one μV/m
DME	Distance Measuring Equipment
DSSS	Direct Sequence Spread Spectrum
DUT	Device-Under-Test
EE	Emergency Exit
EMI	Electromagnetic Interference
EUROCAE	European Organisation for Civil Aviation Equipment
EWI	Eagles Wings Inc.
FAA	Federal Aviation Administration
FCC	Federal Communications Commission
FHSS	Frequency Hopping Spread Spectrum
FRS	Family Radio Service
GFSK	Guassian Frequency Shift Keying
GHz	Gigahertz
GMRS	General Mobile Radio Service
GPS	Global Positioning System
GS	Glideslope
HIRF	High Intensity Radiated Fields
ICAO	International Civil Aviation Organisation
IEEE	Institute of Electrical and Electronics Engineers
ILS	Instrument Landing System
IPL	Interference Path Loss
ISM	Industry, Scientific, and Medical
ITU	International Telecommunication Union
LAP1-8	Laptop computers 1-8. See details in Table 3.2-4
LaRC	Langley Research Center
LOC	Localizer

MAX	Maximum
MHz	Megahertz
Min.	Minimum
MIPL	Minimum Interference Path Loss
MLS	Microwave Landing Systems
MOPS	Minimum Operating Performance Standards
NASA	National Aeronautics and Space Administration
NIC	Network Interface Card
NIST	National Institute of Standards and Technology
PCMCIA	Personal Computer Memory Card Interface Adapter
PC Card	PCMCIA Card
PDA	Personal Digital Assistant
PED	Portable Electronic Device
PLF	Path Loss Factor
PRN	Printer
PS	Ping Storm
QAM	Quadrature Amplitude Modulation
QPSK	Quadrature Phase Shift Keying
RC	Reverberation Chamber, or Mode-Stirred Chamber
RF	Radio Frequency
RTCA	RTCA, Inc.
SAC	Semi-anechoic Chamber
SatCom	Satellite Communication (Aeronautical Mobile Satellite Service)
SD	Secure Digital
StDev	Standard Deviation
TACAN	Tactical Air Navigation
TCAS	Traffic Collision – Avoidance System
TCP/IP	Transmission Control Protocol/ Internet Protocol
TSO	Technical Standard Orders
UAL	United Airlines
UNII	Unlicensed National Information Infrastructure Band
US	United States
USB	Universal Serial Bus
UWB	Ultrawideband
VEE	Visual Engineering Environment
VHF Comm	Very High Frequency Communication – Voice Modulation
VHF-1 Comm	VHF-Comm radio no. 1
VOR	VHF Omnidirectional Range

WECA	Wireless Ethernet Compatibility Alliance
Wi-Fi	Wireless Fidelity
WLAN	Wireless Local Area Network
WPAN	Wireless Personal Area Network
Xfer	Duplex File Transfer

List of Symbols

π	Universal constant = 3.141592654
η_{Tx}	Transmit antenna efficiency factor
A	Device emission power
B	Interference coupling factor, negative of interference path loss in dB
C	Receiver susceptibility threshold
CF	Chamber Calibration Factor (dB)
CLF	Chamber Loading Factor
D_G	Directivity
E	Electric Field Intensity (V/m)
$EIRP$	Effective Isotropic Radiated Power (W)
IL	Empty chamber Insertion Loss
$L_{Chmbr(dB)}$	Chamber loss (dB), or = $-10log_{10}(CLF * IL)$
$L_{RecCable(dB)}$	Receive cable loss (dB)
$L_{XmitCable(dB)}$	Transmit cable loss (dB)
P_c	Carrier frequency power
P_{MaxRec}	Maximum received power measured over one paddle rotation
$P^R(2), P^R(3)$	Power received at points (2) and (3), respectively, in dBm
$P_{SAMeas(dBm)}$	Maximum receive power measured at the spectrum analyzer (dBm) over one stirrer revolution
$P^T(1),$	Power transmitted at point (1), in dBm
P_{TotRad}	Total radiated power within measurement resolution bandwidth
$P_{Xmit(dBm)}$	Power transmitted from source (dBm)
R	Distance (m)
Rx	Receive
S/I	Signal-to-Interference Ratio
TRP	Total Radiated Power (within measurement resolution bandwidth)
Tx	Transmit

Abstract

Measurement processes, data and analysis are provided to address the concern for Wireless Local Area Network devices and two-way radios to cause electromagnetic interference to aircraft navigation radio systems. A radiated emission measurement process is developed and spurious radiated emissions from various devices are characterized using reverberation chambers. Spurious radiated emissions in aircraft radio frequency bands from several wireless network devices are compared with baseline emissions from standard computer laptops and personal digital assistants. In addition, spurious radiated emission data in aircraft radio frequency bands from seven pairs of two-way radios are provided. A description of the measurement process, device modes of operation and the measurement results are reported. Aircraft interference path loss measurements were conducted on four Boeing 747 and Boeing 737 aircraft for several aircraft radio systems. The measurement approach is described and the path loss results are compared with existing data from reference documents, standards, and NASA partnerships. In-band on-channel interference thresholds are compiled from an existing reference document. Using these data, a risk assessment is provided for interference from wireless network devices and two-way radios to aircraft systems, including Localizer, Glideslope, Very High Frequency Omnidirectional Range, Microwave Landing System and Global Positioning System. The report compares the interference risks associated with emissions from wireless network devices and two-way radios against standard laptops and personal digital assistants. Existing receiver interference threshold references are identified as to require more data for better interference risk assessments.

1 Executive Summary

Wireless technologies are widely adopted in the present consumer market. Technologies such as cellular phones and wireless local area networks (WLANs) have brought a revolution in accessibility and productivity. WLANs enable consumers to have convenient access to web-browsing, email, instant messaging and numerous enterprise applications. As travelers become more dependent upon Internet access, airlines are increasingly interested in providing connectivity to their customers while traveling onboard aircraft. While WLAN equipment provided by the airlines for permanent installation on the aircraft must be properly certified, passenger carry-on products are not required to pass the rigorous aircraft radiated field emission standards.

Two-way radio communications, such as Family Radio Service (FRS) and General Mobile Radio Service (GMRS), are also becoming popular. These no-fee radio systems allow family members, friends and business associates to stay in contact during trips, shopping, or where party members may be physically dispersed. Unlike the low power FRS radios with half-watt maximum transmitted power,

GMRS radio can radiate much higher power. Two-watt GMRS radio models, which require a license presently, are highly popular. Many recent models have both FRS and GMRS built-in features. While use of these radios is not presently authorized on aircraft, their low cost and popularity hint that their use by unsuspecting passengers is likely.

With the support of the Federal Aviation Administration (FAA) Aircraft Certification Office and the National Aeronautics and Space Administration (NASA) - Aviation Safety Program - Single Aircraft Accident Prevention Project, radio frequency (RF) emissions from portable WLAN devices and two-way radios were measured. In addition, interference path loss (IPL) measurements were conducted with an airline partner to quantify the attenuation levels for emission from inside the passenger cabin. These emission and path loss data are used to assess potential risks to aircraft systems.

This report documents the spurious radiated emission measurement process and shows the results from WLAN devices and two-way radio testing. Spurious emissions are emissions on frequencies that are outside the necessary bandwidth, and the level of which may be reduced without affecting the corresponding transmissions of information. Out-of-band emissions (emissions at frequencies immediately outside the necessary bandwidth) are excluded. The emission results are compared against emissions from standard laptop computers and Personal Digital Assistants (PDAs), which are used in this report as benchmarks, since these devices are currently allowed for use during certain non-critical phases of flight. In addition, the report documents IPL results measured on four Boeing B747-400 and six Boeing B737-200 aircraft. These airplanes were provided by United Airlines (UAL) for IPL measurements under a contract between NASA Langley Research Center (LaRC) and Eagles Wings Incorporated (EWI). The new IPL results are summarized and presented together with the existing IPL data from other sources, which include references, standards, and results from other NASA cooperative efforts. Interference thresholds summarized from an existing standard are reported. The measured emissions, the overall IPL, and the interference thresholds were used to compute interference safety margins reported in this document. The sections below provide additional details on the measurements, results and the analysis.

Radiated Emission Measurement

Radiated emissions from WLAN devices and two-way radios were measured in two reverberation chambers (RCs) at NASA LaRC. Two chambers were employed to overcome certain frequency and operational limitations associated with highly sensitive emission measurements. WLAN network interface cards (NIC), access points (APs) and a Bluetooth test set were acquired. Preliminary testing was conducted to identify WLAN operational issues in a high multi-path RC environment. The WLAN devices tested include seven Institute of Electrical and Electronics Engineers (IEEE) 802.11b, five IEEE 802.11a, and six Bluetooth devices. As a result of the preliminary testing, WLAN operating modes, channels, and data rates were identified and uniformly adopted for more extensive tests. FRS and GMRS radio operations were simple and no such preliminary testing was needed.

The preliminary testing also involved selecting host laptop computers and PDAs with low emissions so they did not mask emissions from the WLAN devices under test. The screening involved emission measurement of eight laptop computers and two PDAs in various operational modes. The host laptops and PDAs were selected using the criteria of the lowest emissions in the measurement frequency bands while operating in idle and file transfer modes. This screening identified two laptop computers to cover five measurement frequency bands and both PDAs.

The RC emission measurement method used was adopted from an earlier effort to assess the risk of interference from wireless phones to aircraft radio receivers [1]. The RC method was efficient, repeatable, and provided results directly in terms of effective peak radiated power, rather than electric field strength, so that an approximate conversion from field strengths to radiated power was not needed. Proper use of filters prevented high power emissions from the WLAN devices at wireless carrier frequencies from reaching the receiver, preventing undesirable receiver overloading and intermodulation. Filters were also used to block spurious emissions from the WLAN AP antenna from radiating in the chamber and contaminating the environment.

Interference Path Loss Measurement

Path loss measurement was another major effort to help assess risks of interference to aircraft systems from passenger carry-on devices. The measurements were conducted on four Boeing 747-400 and six Boeing 737-200 airplanes provided by UAL during three one-week trips to Southern California Aviation facility in Victorville, California. Several aircraft systems were measured, including Localizer (LOC), Glideslope (GS), Very High Frequency Omnidirectional Range (VOR), Very High Frequency Communication (VHF-Comm.), Global Positioning Systems (GPS), Traffic Collision Avoidance System (TCAS), and Satellite Communication (SatCom). The measurements were conducted with a radiating antenna positioned at windows and doors, while a spectrum analyzer recorded the maximum signals coupled into aircraft antennas. The transmitting antenna was also positioned at locations other than windows and doors on two aircraft, and the end comparison indicates that the door and window measurements indeed capture the minimum IPL values. In addition, the results indicate that for many systems the minimum IPL is strongly influenced by the antenna locations relative to an aircraft door. Therefore, IPL for a particular aircraft is dependent upon antenna installation. The measured IPL data are summarized in this report along with other previously available IPL data, and the computed all-aircraft minimum IPL values are shown.

Interference Safety Margin

Interference analysis was conducted using the WLAN and two-way radios emission results, the IPL (all new and previously available data considered), and the receiver interference thresholds from a standard document. Interference safety margins were calculated for each combination of WLAN/radio device, minimum or average IPL, and minimum or typical interference threshold. As a result, the safety margin can be positive or negative. However, it was seen that WLAN devices, in general, have better safety margins than laptops and PDAs, mainly due to lower emissions in most cases. The FRS/GMRS radios have the worst safety margin in the GS band due to very high spurious emissions. The emissions are also high for FRS/GMRS radios in the Microwave Landing Systems (MLS) band. Yet, the results indicate a very large positive safety margin, and these radios are, therefore, not a concern in this band.

Conclusions

1. Spurious emissions in aircraft radio bands from selected WLAN devices were lower than from laptop computers and PDAs. One exception is IEEE 802.11a device emissions in the MLS band, where emissions from the laptop computers and other WLAN devices were too low to be measured. With that exception, the results indicate that the WLAN devices tested are not any more threatening to the aircraft bands under consideration than the common laptop computers and PDAs. High emissions from IEEE 802.11a devices in the MLS band are not a concern due to a very large positive safety margin.

2. FRS/GMRS radio emissions are much higher than from the laptops/PDAs in the GS and MLS bands. In the GS band, emissions from GMRS/FRS radios can exceed the laptop/PDA maximum emission by as much as 30 dB, and the aircraft emission limit RTCA/DO-160 Category M by as much as 23 dB. In the MLS band, the maximum emissions from GMRS/FRS radios can exceed the laptop/PDA maximum emissions by at least 44 dB, but are below the RTCA/DO-160 Category M emission limit.

3. Spurious emissions from WLAN devices are lower than Federal Communications Commission (FCC) Part 15 limits, but can be higher than aircraft RTCA/DO-160D Category M emission limits in the TCAS, Air Traffic Control Radar Beacon System (ATCRBS), and Distance Measuring Equipment (DME) bands.

4. IPL measurements were conducted to supplement existing data. Analysis of new measurement data supports previous observations that window and door locations capture the lowest IPL values, and that proximity of aircraft antennas to an aircraft door can reduce minimum IPL significantly.

5. Interference safety margin can be positive or negative, and can vary broadly depending on the IPL and interference threshold values used.

Recommended Future Work:

1. Additional receiver interference threshold data are needed for greater confidence level. More tests on a number of receivers from multiple manufacturers are recommended. Signal modulation and types should be considered.

2. Conduct emission measurements and interference analysis on other types of wireless devices, particularly those utilizing newly available RF bands and having multi-band capability. Some of the current and future wireless trends include 2.5G and 3G phones, software-defined-radios, phones/PDAs with built-in camera and other smart features.

3. Assess the potential for emerging radio technologies that overlay existing spectrum (such as Ultra Wideband) to cause interference to aircraft systems.

4. Conduct additional IPL measurements on different types of aircraft where minimal data currently exists.

5. Initiate flight operational assessment of PED electromagnetic interference (EMI) to aircraft radios, addressing safety impact of EMI as affected by navigation data processing and redundancy management within specific avionics packages, including the influence of crew and air traffic control procedures.

2 Introduction

"All portable electronic devices must remain off during taxi, takeoff, approach, and landing until the plane arrives at the gate and the seat-belt sign is turned off." "Passengers may turn on and use cellular phones only when the main cabin door is open". "Any radio transmission using personal communication devices is prohibited". Such announcements are familiar to airplane travelers. These policies stem from the potential for portable electronic devices (PEDs) to interfere with aircraft communication and navigation systems, and are stated in a way that has been applicable to most commercially available products, until recently. With the introduction of increasingly compact, inexpensive, multifunction wireless PEDs, it is more difficult for passengers (and flight attendants) to determine if a device is acting as a transmitter. Sometimes it is ambiguous if a device is turned on at all. In fact, some new wireless technologies incorporate the ability to turn themselves on when packed away in a storage compartment or under a seat.

Wireless technologies have brought a revolution in personal accessibility and productivity, and have created new markets for products and services. WLANs enable convenient and affordable web-browsing, email, instant messaging and numerous enterprise applications in high-traffic public places such as restaurants, coffee shops, shopping malls, convention centers, hotels, and airports. As travelers become more dependent upon Internet access at places away from home or office, airlines are becoming more interested in providing connectivity to their customers while traveling on board aircraft.

The use of unauthorized intentional transmitters, such as WLAN devices, wireless phones and citizen's band radios are of growing concern to the FAA and to the airlines who are responsible for passenger safety. While WLAN equipment provided by the airlines for permanent installation on the aircraft must be properly certified, the passenger carry-on products are not required to pass the rigorous aircraft radiated-field emission standards. Demanding certification for use on aircraft is considered impractical due to enforceability issues that could result in poor customer relations.

FRS and GMRS are becoming popular as family members, friends and business associates desire to stay connected during trips, shopping or where members may be physically dispersed. On an aircraft, unaware passengers may attempt to use these radios to communicate with others whose seats may be assigned at different locations on the aircraft. Use of these radios by American travelers/tourists has been observed in foreign countries where their use was not yet allowed. With two watts of radiated power, the GMRS radio is attractive due to extended range and increased channel capacity compared to the lower-power FRS radio. GMRS radio is readily available but requires a license to operate. However, it is unrealistic to assume that all users are aware of (or willing to comply with) the requirements of application submission and high fees. The popularity and low cost of the FRS and GMRS radios make it reasonable to assume that their use on airplanes by unsuspecting passengers is inevitable.

2.1 Background

This report builds upon a detailed threat assessment of wireless phones previously performed by NASA, and accomplishes objectives identified in the previous NASA work [1]. The previous NASA report introduced a radiated emission measurement process for two dominant digital standards for wireless handsets, and reported detailed radiated emission data for several typical units. The measurement technique was also different in that a new RC method was used that has certain advantages over conventional test methods. The wireless handset data was supplemented with detailed aircraft IPL and navigation radio interference threshold data from numerous reference documents, standards and NASA partnerships. The radiated emission measurement process, path loss data and interference

threshold analysis are directly applied, and extended, for WLANs, Bluetooth devices and FRS/GMRS radios evaluated in this report. The previous NASA report drew extensively from RTCA Special Committee reports published in 1988 (RTCA/DO-199 [2]) and 1996 (RTCA/DO-233 [3]), which remain the foundation for regulatory and advisory guidance for the FAA and other comparable agencies worldwide.

On July 12, 2001, the European Organisation for Civil Aviation Equipment (EUROCAE) held their initial meeting of Working Group 58, tasked to reexamine the issues of PEDs used onboard commercial aircraft. In their second meeting on September 20-21, 2001, the Group identified the following objectives:

1. "To review the EMC issues related to the use of new technology PEDs and related installed services on aircraft by evaluation and comparison of existing studies, measurement of data as necessary, and production of a report."
2. "To propose technical and non-technical solutions for the operation of PEDs on board aircraft for the aviation community, including standards and guidelines as appropriate."
3. "To provide guidelines to non-aviation standardisation fora, in order to help them assist in the maintenance of safety on board aircraft."

EUROCAE Working Group 58 agreed on the following initial Terms of Reference:

1. Evaluate PEDs to identify new technologies, device types and their potential usage on aircraft.
2. Evaluate services, provided by airlines and aircraft manufacturers, which may use non-aeronautical commercial-off-the-shelf (COTS) equipment.
3. Consider both intentional and unintentional radiations from PEDs, and their coupling to electronic systems and antennas.
4. Gather opinions and information from, and collaborate with, interested parties, including aircraft manufacturers, aviation equipment manufacturers, airlines, regulatory authorities and the electronics industry.
5. Work jointly and establish close working relationships with the International Civil Aviation Organisation (ICAO) panels, coordinating groups, regulatory authorities and other standards organisations as appropriate.
6. Produce guidance documentation in a timely manner and in an appropriate format for the use of those concerned with this issue.

These initial Terms of Reference have been slightly modified, and the EUROCAE WG-58 activity continues. An Internet website has been established to consolidate documentation, agendas and schedules for this activity, but is accessible only to subscribers.

On March 20, 2003, the RTCA established Special Committee 202, upon request from the FAA, to "develop guidance related to the use of portable electronic devices on board air carrier aircraft." The guidance "will provide a means for authorities, aircraft operators and aircraft manufacturers to determine acceptable and enforceable policies for passenger and crew use of portable electronic devices." The Terms of Reference were divided into two phases: a near-term PED technology assessment, and a longer-term technology assessment. An Internet website has been established to track meeting schedules, documentation, and terms of reference for the effort, which can be viewed at http://www.rtca.org/comm/sc202.asp.

The EUROCAE working group and RTCA special committee efforts require openly available, high-confidence data upon which to base their analyses and recommendations. The goal of this NASA report is to provide suitable measurement processes, data and analysis that may be used by these committees, airlines and the FAA to establish a sound technical basis for allowing airplane operators and passengers freedom in using new wireless technologies in a manner that will not limit the safe operation of aircraft electronic systems.

The NASA efforts described in this report, as well as those documented in [1], were accomplished with the support of the FAA Aircraft Certification Office and the NASA Aviation Safety Program. Additional path loss data were measured under a cooperative agreement with UAL and EWI. These measurements were conducted for various aircraft radio receivers on four Boeing B747-400 and six Boeing B737-200 aircraft. Utilizing receiver susceptibility threshold data from RTCA/DO-199 and GPS receiver performance specifications, interference safety margins were calculated and presented. The following subsections describe the objectives, the approach to measure spurious emissions, and the report organization.

2.2 Objective

The primary objectives of this work were to develop a radiated emission measurement process for WLAN devices and two-way FRS/GMRS radios, to conduct aircraft IPL measurement, and to provide interference risk assessment of WLAN devices and two-way radios to aircraft systems, including LOC, GS, VOR, and GPS.

2.3 Approach

Assessment of aircraft radio receiver interference is typically accomplished by addressing the three elements of the equation:

$$A + B \geq C , \qquad \text{(Eq. 2.3-1)}$$

at any frequency in the aircraft radio navigation bands, where

"*A*" is the maximum RF emission from the offending device in dBm,

"*B*" is the maximum interference coupling factor in dB; "*-B*", in dB, is commonly referred to as the minimum IPL,

"*C*" is the receiver's minimum in-band, on-channel interference threshold in dBm.

If the minimum interference threshold, "*C*", is lower than the maximum interference signal level at the receiver's antenna port, "(*A* + *B*)", there is a potential for interference.

A primary focus of this effort was to measure the maximum RF emission, "*A*", from WLAN devices and two-way FRS/GMRS radios. In this report, the WLAN devices considered include IEEE 802.11a, IEEE 802.11b, and Bluetooth devices. Technically, Bluetooth is classified under Wireless Personal Area Network (WPAN) but it is grouped under WLAN in this report for simplicity.

The secondary focus was to measure the minimum IPL, "-B", for a number of systems on several B747 and B737 aircraft. The new measured IPL data are summarized in this report and compared to other data previously available.

Receiver interference thresholds "C" were not measured in this effort. Rather, test data from RTCA/DO-199 were used in evaluating interference risks to aircraft systems. DO-199 provided receiver interference threshold data on a limited number of receivers for a few aircraft systems. Additional testing to include more receivers and more systems is highly desirable. Thorough measurement and analysis of receiver susceptibility thresholds requires having access to multiple aircraft receivers and in-depth knowledge of receiver operations and designs. Aircraft radio manufacturers are best equipped to address this issue.

Sections 2.3.1 and 2.3.2 discuss in more detail the emission and path loss measurement approaches.

2.3.1 Emission Measurements of WLAN Devices and Two-Way Radios

To simplify the process and to reduce the number of emission measurements, aircraft radio bands that overlapped, or were near one another were grouped together, and emissions were measured across the entire combined band simultaneously. Five frequency groups, designated as measurement Band 1 to Band 5, covered all aircraft radio bands of interest. Table 2.3-1 correlates the measurement bands to aircraft radio frequencies.

It is assumed that high emissions in any of Bands 1 through 5 would affect all aircraft systems operating in that band. As an example, high emissions in Band 1 are assumed to affect all LOC and VOR systems as a group. No effort was taken to distinguish whether the emissions were in LOC or VOR bands.

Table 2.3-1: Emission Measurement Bands and Corresponding Aircraft Radio Bands.

Measurement Band Designation	Measurement Freq. Range (MHz)	Aircraft Systems Covered	Spectrum (MHz)
Band 1	105 – 120	LOC	108.1 – 111.95
		VOR	108 – 117.95
Band 2	325 – 340	GS	328.6 – 335.4
Band 3	960 – 1250	TCAS	1090
		ATCRBS	1030
		DME	962 - 1213
		GPS L2	1227.60
		GPS L5	1176.45
Band 4	1565 – 1585	GPS L1	1575.42 ± 2
Band 5	5020 - 5100	MLS	5031 – 5090.7

RCs were used to measure RF emissions from a device-under-test (DUT). Using this method, measured RF emissions resulted in "total radiated power" [4]. This method differs from the approach used in RTCA/DO-199, where the total radiated power was estimated from the electric field measured at a given distance from a DUT. Further details about conducting emission measurements in a RC are found in Section 3.

The measurement process began with selecting host computer laptops/PDAs for the WLAN devices. This step ensured that spurious emissions from the intended WLAN devices were not masked by

emissions from a noisy host laptop/PDA. This selection involved measuring emissions from eight different laptops and two PDAs operating in various modes. The laptops/PDAs with the lowest emissions in the idle and file transfer modes in a particular band were chosen for that band. The idle and the file transfer modes were typical laptop modes while emission measurements of the WLAN devices were being conducted. In addition, emission data of the laptops with all operating modes considered established an emission baseline for laptop computers that could be used onboard an aircraft. Emissions from intentional transmitters such as WLAN devices were compared against this baseline. For two-way FRS/GMRS radios, no similar host screening was needed since these devices can operate without a host.

Emission measurements were conducted on five 802.11a, seven 802.11b and six Bluetooth WLAN devices. The WLAN devices were exercised through various modes, channels, and data rates during the emission measurement. Various filter combinations were used in the wireless AP antenna path to allow only the intended wireless signal to radiate for communication with the DUTs, and block spurious emissions from the APs. Additional filters were also used in the measurement path to prevent the wireless signals (from the wireless cards and the AP) from reaching the measuring instrument to cause overloading or intermodulation.

Emissions were also measured on four matched pairs of FRS radios and three matched pairs of GMRS radios. Emissions from a matched pair were measured at the same time, with each radio in turn being in transmit, receive, and idle modes. Thus, a recorded measurement trace includes the maximum emissions from both radios in all three modes. The radios were also cycled through at least two frequency channels during each measurement. Again, filters were employed to prevent overloading of the measurement receiver.

Further details are discussed in Section 3 of this report.

2.3.2 Path Loss Measurements

This effort supplemented the collection of previously available path loss data with measurements on four B747-400 and six B737-200 aircraft. In this effort, three separate measurement trips were made to an aircraft storage facility in Victorville, California to conduct IPL measurement on LOC, VOR, GS, VHF, TCAS, SatCom and GPS systems (if available). The results were plotted for different windows along each aircraft. The *minimum* path losses for the aircraft systems were summarized and shown along with other previously available data ([1], [2], [3], [5] and [21]), and the overall *path loss* statistics were computed for safety margin calculations.

The measurement system included a spectrum analyzer and a tracking source with its frequency tracking (matching) the spectrum analyzer's frequency. The tracking source was used to deliver a known emission level to a matched and efficient transmit antenna simulating radiation from PEDs. The spectrum analyzer continuously swept and registered maximum emissions across the measurement band received by the aircraft antenna. The transmit antenna was pointed toward the windows or it was scanned along door seams. Past studies [5], and also the results of this study, confirmed that window and door locations provided the lowest IPL values. The difference in dB between the transmit antenna output power and power at the receiver's antenna cable port (measured by the spectrum analyzer) was the desired path loss value for that transmit antenna location. The transmit antenna was then moved to a different window/door/seat location and the process repeated until all desired aircraft locations (windows/doors/seats) were included.

2.3.3 Safety Margin Calculations

With device emission "A", path loss "-B" and interference threshold "C" known, the safety margin was calculated as:

$$Safety\ Margin = C - (A + B) \qquad \text{(Eq. 2.3-2)}$$

Results of the safety margin calculations are reported in Section 5.

2.4 Report Organization

Measurement of emissions from WLAN devices and two-way radios is described in Section 3. The method is described in 3.2, and a summary of the results is provided in Section 3.3. Section 3.4 summarizes emission data from non-intentional transmitting laptops and PDAs. Section 3.5 compares results from all measurements reported in Sections 3.3 and 3.4. More detailed emission measurement results are shown in Appendix A for WLAN devices and two-way radios, and in Appendix B for laptops and PDAs.

Section 4 describes IPL measurements and results for Boeing 747 and 737 aircraft, and a comparison with other previously available path loss data. Section 4.1 summarizes the aircraft measurements, with a detailed description in 4.1.1 and results in 4.1.2. Section 4.2 shows the *minimum* and the *average* IPL for each of the measured B737 and B747 aircraft, along with similar data previously reported. Section 4.3 further condenses the data by showing the all-aircraft statistics of the minimum IPL. The lowest and the average values of the minimum IPL were used in the safety margin calculations in Section 5.

Section 5 briefly summarizes the interference threshold data from RTCA/DO-199. In this section, interference safety margins for each aircraft system of interest are calculated and reported from the emission data, the IPL data, and the susceptibility thresholds.

3 WLAN and Radio RF Emissions

3.1 Wireless Overview

IEEE 802.11a, IEEE 802.11b, and Bluetooth wireless network technologies and FRS/GMRS radios are described in this section. Table 3.1-1 lists types of devices used for this assessment with associated transmission frequency bands and operating parameters. In addition, the power used during radiated emission testing discussed in this report and the maximum permitted output powers, as specified by the corresponding standards or regulatory limits, are listed.

3.1.1 IEEE 802.11a

IEEE 802.11a is a very high-speed, high-bandwidth standard and a variant of the IEEE 802.11 standard. It expands on the 802.11 network standard to define WLAN operating parameters, providing access to outside networks for wireless devices, including local intercommunication. The 802.11a standard requires that data rates of 6, 12, and 24 Mbits/s must be supported; however, maximum rates of 54 Mbits/s are common. Each data rate uses a particular modulation technique to encode data. Higher data rates are achieved by employing advanced modulation techniques. Devices using 802.11a operate in the 5 GHz Unlicensed National Information Infrastructure Band (UNII). The bandwidth of 300 MHz is

composed of three bands that legally operate in the US; the first band of 5.15 to 5.25 GHz uses 50 mW maximum power, the second band of 5.25 to 5.35 GHz uses 200 mW maximum power, and a third band of 5.725 to 5.825 GHz uses 800 mW maximum power [6]. The first and second bands contain eight non-overlapping 20 MHz channels. A typical application of 802.11a technology is a wireless NIC inserted into a laptop Personal Computer Memory Card Interface Adapter (PCMCIA) slot. The NIC converts the laptop, a non-intentional transmitter, to a wireless PED, capable of transmission and intercommunication with other wireless devices or APs.

3.1.2 IEEE 802.11b

The IEEE 802.11b standard provides location independent access to an outside network between wireless data devices, including intercommunication on a local scale. Primarily an extension of the 802.11 standard, it defines additional operational parameters for high-rate data transfers on WLANs while maintaining 802.11 protocols. Devices using 802.11b operate in the 2.4 GHz band, which is divided into fourteen 22 MHz channels, eleven of which legally operate in the US. Adjacent channels partially overlap, except for three of the 14, which are completely non-overlapping. The 802.11b standard utilizes a Direct Sequence Spread Spectrum (DSSS) modulation mode, as defined by 802.11, and advanced coding techniques to achieve higher data rates of 5.5 Mbit/s and 11 Mbit/s. The coding techniques employ different modulation schemes at different data rates. The FCC allows a maximum output power of 1000 mW. However, if a power level greater than 100 mW is used, then power control must be provided by the system [6]. A distance range of 100 meters is typical, but ranges are dependent upon environmental obstacles and power. A typical application of 802.11b technology is a wireless NIC inserted into a laptop PCMCIA slot. As with 802.11a devices, a non-intentional transmitter is converted to an intentional transmitter that is capable of intercommunication with other wireless devices or APs.

3.1.3 Bluetooth

Bluetooth is a short-range radio technology with the capability to link together different wireless devices providing for data and limited voice communication. Bluetooth uses 79 channels separated by 1 MHz each, from 2.4 to 2.48 GHz. The Bluetooth standard supports development of low cost and low power wireless devices. The specification allows for three power classes [7]. Power control is required for devices utilizing class one levels, and must be able to control and limit transmit power over 1 mW (0 dBm) [7]. Power control is optional at levels under 0 dBm, but may be employed in order to conserve power. Bluetooth units operate with a maximum data rate of 11 Mbps, and a power level up to 100 mW. The nominal distance between devices is 0.3 to 10 meters; however, greater distances are achieved with higher power. It uses Gaussian Frequency Shift Keying (GFSK) modulation combined with Frequency-Hopping Spread Spectrum (FHSS) techniques for data transmission [7]. A Bluetooth transmitter hops among 79 frequencies at a rate of 1600 hops per second.

3.1.4 FRS/GMRS Radios

FRS and GMRS radios are legal, modern, two-way communication devices in the US and Canada. These devices are more compact and more efficient than their walkie-talkie predecessors. They also have a longer communication range, less distortion, better signal reception, and more effective penetration of building structures. Both types of radios utilize 38 subcodes in each of the main channels, which enable users to achieve a semi-private conversation. A subcode is an interference filter allowing only the signals designated to a particular subcode on a channel to be heard by the users, blocking all other signals.

Several users in fairly close proximity, fewer than two miles, are able to communicate with unlicensed FRS devices. However, if communication beyond 2 miles is needed, a licensed-GMRS device may be used. GMRS regulations do not permit superficial chatter between individuals on this service, unlike the FRS radio regulations. GMRS has a larger coverage area because of the higher output power and the ability to use repeaters in the coverage area. Table 3.1-1 provides a comparison of the two radios.

Table 3.1-1: Wireless Technology Parameters

Wireless Technology	Frequency Band (GHz)	Typical Data Rates (Mbps)	Number of Channels	Maximum Output Power per Std. / per Test (mW)	Typical Range
802.11a	5.15 – 5.825	6, 12, 24, 54	12*	800 / 40 & 200	50 meters
802.11b	2.4 – 2.4835	1, 2, 5.5, 11	11*	1000 / 100	24 – 100 meters
Bluetooth	2.4 – 2.4835	1	79'	100 / < 1**	10 – 100 meters
FRS Radio	0.4625675 – 0.4677175	NA	14	500 / 500	2 miles
GMRS Radio	0.4625500 – 0.4677250	NA	23***	50000*** / 2000	5 miles

* Legal channels in US
** Less than 1 mW, varied by channel
*** FCC Part 95 Subpart E
' Utilizes FHSS over all channels

3.2 Measurement Process

This section incorporates discussions on preliminary investigations; emission testing conducted on laptop computers, PDAs, and a printer used as hosts for WLAN devices; and, device-focused tests conducted to measure radiated spurious emissions from wireless devices installed in a host. Determination of testing parameters is discussed, including procedures, RF filtering, host devices, WLAN devices, and test configurations. Several figures are included to illustrate the test environment, setup, and instrumentation. Tables are presented which include information on measurement frequency bands, measurement bandwidths, host and AP characterization, and WLAN configurations. A diagram of the test facility is presented with a discussion of NASA-LaRC High-Intensity Radiated Fields (HIRF) Laboratory RCs. The radiated emission test procedure is briefly discussed and includes calibration and emission measurement methods. Test matrices for WLAN devices and FRS and GMRS radios are presented to illustrate test modes. Finally, the data reduction process is discussed and the results are linked to data charts found in this report.

The following sections describe the measurement process by presenting the measurement method used, the types of preliminary testing conducted, the specifics of the device-focused testing on WLAN devices, and the data reduction process.

3.2.1 Measurement Method

Overview

The goal of this effort was to develop a process and representative data for measuring spurious radiated emissions in aircraft communication and navigation (com/nav) receiver bands from wireless

devices meeting IEEE 802.11b, IEEE 802.11a, Bluetooth, FRS and GMRS radio standards. The measurement process for spurious radiated emissions incorporates RF measurement instrumentation, specialized data acquisition software, generation and application of calibration data, and the use of RCs [1]. Preliminary PED and WLAN device performance testing was conducted in both a Semi-Anechoic Chamber (SAC) and a RC; however, a RC was used for all emission testing in order to provide more comprehensive test results and to expedite the test process. Additional advantages of using the RC method are described in the next section.

Test Facility Description

The NASA-LaRC HIRF Laboratory has three separate RCs, as seen in Figure 3.2-1. This facility is capable of performing radiated susceptibility tests and emission tests using either one chamber at a time or in two or three chambers simultaneously. Using multiple chambers allows for distributed testing of systems, creating different electromagnetic environments in each chamber utilized. The National Institute of Standards and Technology (NIST) has characterized the field uniformity of the NASA-LaRC RCs; details regarding their performance are located in [14]. Characterization of the chambers by NIST indicates a high degree of electromagnetic field uniformity performance within the stated useable frequencies. A chamber's lowest useable frequency is determined by its construction and geometry, and a sufficient mode density within the chamber to provide a uniform electromagnetic environment [13].

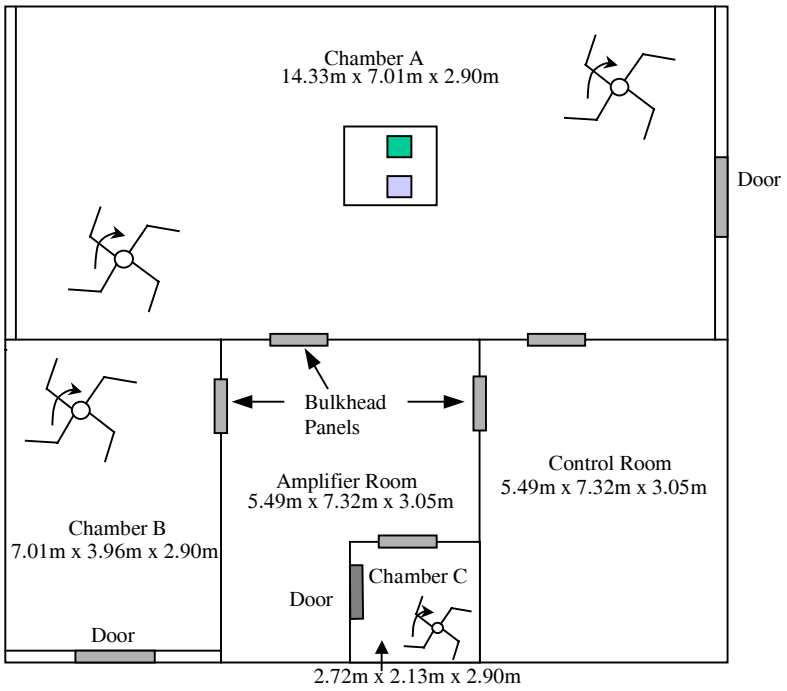

Figure 3.2-1: Layout and dimensions of the HIRF Laboratory at NASA LaRC.

The lowest useable frequency for Chamber A is approximately 100 MHz with +/-2 dB variation [14], and it accommodates test measurement frequency Bands 1 and 2 (Table 2.3-1). The lowest useable frequency for Chamber C is approximately 300 MHz with +/-2 dB variation, and it accommodates measurement frequency Bands 3, 4, and 5. Chamber A has the capability to test all the emission measurement bands. However, intermittent low-level noise interference was observed in the higher

bands, and Chamber C was used instead. Chamber B, which was unavailable at the time, could also be used in the future with its 150 MHz lowest usable frequency.

Radiated emission measurements in RCs produce results in terms of radiated power, which is preferred, rather than electric fields as in a SAC. Radiated emissions in term of power can be applied directly into Eq. 2.3-1 for interference risk assessment. Compared with the SAC method, the advantages of the RC method also include repeatability and speed when a large number of aspect angles in the SAC are considered. The RC method does not suffer from *measurement uncertainty* caused by multipath effects. However, establishing and maintaining connectivity with a wireless DUT can be much more difficult in a RC than in a SAC due to severe multipath interference. In addition, Section 3.2.2 provides more details on connectivity issues associated with WLAN devices in a reverberation chamber.

The RC method, however, may not be appropriate for measuring emission signals with very short pulse durations [15]. Due to high chamber quality factor, the chamber time-constant should not be greater than 0.4 of the pulse-width of the modulated signal. This requirement ensures that once a pulsed signal is turned on, the field environment in the chamber reaches (near) steady-state level before the pulse is turned off. RF absorber can be added to the chamber to lower the time-constant; however, emission signal characteristics must be known in advance for all DUTs in all measurement bands. In addition, measurement sensitivity would be reduced. A method for measuring chamber quality factor and time-constant is described in [15]. Absorber was not added in this study.

For the RCs used, the chamber time-constants vary with frequency, and are about 0.5 to 2 microseconds in the measurement bands of interest. It is assumed that most RF emission signals measured in this effort are continuous-wave (CW), or pulse modulated signals of five microseconds (= 2 microseconds / 0.4) or longer.

Description of Measurement Method

Figure 3.2-2 shows the emission test setup in an RC. Tests conducted in RCs rely on several different methods to produce a statistically uniform and isotropic electromagnetic environment (field statistics measured over one stirrer revolution are isotropic and spatially uniform). Two of these methods are mode-stirred and mode-tuned [13]. Stirrers with reflective surfaces are rotated continuously during mode-stirring, or stepped at equal intervals for a complete rotation during mode-tuning. For measurements in this report, the mode-stirred method was adopted due to ease of setup, implementation, and significant speed improvements over the mode-tuned method. While the mode-tuned method can be more accurate in immunity testing applications (especially for DUTs with slow response time), the mode-stirred method is superior for most emission measurements due to speed. With a spectrum analyzer for measuring receive power, the emission measurement system can respond fast enough to the changing fields caused by the continuously rotated stirrers. Settling-time delays for stirrer stepping in mode-tuned operations are eliminated, resulting in significant speed improvements. In addition, combining mode-stirred operations with continuous frequency sweeping can further expedite the measurements.

Measurement uncertainty levels can be lowered by selecting the number of measurement points in a stirrer revolution approximately equal to the number of calibration points. In addition, the number of measurements during one stirrer revolution should be as large as possible within constraints of instrument capabilities and test time to reduce uncertainties. Using the mode-stirred method, several thousand measurements per stirrer revolution are easily achievable with a spectrum analyzer. On the other hand, the mode-tuned method with the number of measurements exceeding 100 per stirrer revolution is typically

considered impractical due to excessive test time. The mode-stirred method's short calibration times also allow for frequent chamber calibrations to correct for DUT operator changes during long test times.

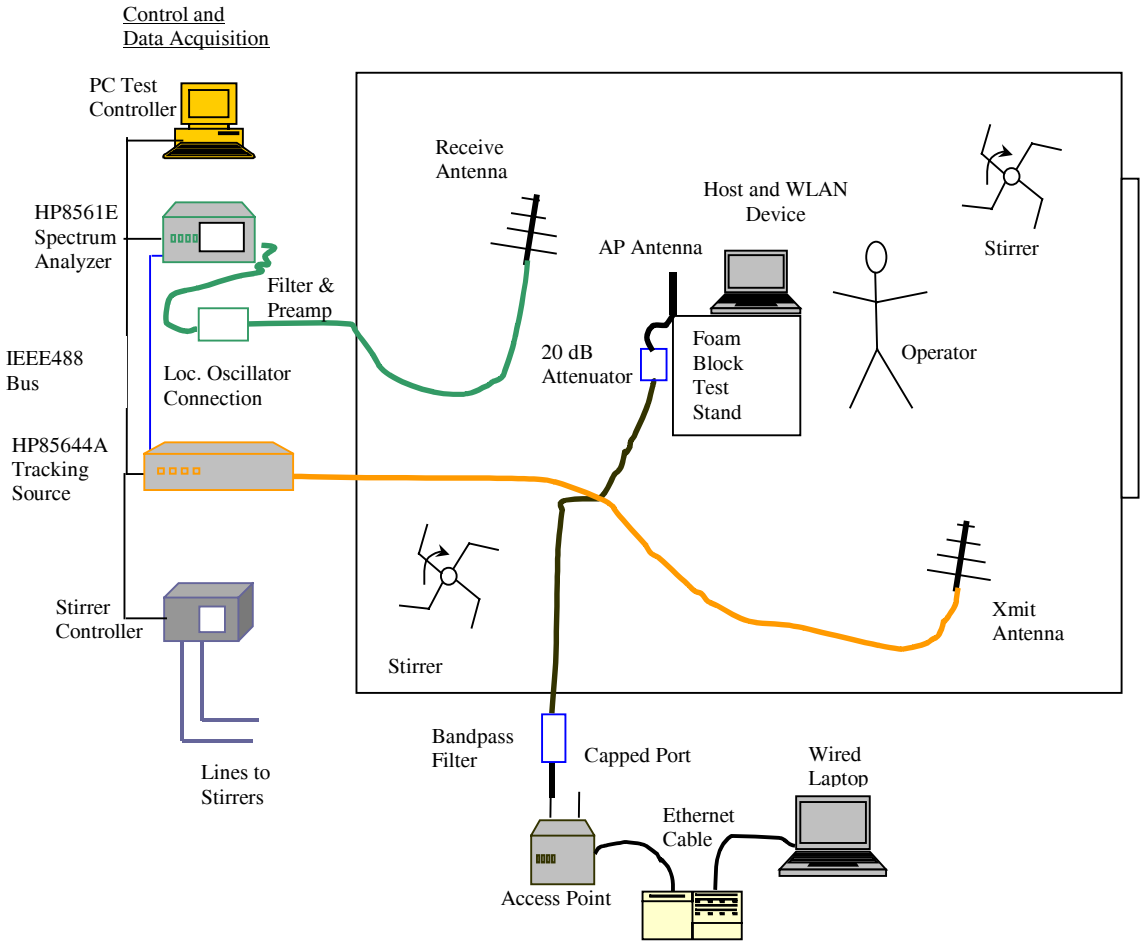

Figure 3.2-2: RC and WLAN emission test configuration.

Emission measurements using the mode-stirred method typically involve [15]: 1) Empty chamber insertion loss measurement; 2) Measurement of chamber loading, caused by the presence of a test operator and test equipment inside the chamber; and 3) Measurement of maximum receive power over a paddle rotation of the stirrer with the DUT powered on in various test modes. The total radiated power within the measurement resolution bandwidth can be calculated using [15, appendix E]:

$$P_{TotRad} = (P_{MaxRec} * \eta_{Tx}) / (CLF * IL), \qquad \text{(Eq. 3.2-1)}$$

where

P_{TotRad} = total radiated power within the measurement resolution bandwidth,

P_{MaxRec} = maximum received power measured over one complete paddle rotation,

CLF = chamber loading factor, or the additional loading effects caused by the presence of objects or operators in the test chamber,

η_{Tx} = efficiency factor of the transmit antenna used in chamber calibration and assumed to be unity for the antennas used,

IL = empty chamber insertion loss, pre-determined during chamber calibration.

IL is measured during chamber calibration, and is defined as the ratio of the maximum receive power and the transmitted power in a stirrer revolution [15: appendix B]:

$$IL = P_{MaxRec} / P_{Input} \ , \qquad \text{(Eq. 3.2-2)}$$

where P_{MaxRec} and P_{Input} are the maximum received power and the transmit power at the antennas, respectively.

In [15], *IL* is first measured and averaged over multiple locations for improved uncertainties. *CLF* is then measured once (one location) when test objects or personnel are introduced into the test chamber. Correction for *CLF* is applied only when the values exceed a given threshold (3 dB is specified in [15]). In this effort, a simplified one-step process was used instead: (*CLF*IL*) combination was measured together. This one-step process requires that the DUTs and DUT operator be present in the chamber during calibration. The chamber loading factor measurement is no longer needed, eliminating uncertainties about whether a correction for *CLF* should be applied. To reduce the burden on DUT operators, (*CLF*IL*) was measured at one location rather than averaged over multiple locations. The effect is an acceptable small increase in uncertainty (of about two dB or less depending on chamber field uniformity and frequency).

In an actual setup, it is often convenient to include transmit and receive path losses in the chamber calibration measurements. These path losses account for the presence of test cables, in-line amplifiers, attenuators and filters for various purposes. Transmit path losses are associated with components connecting the source output and the transmit antenna, whereas receive path losses are associated with components connecting the receive antenna and the spectrum analyzer input. As result, chamber calibration factor (*CF*), in dB, is introduced:

$$\begin{aligned} CF &= (P_{Xmit(dBm)} - P_{SAMeas(dBm)}) \\ &= L_{Chmbr(dB)} + L_{RecCable(dB)} + L_{XmitCable(dB)} \ , \end{aligned} \qquad \text{(Eq. 3.2-3)}$$

where

CF = chamber Calibration Factor (dB),

$L_{Chmbr(dB)}$ = chamber loss (dB), or

= $-10log_{10}(CLF * IL)$,

$L_{RecCable(dB)}$ = receive cable loss (dB),

$L_{XmitCable(dB)}$ = transmit cable loss (dB),

$P_{SAMeas(dBm)}$ = maximum receive power measured at the spectrum analyzer (dBm) over one stirrer revolution,

$P_{Xmit(dBm)}$ = power transmitted from source (dBm).

Passive losses (not to include amplifier gains) are defined to be positive in dB. The total radiated power in dBm can be computed using:

$$P_{TotRad(dBm)} = P_{SAMeas(dBm)} - L_{XmitCable(dB)} + CF . \quad \text{(Eq. 3.2-4)}$$

As shown in Figure 3.2-2, measurement instrumentation included a spectrum analyzer, a tracking source (frequency-coupled with the spectrum analyzer), a computer, a stirrer controller, transmit and receive antennas, RF filters, pre-amplifiers, and an IEEE-488 bus. The measurement procedure begins by performing a transmit path loss calibration. Transmit path losses are measured at each frequency by injecting a known power from the tracking source through the cable to the antenna connector and using a spectrum analyzer to measure the loss. Next, a chamber calibration is performed. A known level of power is delivered from the source into the chamber through the transmit antenna while the stirrer(s) are continuously rotated at a predetermined rate. The spectrum analyzer is used to record the maximum power coupled into the receive antenna (and the receive path) while performing synchronized frequency sweeps with the tracking source across the measurement bands. Eq. 3.2-3 is applied to determine the *CF* [1,12].

The source is then removed, and the transmit path connection terminated, to avoid leakage from the source into the chamber. With the DUT powered off, a radiated emission measurement is conducted to measure noise floor levels in each band. Then the DUT is powered on and a radiated emission measurement performed at each frequency with the DUT placed in each test mode. During the emission measurements, the spectrum analyzer is put on maximum hold mode while continuously sweeping over the measurement frequency band. The control software applies the equation Eq. 3.2-4 to normalize the measured power with the calibration data [1].

Figure 3.2-2 shows the position of a host and WLAN device in the center of the chamber, represented by a laptop computer on a foam block test stand. The AP antenna is also located on the same test stand. Utilizing the mode-stirred method, the two stirrers located in the corners of the chamber were continuously rotated at 5 rpm during chamber calibrations and emissions testing. Also illustrated is the control and data acquisition system. Note the line labeled Local Oscillator Connection. This line actually represents several connections between the tracking source and spectrum analyzer that ensure frequency synchronization. RF filters and a preamplifier are indicated in the receive path. The wireless network is illustrated outside the chamber, and includes an AP, a router, a wired laptop, and a bandpass filter inline with the AP antenna. A 20 dB attenuator is located inside the chamber at the AP antenna. This attenuator was used to improve wireless network communications by reducing signal overload caused by close proximity of the AP antenna and wireless card. The AP antenna and the wireless card were placed close to each other to overcome multipath interference. The AP antenna port that was not used was capped with a 50-ohm termination to prevent signals outside the chamber from coupling in through the AP.

3.2.2 Preliminary Testing

Overview

Before radiated spurious emission measurements began, several preliminary and exploratory tests were performed. The requirements for filtering were analyzed and specific parameters were determined for selecting filters and preamplifiers. In addition, emission tests were conducted on PEDs in order to establish host baselines, and APs and WLAN devices were characterized and selected.

During preliminary and emission testing of WLAN devices, two tests were performed, ping storm and duplex file transfer. Ping was used to probe the target, a WLAN device, and determine if the network was functioning correctly. A network ping sends a null packet, which is a very small packet of 8 bytes, plus standard Transmission Control Protocol/ Internet Protocol (TCP/IP) overhead over the network. This packet contains enough information to locate a particular receiving device or client using its IP address. The receiving device will then send a minimal response. The round-trip usually takes only milliseconds and indicates that the devices are communicating and that the network is operating correctly. A ping storm occurs when a ping is sent continuously over the network. Duplex file transfers between laptops were also conducted. A data file from a wired laptop was sent to a WLAN laptop and vice versa, simultaneously. These types of tests were performed during AP characterization and radiated emissions measurement testing.

In addition, emissions tests were conducted on eight laptop computers and two PDAs in the five measurement frequency bands using several different operating modes. The resulting emissions data were analyzed and compared to determine from measured emission levels which laptop computers to use as hosts for the WLAN devices during emissions tests.

Determination of Required Filtering

Tests were performed in a RC using an HP85644A sweeping source to determine if representative device emissions caused intermodulation or false spurious emissions within the measurement system in each measurement frequency band. These tests were conducted with required preamplifiers in place, and band-specific filters to avoid overdriving the preamplifiers. Figure 3.2-2 illustrates the receive path used during calibration and emission testing with filters and preamplifier in place. Tables 3.2-1, 3.2-2, and 3.2-3 give the designated RC, preamplifier, receive antennas, spectrum analyzer settings, and filters used during calibration and emission measurements for each threat type and frequency band.

Table 3.2-1: FRS/GMRS Threat Source (440 – 470 MHz)

Freq. Band	Cbr.	Pre-Amplifier Used	Receive Antenna	Spectrum Analyzer Settings	Specified filter before Pre-Amplifier
1	A	Miteq AU-1291-N-1103-1179-WP, 60 dB; HP8491B Attenuator, 10 dB	AH SAS-200/514	HP 8561E RBW= 10kHz Atten.= 0dB	K&L 8IL40-336/U468 Lowpass Cutoff Freq. 336 MHz
2	A	Miteq AU-1291-N-1103-1179-WP, 60 dB; HP8491B Attenuator, 10 dB	AH SAS-200/514	HP 8561E RBW= 10kHz Atten.= 0dB	K&L 8IL40-336/U468 Lowpass Cutoff Freq. 336 MHz
3	C	HP83017A, 40dB	AH SAS-200/571	HP 8561E RBW= 100kHz Atten.= 0dB	K&L 4IH30-926/U1600 (2) Highpass Cutoff Freq. 926 MHz
4	C	Antenna Integrated, 55dB	µpulse 2104NW	HP 8561E RBW= 10kHz Atten.= 0dB	K&L 4IH30-926/U1600 (2) Highpass Cutoff Freq. 926 MHz
5	C	HP83017A, 40dB	AH SAS-200/571	HP 8561E RBW= 30kHz Atten.= 0dB	K&L 9FV30-5061/X60 Bandpass 5031 – 5091 MHz

Table 3.2-2: IEEE802.11b, Bluetooth Threat Source (2400 – 2500 MHz)

Freq. Band	Cbr.	Pre-Amplifier Used	Receive Antenna	Spectrum Analyzer Settings	Specified filter before Pre-Amplifier
1	A	Miteq AU-1291-N-1103-1179-WP, 60 dB; HP8491B Attenuator, 10 dB	AH SAS-200/514	HP 8561E RBW= 10kHz Atten.= 0dB	K&L 4IL30-600/U2497 Lowpass Cutoff Freq. 600 MHz
2	A	Miteq AU-1291-N-1103-1179-WP, 60 dB; HP8491B Attenuator, 10 dB	AH SAS-200/514	HP 8561E RBW= 10kHz Atten.= 0dB	K&L 4IL30-600/U2497 Lowpass Cutoff Freq. 600 MHz
3	C	HP 83017A, 40dB	AH SAS-200/571	HP 8561E RBW= 100kHz Atten.= 0dB	K&L 6IL30-1600/U2497 Lowpass Cutoff Freq. 1600 MHz
4	C	Antenna Integrated, 55dB	µpulse 2104NW	HP 8561E RBW= 10kHz Atten.= 0dB	K&L 6IL30-1600/U2497 Lowpass Cutoff Freq. 1600 MHz
5	C	HP83017A, 40dB	AH SAS-200/571	HP 8561E RBW= 30kHz Atten.= 0dB	K&L 4FV30-5050/X100 Bandpass 5000-5100 MHz

Table 3.2-3: IEEE802.11a Threat Source (5150 – 5825 MHz)

Freq. Band	Cbr.	Pre-Amplifier Used	Receive Antenna	Spectrum Analyzer Settings	Specified filter before Pre-Amplifier?
1	A	Miteq AU-1291-N-1103-1179-WP, 60dB; HP8491B Attenuator, 10 dB	AH SAS-200/514	HP 8561E RBW= 10kHz Atten.= 0dB	K&L 6IL30-1600/U2497 Lowpass Cutoff Freq. 1600 MHz
2	A	Miteq AU-1291-N-1103-1179-WP, 60 dB; HP8491B Attenuator, 10 dB	AH SAS-200/514	HP 8561E RBW= 10kHz Atten.= 0dB	K&L 6IL30-1600/U2497 Lowpass Cutoff Freq. 1600 MHz
3	C	HP 8301&A, 40dB	AH SAS-200/571	HP 8561E RBW= 100kHz Atten.= 0dB	K&L 6L250-4000/T1800(2) Lowpass Cutoff Freq. 4000 MHz
4	C	Antenna Integrated, 55dB	µpulse 2104NW	HP 8561E RBW= 10kHz Atten.= 0dB	K&L 6L250-4000/T1800 Lowpass Cutoff Freq. 4000 MHz
5	C	HP83017A, 40dB	AH SAS-200/571	HP 8561E RBW= 30kHz Atten.= 0dB	K&L 9FV30-5061/X60 Bandpass 5031 – 5091 MHz

Host Device Baseline

WLAN devices come in two different forms: 1) a removable PC card; or 2) integrated into an electronic system, which enables its host device to communicate with a mobile or fixed network using assigned radio frequencies. WLAN transmitters do not function independently and must be installed in a host device. A host is a PED that a user chooses to be mobile and linked to other PEDs in order to exchange information. A baseline of spurious radiated emissions for each possible host was measured in the five measurement frequency bands. This phase of testing determined the "quietest", or lowest peak radiated emission power for each PED, and was used to determine hosts for WLAN device testing. Various laptop computers were used as test objects. Table 3.2-4 shows the laptops, PDAs, and a mobile printer considered.

Laptop Computers

Spurious radiated emissions were recorded for all five measurement frequency bands with each of the eight laptops operating in five modes. Modes are processing tasks that may be performed by a laptop while in use. Radiated emissions from the modes (idle, flowerbox screensaver, file transfer, CD, and DVD) were measured separately and then plotted with each other to achieve a maximum radiated peak envelope of the laptop, which is discussed further in Section 3.4. The flowerbox screensaver was selected to be a large, smooth, checkerboard cube pattern that spins and blooms at maximum complexity. The file transfer mode transfers a file from the hard drive to the PCMCIA slot mounted microdrive. Idle mode testing is conducted as a normal desktop screen is displayed. In order to exercise the video and audio cards, a CD and DVD were played. Appendix B contains results of the plotted data.

In order to determine the emissions from the WLAN devices, laptop emissions were independently measured to create a baseline. Combining idle and file transfer modes created a baseline, which is directly compared with the DUT (WLAN device paired with its host) idle, ping storm, and file transfer values across the measurement frequency band. This comparison reveals what effects the WLAN device adds to the host emission levels. The baseline was used to determine the "quietest" host in each of the measurement bands. LAP4 and LAP6 were chosen as hosts since they had the lowest peak radiated emission power baseline levels in some measurement frequency bands. LAP4 is the host for WLANs tested in RC A, which was configured to test Bands 1 and 2. LAP6 was the host for WLANs tested in RC C, which was configured to test Bands 3, 4, and 5. Figure 3.2-3 illustrates the configuration for a chamber with a tracking source (for calibration), a spectrum analyzer, transmit and receive antennas (log periodic, GPS, and horn), a laptop computer, and an operator.

PDA and Printer

A PDA baseline consisted of the idle and file transfer modes. File transfer in this case was performing a backup operation to a secure digital or compact flash card.

The battery powered printer was used as a host for a BlueTooth – USB printer adapter. The printer's baseline solely consisted of the idle mode with the unit powered on. Peak radiated emission power levels from these hosts are located in Appendix B. Host baselines are compared with the DUT emission measurements to determine how the WLAN affects the host emission levels.

Table 3.2-4: Laptop, PDA, and Mobile Printer Models

Host Designation	Manufacturer	Model
LAP1	Dell	Latitude C640
LAP2	HP	Pavilion n6395
LAP3	Sony Vaio & Dock	PCG-641R PCGA-DSM51
LAP4	Dell	Latitude C800
LAP5	Fujitsu	Lifebook
LAP6	Panasonic	Toughbook CF-47
LAP7	Fujitsu	Lifebook CP109733
LAP8	Gateway	450SX4
PDA1	Palm	m515
PDA2	Toshiba	e740
PRN	Hewlett Packard	DeskJet 350

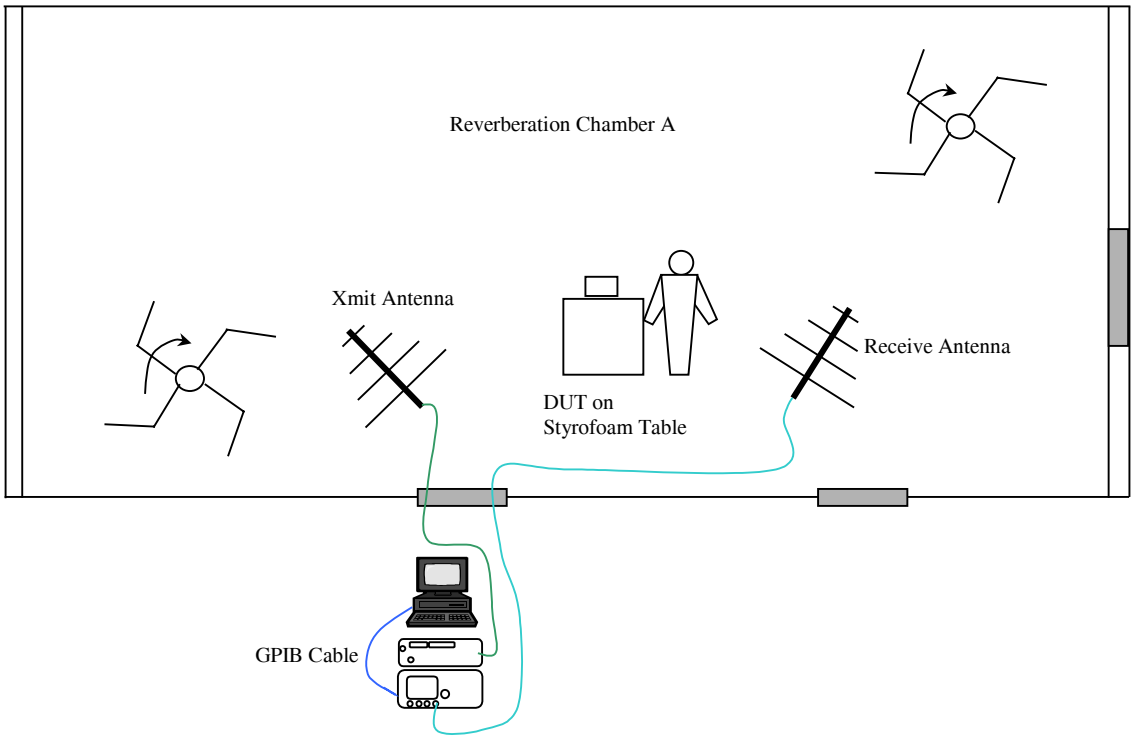

Figure 3.2-3: Setup for host baseline in RC A

Test Set and Wireless Device Characterization and Selection

Prior to conducting radiated emission testing, WLAN APs and a Bluetooth test set were characterized to determine operating limitations, performance, and noise levels. Two 802.11a APs, two 802.11b APs, and one Bluetooth test set were evaluated. The Bluetooth test set and APs, also utilized as test sets, served as DUT controllers for setting WLAN parameters such as data rates, channels, and power. In addition, the test sets and wireless device combinations were evaluated.

802.11a and 802.11b Data Rate and Channel Control

The ability of APs and WLAN devices to control data rates, channels, and power was tested and verified. Various AP and wireless PC card combinations were tested to determine interoperability and performance. WLANs were set up and operated in appropriate configurations (Figure 3.2-4) in a SAC and a RC. A network configuration consisted of an AP, acting as a bridge between devices or clients, and a wireless base station connected to a router that functioned as server for IP addresses; a wired laptop, connected to the router; and a laptop with a wireless NIC installed in the computers PCMCIA slot. Each AP was configured as required by using TCP/IP network links and a browser on the wired laptop that interfaced with AP software to setup and control operational parameters. Another laptop with a wireless PC card inserted and interface software installed was used to communicate with an AP through the wireless network. WLAN cards were tested in infrastructure mode only, one at a time.

Figure 3.2-4 shows a diagram of the operational evaluation setup of the WLAN in a RC. Tests were conducted to determine the data rates and channels to be used during emissions testing. For testing the capabilities and performance of APs and PC cards, a ping storm was initiated from the AP control wired

laptop to the WLAN laptop (Figure 3.2-4) while various data rates and channels were applied. Duplex file transfers between laptops were also conducted. A data file from the wired laptop was sent to the WLAN laptop with PC card and vise versa, simultaneously. Again, various data rates and channels were tested while transferring files.

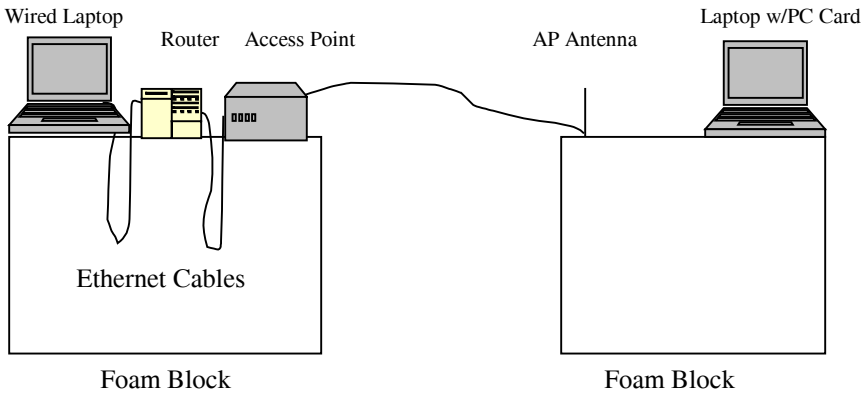

Figure 3.2-4: Preliminary testing WLAN configuration.

Figure 3.2-5 contains pictures of the preliminary testing setup in a RC. Note that a log periodic receive antenna and a spectrum analyzer were used to monitor the spurious signals in the measurement bands. The wired and wireless laptops are shown, as well as the AP with attached antennas and network router.

Figure 3.2-5: Preliminary AP and WLAN device evaluation testing in RC.

Continuous operation in a RC was more difficult to maintain than in a SAC due to multipath propagation conditions. Multipath loss occurs as the RF signal bounces off the chamber walls and rotating paddles within the chamber enroute from the AP antenna to the WLAN device. The rotating paddles are the greatest contributor to this loss. As a result, the signal can take more than one path,

arriving at the WLAN device as multiple or attenuated signals. WLAN performance was significantly impacted by these losses. 802.11a device communications were more difficult to maintain in an RC than were 802.11b device communications. In these cases, the AP antenna was placed at a distance approximately one to three inches from the PC WLAN card in order to establish the network connection. Reducing the AP antenna and card distance did improve connection stability by reducing the effect of multipath signals. During emission testing, a 20dB attenuator was added at the AP antenna to prevent the WLAN card and AP antenna from overpowering each other when the two were in close proximity.

The more robust APs and cards were able to operate continuously with fewer dropouts and quicker recovery. Many of the faster data rates were difficult to sustain in this multipath environment. The selection of data rates during emission testing was determined largely by the capability of the AP/card combination to maintain association and communication and to perform in a robust manner. Data rates were selected based on the AP operability at each rate, and the desire to test as many data rates and modulation schemes as possible.

Preliminary operational testing of APs and PC cards was used to determine channel selections. Changing channels moves the transmission signal from one frequency to another within the larger operational frequency band for a particular type of device. The 802.11a WLAN devices used during testing were limited to the first two operational bands (5.15 to 5.25 GHz and 5.25 to 5.35 GHz). The availability of certain channels was further limited by equipment selected.

802.11a and 802.11b WLAN Operational Evaluation

APs were tested to determine their operational capability in a RC environment by verifying transmission signals and identifying any spurious signal emissions. Tests were conducted to determine if test sets emitted signals through their antennas and produced noise in the five measurement bands. Radiated emissions were measured in a RC with APs active, but no PC cards or other WLAN devices present. No significant spurious signals were noted during the preliminary tests of the APs; however, bandpass filters were added inline between the APs and antennas during emissions testing to ensure that no out-of-band emissions were radiated into the chamber.

Results of 802.11a and 802.11b Preliminary Testing

All data rates and channels allowed by the APs, test set, and cards were exercised during preliminary operational testing. Among various AP and card combinations, there were configuration and operational variations. While some WLAN cards automatically configure to the associated AP data rate and channel, others do not, and can be set independently. Communication and setup interfaces varied in ease-of-use and capability. Among the various devices tested, some had a greater number of available data rates, channels, and modes. The ability to control power levels proved to be very limited; therefore, PC cards were configured and maintained at maximum power levels. Power level maximums were 200 mW for 802.11a devices and 100 mW for 802.11b devices.

Ultimately, two APs, one for 802.11a tests and one for 802.11b tests, were selected based on ease-of-use, overall capability, and robust behavior. The selected APs each had removable antennas, adjustable power settings, and short delays during configuration changes. Limiting test conditions were largely associated with PC cards. For instance, out of eight 802.11a PC cards, two were not capable of turbo mode, thereby, limiting data rates and channels. Certain brands of PC cards were unable to maintain higher data rates reliably and produced numerous dropouts and disassociations from the AP. Except for duplicates, all PC cards tested during the preliminary stage were used during emissions testing. A total of

five 802.11a PC cards and six 802.11b PC cards were selected for emissions testing. The 802.11a selected data rates and associated modulation schemes are listed in Table 3.2-5, and selected channels and maximum output power are listed in Table 3.2-6. The 802.11a AP chosen for use during emissions testing had a high-speed or turbo mode capability that allowed for three additional channels. In addition to the normal channels shown in Table 3.2-6, channels 42, 50, and 58 were also used when operating in turbo mode. The 802.11b selected data rates and associated modulation schemes are listed in Table 3.2-7, and selected channels and maximum output power are listed in Table 3.2-8. Table 3.2-8 shows that the channel numbers chosen for 803.11b emissions testing were 1, 6, and 11, as these channels are non-overlapping in frequency bandwidth. .

Table 3.2-5: 802.11a Selected Data Rates

Data Rate (Mbps)	Modulation**
6	BPSK
12	QPSK
24	16-QAM
36*	16-QAM

*Available in turbo mode.
**BPSK – Binary Phased Shift Keying, QPSK – Quadrature Phased Shift Keying, 16-QAM – 16 bit Quadrature Amplitude Modulation

Table 3.2-6: 802.11a Selected Channels.

Channel Numbers	Frequency (MHz)	Maximum Output Power
36	5180	40 mW
42*	-	40 mW
48	5240	40 mW
50*	-	-
58*	-	200 mW
64	5320	200 mW

* Turbo Mode Channels

Table 3.2-7 802.11b Selected Data Rates

Data Rates (Mbps)	Modulation*
1	BPSK
2	QPSK
11	QPSK

*BPSK – Binary Phased Shift Keying, QPSK – Quadrature Phased Shift Keying

Table 3.2-8: 802.11b Selected Channels

Channel Numbers	Frequency (MHz)	Maximum Output Power
1	2412	100 mW
6	2437	100 mW
11	2462	100 mW

Bluetooth Test Set Operational Evaluation and Characterization

An evaluation of an Agilent Technologies E1852B Bluetooth Test Set was conducted to determine if the operational modes of COTS Bluetooth devices could be controlled by the test set. A laptop installed with Agilent's Bluetooth test set interface software was used to send inquire and page commands in normal mode. A communication link between the test set and a Bluetooth device occurs when the test set detects any Bluetooth device in its coverage area by using device address inquiries. The Bluetooth device address is selected to establish a connection and to implement a normal mode page communication link. A normal mode connection sends null packets with a header over the network to the Bluetooth device, which returns a reply to the Bluetooth test set. Once a connection is made, it will remain in place until the operator releases it. All off-the-shelf Bluetooth devices tested were unable to establish a connection through the test mode page because manufacturers remove this feature before devices reach production phase. Test mode allows a payload to be attached with the header to simulate a file transfer.

An investigation of noise floor signal and response from the Bluetooth test set was conducted in the reverberation and semi-anechoic chambers. Figure 3.2-6 illustrates the setup used in the RC and the SAC. The Bluetooth test set was able to inquire a Bluetooth device inside the chamber and remain connected after a page. Since multipath phenomenon exists inside RCs, there is a potential for signals to couple through the Bluetooth antenna to the test set causing interference. At this point, a hardware reset was implemented, which returned the test set to normal. The Bluetooth test set SAC investigation verified that multipath signals caused interference on the test set in the RC. The test set functioned properly in the SAC. Observations of the Bluetooth test set transmission signal into the RC or SAC resulted in no significant spurious signals displayed on the spectrum analyzer.

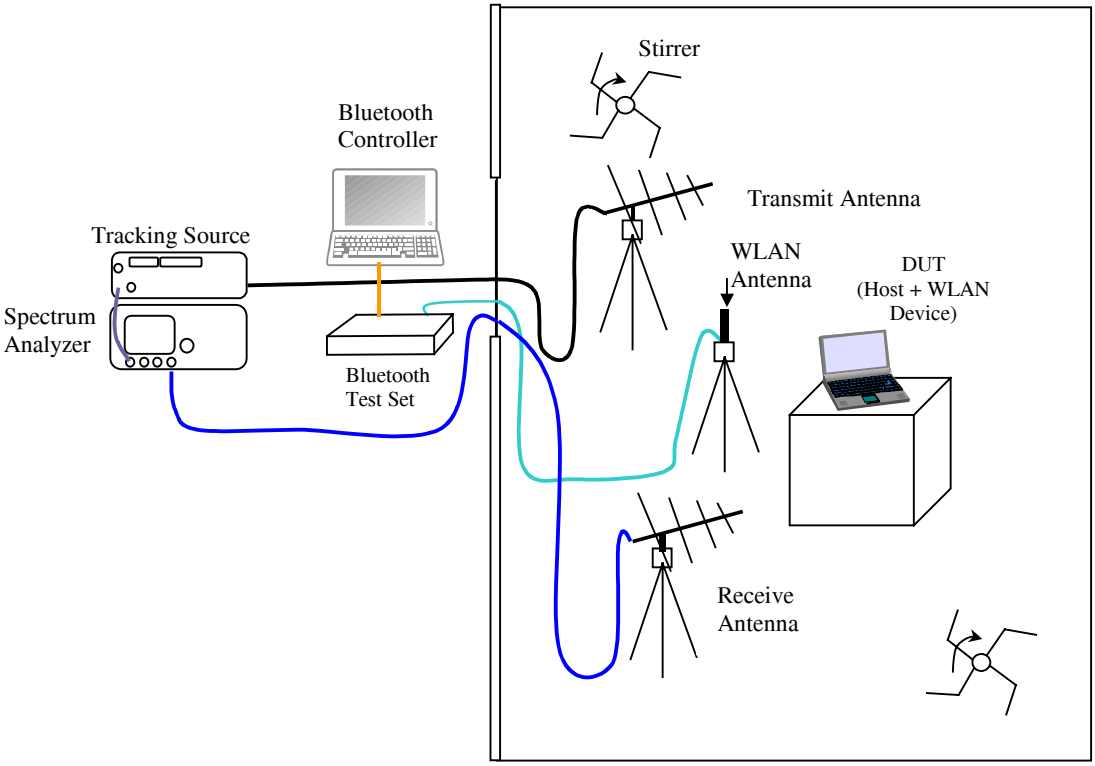

Figure 3.2-6: Bluetooth test set evaluation configuration in RC.

3.2.3 Device-Focused Testing

Overview

Measurements of spurious radiated emissions were conducted on 802.11a, 802.11b, and Bluetooth WLAN devices, and FRS and GMRS radios in five measurement frequency bands. Devices tested include five 802.11a PC cards, six 802.11b PC cards, two PDA-based 802.11b and Bluetooth cards, and six Bluetooth devices. In addition, fourteen FRS/GMRS radios were paired and tested. Host baseline test results were used to select laptops for use during emission testing.

Several industry standards were consulted to determine and justify measurement parameters. This section includes tables listing measurement parameters, such as test measurement bands, resolution bandwidths, sweep times, dwell times, and noise floor estimates. An analysis was conducted to determine minimum test times or dwell times required in a RC in order to ensure adequate measurement sampling. Instrument and preamplifier noise measurements were conducted and combined with other losses and gains to determine the minimum measurement sensitivity for each of the five measurement bands.

The test procedure is further detailed in this section and applied for testing wireless devices. Examples of test matrices for each type of device tested are presented in order to describe the components of a typical emission test.

Included in this section are the following topics that describe the device-focused testing of WLAN devices: the selection and use of test instrumentation parameters; an analysis of measurement sensitivity; a description of the WLAN devices and radios selected for testing; radiated emission measurement test details; examples of test matrices; multipath interference issues; and, finally, the data reduction process.

Frequency Bands, Measurement Bandwidth and Scan Time

Spurious radiated emissions from PEDs may be caused by internal oscillators, clocks, data buses, motors and any other circuitry that generates currents and voltages in the device that vary over time. By their very nature, spurious radiated emissions from randomly selected PEDs have widely varying time, frequency and bandwidth characteristics. The specific time, frequency and bandwidth characteristics of a particular PED emitter are vitally important in determining the exact potential or that emitter to cause harmful EMI to a particular victim system. Unfortunately, it becomes prohibitively difficult to measure every possible signal characteristic that may be generated by every PED. Because of this difficulty, standard procedures for measuring spurious radiated emissions from electronic equipment must make compromises in terms of dwell time and measurement bandwidth, over different regions of the RF spectrum. Narrow measurement bandwidths result in improved sensitivity and frequency resolution, but carry a penalty in longer measurement times (slower sweeps or more frequency samples required over a frequency band), and will underestimate the amplitude of spurious signals with bandwidth larger than the measurement bandwidth. For certain complex or multifunction PEDs, spurious radiated emissions may be intermittent or present only during specific operating modes. In this case, the measurement time (or dwell time) at a particular frequency needs to be adequate to provide confidence that the maximum emission amplitude has been measured.

Test parameters used in spurious radiated emission testing for this report, such as frequency bands, measurement bandwidth, and scan time were based upon those used in [1], with the addition of the MLS frequency band. The RTCA/DO-233 procedure [3] recommended that measuring-equipment bandwidths be chosen so ambient levels are at least 6 dB below emission limits, and it specified minimum

measurement times based upon MIL-STD-462D [8]. DO-233 recommended a single, slow sweep over each frequency band, to meet the required measurement time. As a spectrum analyzer operates, it displays the amplitude at each frequency during a sweep. Because the RC boundary condition changes with stirrer position, multiple measurement samples are required at different stirrer positions in order to find the maximum coupling amplitude. More samples are required by RTCA/DO-160D at lower frequencies to provide confidence that the peak amplitude was accurately measured. However, care must be taken to ensure that peaks are not missed at higher frequencies as well. To reduce test time for the mode-stirred measurements, multiple short sweeps were used instead of a single long sweep, while continuously rotating the chamber stirrers.

There are several references applicable to measurement bandwidths. Some of these references are listed in Table 3.2-9. RTCA/DO-160D is directly applicable to assess the potential for spurious radiated emissions to interfere with commercial aircraft communication/navigation systems, and specifies that bandwidths of 10 kHz "…shall be used in the notches with no correction factor being applied". (Notches apply to aircraft communication/navigation receive bands, including GPS and MLS.) The purpose for the reduced bandwidth is to improve measurement sensitivity. This is reasonable for VOR, LOC and GS (Bands 1 and 2) because the channel bandwidths are no greater than 10 kHz. A resolution bandwidth of 10 kHz is selected for GPS (Band 4), in keeping with the RTCA/DO-160D recommendation, while allowing reasonably short-duration sweep times. A resolution bandwidth of 10 kHz for the DME/ATCRBS/TCAS frequency band (Band 3) results in excessively long sweep times; therefore, a resolution bandwidth of 100 kHz is selected for Band 3. This bandwidth is in line with standards that recommend a 100 kHz measurement bandwidth below 1000 MHz and allows for a reasonably short-duration sweep time. The selected parameters for frequency bands, measurement bandwidth, and scan times are shown in Table 3.2-10.

The HP8561E spectrum analyzer requires two seconds to sweep from 5020 to 5100 MHz with a 10 kHz resolution bandwidth. Because of this long sweep time, a 30 kHz resolution bandwidth is selected as a compromise for best sensitivity, while minimizing measurement time. The selected parameters for MLS are shown as Band 5 in Table 3.2-10.

As previously stated, the RTCA/DO-233 procedure specified minimum measurement times based upon MIL-STD-462D. Using RTCA/DO-233, Appendix A, Section 1.3, the minimum dwell time is specified to be 15 ms/kHz. As the resolution bandwidth is increased, the sweep time decreases by the same factor. Table 3.2-11 shows the minimum required test times the DO-233 procedure specifies for frequency Bands 1 to 5.

Table 3.2-9: Measurement Bandwidth, Several Standards Compared

Frequency Band	**RTCA DO-160D [9]**	**RTCA DO-233 [3]**	**ANSI C63.4-2000 [10]**	**ETSI EN 301 908-7 V1.1.1 [11]**	**MIL-STD-462D [8]**
30-400 MHz	10 kHz	100 kHz	100 kHz	100 kHz	100 kHz
400- 1000 MHz	100 kHz*	100 kHz	100 kHz	100 kHz	100 kHz
Over 1000 MHz	1 MHz*	1 MHz	1 MHz	1 MHz	1 MHz

* Specified to be 10 kHz in aircraft commuication/navigation bands for categories M & H.

Table 3.2-10: Measurement Bandwidths and Sweep Times for Measuring Spurious Radiated Emissions in Aircraft Radio Frequency Bands

Frequency Band Designation & (Chamber)	Aircraft Systems	MHz	Resolution Bandwidth kHz	Spectrum Analyzer Sweep Time (ms) (HP8561E)
1 (A)	VOR & ILS LOC	105 – 120	10	375
2 (A)	ILS GS	325 – 340	10	375
3 (C)	DME, TCAS, ATCRBS, GPS L2	960 – 1250	100	73
4 (C)	GPS L1	1565 – 1585	10	500
5 (C)	MLS	5020 - 5100	30	230

An implied assumption of the minimum required test time estimated in Table 3.2-11, is that the PED is stationary, and oriented to provide maximum coupling to the test antenna at a given frequency. For RC testing, it is necessary to perform more measurements at lower frequencies to gain confidence that an accurate estimate of the maximum amplitude has been obtained. Table 3.2-12 shows the most recent recommendations for a desired number of independent samples for calibrating RCs (DO-160D, Change 1 [9]). Assuming the stirrer rotation rate is not an even multiple of the spectrum analyzer sweep rate, it can be assumed that each spectrum analyzer sweep provides an independent sample for each frequency. Multiplying the required number of independent samples by the sweep time can provide an estimate of minimum measurement time as shown in Table 3.2-12. The optimal measurement time in a RC can be based on a statistical combination of the minimum measurement times estimated in Tables 3.2-11 and 3.2-12, and will always be less than the multiple of the two. This is because the minimum measurement times in Table 3.2-11 assume unchanging electromagnetic boundary conditions in the chamber, and the measurement times in Table 3.2-12 prescribe the time required to obtain adequate samples of these independent boundary conditions. The spectrum analyzer display can monitor how quickly the maximum level stabilizes. Experience has shown that RC measurement times of 120 seconds are adequate to determine peak emissions amplitude for each mode and band.

Table 3.2-11: Estimation of Minimum Required Measurement Time Using RTCA/DO-233, Appendix A Guideline.

A	B	C	D	E	F	G	H
Frequency Band Designation	**Sweep Bandwidth (MHz)**	**Sweep Time (ms)**	**Dwell Time per Sweep (ms/MHz) [C/B]**	**Meas Bandwidth (kHz)**	**DO-233 Min Meas Time (ms/kHz) [(0.015*1000)/E)]**	**Sweeps Rqd for DO-233 Min Meas Time [F/(D/1000)]**	**Min Rqd. Test Time (sec) [G*(C/1000)]**
1	15	375	25.00	10	1.50	60	22.5
2	15	375	25.00	10	1.50	60	22.5
3	290	73	0.25	100	0.15	596	43.5
4	20	500	25.00	10	1.50	60	30.0
5	80	230	2.88	30	0.50	174	40.0

Table 3.2-12: Estimation of Minimum Required Measurement Time in a RC

A	B	C	D
Frequency Band Designation	**Indep. Samples Rqd. for Rvb. Cbr. Cal.**	**Sweep Time (ms)**	**Min Meas Time Assuming Indep. Samples (sec) [B*(C/1000)]**
1	60 (RC A)	375	22.5
2	60 (RC A)	375	22.5
3	18 (RC C)	73	1.3
4	18 (RC C)	500	9.0
5	18 (RC C)	230	4.1

Amplitude Measurement Sensitivity

Using the frequency band, resolution bandwidth, and designated chamber presented in Table 3.2-10 and the preamplifiers specified in Tables 3.2-1 through 3.2-3, the spectrum analyzer noise floor and preamplifier noise power were measured for each of the five frequency bands, and the results are shown in Table 3.2-13. Note that minimum measurement sensitivity is estimated to be 6 dB above the adjusted noise floor. The RC losses were taken from previous test data or estimated. From these measurements and specifications, the estimated minimum sensitivity for each frequency band was computed and shown in Table 3.2-13, Column F.

Table 3.2-13: Estimation of Minimum Measurement Sensitivities

A	B	C	D	E	F
Frequency Band Designation	**Spec. Analyzer Noise Floor (dBm)**	**Pre-Amp Gain (dB)**	**Pre-Amp Noise Power (dB)**	**Reverb Cbr Loss (dB)***	**Estimated Minimum Sensitivity (dBm) [B-C+D+E+6]**
1	-93	61	24	6 (RC A)	-118
2	-93	61	24	10 (RC A)	-114
3	-82	50	23	15 (RC C)	-88
4	-93	55	25	25 (RC C)	-92
5	-88	40	11	40 (RC C)	-71

* Data based on previous test conducted in chambers

Description of WLAN Devices and Two-Way Radios

The off-the-shelf wireless devices tested conformed very well to specified standards and interoperability criteria. Tables 3.2-14, 3.2-15, and 3.2-16 lists the brands and model numbers of devices tested in each wireless standard. Figure 3.2-7 shows the WLAN devices used in this effort. 802.11b devices have a transmit output power range from a 5 mW to 30 mW minimum or 100 mW maximum value. A user is able to expand or confine a transmission area with respect to other wireless devices operating nearby, when an option to adjust the transmit power level is available in the utility software. Several manufacturers of NICs, universal serial bus (USB), or secure digital (SD) devices provide users with additional control options or data rates. The 11B-2, 11B-3, 11B-5, 11B12 and 11B-13 cards are among the 802.11b NICs which have the capability to control the transmit output power. The 11B-2 card

was set to its maximum output power of 30 mW, whereas 11B-3, 11B-5, 11B-12 and 11B-13 were set to their maximum output power of 100 mW. The exact output powers for the other 802.11b devices were unknown, since the PC cards' utility software did not contain any feedback to display the value of the output power levels of the cards. However, 11B-7 and 11B-11 are interoperable with the other adapters, so they are accepted to be within the output power range. Several 802.11a devices contain additional data rates that are not dictated by the IEEE 802.11a standard.

Table 3.2-14: 802.11a Devices Tested

DUT Designation	Manufacturer	Model	Serial Number	Host Designation	Max Output Power Ch. Dependent
11A-1	Proxim	Harmony	052040EX3NVR	LAP4/LAP6	50 mW, 200 mW
11A-2	Proxim	Harmony	051490E0ENVR	LAP/LAP6	50 mW, 200 mW
11A-3	Linksys	WPC11	MBY2402094	LAP/LAP6	50 mW, 200 mW
11A-5	Intel	WCB5000	9009TB00C5B6	LAP/LAP6	40 mW, 200 mW
11A-6	NetGear	WAB501	WAB5A29ZC000671	LAP/LAP6	50 mW, 200 mW

Table 3.2-15: 802.11b Devices Tested

DUT Designation	Manufacturer	Model	Serial Number	Host Designation	Maximum Output Power
11B-2	Cisco	340	VMS053313RR	LAP4/LAP6	30 mW
11B-3	Cisco	350	VMS0535026D	LAP4/LAP6	100 mW
11B-5	Symbol Tech.	Spectrum 24 PCc	00A0F830E7EE	LAP4/LAP6	100 mW
11B-7	Linksys	WPC54	G3001203652	LAP4/LAP6	95 mW
11B-11	Toshiba	E740	62058024L	PDA-2	N/A
11B-12	D-Link Air	DWL-65OH	H252123003470	LAP4/LAP6	100 mW
11B-13	NetGear	WAB501	WAB5A29ZC000671	LAP4/LAP6	100 mW

Table 3.2-16: Bluetooth Devices Tested

DUT Designation	Manufacturer	Model	Serial Number	Host Designation
BLUE-2	3-Com		HHR13D2800	LAP4/LAP6
BLUE-6	TDK	Dongle	SB10008256	LAP4/LAP6
BLUE-8	Troy	Windport	FI-PCM109-68610-24A-0242	LAP4/LAP6
BLUE-10	Anycom		Prn Adap	PRN
BLUE-11	Anycom		PC Card	LAP4/LAP6
BLUE-12	Toshiba	Palm Bluetooth Card	120015892B	PDA-1 (SD Card)

Figure 3.2-7: WLAN devices in the form of NICs, a USB dongle, a SD card and integrated into the PDA.

At the time the 802.11a NICs were purchased, a "Wi-Fi5" certified logo for interoperability was not displayed on the cards. Wireless Ethernet Compatibility Alliance (WECA) did not test 802.11a cards for interoperability, because there was only one chipset manufacturer in every brand of card. Although, WECA certification of an 802.11a NIC only tests interoperability based on the IEEE 802.11a standard. The standard only specifies data rates up to 54 Mbps, whereas 802.11a NIC manufacturers offer additional data rates in a turbo or 2X mode using proprietary methods. Yet all adapters with this capability were able to communicate with the brand of AP used during tests when operated outside the chamber. All adapters and APs with this capability were able to communicate outside the chamber with ease, and a few hindrances arose during data collection in the chamber. Table 3.2-17 lists the NICs tested with mode capability.

Table 3.2-17: 802.11a Turbo Data Rates

Manufacturer	Turbo Mode Data Rates
11A-1/11A-2	12,18,24,36,48,72, 96,108 Mbps
11A-3	Up to 72 Mbps
11A-5	N/A
11A-6	Up to 108 Mbps

Users can set the data rates on NICs; however, during testing, the data rate field was set to automatic. Rates were changed at the AP, and the NICs adjusted their rate accordingly. The AP interface software was used to enable the antenna port used during testing to transmit and receive information. Data collection for 802.11a/b had a few challenging cases which will be discussed later in this section; but overall data were collected as expected from preliminary testing results.

Bluetooth devices, as seen in the third group of Figure 3.2-7, did not have any option controls and usually had a stable link with the test set. Usually, reseating the Bluetooth device with its host solved most of the connection failures that occurred between the Bluetooth device and test set.

FRS and GMRS radios were tested as a pair in the RC with an operator switching channels and transmitting audio. Two-way radio tests were straight forward. Table 3.2-18 lists the brands and models of devices tested. Figure 3.2-8 shows both types of paired radios used in this effort.

Figure 3.2-8: 4 pairs of FRS and 3 pairs of GMRS radios.

Table 3.2-18: FRS and GMRS Radios Tested

Pair Designation	**Manufacturer**	**Model**	**Serial Numbers**
FRS-1	Motorola	T5420	165WCB0L6H
FRS-2	Motorola	T5420	165WCB0L7T
FRS-3	Cobra	FRS 225	L201279758
FRS-4	Cobra	FRS 225	L201273388
FRS-5	Audiovox	FR-1438	112105119
FRS-6	Audiovox	FR-1438	112105121
FRS-7	Midland	75-17	00516539
FRS-8	Midland	75-17	00516537
GMR-1	Motorola	T6400	175TBWY469
GMR-2	Motorola	T6400	175TBX1332
GMR-3	Audiovox	GMRS1535	TTK0111 0019481
GMR-4	Audiovox	GMRS1535	TTK0111 0019501
GMR-5	Midland	G-11C2	15011596
GMR-6	Midland	G-11C2	15011610

Wireless Device and Two-Way Radio Radiated Emission Measurements

Radiated emissions tests were performed in two of the NASA-LaRC RCs, Chambers A and C. Two different chambers were used due to chamber characteristics and noise level in specific frequency bands. The chamber configuration and test instrumentation used during calibration and emission measurements are illustrated in Figure 3.2-2. Test instrumentation consisted of an HP8561E Spectrum Analyzer, an HP85644A Tracking Source, RF filters, pre-amplifiers, transmit and receive antennas, and a control laptop computer. Transmit and receive antennas were appropriate for the measurement frequency bands and included log periodic, dual-ridge horn, and GPS survey. To obtain a lower noise floor, amplify signals, and to block out-of-band signals relative to the wireless device transmission frequencies, RF filters and preamplifiers were included in the receive path.

The previously described measurement method (Section 3.2 Measurement Method) was utilized for all calibrations and radiated emission tests. The position of a host/WLAN device and AP antenna were similar to positions indicated in Figure 3.2-2. During calibration measurements, the host and WLAN device inside the chamber and the test set outside the chamber were powered off. The operator was

grounded during tests to prevent electrostatic discharge voltages from effecting measurements. Using the control software, power measurements were normalized with the calibrated data and the results were recorded for each frequency within the test band.

Noise floor measurements were conducted to determine the ambient environment with hosts, WLAN devices, and an operator inside the chamber, but with the host/WLAN powered off and the Bluetooth test set or AP powered on. These measurements were used to verify a quiet RF environment before proceeding with radiated emissions tests.

A minimum test dwell time of 120 seconds was used for all tests where the RC characteristics affected the measurements. A dwell time is defined as the time applied for the duration of one test, which consisted of either a calibration measurement or an emission measurement where the DUT performed in a test mode, at a specific data rate and channel. Transmit cable calibration measurements required only two sec, as no RC was needed. RC and receive path calibration measurements were conducted for a dwell time of 120 seconds. Emission test dwell times varied depending on the number of channels accessed during a test.

Figure 3.2-9: RC and 802.11a WLAN setup for Band 4 (1565 MHZ – 1585 MHZ).

Figure 3.2-9 provides a picture of the emissions test setup in Chamber C. Included in the picture are the GPS receive antenna, a dual-ridge-horn transmit antenna, a host laptop with wireless PC card installed, and an AP antenna. The stirrer, which is not seen in the picture, was located directly across the chamber from the horn antenna.

Figure 3.2-10 illustrates the control and data acquisition hardware located outside an RC. Pictured are the HP8561E Spectrum Analyzer and the HP85664A Tracking Source. The local oscillators and four other ports of the spectrum analyzer and tracking source were connected in order to synchronize frequencies. The picture also illustrates the receive path including cable, filters and preamplifier resting on top of the tracking source. Agilent Visual Engineering Environment (VEE) software was used to develop control and data recording software that was run on a laptop computer.

Figure 3.2-10: Control and data acquisition setup outside the RC.

The 802.11a and 802.11b APs, located outside the chamber, were used as test sets to control data transfers and switch data rates and channels while operating in ping storm (PS) and duplex file transfer (Xfer) modes. Emission tests were conducted on one WLAN device at a time. The data link between the test set and the WLAN device was exercised using three operational modes: idle, PS, and Xfer, while swiching data rates and channels. A test consisted of a mode, a data rate, and three channels. During a three-minute dwell time, channel switching was conducted at one-minute intervals. This allowed approximately one minute of test time at each channel. Host baseline test results were used to select laptops for use during emission testing of wireless devices. Selected hosts also included PDAs that operated with WLAN cards installed and a printer with wireless capabilities.

During Bluetooth device emissions testing, an Agilent Technologies E1852B Bluetooth Test Set, located outside the chamber, was used to control test modes. Bluetooth emissions tests were performed using both idle and normal paging modes. Since Bluetooth protocol uses frequency-hopping techniques, no channel switching was done. During a test, a spectrum analyzer was swept for a two-minute dwell time and then data were recorded.

FRS and GMRS radios were tested in pairs in idle mode and voice transmit/receive modes. During FRS/GMRS radio emissions testing, the operator used two radios, one in each hand, and talked into one radio while receiving with the other radio. Channels were switched every two minutes.

Test Matrix

Tables 3.2-19 and 3.2-20 are portions of the 802.11a and 802.11b test matrices used during radiated emission testing. The tables include DUT numbers, test modes and channels, and frequency-band numbers. Note that tests using idle, PS, and Xfer modes were conducted. Selected data rates and channels are indicated for PS and Xfer modes. The illustrated combination of modes, data rates, and channels was repeated for each 802.11a and 802.11b WLAN device in the five measurement frequency bands.

Table 3.2-19: 802.11a Test Matrix

Device Under Test	Test Modes and Channels	Bands
11A-1	Idle	1-5
11A-1	Ping Storm AP Data Rate 6 Channels 36 48 64	1-5
11A-1	Ping Storm AP Data Rate 12 Channels 36 48 64	1-5
11A-1	Ping Storm AP Data Rate 24 Channels 36 48 64	1-5
11A-1	Ping Storm AP Data Rate 36 Turbo Channel 42 50 58	1-5
11A-1	Duplex File Xfer AP Data Rate 6 Channel 36 48 64	1-5
11A-1	Duplex File Xfer AP Data Rate 12 Channel 36 48 64	1-5
11A-1	Duplex File Xfer AP Data Rate 24 Channel 36 48 64	1-5
11A-1	Duplex File Xfer AP Data Rate 36 Turbo Channel 42 50 58	1-5

Table 3.2-20: 802.11b Test Matrix

Device Under Test	Test Modes and Channels	Bands
11B-1	Idle	1-5
11B-1	Ping Storm AP Data Rate 1 Channels 1 6 11	1-5
11B-1	Ping Storm AP Data Rate 2 Channels 1 6 11	1-5
11B-1	Ping Storm AP Data Rate 11 Channels 1 6 11	1-5
11B-1	Duplex File Xfer AP Data Rate 1 Channels 1 6 11	1-5
11B-1	Duplex File Xfer AP Data Rate 2 Channels 1 6 11	1-5
11B-1	Duplex File Xfer AP Data Rate 11 Channels 1 6 11	1-5

Table 3.2-21 illustrates the test matrix used for radiated emissions measurements conducted on Bluetooth WLAN devices. As in the previously illustrated matrices, DUT numbers, test modes, and frequency bands are included. Only two modes were used, idle and normal paging. All Bluetooth devices were tested using this matrix in the five measurement frequency bands.

Table 3.2-21: Bluetooth Test Matrix

Device Under Test	Test Modes	Bands
BLUE-1	Idle	1-5
BLUE-1	Normal Paging	1-5

Table 3.2-22 demonstrates a portion of the test matrix used during radiated emissions testing on FRS and GMRS radios. The tests required that two radios be paired for communication and transmission. The matrix illustrates the radio numbers and pairs, test modes, and frequency bands. The matrix was applied for frequency Bands 1 through 5.

Table 3.2-22: FRS/GMRS Radios Test Matrix

Device Under Test	Test Modes	Bands
FRS1&2	Idle	1-5
FRS1&2	Xmit Voice Count, Channels 1&14	1-5
FRS3&4	Idle	1-5
FRS3&4	Xmit Voice Count, Channel 1&14	1-5
FRS5&6	Idle	1-5
FRS5&6	Xmit Voice Count, Channels 1&14	1-5
FRS7&8	Idle	1-5
FRS7&8	Xmit Voice Count, Channel 1&14	1-5
GMR1&2	Idle	1-5
GMR1&2	Xmit Voice Count, Channel 7&14&15	1-5
GMR3&4	Idle	1-5
GMR3&4	Xmit Voice Count, Channels 1&15	1-5
GMR5&6	Xmit	1-5
GMR5&6	Xmit Voice Count, Channels 1&15	1-5

WLAN Device Multipath Interference

During radiated emission testing in an RC, multipath interference continued to occasionally affect communication between APs and WLAN devices. When interference occurred, it caused loss of communication between the AP and the WLAN device, making it necessary to repeat tests. Every effort was made to maintain communication for an adequate dwell time in order to collect a complete data set of measurements. Implementing one or more of the following methods removed many of the multipath interference affects:

1) The AP antenna and WLAN device were placed about one to three inches apart.

2) A 20 dB attenuator was inserted inline with the AP antenna.

3) Metal shielding was placed around the DUT, as shown in Figure 3.2-11, to avoid a direct path between the AP antenna and the stirrers.

4) Only one stirrer was used in Chamber A if communication failed after two attempts to collect data.

Other methods utilized to maintain or reestablish communication were available through the WLAN PC card. The software interfaces for each WLAN PC card provided communication status and a means to rescan for devices. When a rescan failed the NIC was reseated by ejecting it from the PCMCIA slot and then reinstalling it. While this slowed the testing process, it did allow the devices to re-associate.

Disassociation between the 802.11a/b APs and NICs occasionally occurred as a result of channel changes during testing, and recovery was sometimes difficult. A specific example is that 802.11a cards had difficulty maintaining association with an AP during turbo mode tests. In these cases, data were collected for the specified dwell time with the DUT cycling through one or two of the test channels depending on communication status. Where association could not be maintained during a channel

change, the data collected do not contain measurements for that next channel and is, therefore, incomplete. Test log entries were made to indicate incomplete test cases and detail the problems encountered. In some cases data were collected on just one channel for three minutes. However, based on data from completed tests, changing channels during 802.11a/b device testing did not significantly alter the peak radiated emission measurements and did not affect the final results.

Table 3.2-24 provides further detail on incomplete tests due to multipath interference. Details include specific device designation, data rate, and mode, and the channels not reflected in the data due to inadequate communication.

Other than the multipath interference disruptions, the data collection process proceeded with only a few technical inconveniences. The full scope of the testing is indicated in Table 3.2-23 where the total number of test cases for 802.11a/b devices is computed. Out of the combined total of test cases between the two technologies, only 4.5% are incomplete.

Table 3.2-23: Provides the Total Number of Test Cases Taken for Each Wireless Technology Standard

Wireless Technology	Number of Devices	Number of Test Cases Per Device	Number of Test Bands	Total Test Cases
802.11a	5	9	5	225
802.11b	7	7	5	245

Table 3.2-24: Incomplete Test Due To Multipath Interference

WLAN Device	Data Rates	Test Mode	Omitted Channels	Band	Comments
11B-7	1	Ping Storm	6 & 11	1	
	11	File Transfer	11	3	
	11	Ping Storm, File Transfer	6 & 11	4	
	11	Ping Storm, File Transfer	6 & 11	5	
11B-11	11	Ping Storm	11	2	
	2	Ping Storm	11	3	
	1	Ping Storm	11	5	
	11	Ping Storm	11	5	
11A-1	12	Ping Storm	64	2	
11A-2	12	File Transfer	48 & 64	1	
11A-3	12	File Transfer	48 & 64	1	
	24	File Transfer	48 & 64	1	
	12	File Transfer	48 & 64	2	
	36 (turbo)	Ping Storm, File Transfer	all	3,4,5	Omitted

Figure 3.2-11: Metal shielding to reduce multipath interference to the AP antenna.

3.2.4 Data Reduction

IEEE 802.11a, IEEE 802.11b, and Bluetooth

Figures 3.2-13 and 3.2-14 illustrate the data reduction process and results. The process was applied to the PED baseline test data set and wireless device emission data set in each frequency band. For the purpose of comparison and analysis, large amounts of data were reduced by creating data envelopes, which are representative of the maximum measurements for each PED and each WLAN device and host combination. Ultimately, these data envelopes were reduced to two composite data envelopes, a PED composite envelope and a WLAN device composite envelope, that represent the maximum magnitudes of all PEDs and all WLAN devices. The end of the process results in data plots found in Sections 3.3, 3.4, and 3.5 comparing PED and WLAN device emissions.

A general data reduction process is illustrated in Figure 3.2-13. Implementing this process creates data envelopes from data sets by determining the maximum (MAX) magnitudes for each frequency within a frequency band. The oval shapes illustrated in the figures represent data plots produced for each of the five frequency bands. The DUT notation represents PED, host device, or combination of WLAN device and host. As input to the reduction process, DUT Data represents measurement data collected during PED/host and WLAN device testing using several operating modes. Figure 3.2-13 demonstrates the generation of DUT envelopes using measurement data and the creation of composite envelopes from individual DUT envelopes.

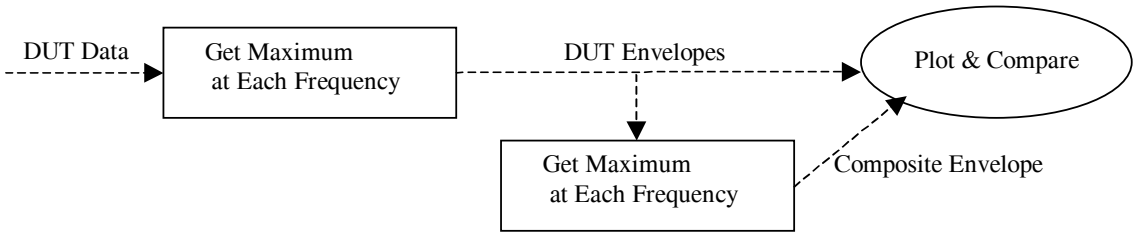

Figure 3.2-13: Data reduction process.

In this section the notation WLAN is used to refer to a WLAN device and host combination, where the host was selected based on lowest emission levels from all PEDs tested (Section 3.2.2 Host Device Baseline). WLAN and PED measurement data are illustrated in Appendices A and B, respectively. The reduction of this data followed the general process illustrated in Figure 3.2-13.

The following algorithms summarize the generation of data envelopes and use DUT to refer to PED or WLAN data.

For each frequency band, and for each DUT,

$$Max\,[DUT\ \ Emissions\ ]_{All\ \_\ Modes} \ \Rightarrow\ DUT_{Envelope}$$

For each frequency band,

$$Max\,[DUT\ \ Envelope\ ]_{All\ \_\ DUT} \ \Rightarrow\ All\ \_\ DUT\ _{Composite\ \_\ Env}$$

Conforming to the data reduction process individual PED and WLAN envelopes, and PED and WLAN composite envelopes were generated. PED envelopes are plotted and reported in Section 3.4. WLAN envelopes are plotted and shown in Section 3.3.

Figure 3.2-14 shows the last step in the data reduction process, which plots and compares the final PED composite envelope and the final WLAN composite envelope. The two composite envelopes were plotted together for each frequency band and are reported in Section 3.5.

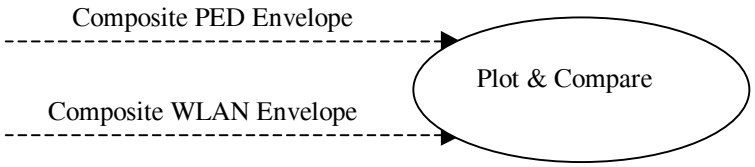

Figure 3.2-14: Composite PEDs and Composite WLAN data reduction and plot (See Section 3.5).

3.3 Test Results of WLAN Devices

This section describes the results from the radiated emission tests conducted on WLAN devices. The following charts illustrate the WLAN devices' data envelopes organized by measurement frequency bands. Sections are labeled with the appropriate frequency bands and include data acquired during radiated emissions testing using WLAN devices combined with a host based on 802.11a, 802.11b, and Bluetooth standards, and FRS radios and GMRS radios. Each chart contains plots of individual WLAN device envelopes, and an envelope that represents the maximums of all WLAN devices. Individual devices are designated with a number-letter combination, such as 11A-1, 11B-5, Blue-2, FRS1&2, or GMR3&4, whereas the envelope of all WLAN devices is simply labeled 11A, 11B, Blue, FRS, or GMR. Individual WLAN device envelopes were generated from measured emission data including all PS tests, Xfer tests, and idle mode tests. Noise floor data is plotted on charts in Appendix B that illustrate

individual WLAN device data in each test mode. A WLAN Devices Composite Envelope is the maximum at each frequency of all of the individual WLAN Device Envelopes. Note that the WLAN Device Composite Envelopes are plotted in green. In all cases, the green Composite Envelope plot masks portions or all of individual device traces directly underneath, making it difficult to recognize the presence of the individual traces beneath. A description of the processes used for the reduction of data and the generation of envelopes is found in Section 3.2.4. Envelope plots that include all WLAN devices are also used in charts in Section 3.5.

The individual WLAN device envelopes were analyzed, and it was determined that devices with the highest emissions were randomly distributed across frequency bands, and that no one device can be designated as the dominant emitter in all five measurement bands.

3.3.1 Band 1 (105 MHz to 120 MHz)

Data presented in Figures 3.3-1 to 3.3-5 were acquired in the aircraft systems frequency band assigned to VOR and ILS LOC systems. Each figure plots envelopes for each individual WLAN device and an envelope representing all WLAN devices as related to each standard.

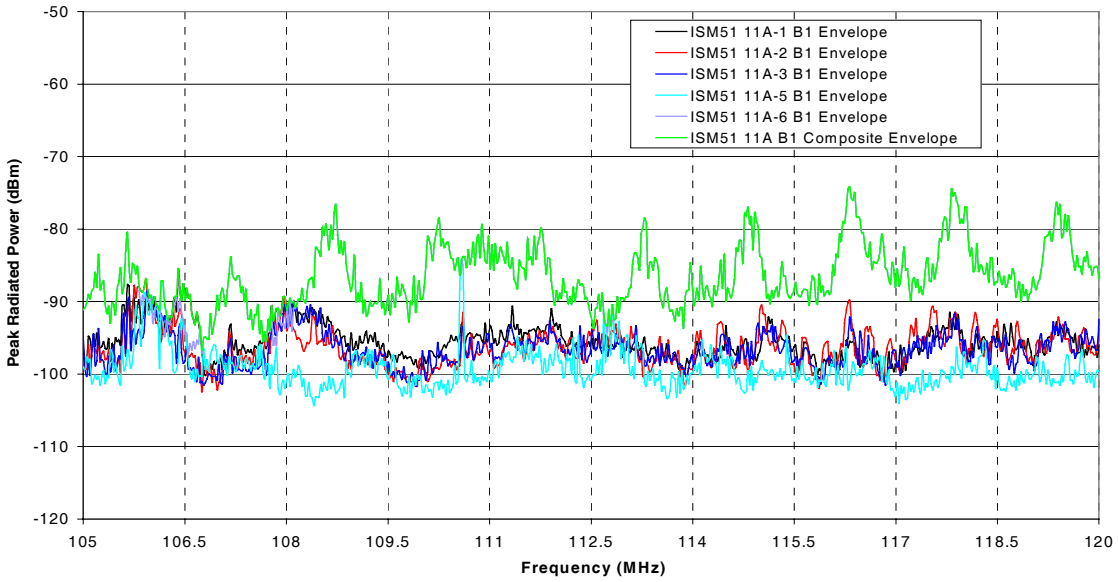

Figure 3.3-1: Individual 802.11a WLAN Device Envelopes and 802.11a WLAN Devices Composite Envelope for Band 1.

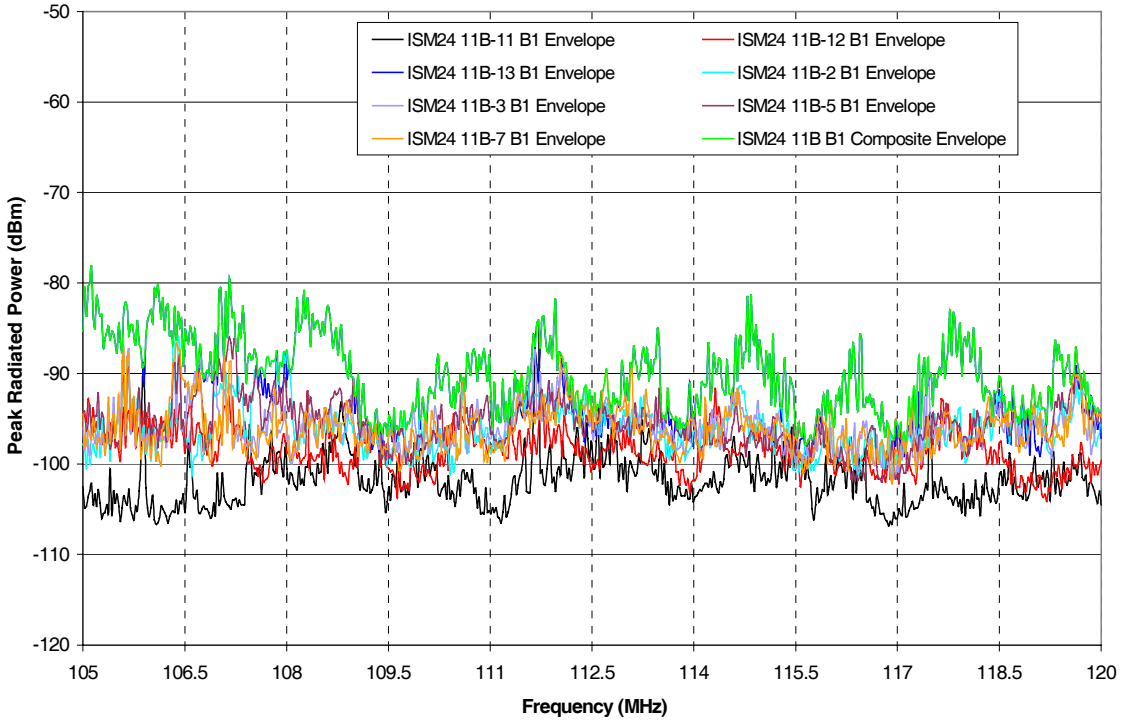

Figure 3.3-2: Individual 802.11b WLAN Device Envelopes and 802.11b WLAN Devices Composite Envelope for Band 1.

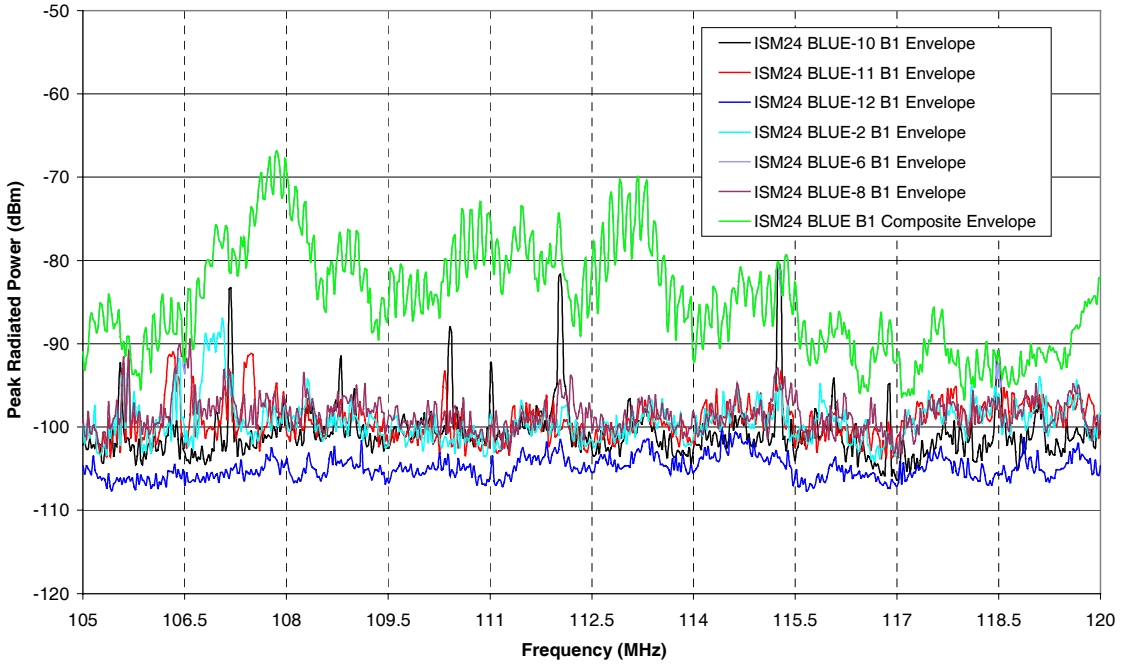

Figure 3.3-3: Individual Bluetooth WLAN Device Enelopes and Bluetooth WLAN Devices Composite Envelope for Band 1.

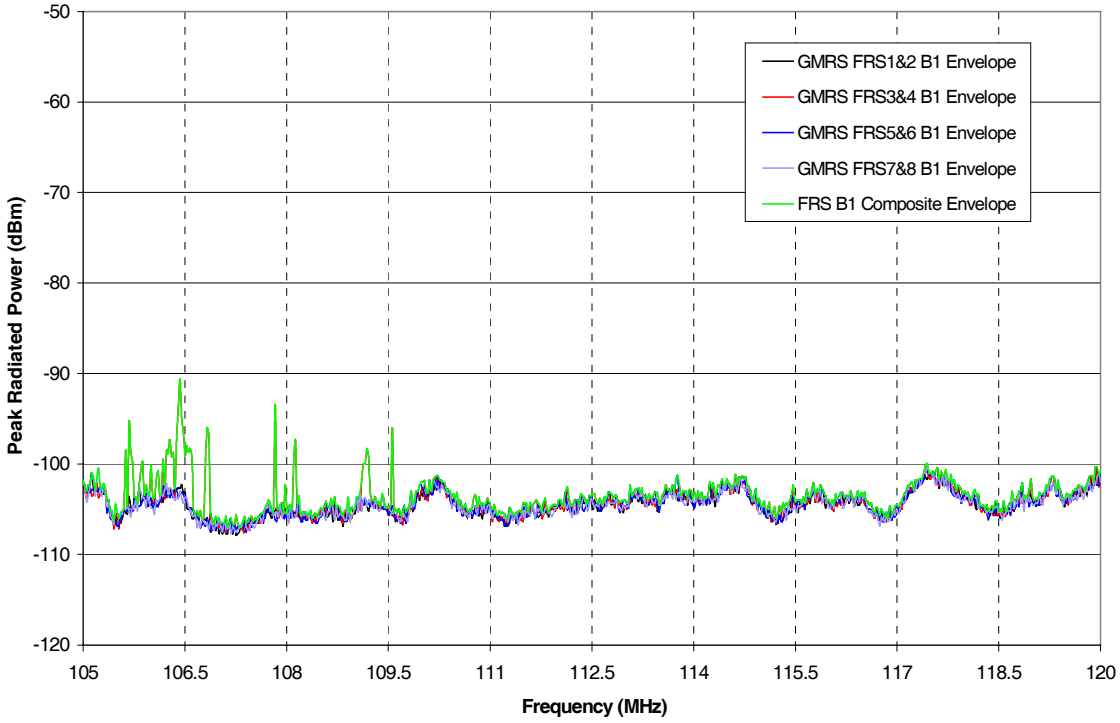

Figure 3.3-4: Individual FRS Radio Envelopes and All FRS Radios Composite Envelope for Band 1.

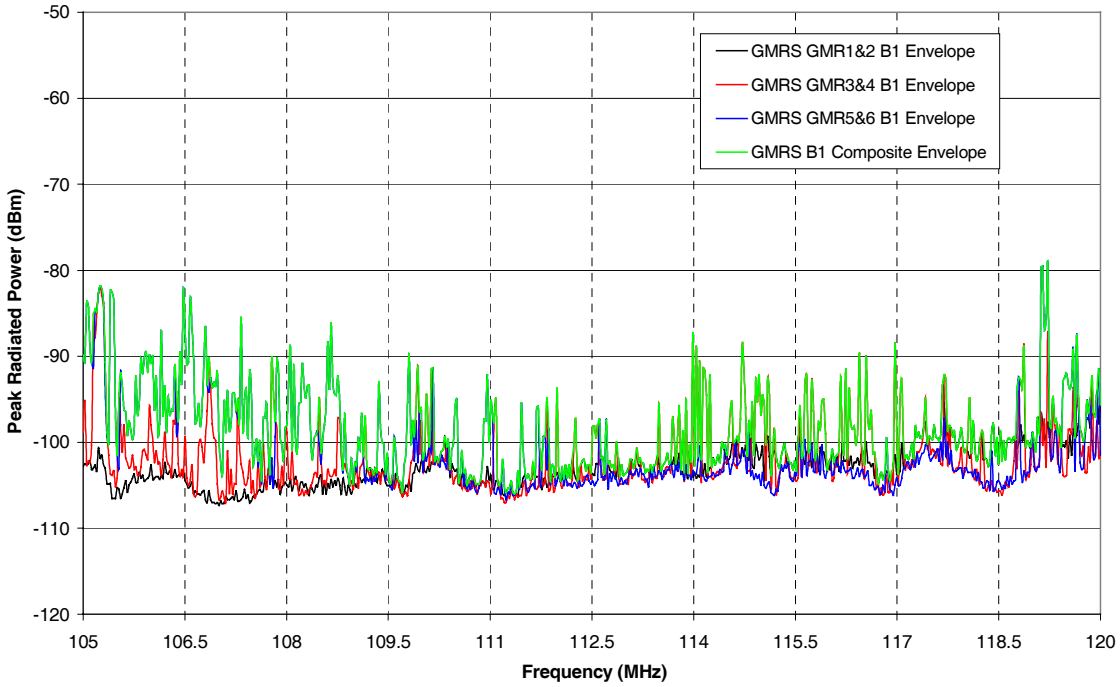

Figure 3.3-5: Individual GMRS Radio Envelopes and All GMRS Radios Composite Envelope for Band 1.

3.3.2 Band 2 (325 MHz to 340 MHz)

Data presented in Figures 3.3-6 to 3.3-10 were acquired in the aircraft systems frequency band assigned to ILS GS systems. Each figure plots envelopes for each individual WLAN device and an envelope representing all WLAN devices as related to each standard.

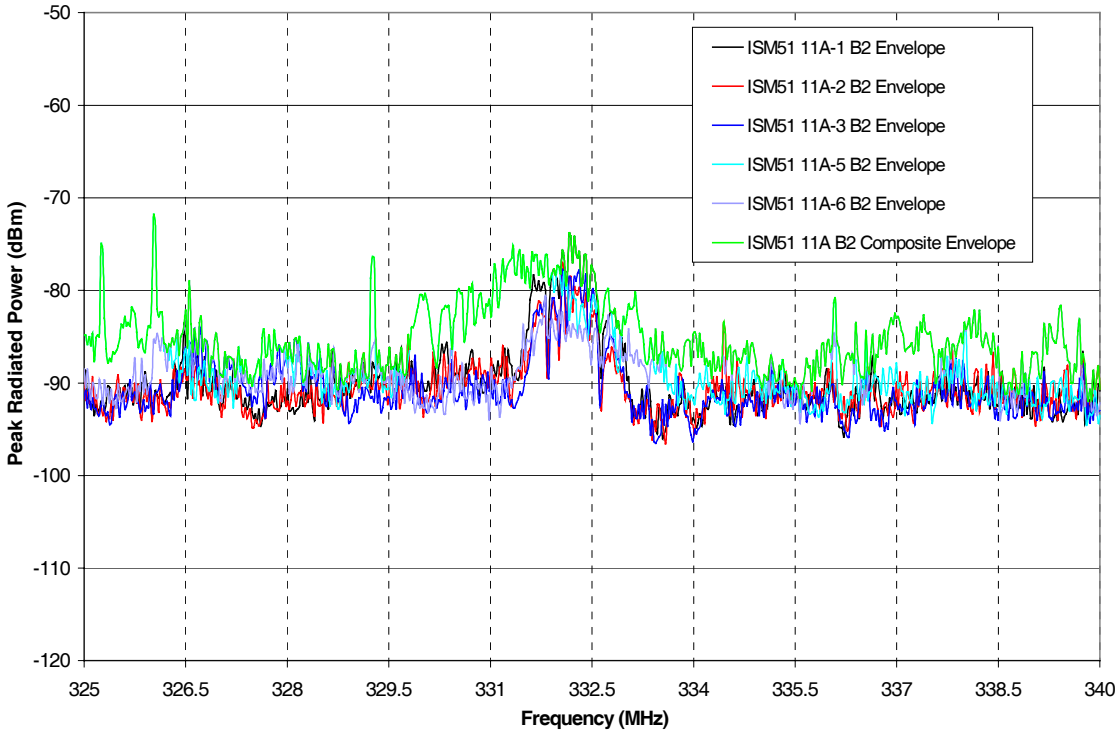

Figure 3.3-6: Individual 802.11a WLAN Device Envelopes and 802.11a WLAN Devices Composite Envelope for Band 2.

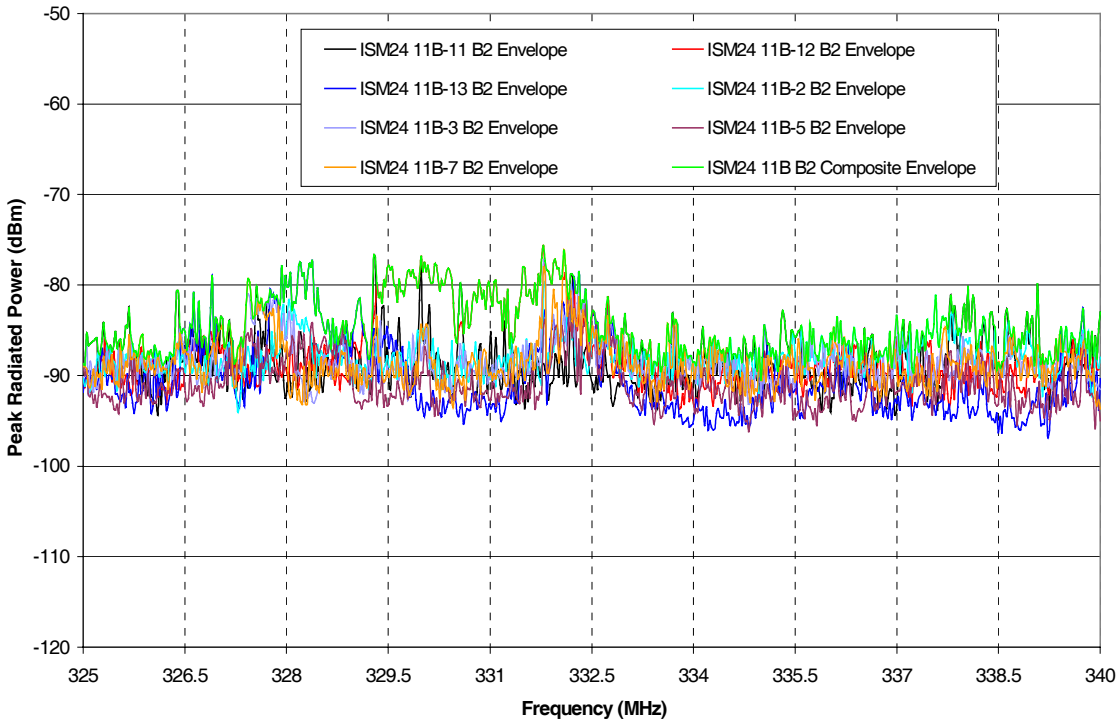

Figure 3.3-7: Individual 802.11b WLAN Device Envelopes and 802.11b WLAN Devices Composite Envelope for Band 2.

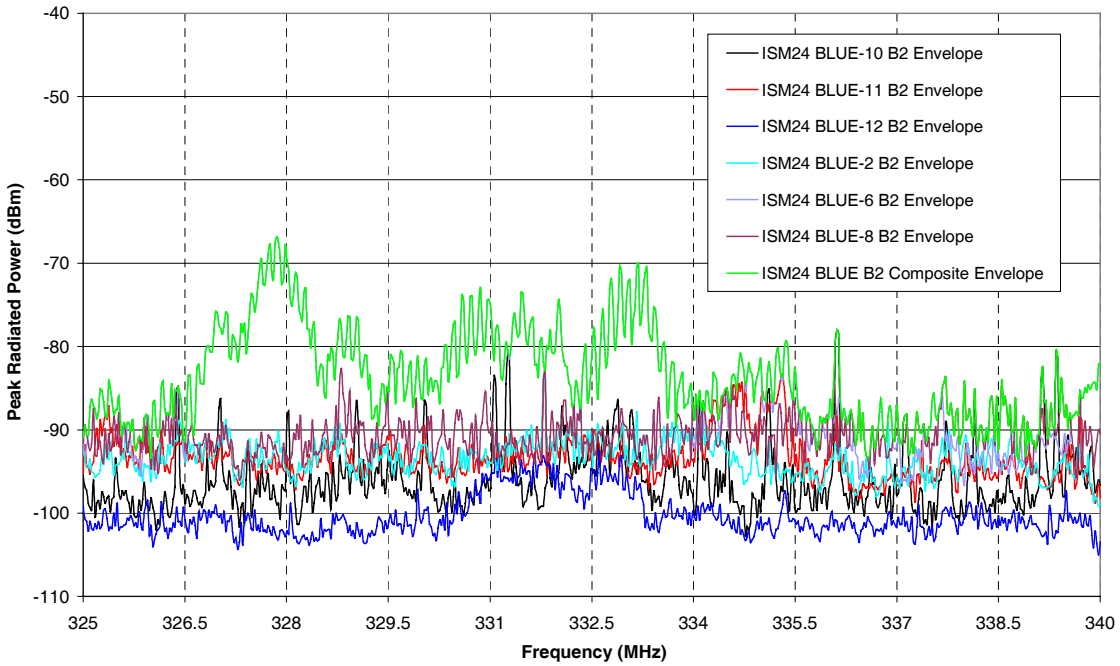

Figure 3.3-8: Individual Bluetooth WLAN Device Envelopes and Bluetooth WLAN Composite Devices Envelope for Band 2.

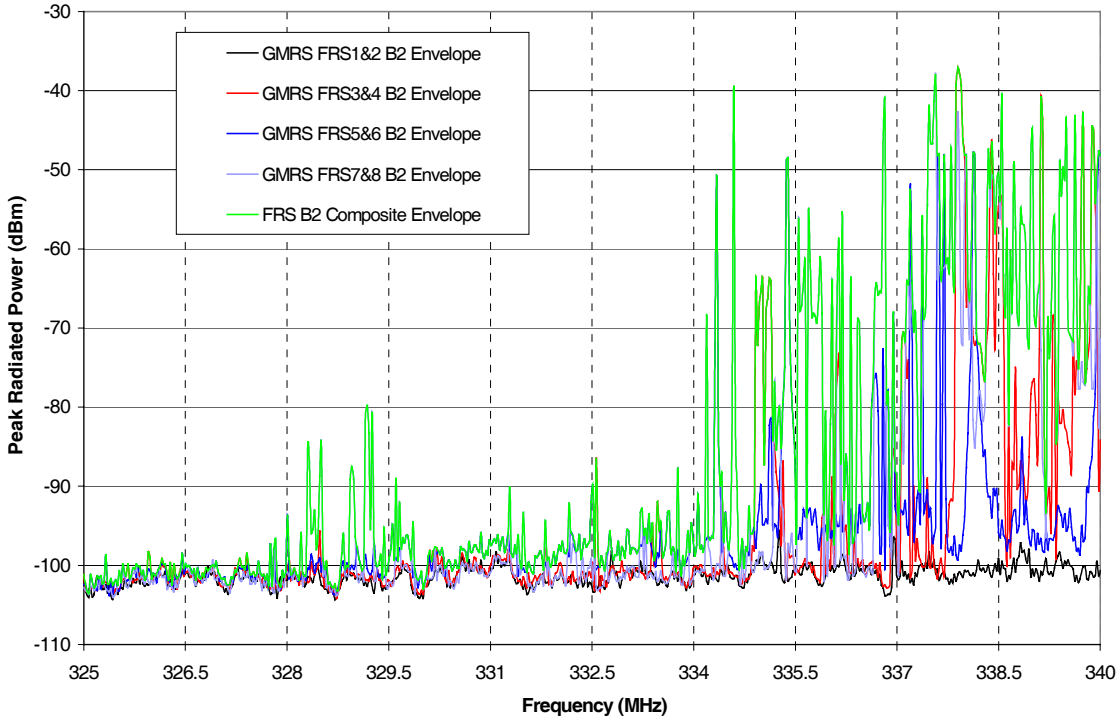

Figure 3.3-9: Individual FRS Radio Envelopes and FRS Radios Composite Envelope for Band 2.

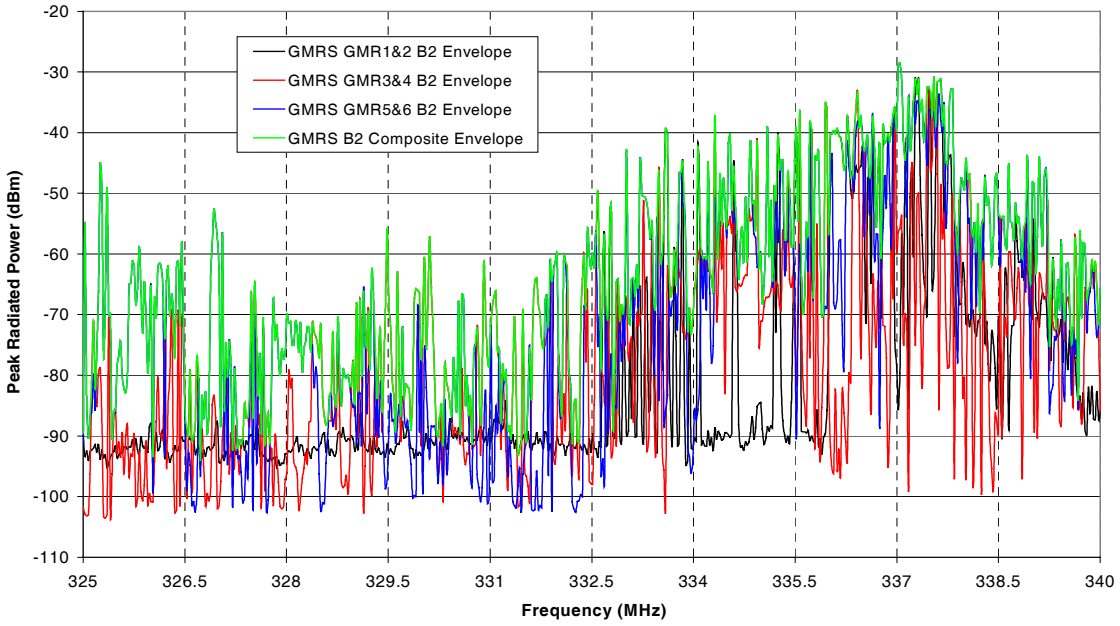

Figure 3.3-10: Individual GMRS Radio Envelopes and GMRS Radios Composite Envelope for Band 2.

3.3.3 Band 3 (960 MHz to 1250 MHz)

Data presented in Figures 3.3-11 to 3.3-15 were acquired in the aircraft systems frequency band assigned to DME, TCAS, ATCRBS, and GPS L2 systems. Each figure plots envelopes for each individual WLAN device and an envelope representing all WLAN devices as related to each standard.

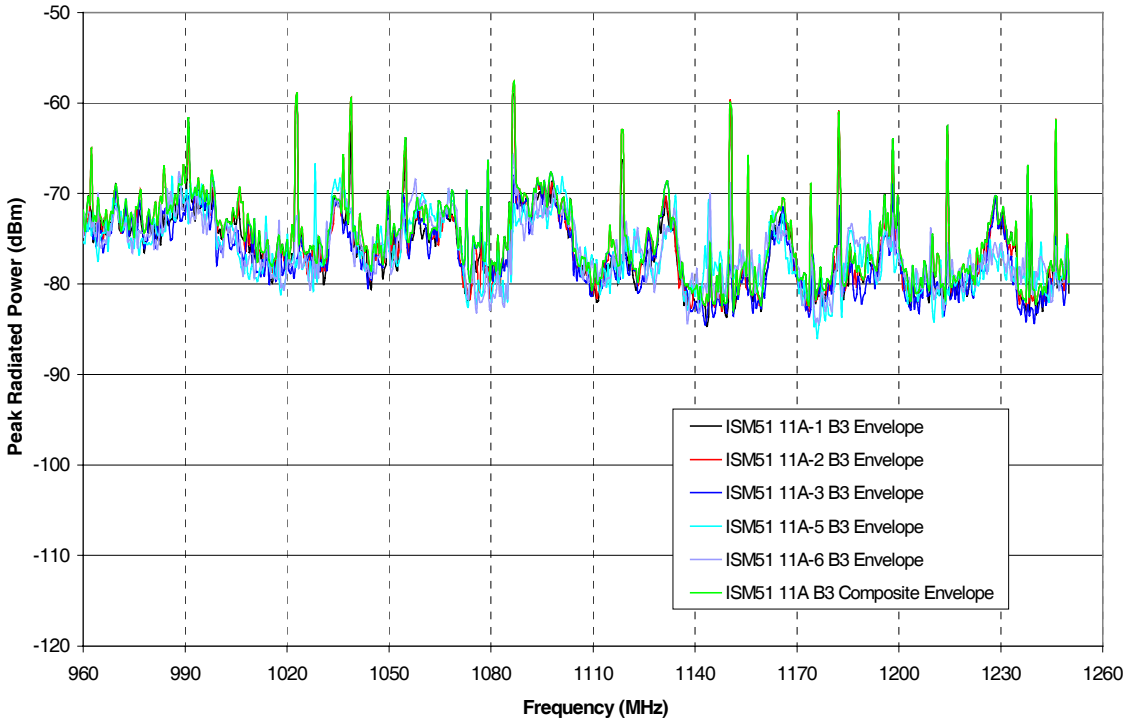

Figure 3.3-11: Individual 802.11a WLAN Device Envelopes and 802.11a WLAN Devices Composite Envelope for Band 3.

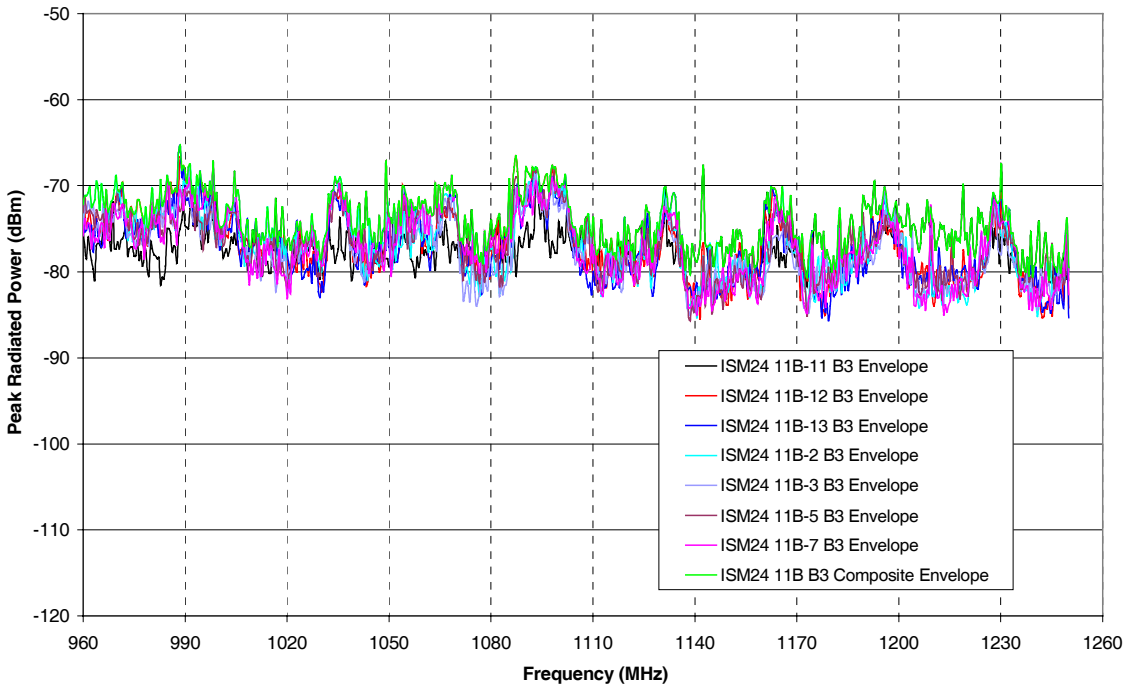

Figure 3.3-12: Individual 802.11b WLAN Device Envelopes and 802.11b WLAN Devices Composite Envelope for Band 3.

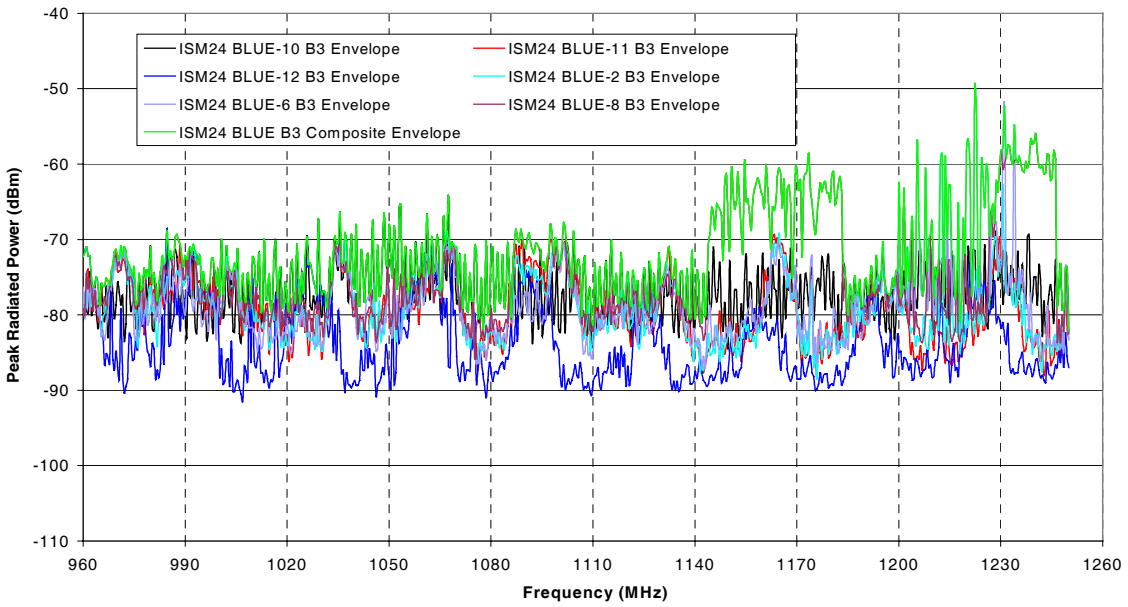

Figure 3.3-13: Individual Bluetooth WLAN Device Envelopes and Bluetooth WLAN Devices Composite Envelope for Band 3.

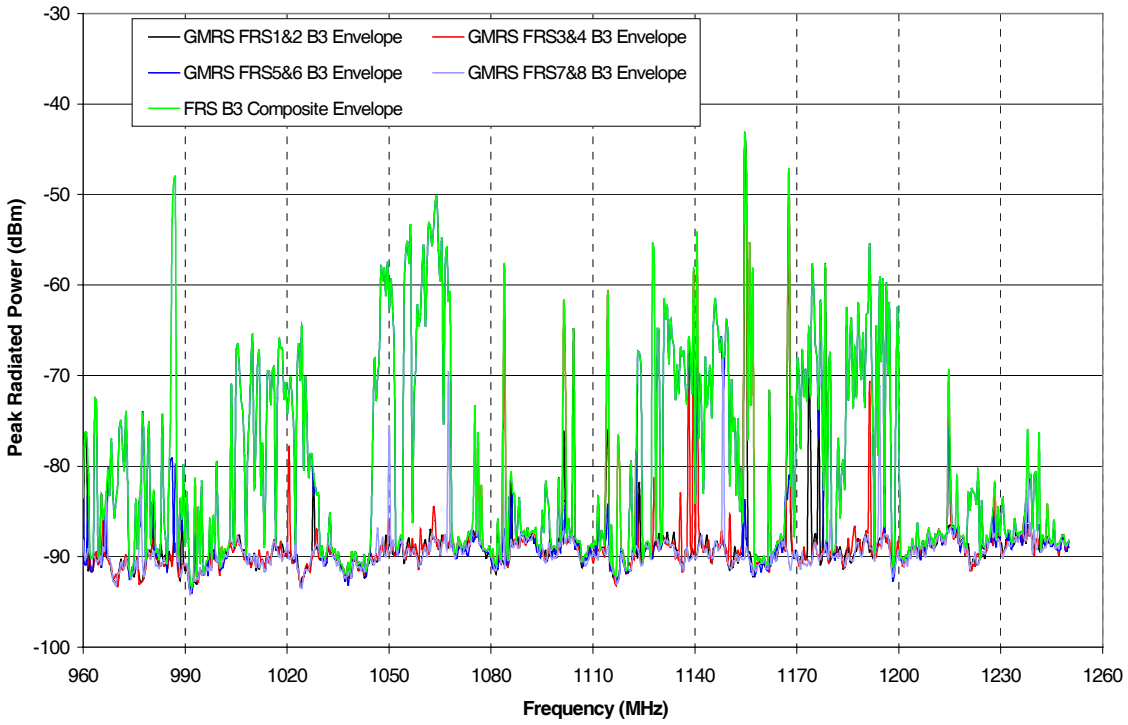

Figure 3.3-14: Individual FRS Radio Envelopes and FRS Radios Composite Envelope for Band 3.

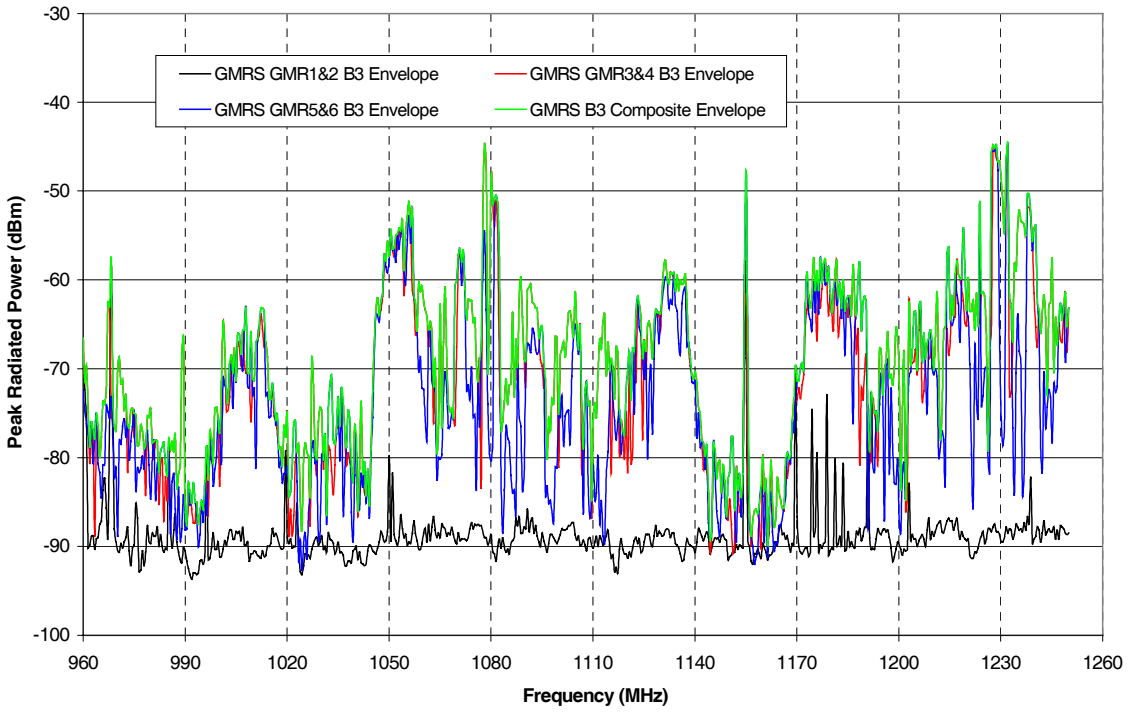

Figure 3.3-15: Individual GMRS Radio Envelopes and GMRS Radios Composite Envelope for Band 3.

3.3.4 Band 4 (1565 MHz to 1585 MHz)

Data presented in Figures 3.3-16 to 3.3-20 were acquired in the aircraft systems frequency band assigned to GPS L1 systems. Each figure plots envelopes for each individual WLAN device and an envelope representing all WLAN devices as related to each standard.

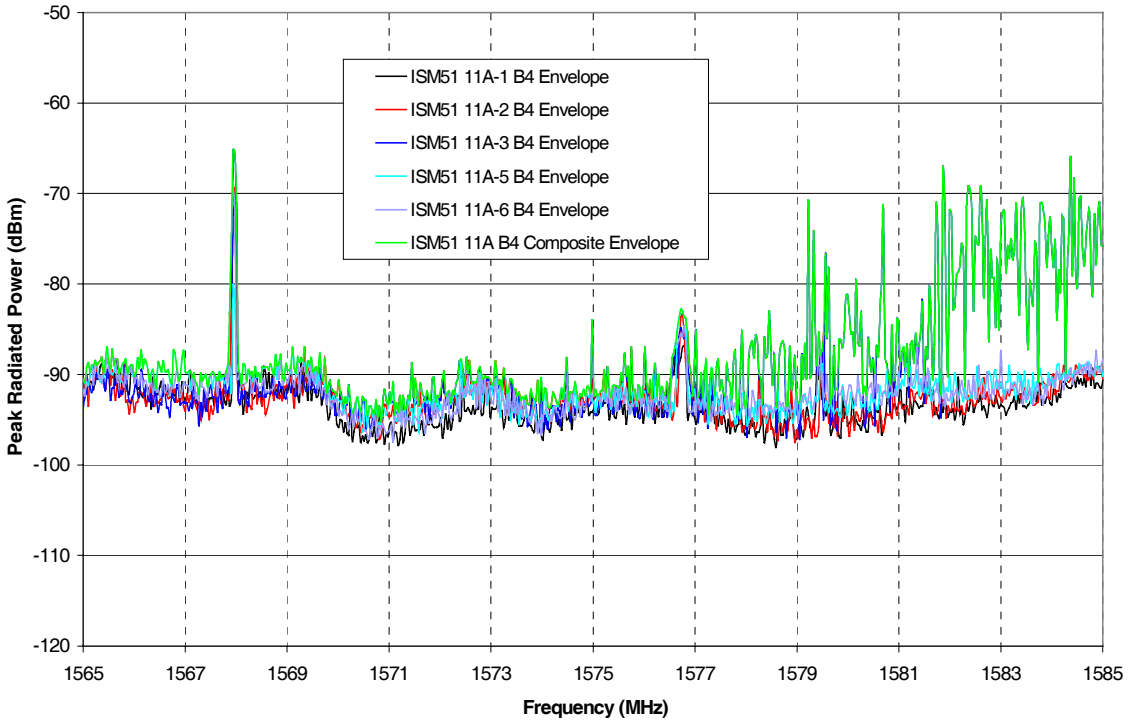

Figure 3.3-16: Individual 802.11a WLAN Device Envelopes and 802.11a WLAN Devices Composite Envelope for Band 4.

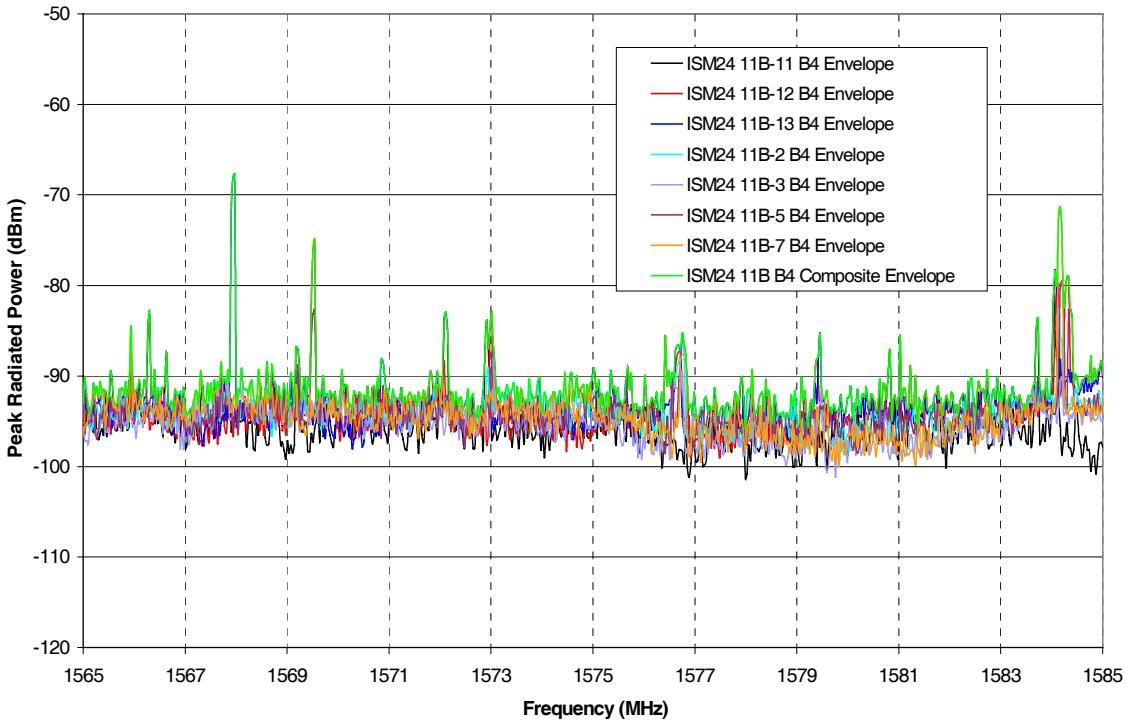

Figure 3.3-17: Individual 802.11b WLAN Device Envelopes and 802.11b WLAN Devices Composite Envelope for Band 4.

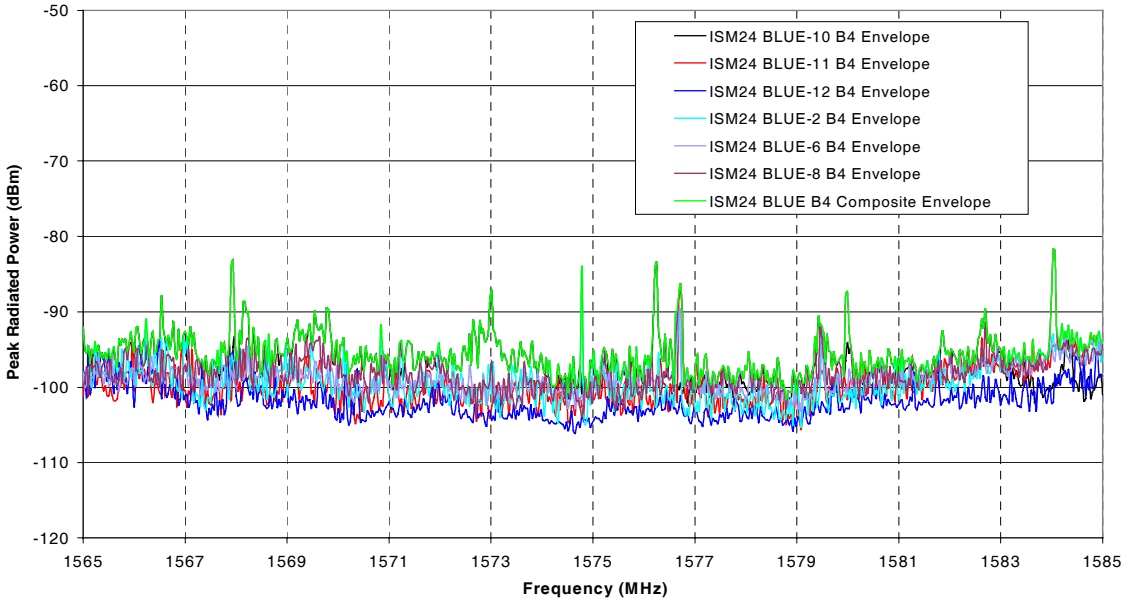

Figure 3.3-18: Individual Bluetooth WLAN Device Envelopes and Bluetooth WLAN Devices Composite Envelope for Band 4.

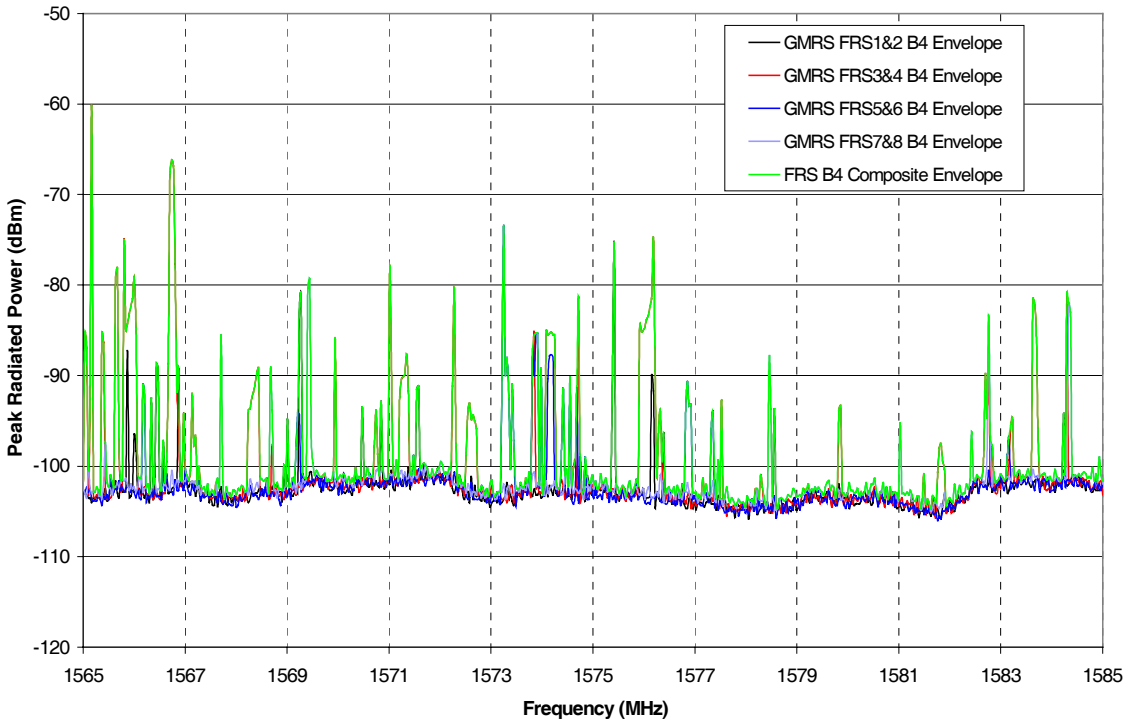

Figure 3.3-19: Individual FRS Radio Envelopes and FRS Radios Composite Envelope for Band 4.

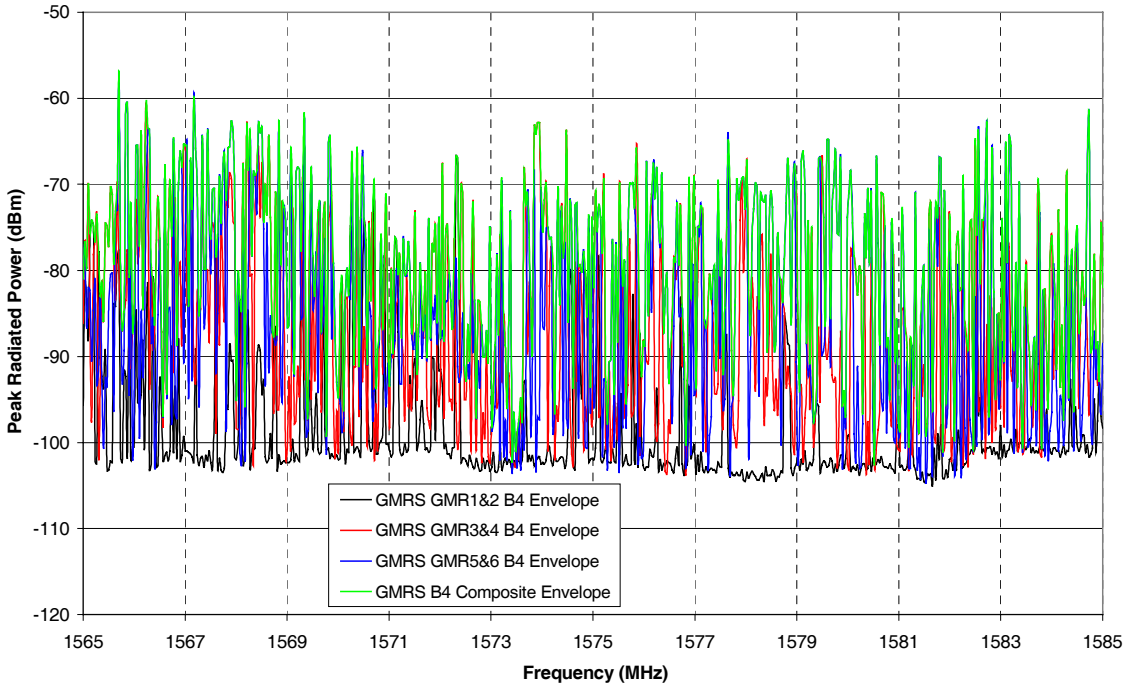

Figure 3.3-20: Individual GMRS Radio Envelopes and GMRS Radios Composite Envelope for Band 4.

3.3.5 Band 5 (5020 MHz to 5100 MHz)

Data presented in Figures 3.3-21 to 3.3-25 were acquired in the aircraft systems frequency band assigned to MLS systems. Each figure plots envelopes for each individual WLAN device and an envelope representing all WLAN devices as related to each standard.

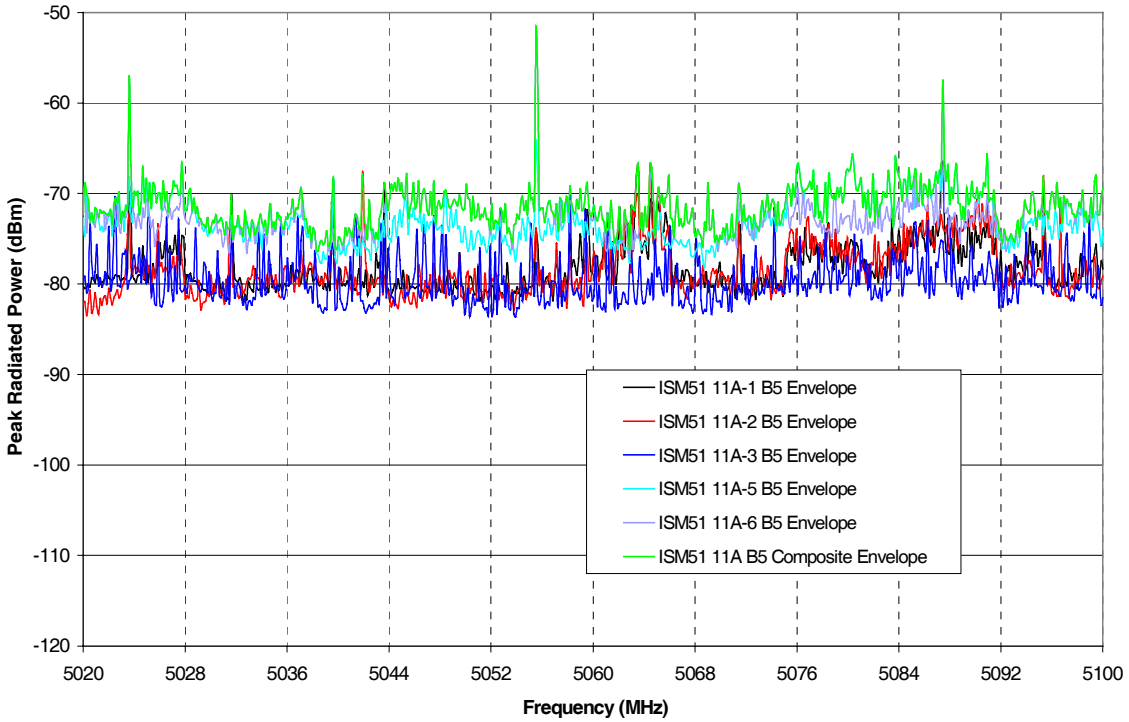

Figure 3.3-21: Individual 802.11a WLAN Device Envelopes and 802.11a WLAN Devices Composite Envelope for Band 5.

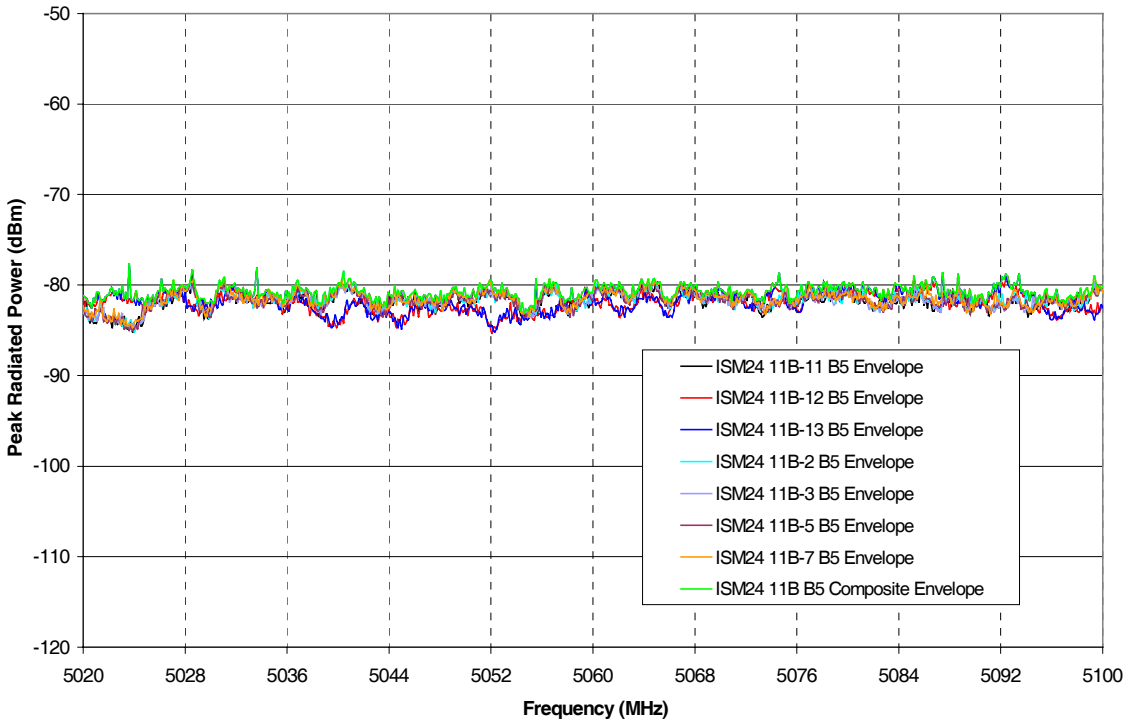

Figure 3.3-22: Individual 802.11b WLAN Device Envelope and 802.11b WLAN Devices Composite Envelope for Band 5.

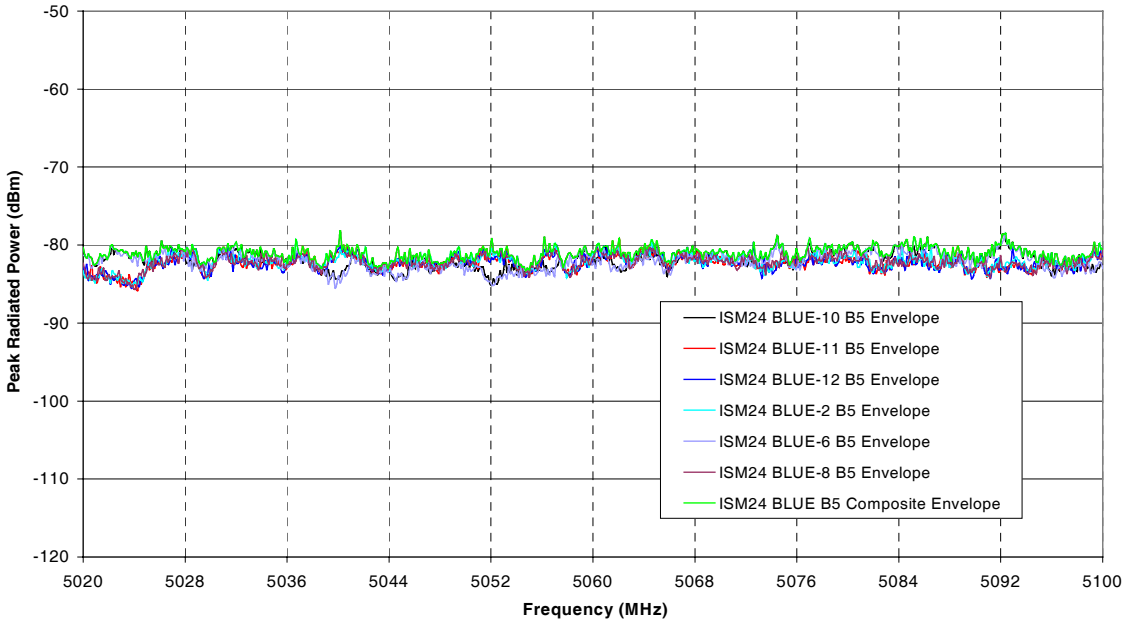

Figure 3.3-23: Individual Bluetooth WLAN Device Envelopes and Bluetooth WLAN Devices Composite Envelope for Band 5.

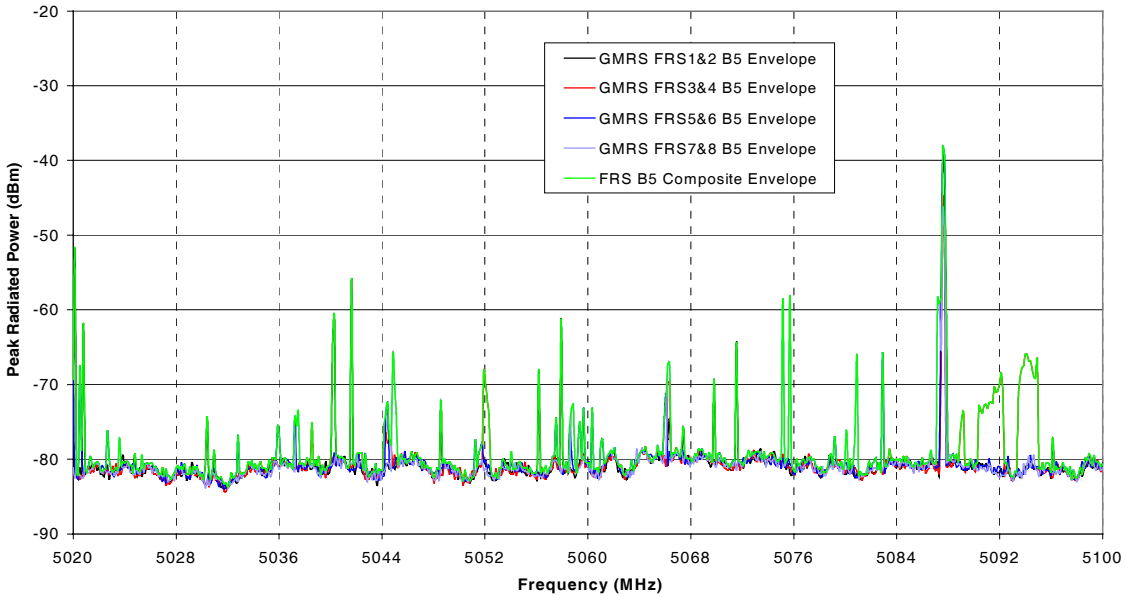

Figure 3.3-24: Individual FRS Radio Envelopes and FRS Radios Composite Envelope for Band 5.

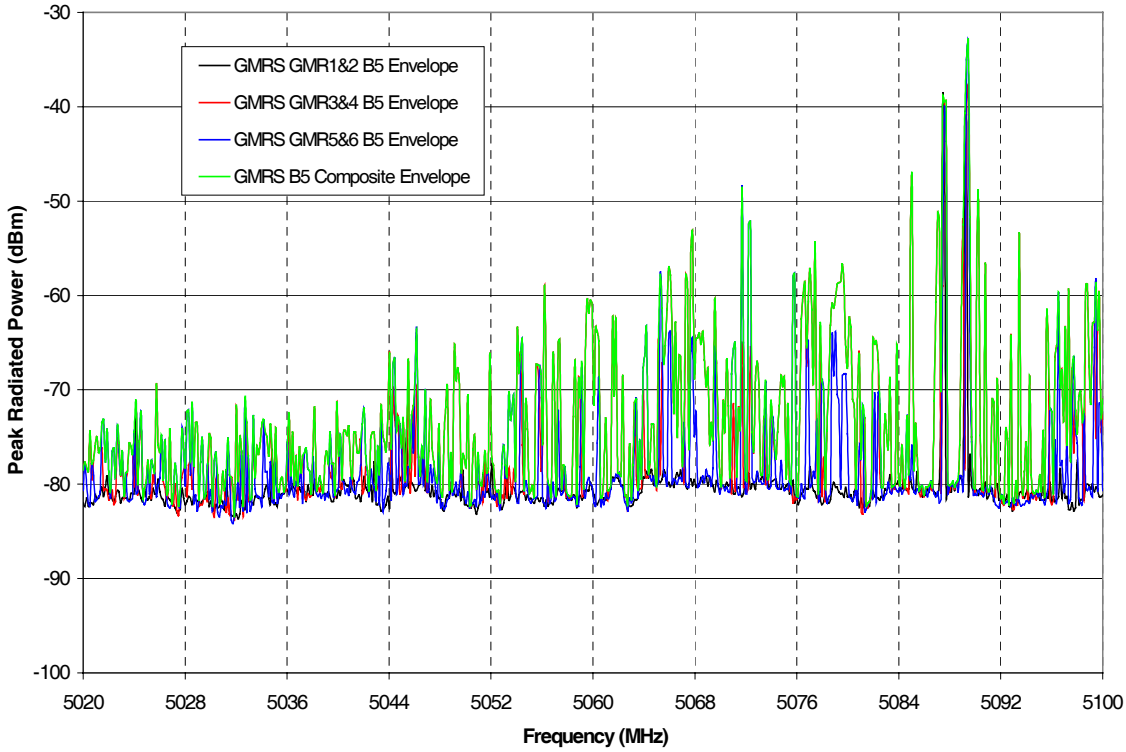

Figure 3.3-25: Individual GMRS Radio Envelopes and GMRS Radios Composite Envelope for Band 5.

3.4 Summary of Emission From Standard Laptops and PDAs

This section describes the results from the radiated emission tests conducted on laptop computers and PDAs. The following charts illustrate the PED data envelopes organized by measurement frequency bands. Charts are labeled with the appropriate frequency bands and include the reduced data acquired during radiated emissions testing using PEDs, such as laptop computers, PDAs and a printer. Noise floor data are plotted on charts in Appendix A that illustrate individual PED data in each test mode. Each chart contains plots of individual PED envelopes, and a composite envelope that includes all PEDs. In addition to the PEDs selected as hosts during WLAN emission testing, the PED envelopes presented here include all PEDs tested. The individual PED's designations are listed in the chart legends. Individual PED envelopes were generated from measured emissions data, including idle mode and all other PED test modes. The PEDs composite envelope is the maximum at each frequency of all the individual PED envelopes. Note that the PEDs composite envelopes are plotted in red. A description of the processes used for the reduction of data and the generation of envelopes is found in Section 3.2.4. Envelope plots that include all PEDs are also used in charts in Section 3.5.

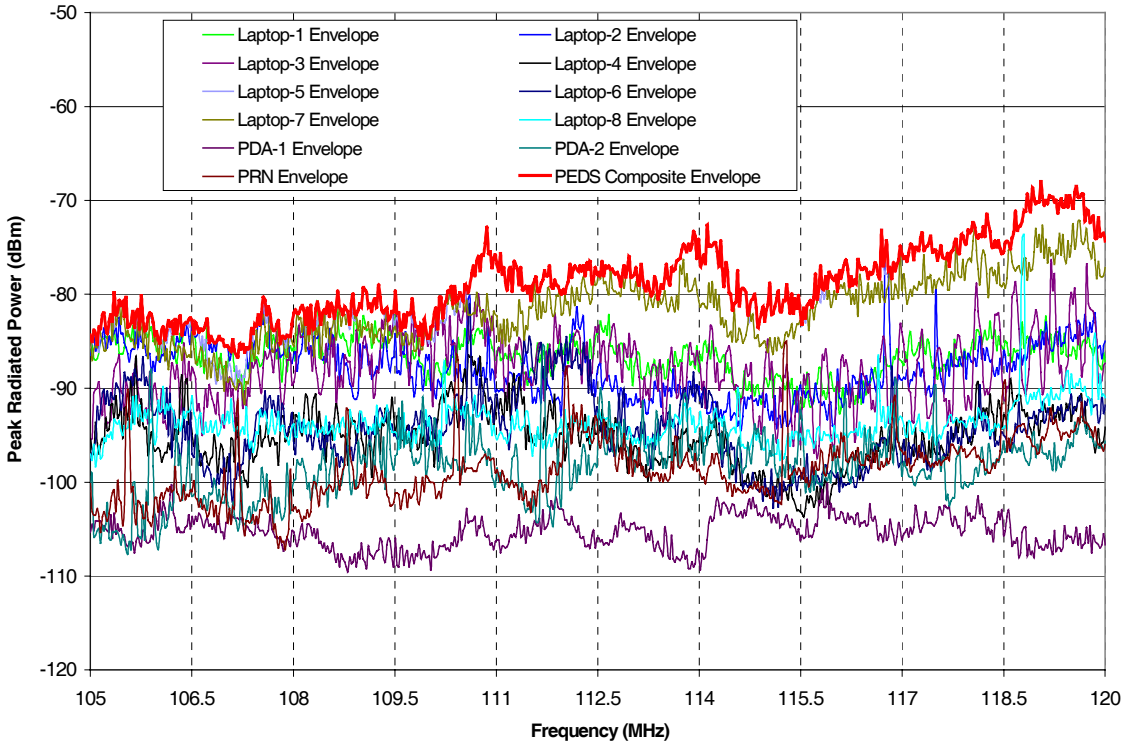

Figure 3.4-1: Individual PED Envelopes and PEDS Composite Envelope for Band 1 (105 MHz to 120 MHz).

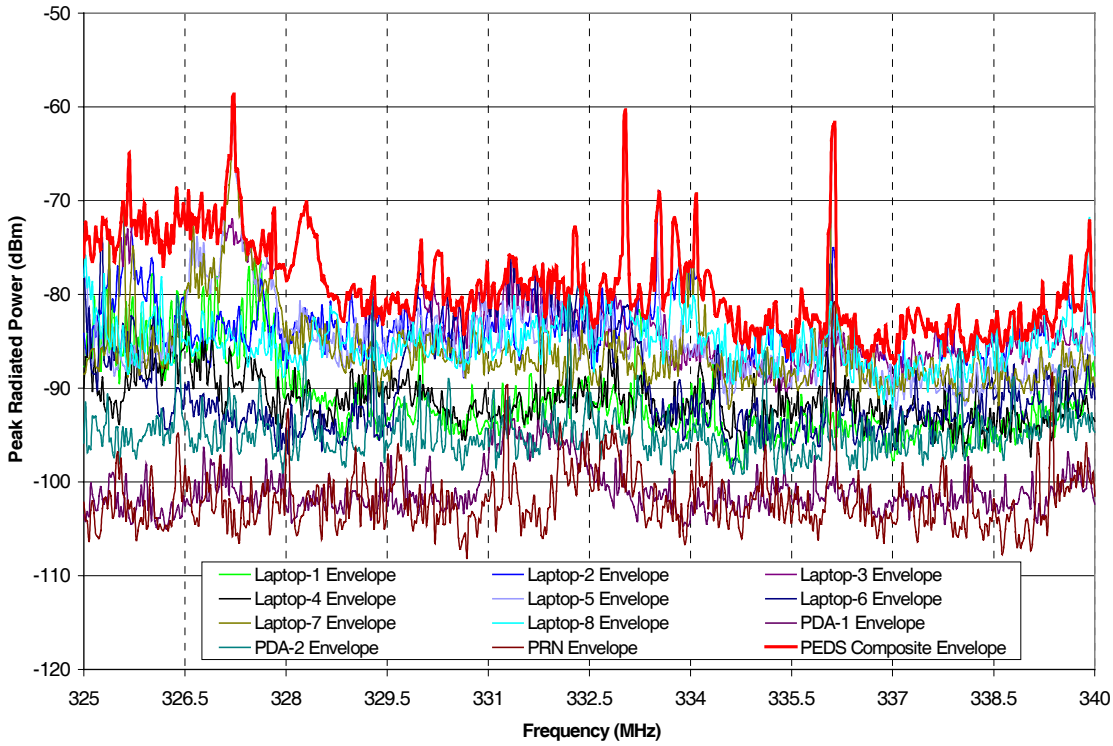

Figure 3.4-2: Individual PED Envelopes and PEDS Composite Envelope for Band 2 (325 MHz to 340 MHz).

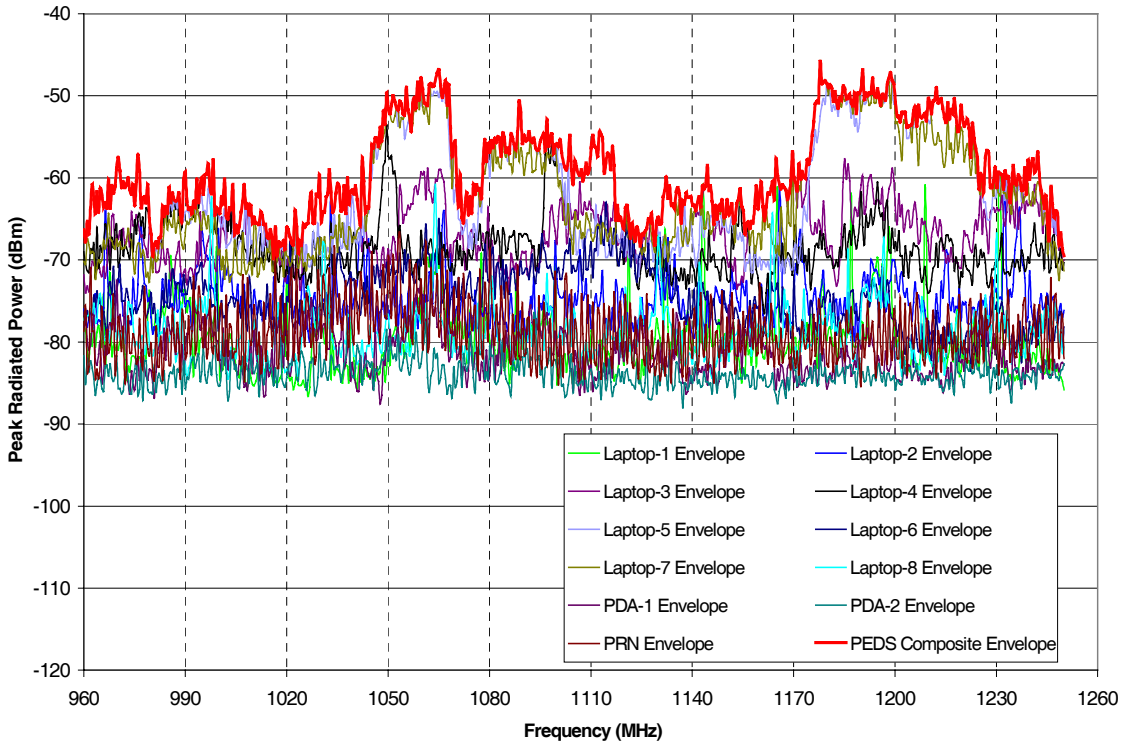

Figure 3.4-3: Individual PED Envelopes and PEDS Composite Envelope for Band 3 (960 MHz to 1250 MHz).

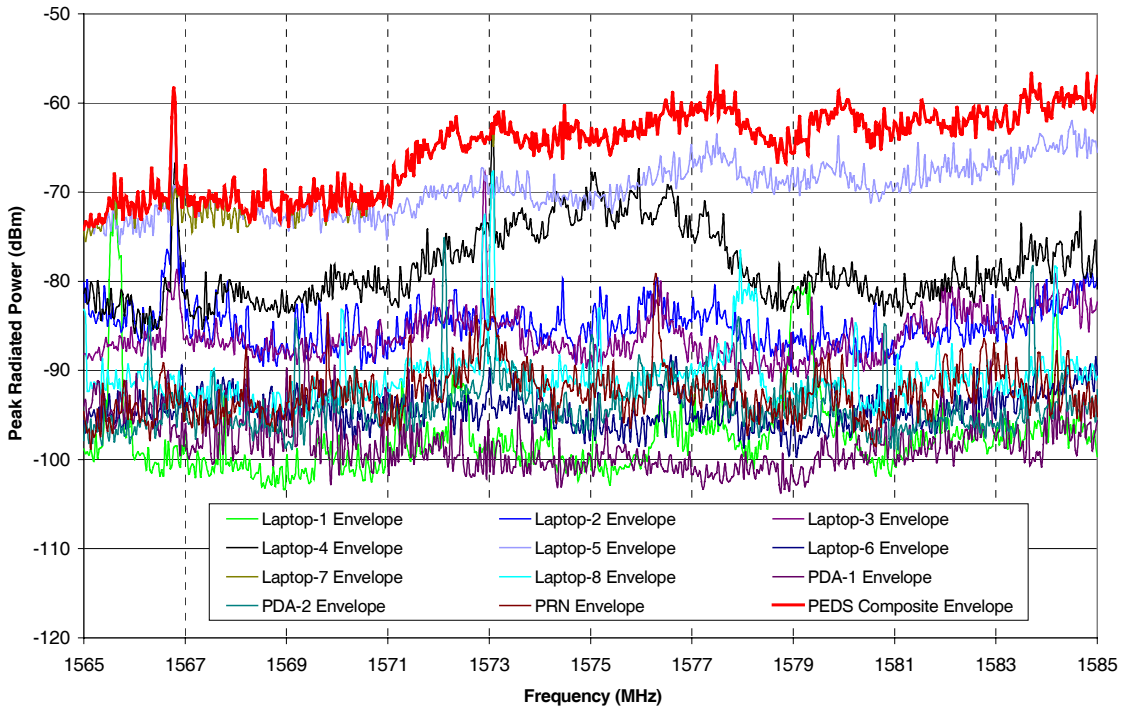

Figure 3.4-4: Individual PED Envelopes and PEDS Composite Envelope for Band 4 (1565 MHz to 1585 MHz).

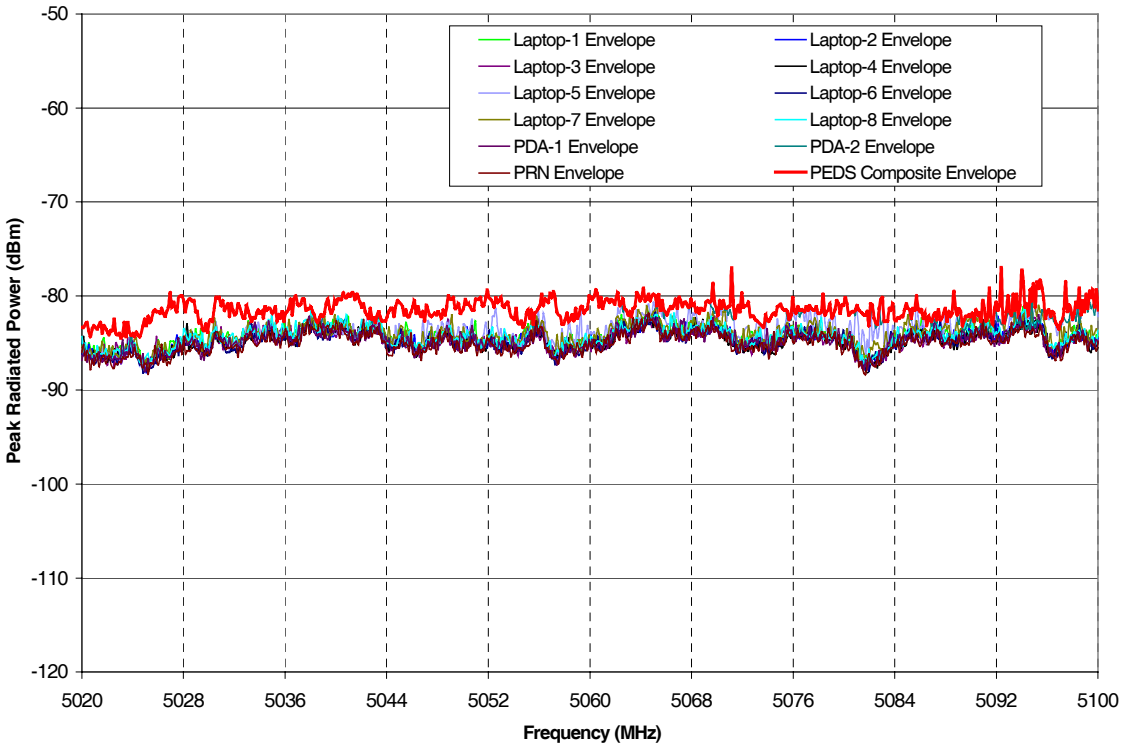

Figure 3.4-5: Individual PED Envelopes and PEDS Composite Envelope for Band 5 (5020 MHz to 5100 MHz).

3.5 Comparison of Emissions From Intentionally- and Unintentionally-Transmitting PEDs

The following charts illustrate envelopes that include data from all unintentionally-transmitting PEDs, and all intentionally-transmitting 802.11a, 802.11b, and Bluetooth WLAN devices organized by measurement frequency bands. Sections are labeled with the appropriate frequency bands and include five charts of reduced data produced from data acquired during radiated emissions testing of PEDs and WLAN devices. Three charts in each section contain a plot of a PED composite envelope that includes all PEDs, and a WLAN composite envelope that includes all WLAN devices. Noise floor data are plotted on charts in Appendices A and B that include data on individual WLAN devices and individual PED devices in each test mode. The generation of PED envelopes is described in Section 3.4. Note that the PED composite envelopes are plotted in red. The reduction of the WLAN device data to a WLAN composite envelope is defined in Section 3.3. The WLAN composite envelope plots are presented here in green. The envelopes for data acquired during emissions testing of FRS and GMRS radios are included in two of the five charts for each frequency band. A description of the processes used for the reduction of data and the generation of envelopes is found in Section 3.2.4.

In general, the data presented in the PED envelope and WLAN device envelope comparison charts indicate that radiated emissions from WLAN devices are not higher than PED emissions. One exception occurs in Figure 3.5-21 that illustrates Band 5 (5020 MHz to 5100 MHz), having the WLAN envelope higher than the PED envelope. Since the transmission frequency of 5.4 GHz for 802.11a devices is relatively close to frequency Band 5, this difference is expected.

Note that in Bands 2, 3, 4, and 5, the FRS and GMRS radio emissions are significantly higher than any of the tested WLAN devices. In Bands 2 and 5, the radio emissions are higher than all the PEDs.

3.5.1 Band 1 (105 MHz to 120 MHz)

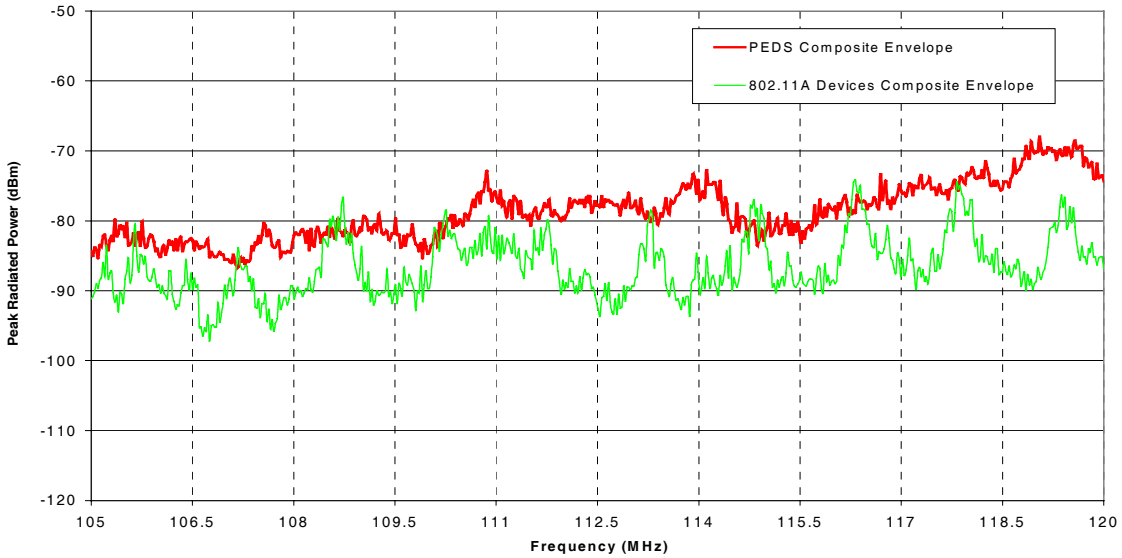

Figure 3.5-1: 802.11a Composite WLAN Devices Envelope and PEDs Composite Envelope for Band 1.

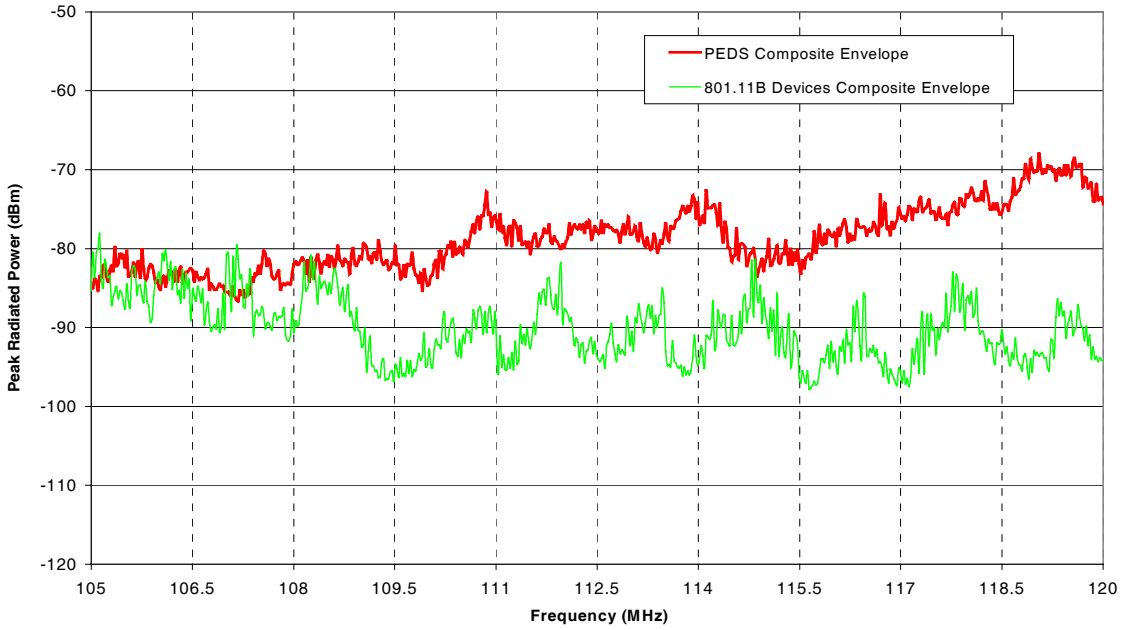

Figure 3.5-2: 802.11b Composite WLAN Devices Envelope and PEDs Composite Envelope for Band 1.

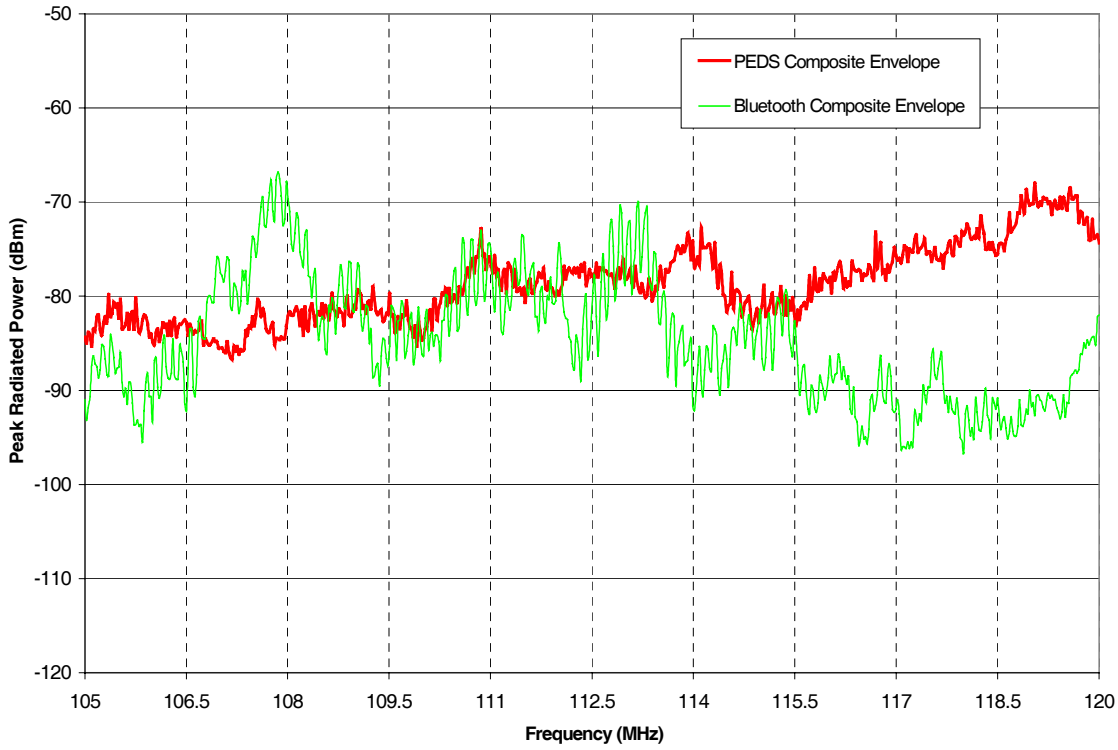

Figure 3.5-3: Bluetooth WLAN Devices Composite Envelope and PEDs Composite Envelope for Band 1.

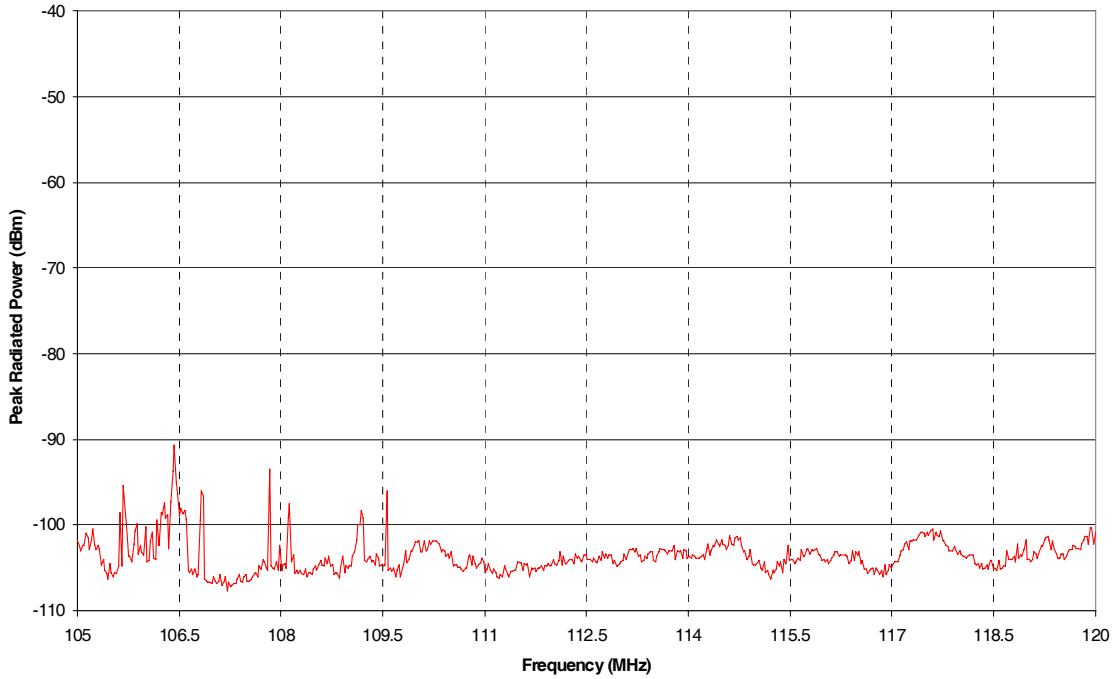

Figure 3.5-4: FRS Radios Composite Envelope for Band 1.

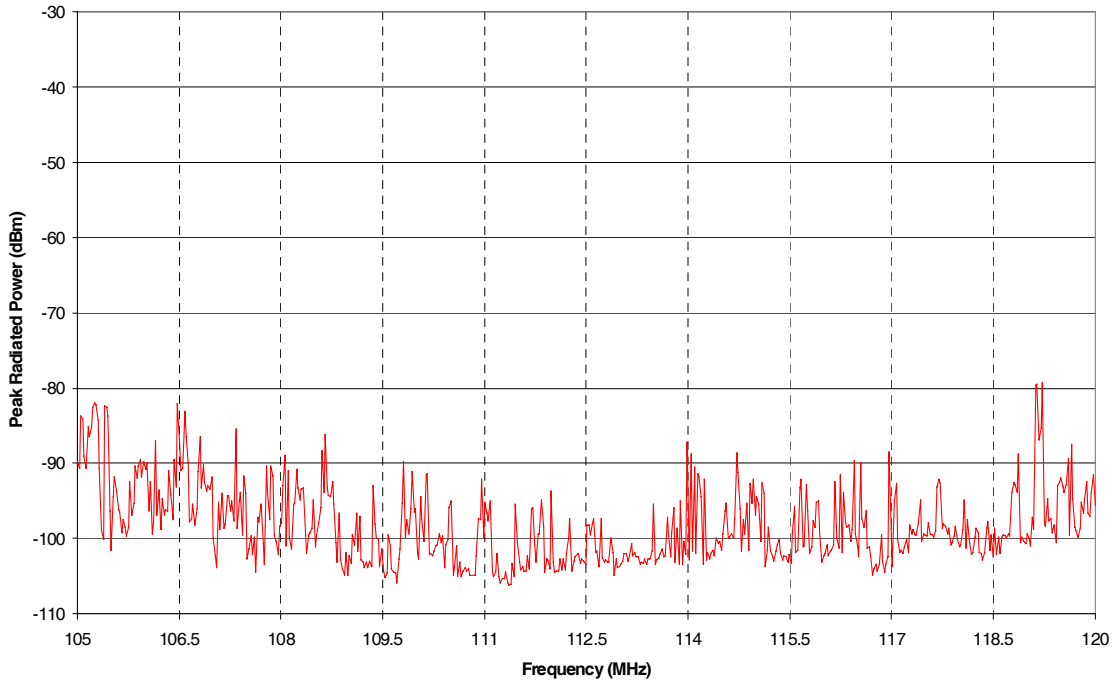

Figure 3.5-5: GMRS Radios Composite Envelope for Band 1.

3.5.2 Band 2 (325 MHz to 340 MHz)

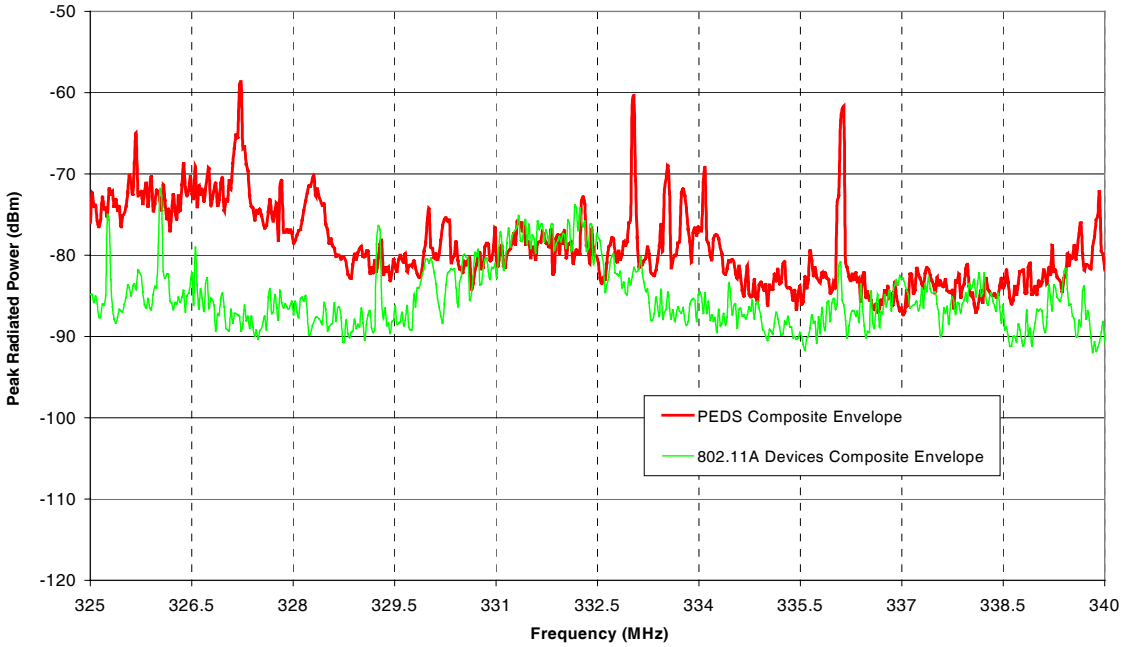

Figure 3.5-6: 802.11a WLAN Devices Composite Envelope and PEDs Composite Envelope for Band 2.

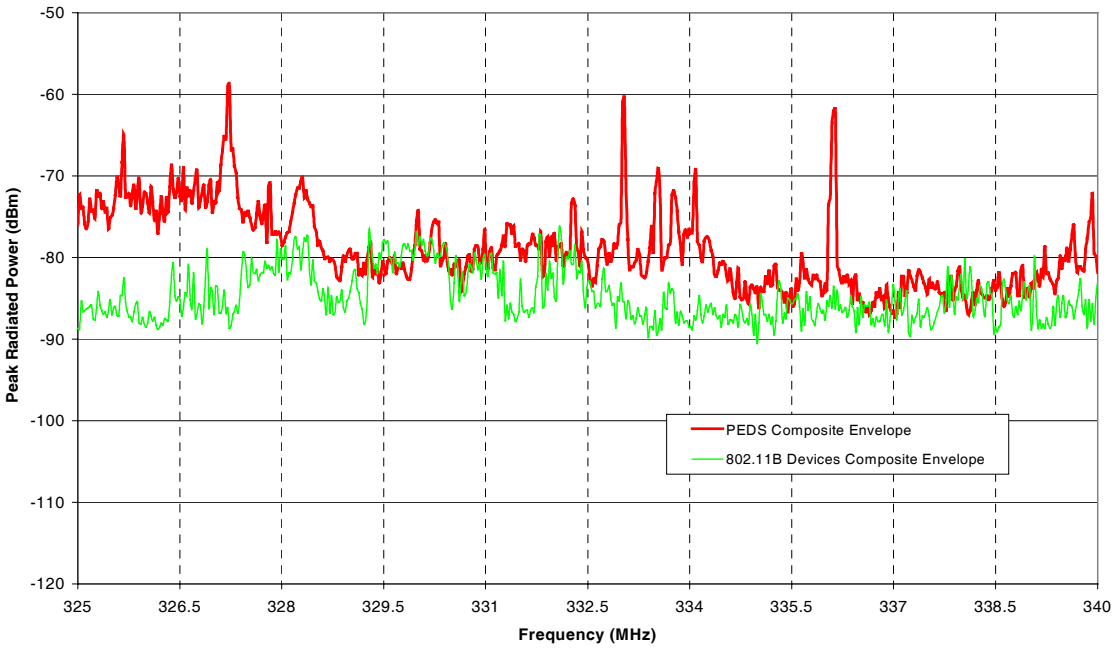

Figure 3.5-7: 802.11b WLAN Devices Composite Envelope and PEDs Composite Envelope for Band 2.

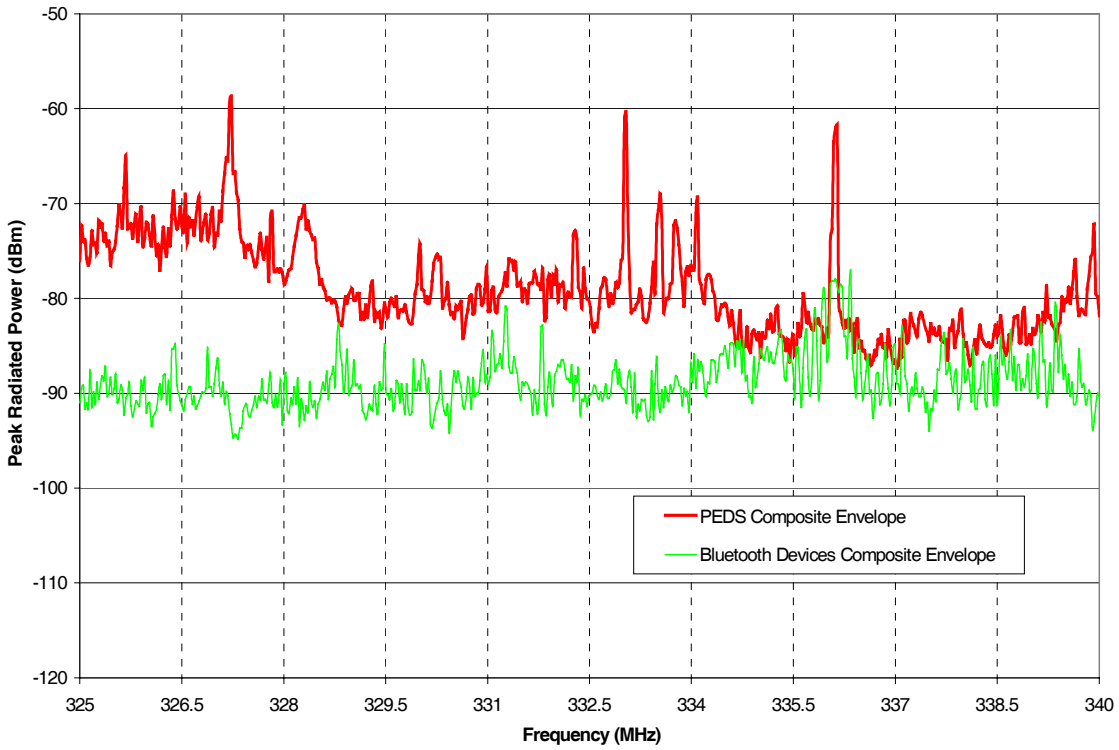

Figure 3.5-8: Bluetooth WLAN Devices Composite Envelope and PEDs Composite Envelope for Band 2.

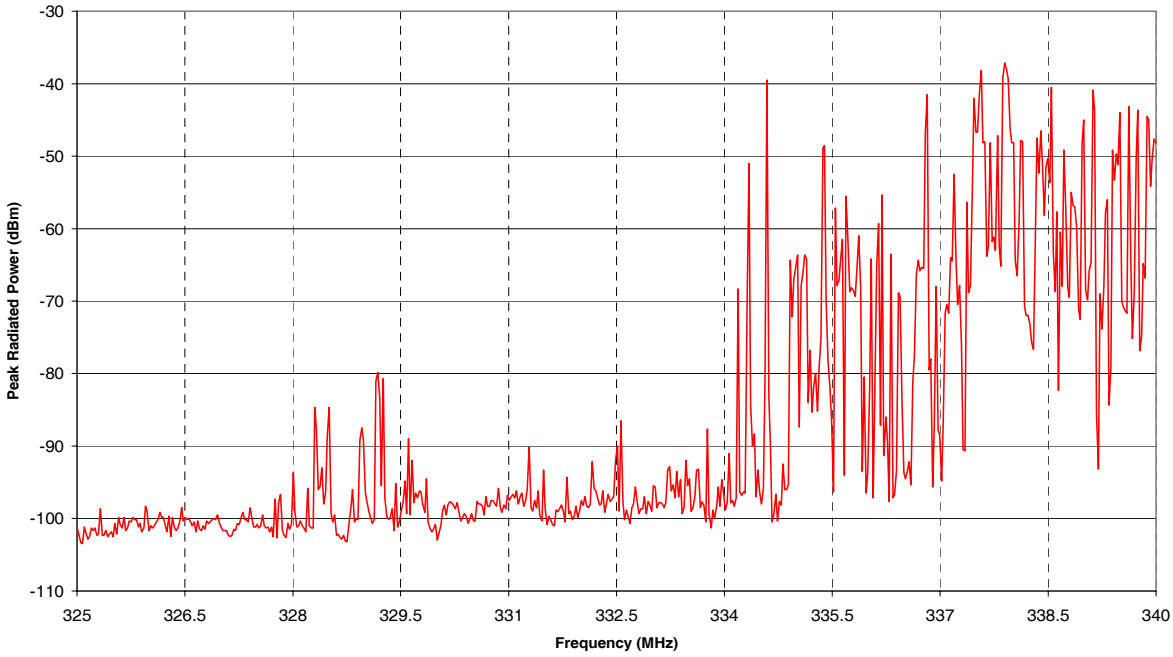

Figure 3.5-9: FRS Radios Composite Envelope for Band 2.

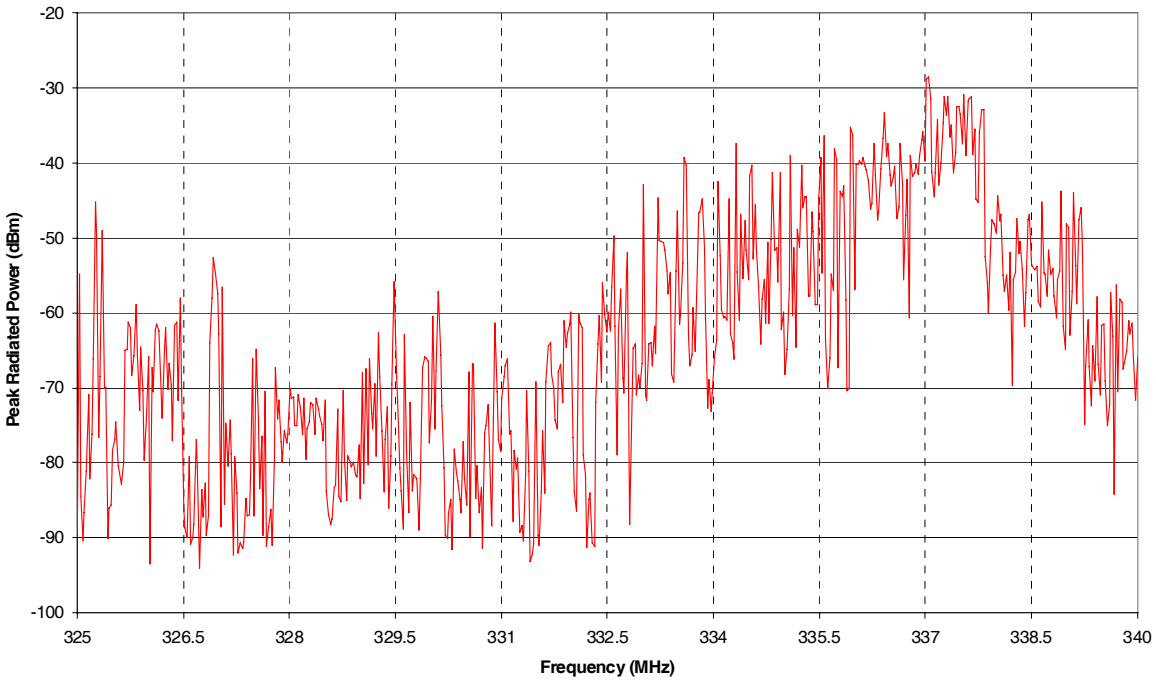

Figure 3.5-10: GMRS Radios Composite Envelope for Band 2.

3.5.3 Band 3 (960 MHz to 1250 MHz)

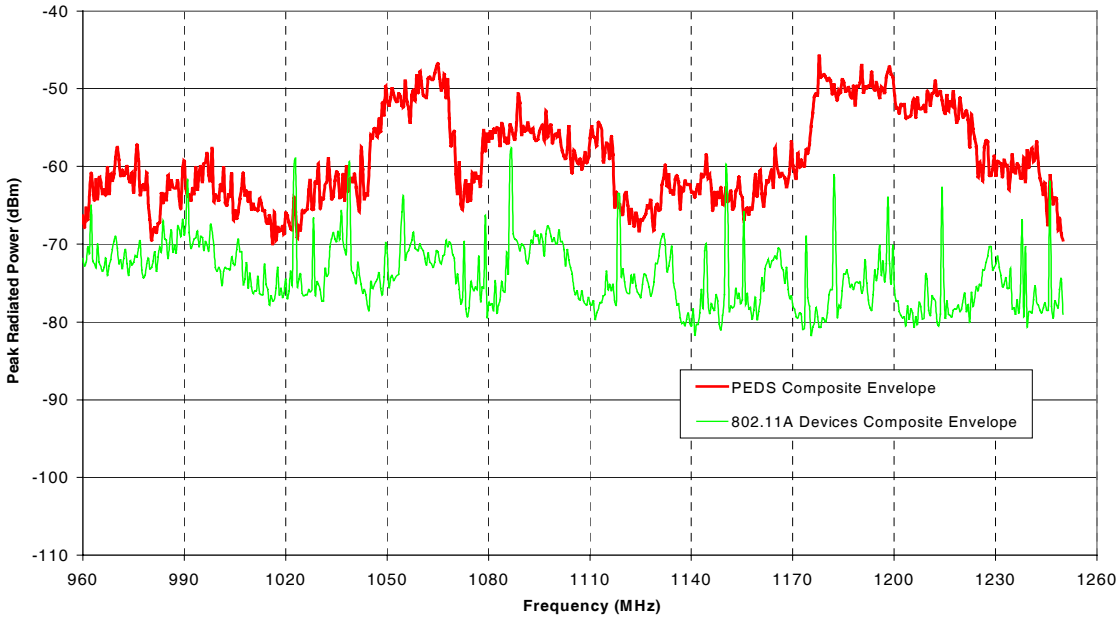

Figure 3.5-11: 802.11a WLAN Devices Composite Envelope and PEDs Composite Envelope for Band 3.

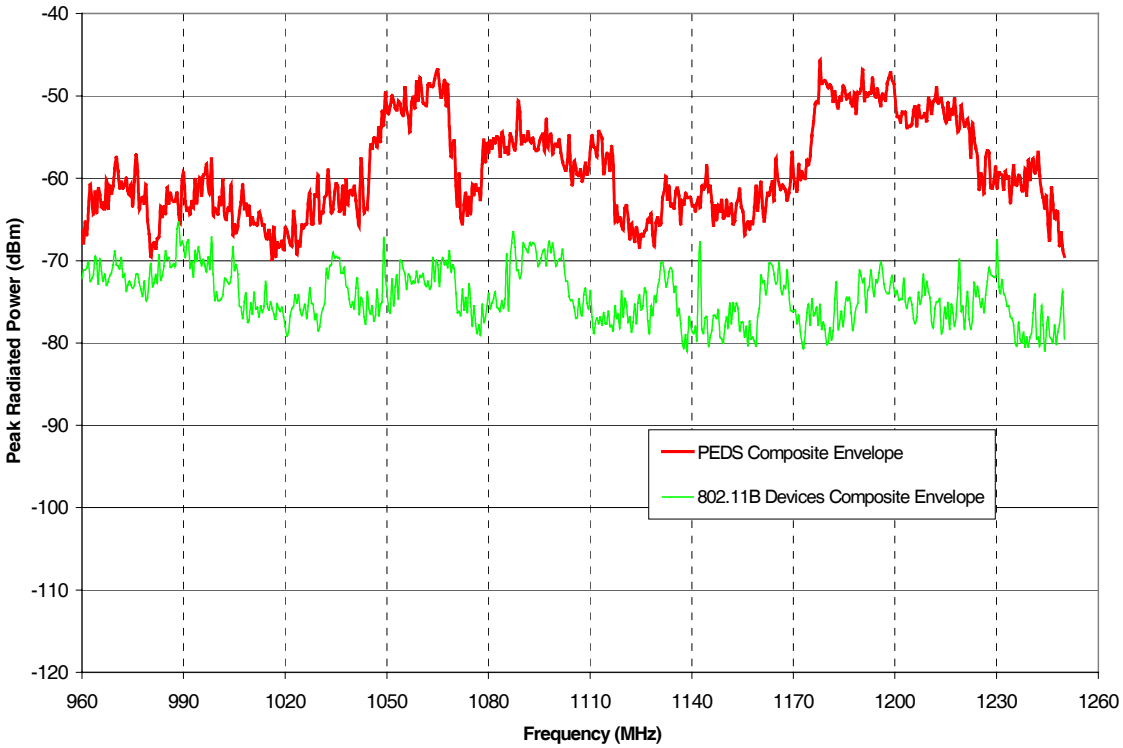

Figure 3.5-12: 802.11b WLAN Devices Composite Envelope and PEDs Composite Envelope for Band 3.

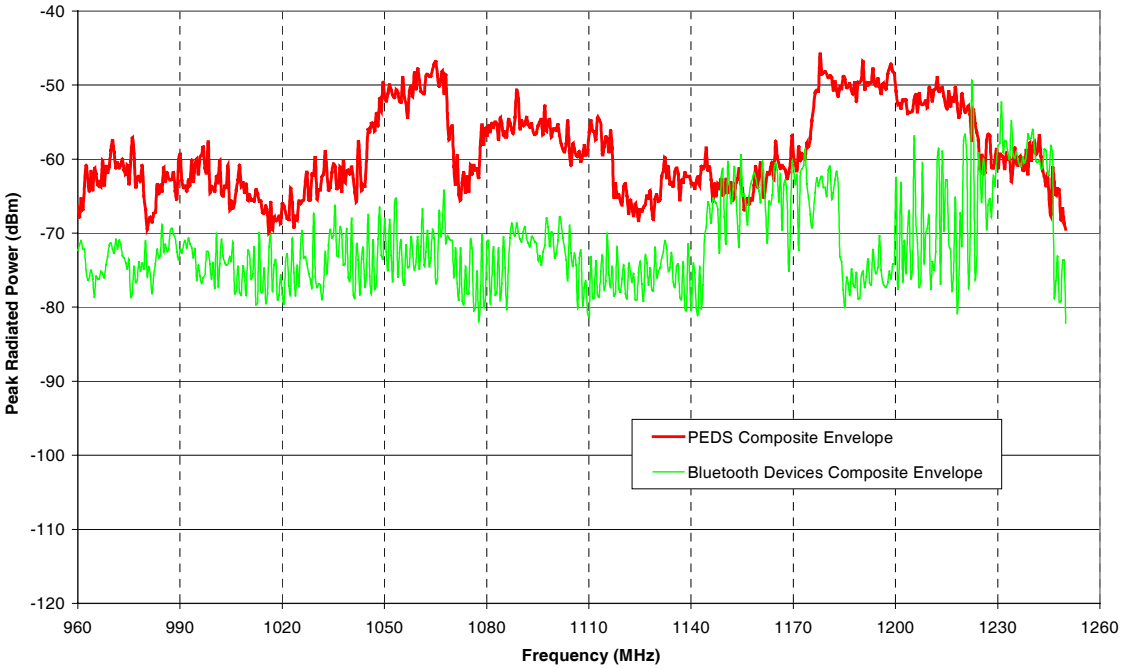

Figure 3.5-13: Bluetooth WLAN Devices Composite Envelope and PEDs Composite Envelope for Band 3.

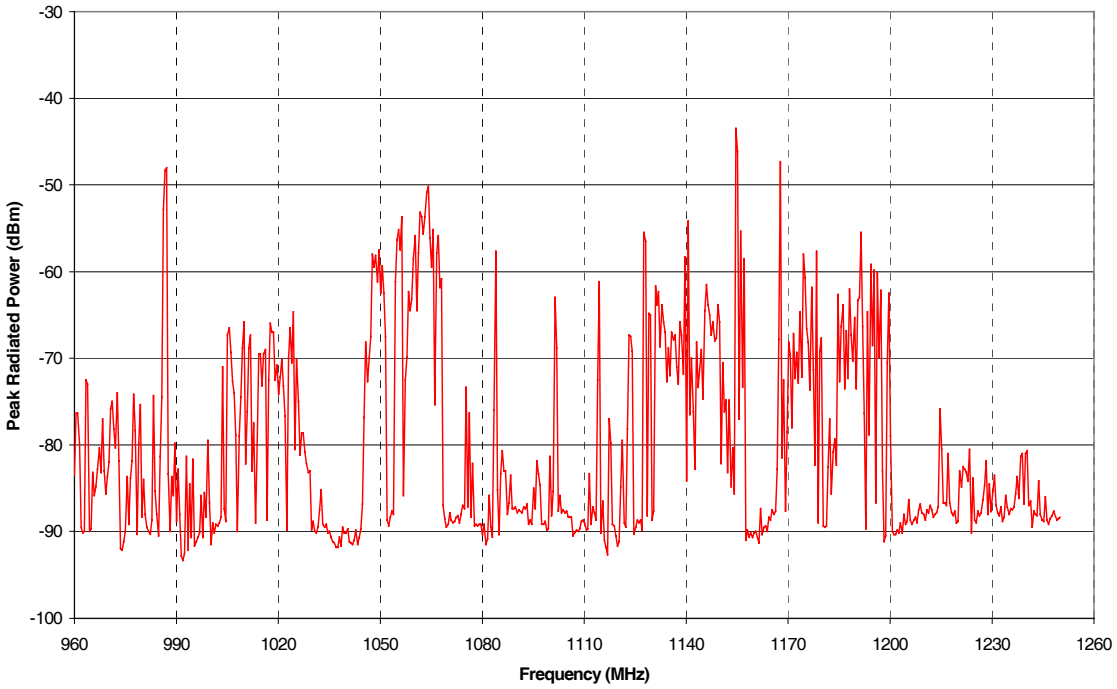

Figure 3.5-14: FRS Radios Composite Envelope for Band 3.

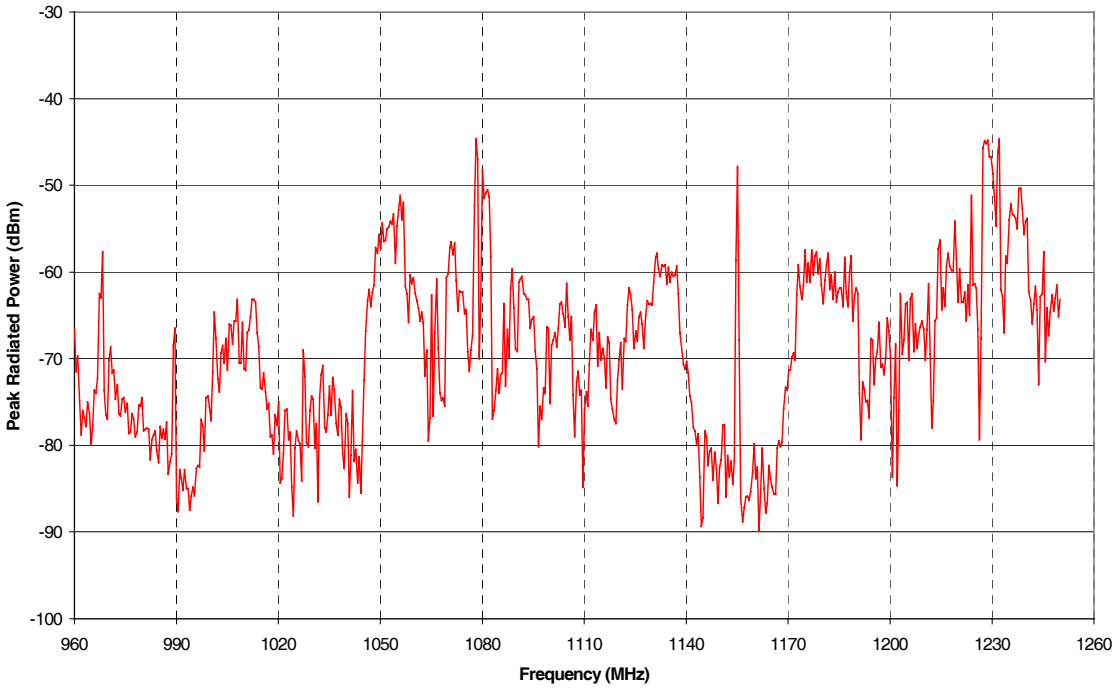

Figure 3.5-15: GMRS Radios Composite Envelope for Band 3.

3.5.4 Band 4 (1565 MHz to 1585 MHz)

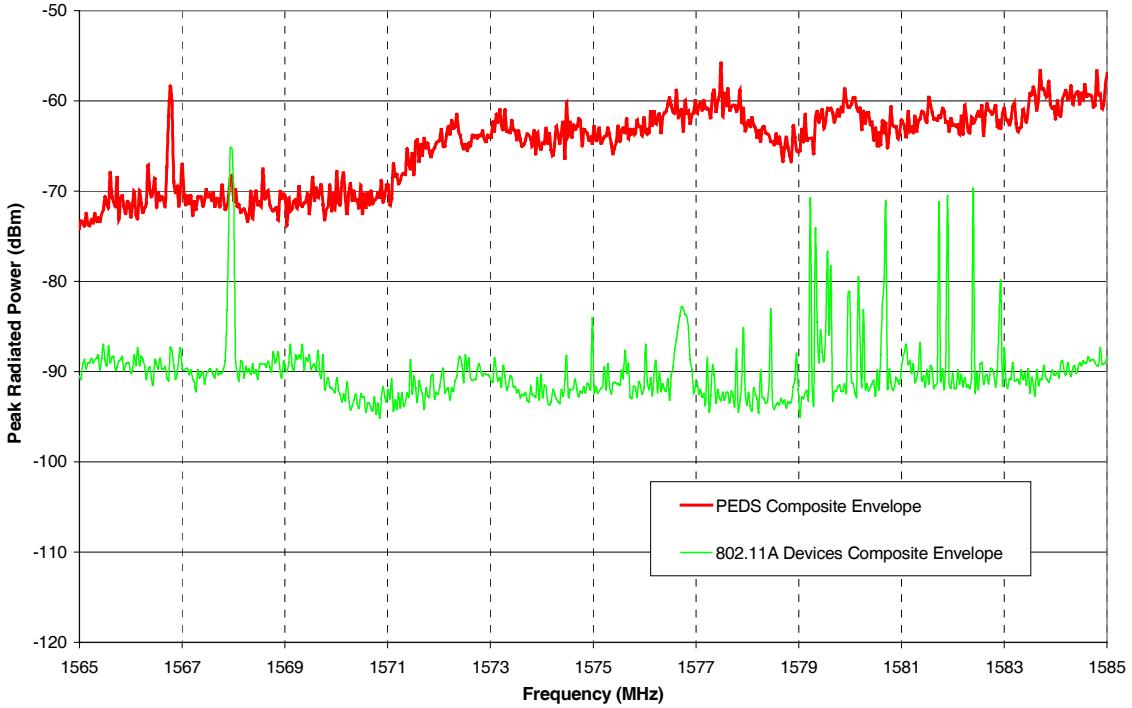

Figure 3.5-16: 802.11a WLAN Devices Composite Envelope and PEDs Composite Envelope for Band 4.

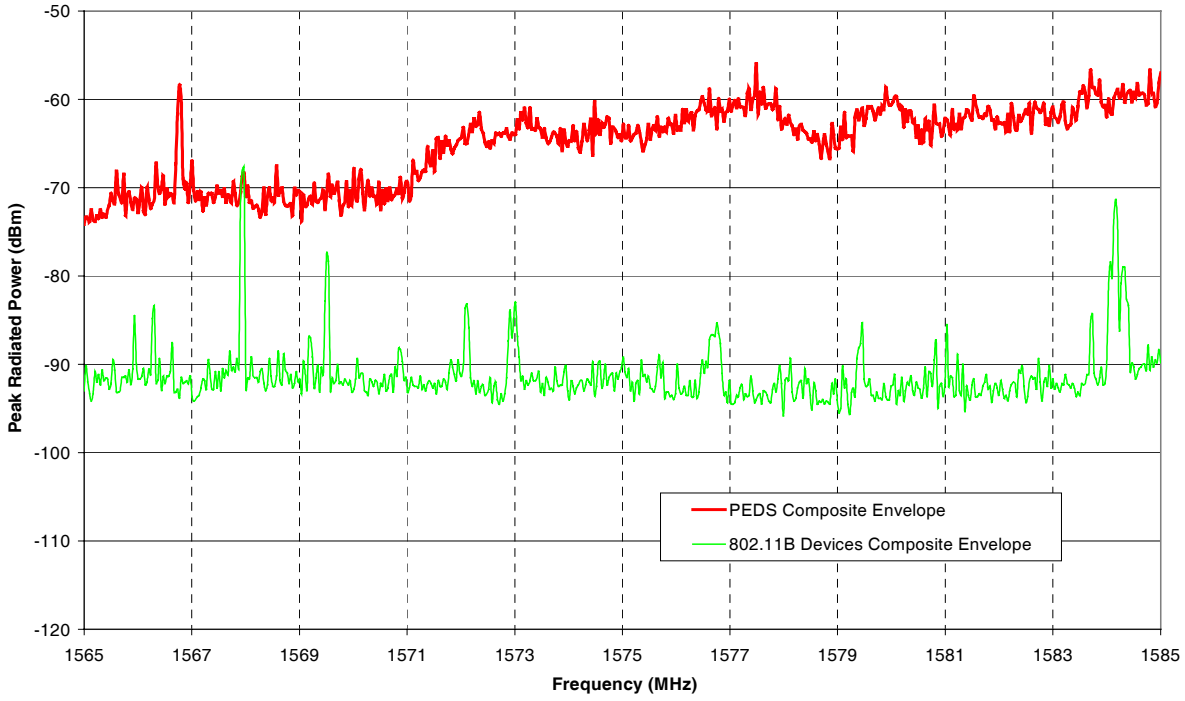

Figure 3.5-17: 802.11b WLAN Devices Composite Envelope and PEDs Composite Envelope for Band 4.

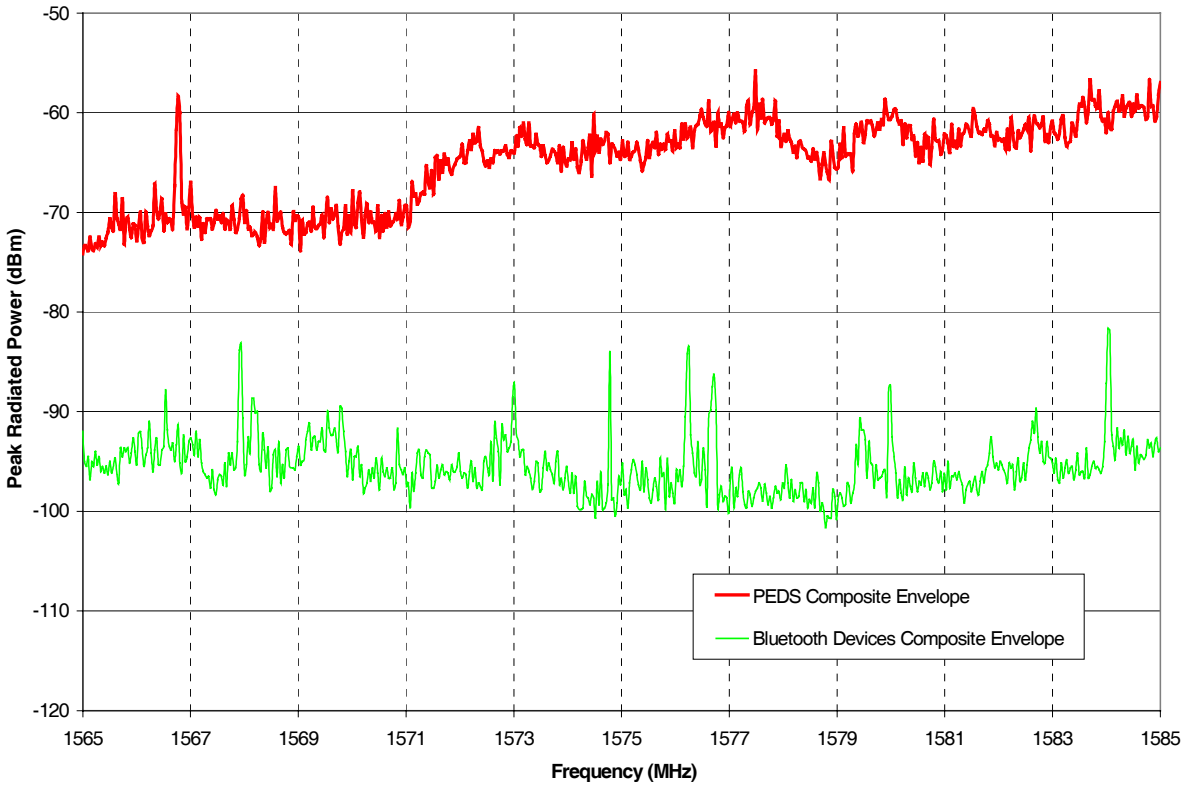

Figure 3.5-18: Bluetooth WLAN Devices Composite Envelope and PEDs Composite Envelope for Band 4.

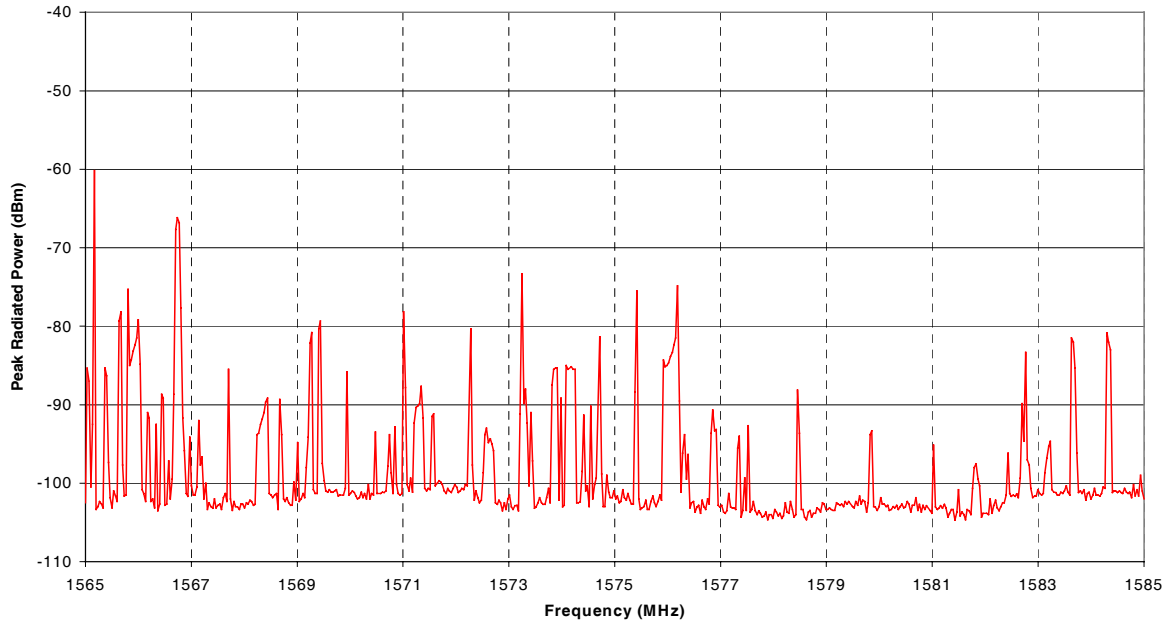

Figure 3.5-19: FRS Radios Composite Envelope for Band 4.

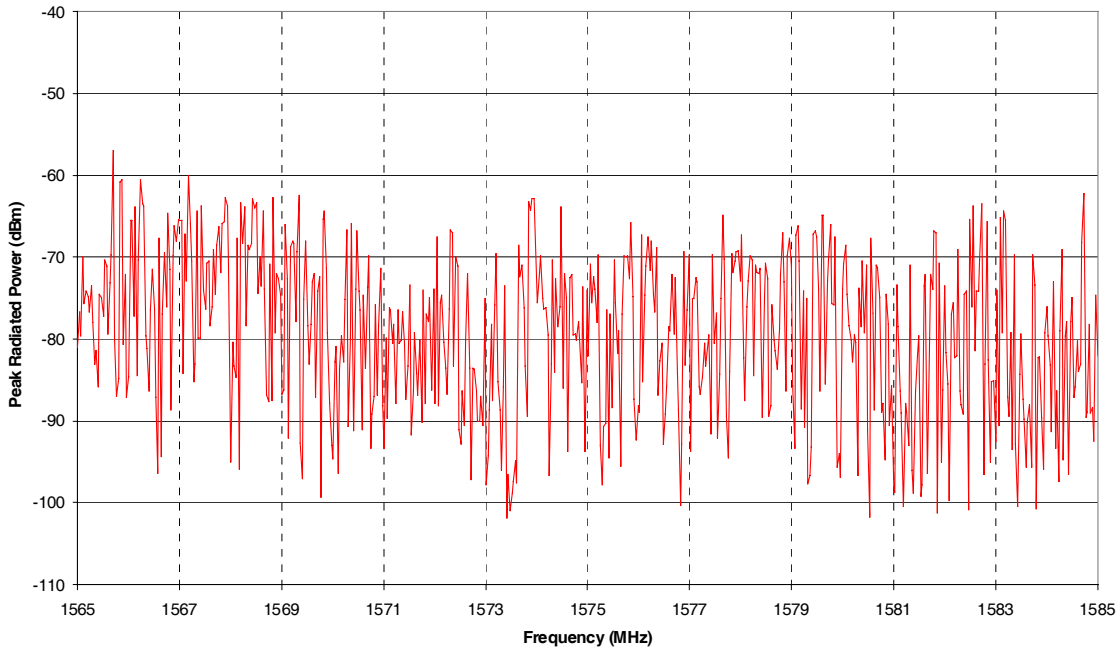

Figure 3.5-20: GMRS Radios Composite Envelope for Band 4.

3.5.5 Band 5 (5020 MHz to 5100 MHz)

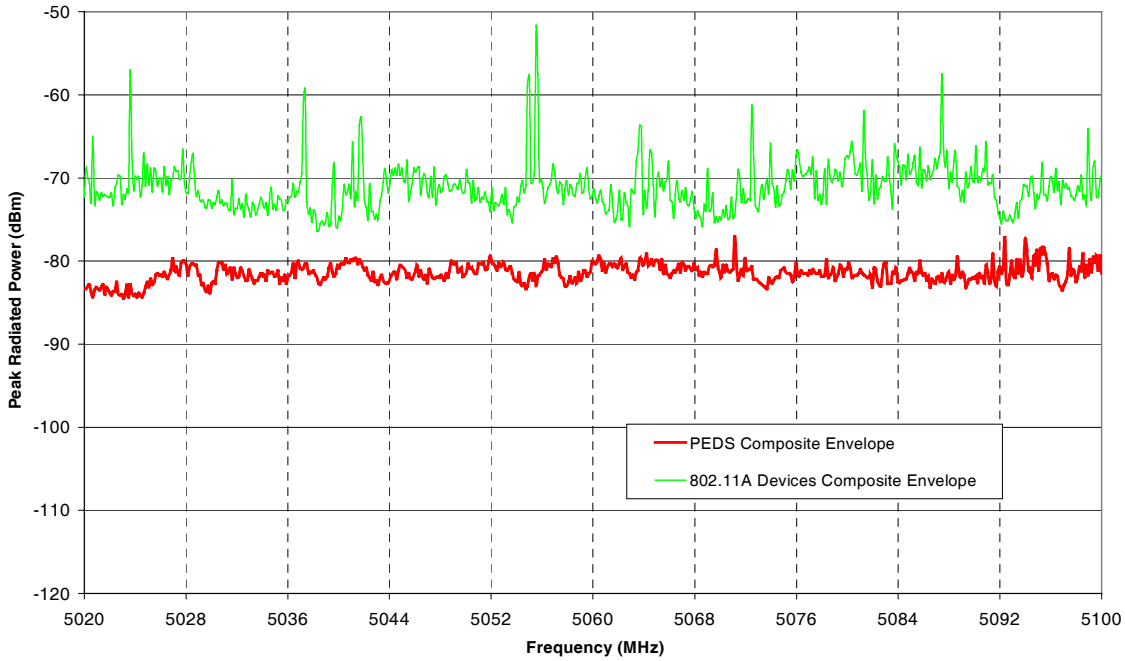

Figure 3.5-21: 802.11a WLAN Devices Composite Envelope and PEDs Composite Envelope for Band 5.

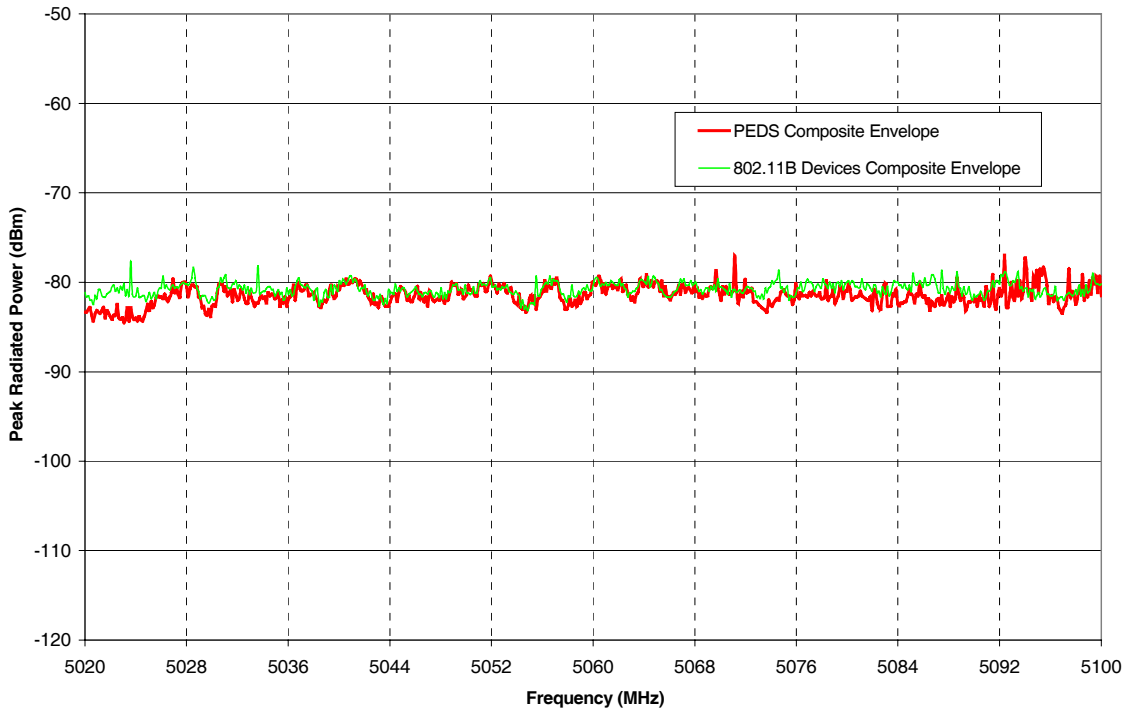

Figure 3.5-22: 802.11b WLAN Devices Composite Envelope and PEDs Composite Envelope for Band 5.

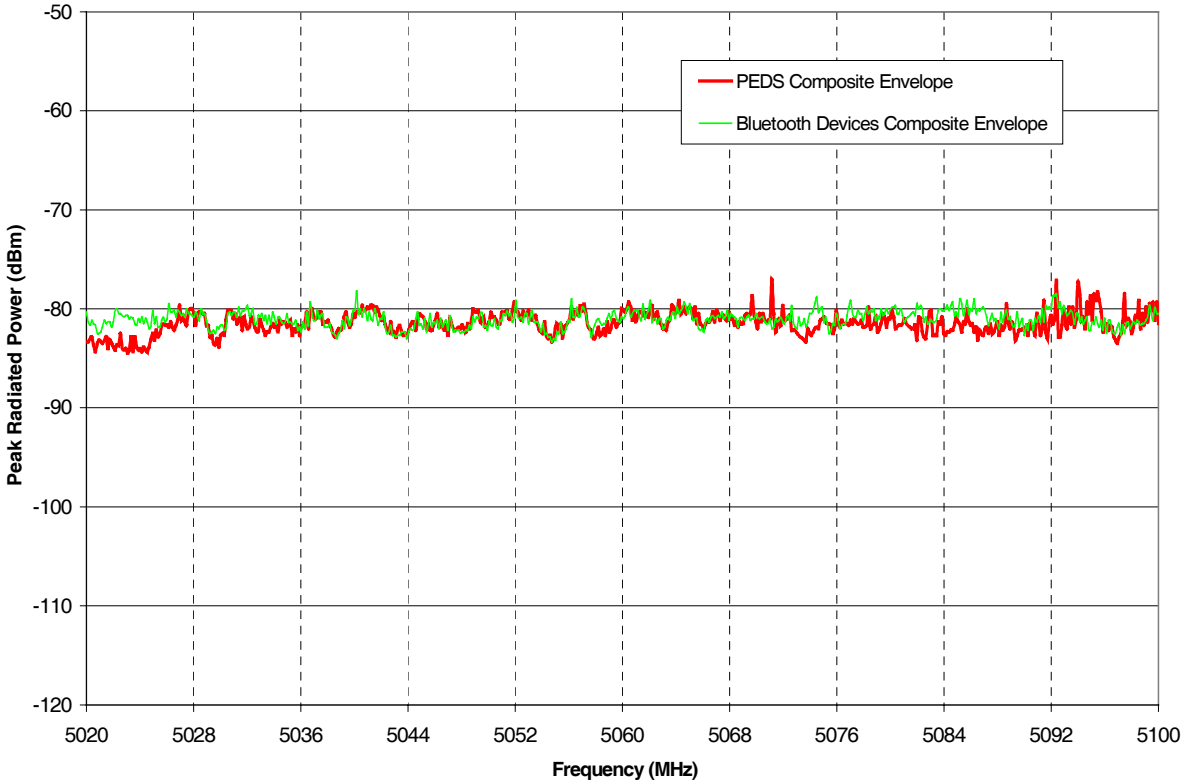

Figure 3.5-23: Bluetooth WLAN Devices Composite Envelope and PEDs Composite Envelope for Band 5.

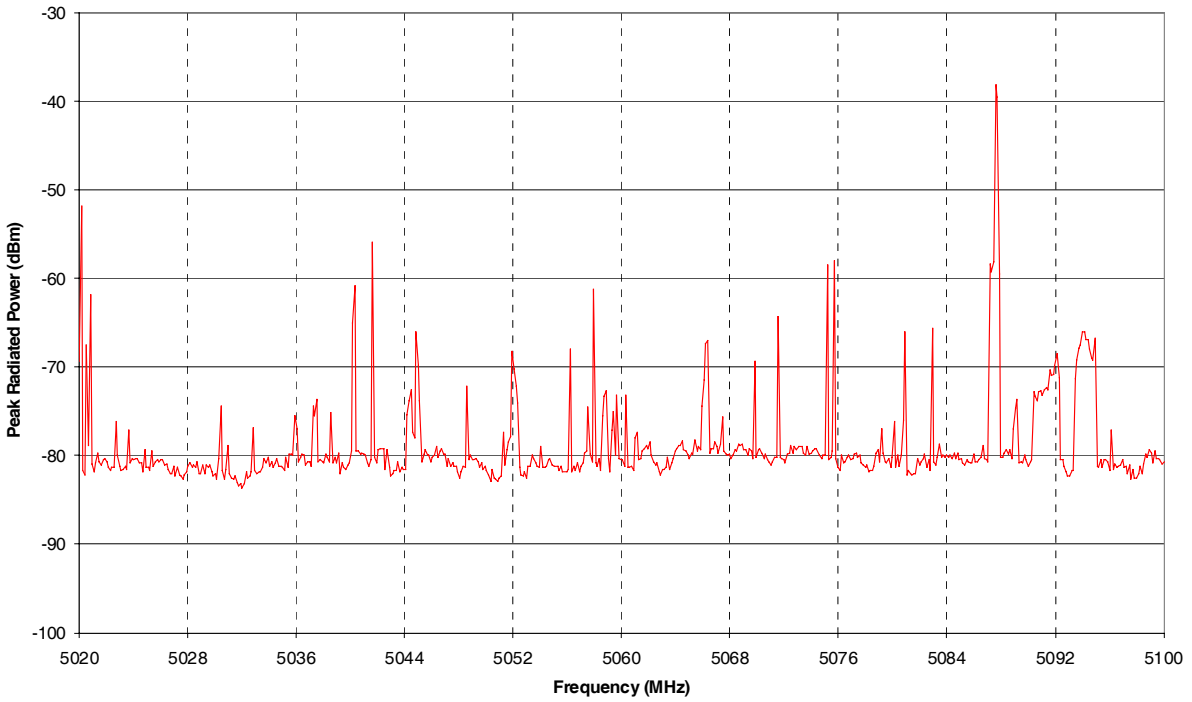

Figure 3.5-24: FRS Radios Composite Envelope for Band 5.

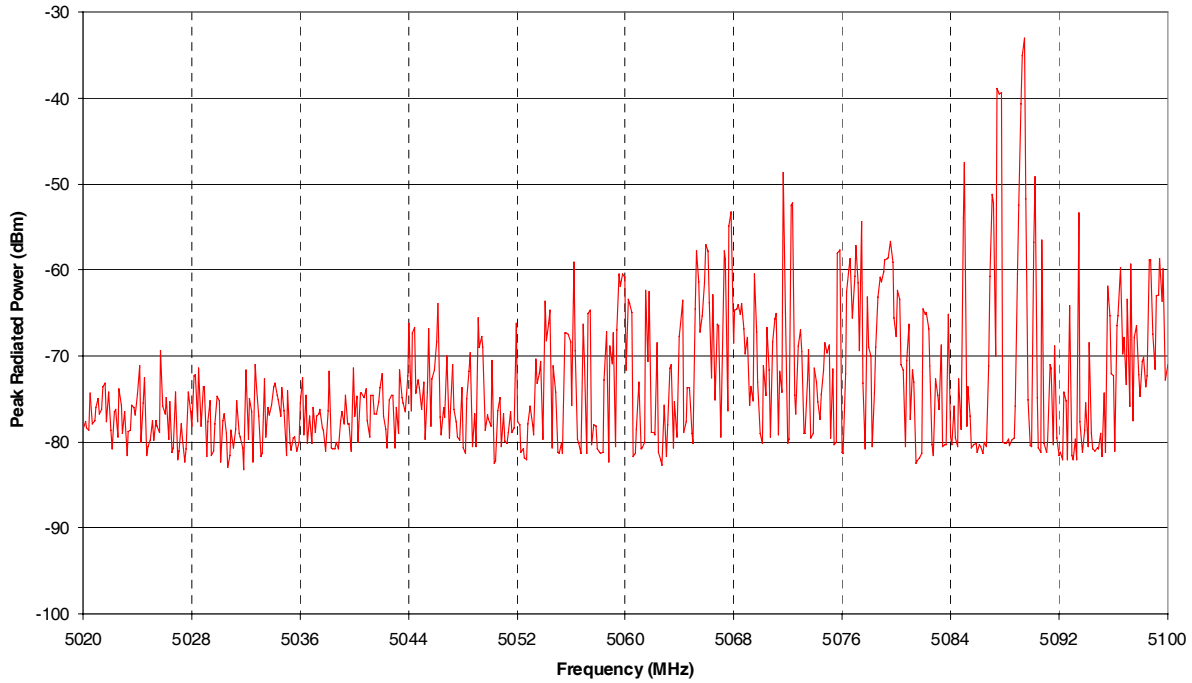

Figure 3.5-25: GMRS Radios Composite Envelope for Band 5.

3.6 Summary of Maximum Emissions from WLAN Devices and FRS/GMRS Radios

This section summarizes maximum emission results reported in earlier sections for WLAN devices, two-way radios and computer laptops/PDAs. In addition, comparisons with corresponding FCC and RTCA/DO-160 [9] emission limits are reported.

3.6.1 Summary of Maximum Emission Results

Table 3.6-1 summarizes previously presented emission data by reporting the maximum emission value of different device groups for each measurement band. The device groups include 802.11b, 802.11a, Bluetooth, FRS radio, GMRS radio, and Laptop/PDAs. The corresponding aircraft radio-navigation systems with frequency spectrum aligned within the emission measurement bands are also shown. These systems are potentially affected by any high emissions within the their measurement bands. These emission data from Table 3.6-1 are used in the safety margin calculations in Section 5.

Figure 3.6-1 plots emission data from Table 3.6-1. It can be observed that emission from the GMRS radios are the highest, followed by FRS radios. Highest emissions are from the GMRS radio at –28.5 dBm in Band 2 and –33 dBm in Band 5. (Note: lines in Figure 3.6-1 are for linking the data points at the markers. Their magnitudes between the markers have no significant values). In Band 2, the GMRS radio emission exceeded the laptop/PDA emission by about 30 dB.

Figure 3.6-1 also shows that maximum emissions from the WLAN devices are generally *lower* than maximum emissions from the laptop/PDA devices in all five bands. One exception is 802.11a emissions in Band 5 with the maximum emission level at –52 dBm. High emission from 802.11a devices in this band is not unexpected since both the 802.11a band and Band 5 are close in the 5-GHz range. MLS is the only system in this band, and the risk to MLS is viewed as low due to lack of installed MLS systems in the US.

Emissions in Band 5 from other WLAN devices and laptop/PDA devices are lower in the measurement noise floor as evidenced by data aggregated near –78 dBm.

Table 3.6-1 Maximum Emission from WLAN Devices/ Two-way Radios in Aircraft Bands (in dBm)

Measurement Band	Frequency (MHz)	802.11b	Blue-tooth	802.11a	FRS Radio	GMRS Radio	Laptops PDAs	Aircraft Bands
Band 1	105 - 120	-78.2	-66.8	-74.2	-90.7	-79.3	-68.0	**LOC, VOR**
Band 2	325 - 340	-75.7	-77.2	-71.8	-37.2	-28.5	-58.7	**GS**
Band 3	960 - 1250	-65.3	-49.7	-57.7	-43.5	-44.7	-45.7	**TCAS, ATC, DME/TACAN, GPS L2**
Band 4	1565 -1585	-67.7	-81.7	-65.2	-60.2	-57.0	-55.8	**GPS L1**
Band 5	5020 - 5100	-77.7	-78.2	-52.0	-38.2	-33.0	-77.0	**MLS**

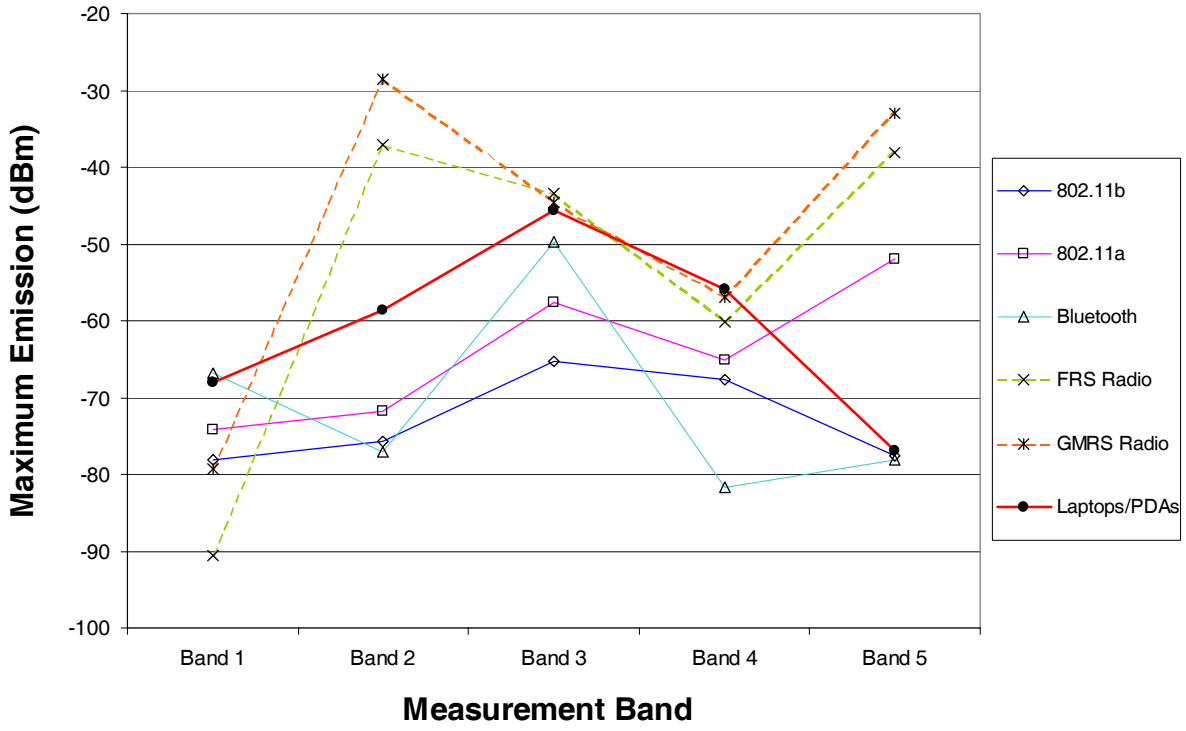

Figure 3.6-1: Maximum emission from WLAN, Bluetooth devices, FRS/GMRS radios and Laptops/PDAs.

3.6.2 Comparison with Emission Limits

Table 3.6-2 shows the FCC Part 15.109 [16] and 15.209 [17] limits for unintentional and intentional radiators, the RTCA/DO-160 Category M limits, and the FCC spurious emission limits for FRS/GMRS radios (FCC 95.635 [18]). RTCA/DO-160 Category M emission limit is selected for comparisons with spurious emissions from passenger carry-on electronic devices since these devices can be located in the passenger cabin or in the cockpit of a transport aircraft, where apertures (such as windows) are electromagnetically significant. The quote below is the definition for Category M radiated emissions limit specified in RTCA/DO-160 Section 21 [9]:

> "*Category **M**:*
> *This category is defined for equipment and interconnected wiring located in areas where apertures are em significant and not directly in view of radio receiver's antenna. This category may be suitable for equipment and associated interconnecting wiring located in the passenger cabin or in the cockpit of a transport aircraft.*"

For the RTCA/DO-160 Category M limit listed in Table 3.6-2, the limit value for each *measurement band* is chosen to be the lowest limit of the *aircraft bands* within it. As an illustration, the emission measurement Band 3 would cover TCAS, ATCRBS, DME, GPS L2 and GPS L5. The emission limit for the whole measurement band is chosen to be the lowest limit of all the systems listed. In this case, the lowest value is 50 dBμV/m for TCAS, DME and ATCRBS since the limits for GPS L2 and GPS L5 are

higher. In addition, the emission limit for each aircraft radio band is chosen to be the lowest value between its lowest and highest frequency limits.

To compare with measured emission data in dBm, the field limits in FCC Part 15 and the RTCA/DO-160 Category M are converted to the equivalent Effective Isotropic Radiated Power (*EIRP*) using Equation 3.6-1.

$$EIRP = \frac{E^2 \cdot 4\pi R^2}{120\pi} \qquad \text{(Eq. 3.6-1)}$$

where *EIRP* = Effective Isotropic Radiated Power (*W*)

E = Electric Field Intensity at distance R (*V/m*)

R = Distance (*m*)

Ideally, *E* field measurement is taken in the direction of maximum radiation from the test device. To convert power, *EIRP,* from watts to dBm, use the expression *10 * log(1000*EIRP).* For the RTCA/DO-160 limit given in *dBμV/m*, the unit is converted to *V/m* before applying Equation 3.6-1.

Table 3.6-2: Estimated FCC and RTCA spurious radiated emission limits

	FCC Part 15 Limit (μV/m @ 3m)	**RTCA/DO-160 Category M Limit** (dBμV/m @ 1m)	**FCC Part 15 Limit** (*EIRP*, dBm)	**RTCA/DO-160 Category M Limit** (*EIRP*, dBm)	**FCC FRS/GMRS Radio Limit** (*TRP*,dBm)
Band 1	150	35	**-51.7**	**-69.8**	**-13**
Band 2	200	52.9	**-49.2**	**-51.9**	**-13**
Band 3	500	50	**-41.2**	**-54.8**	**-13**
Band 4	500	53	**-41.2**	**-51.8**	**-13**
Band 5	500	71.8	**-41.2**	**-33.0**	**-13**

Emissions measured using a RC, on the other hand, provide results in "total radiated power" (*TRP*) within the measurement resolution bandwidth. *TRP* is different from *EIRP* except for antennas or devices with an isotropic radiation pattern. Rather,

$$EIRP \text{ (dBm)} = TRP \text{ (dBm)} + D_G \text{ (dB)}, \qquad \text{(Eq. 3.6-2)}$$

where D_G is *directivity,* or maximum *directive gain* of the test device. Directive gain of any device is a measure of radiated power as a function of aspect angle referenced to the isotropic value.

For spurious emissions, D_G is the directivity at the spurious emission frequency of interest. D_G is usually difficult to measure or calculate since maximum radiation angles and radiation mechanisms for *spurious* emissions are often not known. Maximum theoretical estimation of D_G based on device size tends to significantly over-estimate the real directivity, especially at high frequency, because the device geometry is typically not designed to radiate efficiently as an antenna as assumed in the theoretical

estimation. There are other theoretical statistical developments to estimate the "expected" directivity for non-intentional radiators [19]. These developments are yet to be validated or widely accepted. Additional details on expected directivity are discussed in Section 3.6.3.

For simplicity, we assume that the WLAN devices (plus the host computer laptops/PDAs) have unity D_G for spurious emission. Thus, *TRP* is assumed to be the same as *EIRP* at all spurious frequencies of interest. This assumption introduces an uncertainty level equal to D_G, according to Equation 3.6-2. For a dipole antenna with small electrical length, D_G is close to 1.76 dBi (or dB relative to isotropic). For a half-wave dipole, D_G is close to 2.15 dBi. Thus, it is reasonable to assume for devices up to one-half a wavelength in size, the uncertainties should not be much more than 2-5 dB. This level of uncertainty is considered acceptable for a first order comparison.

Section 3.6.3 computes the "expected" directivity using formulas provided in [19]. For a device 0.5 m in size (approximately the maximum size of an open laptop computer), the expected directivity is between 5 dB near 100 MHz and 9 dB near 5 GHz. These expected directivity values are provided for information purposes only. The method used is yet to be proven or widely accepted.

For FRS and GMRS radios, FCC 95.635 [18] dictates the attenuation for frequency *outside* of the vicinity of the center frequency is at least $43 + 10\log(P_c)$ *dB*, where P_c is carrier frequency power in watts. For 0.5-watt FRS radios and 2-watt GMRS radios, the attenuation below carrier power is 40 dB for FRS radios and 46 dB for GMRS radios. As a result, the calculated emission limits are -13 dBm for both FRS and GMRS radios.

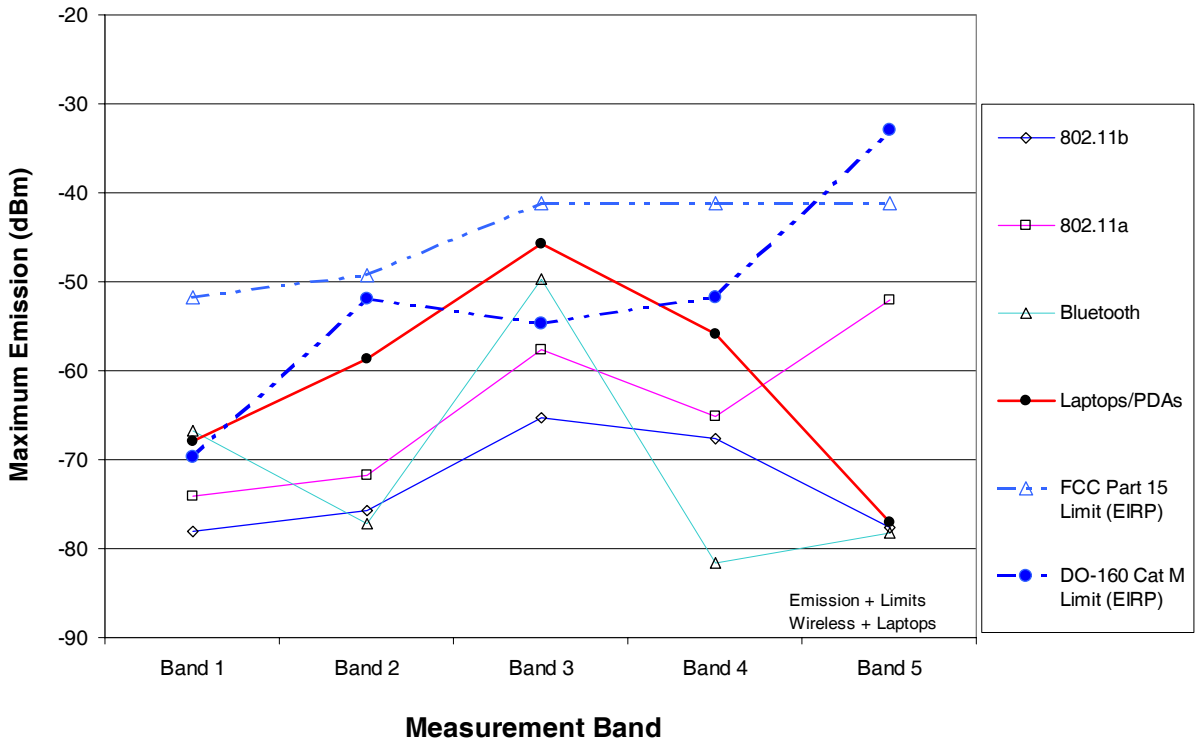

Figure 3.6-2: Maximum emissions from WLAN devices, laptops/PDAs and comparison with FCC and RTCA/DO-160 equivalent *EIRP* limits.

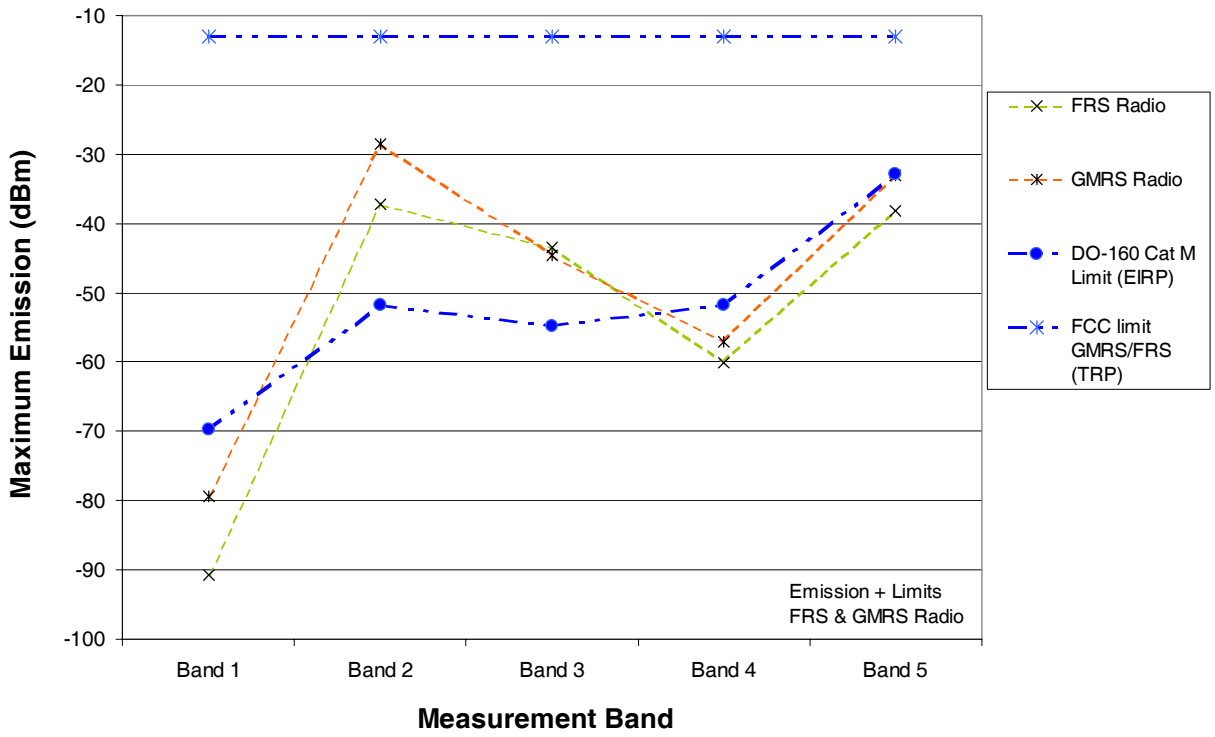

Figure 3.6-3: Maximum emission from two-way FRS/GMRS radios and comparison with FCC limits.

Figure 3.6-2 shows emissions from laptops/PDAs and WLAN devices are lower than corresponding FCC equivalent *EIRP* limits. However, emissions from laptops/PDAs and Bluetooth devices are higher than the RTCA/DO-160 Category M equivalent *EIRP* limits in Band 1 and Band 3. In addition, WLAN device emissions are lower than the emissions from the laptops/PDAs, except for 802.11a emissions in Band 5. It can be argued that emissions from the measured WLAN devices, while being higher than RTCA/DO-160 Cat M limits, do not pose significantly higher risk to aircraft radio receivers than emissions from standard laptop/PDA devices.

For FRS/GMRS radios, Figure 3.6-3 shows emissions are still below the FCC maximum out-of-band emission limit of –13 dBm for these devices. Figures 3.6-1 and 3.6-3 show spurious emissions in GS band from GMRS radios can be **23** dB higher than RTCA/DO-160D Category M limit, and **30** dB higher than the maximum laptop/PDA emissions in the same band. The threat of interference from these two-way radios can be significantly higher than from the laptops/PDAs.

3.6.3 Expected Directivity Estimation

The comparisons above were between the *TRP* from the devices and the FCC Part 15 and RTCA/DO-160 Cat. M equivalent *EIRP* limits, assuming unity directivity. For devices with directivity different than unity, the limits must be adjusted downward by the amounts equal to the devices directivity in dB, which can vary with device size, frequency and geometry.

Reference [19] provides a method to estimate the *expected* directivity derived from a statistical approach. Using equations given, expected directivity of a device can be estimated if its maximum

dimension is known. For a laptop computer with the maximum dimension of 0.5 m (open screen configuration), the expected directivity is shown in Figure 3.6-4. This figure shows the results of three calculations: 1) theoretical maximum directivity for a high gain antenna of the same size, 2) expected directivity for 1-planar cut measurement, and 3) expected directivity for 3-planar cut measurement. The 3-planar cut expected directivity is between five and eight dB for frequencies in Band 4 (GPS) and below, and less than nine dB in Band 5 (MLS).

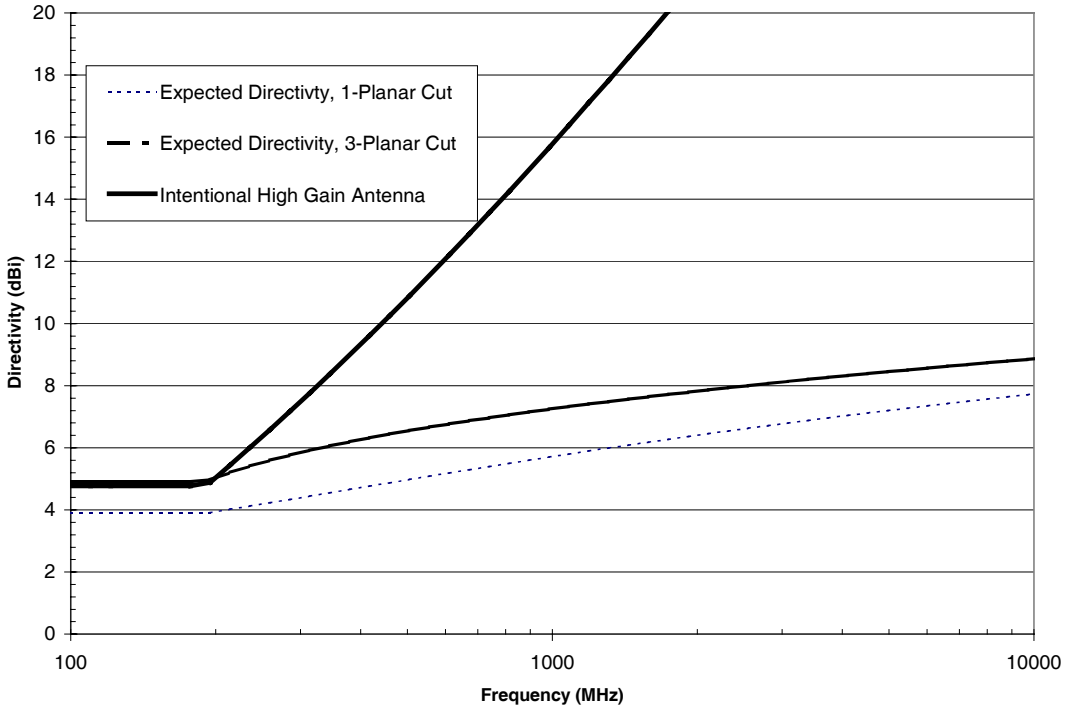

Figure 3.6-4: Expected spurious emission directivity of a 0.5 m device.

4 Aircraft Interference Path Loss Determination

Aircraft IPL is the second of the three components needed for assessing the potential of interference from RF sources to aircraft receivers. Using World Jet Inventory [20] as a guide, there are about 35 different types of operational, commercial jet airplanes built in the US and Western Europe with a capacity of 30 seats or more. Each aircraft type and series has a unique configuration of antenna placements and radio receiver installations. These variations may result in widely different IPL values.

The following sections describe a recent effort to measure IPL for various radio receiver systems on six B737s and four B747s. The IPL results are summarized and presented along with other previously available data for comparison.

4.1 Interference Path Loss Measurements on B737s and B747s

Previous investigations [1] identified deficiencies in available IPL data for a reasonable risk assessment of interference to receiver systems from PEDs. To address that issue, NASA entered into a cooperative agreement with UAL and EWI to conduct additional IPL measurements and to address several technical issues. One issue was to measure additional IPL data using a thorough and consistent set of procedures. Another issue concerned aircraft-to-aircraft repeatability. This repeatability issue resulted in measurements on six similar B737-200 and four similar B747-400 aircraft. The aircraft in each of the two groups were acquired by UAL at approximately the same time, and, therefore were similarly configured.

Other technical issues include investigating the effectiveness of risk mitigation techniques, such as treating exit door seams and windows with conductive tape and films. New instrumentation tools for assessing health of aircraft cables and antennas were demonstrated. Preliminary on-aircraft operational testing of susceptibility of aircraft systems to Ultrawideband (UWB) interference signals was also conducted when the schedule permitted [21].

For this report, only the IPL results from unmodified aircraft configurations that are relevant to wireless interference are reported. IPL data of modified aircraft configurations for side studies, which may have conductive tapes and film over aircraft windows and doors, are excluded. These configurations are not representative of an in-service aircraft.

The IPL measurements were performed during three one-week visits to the Southern California Aviation facility in Victorville, California. UAL provided the flight-ready airplanes, along with fuel, engineering and mechanic support for this effort. These airplanes were temporarily put in storage configuration due to September 11 terrorist events that resulted in lower demand in passenger travel and an increase in surplus capacity. NASA provided measurement instrumentation, data acquisition and test control software development and support, and staff. EWI was tasked to lead the overall effort and to conduct analysis.

IPL measurements were conducted on the six B737-200 airplanes for the VOR/LOC, VHF-1 Comm., GS, TCAS, and GPS systems. The interference source, simulated with dipole and horn antennas, was positioned to radiate toward each of the windows and the door exits on one side of the aircraft. In addition, full IPL measurements were also conducted on two B737s with the transmit antenna positioned at all seat locations including locations between seats (on one side of the aircraft).

IPL measurements were also conducted on the four B747-400 aircraft for the LOC, VHF-1 Comm., GS, TCAS, GPS and SatCom systems. Due to large aircraft size and the number of windows and doors, IPL was measured with the transmitting antenna positioned only at selected windows considered closest to the receiving aircraft antenna and to provide the lowest path loss values. For systems with antennas on top of the aircraft, including VHF-1 Comm., GS, TCAS, GPS and SatCom, these locations include all windows on one side of the *upper deck*. For LOC and GS systems with their antennas located behind the nose radome, IPL measurements were conducted (with the transmit antenna) at the first 20 windows on one side of the *lower deck*. These windows were closest to the antennas in the radome. Figure 4.1-1 shows images of B737 and B747 aircraft at the measurement site.

The following subsections, 4.1.1 and 4.1.2, describe the measurement method and IPL results.

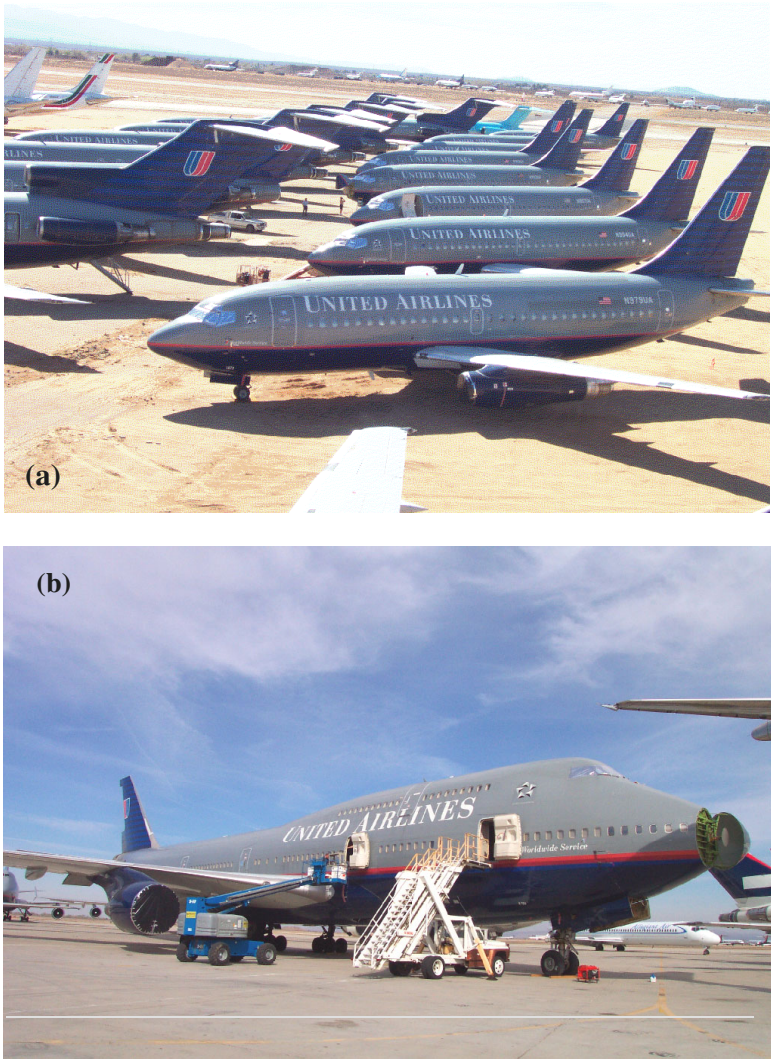

Figure 4.1-1: (a) B737-200 and (b) B747-400 aircraft at the measurement site.

4.1.1 IPL Measurement Method

It is assumed that for PEDs interference problems, the interference source is located within the passenger cabin, and the victims are aircraft radio receiver systems. A common path of PED interference is through the windows or door seams, along the aircraft body, and into the aircraft antennas. The interference signal picked up by the antennas is channeled back into the receivers to potentially cause interference if they are higher than the receiver interference thresholds.

Figures 4.1-2 and 4.1-3 illustrate typical radio receiver interference coupling paths and a setup for conducting IPL measurements. The setup shows a tracking source is used to provide RF power to the transmit antenna, and a spectrum analyzer is used to measure the signal received by the aircraft antenna. The frequency-coupled spectrum analyzer and tracking source pair allows for frequency sweeps, resulting in more thorough measurements and reduced test time. Swept CW was preferred over discrete frequency measurement, according to RTCA/DO-233. A pair of test cables is used to connect the instruments to the

aircraft antenna cable and to the transmit antenna. An optional amplifier may be needed to increase the signal strength depending upon the capability of the tracking source and the path loss level. A pre-amplifier may be needed in the receive path near the spectrum analyzer for increased dynamic range. This pre-amplifier (not shown in Figure 4.1-3) may be internal to the spectrum analyzer.

In the actual measurements, two independent measurement systems were used for concurrent measurements on two airplanes at a time. While the basic set up for each system was the same as shown in Figure 4.1-3, the performance and capabilities of the instruments were different. This difference caused amplifiers and pre-amplifiers to be used in one setup but not the other. In one setup, the tracking source and the spectrum analyzer were combined in one unit with an internal pre-amplifier. The other set up included a separate spectrum analyzer and a tracking source that delivered much higher output power. In either case, correction factors were applied to ensure correct final IPL results.

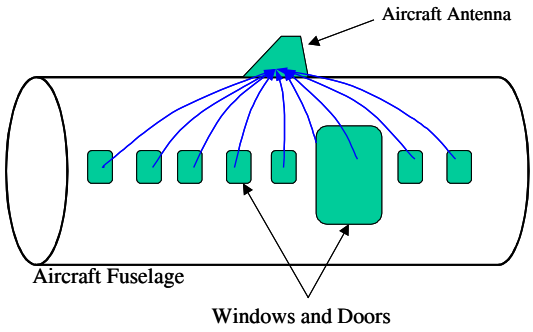

Figure 4.1-2: A typical radio receiver interference coupling path for a top mounted aircraft antenna.

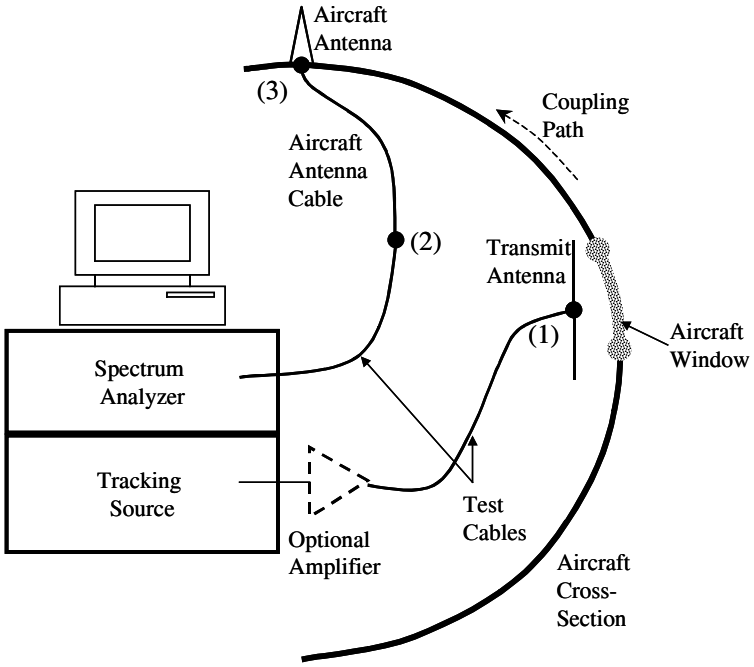

Figure 4.1-3: A typical setup for conducting an IPL measurement.

In Figure 4.1-3, IPL is defined to be the ratio, or the difference in dB, between the power radiated from the transmit antenna at location (1) to the power received at location (2). For GPS, IPL is defined to be the difference in power between location (1) and (3). Or,

$$IPL = P^{T}_{(1)} - P^{R}_{(2)} \quad \text{for most systems, and} \qquad \text{(Eq. 4.1-1)}$$

$$IPL = P^{T}_{(1)} - P^{R}_{(3)} \quad \text{for GPS,} \qquad \text{(Eq. 4.1-2)}$$

where $P^{T}_{(1)}$ is power transmitted at point (1), and $P^{R}_{(2)}$, and $P^{R}_{(3)}$ are power received at points (2) and (3), in dBm, respectively.

The antennas used in the measurement include dipoles (a set of dipoles with baluns covering different frequency ranges) for frequencies in the GS band and below, and a dual-ridge horn antenna for the frequencies in the TCAS band and above. No corrections were made to account for the transmit antenna gain as performed on many data sets documented in RTCA/DO-199 and RTCA/DO-233. The proximity of the transmit antennas and their surroundings, such as walls, seats, windows, table trays, would have large affects on the true antenna gain, and that free-space antenna gain is viewed as not the appropriate correction factor. The true antenna gain is not known in the presence of the obstacles. Transmit antenna gain correction was not applied to at least one set of data in RTCA/DO-199. It was also unclear if the same gain correction was made to *all* data in DO-233. In this effort, it is considered best not to correct for the free space antenna gain in the definition for IPL for the reasons stated. However, free-space antenna gains, as provided by the antenna manufacturers, are shown in Table 4.1-1 that can be used to factor in the transmit antenna free-space gain, if so desired.

Table 4.1-1: Transmit Antenna Free-Space Gain (dBi)

Aircraft Systems	Spectrum (MHz)	Measurement Frequency Range (MHz)	Transmit Antenna Type	Free-Space Antenna Gain (dBi)
VHF-Com	118 – 137	116-138	Dipole	2.1
LOC/VOR	LOC: 108.1 – 111.95 VOR: 108 – 117.95	108-118	Dipole	0.9
GS	328.6 – 335.4	325-340	Dipole	1.9
TCAS	1090	1080 – 1100	Dual-Ridge Horn	7.4
GPS (L1)	1575.42 ± 2	1565 – 1585	Dual-Ridge Horn	9.6
SatCom	1545-1559	1530 – 1561	Dual-Ridge Horn	9.6

In the actual measurement, the test cables at (1) and (2) were connected together and a "through" swept measurement was made for the total system loss. The test cables were then reconnected at points (1) and (2) (points (1) and (3) for GPS) and another swept-frequency measurement was made. The instrument settings were maintained to be the same as during the "through" system loss measurement . The receive power difference between the maximum of the first measurement data and the maximum of the second measurement data gave the IPL for that particular transmit antenna location. This calculation for IPL was conducted during data post-processing.

As shown in Figure 4.1-3, a transmit antenna was used to simulate an interference source. The tuned dipole transmit antenna was used for measurements in the LOC, VOR and GS bands, and a dual-ridge-horn antenna was used for measurements in the TCAS, GPS and SatCom bands.

For most systems, IPL included aircraft cable loss, since receiver susceptibility thresholds were specified at the receiver antenna port. For GPS, interference thresholds were specified at the output of a passive GPS antenna. Thus, IPL for GPS should not include the antenna cable loss. The test cable should connect directly to the GPS antenna output or very close to it, and the spectrum analyzer measured the power at the output of the antenna directly. Since the aircraft active GPS antenna was powered with the help of a DC bias-tee, the bias-tee was included in the total system loss measurement.

The active GPS antenna pre-amplifier gain was removed during post processing, giving higher IPL. This step was required in the GPS receiver's Minimum Operating Performance Standards (MOPS), as the interference threshold was specified at the output of a passive antenna, or at the output of an active GPS antenna, but before the pre-amplifier stage.

The measurement process for each system on each aircraft typically involved the following steps:

1. Conduct 1-meter path loss measurement. IPL was measured with the transmit antenna positioned one meter from the aircraft antenna. This simple step established a baseline measurement and helped detect any excessive aircraft antenna cable loss. Excessive cable loss could indicate possible signs of connector corrosion in the path. These data were not needed to compute the IPL.

2. Configure the spectrum analyzer to the proper reference level, resolution bandwidth, attenuation level and desired measurement frequency band. Configure the tracking source to track the frequency sweep of the spectrum analyzer. Set the tracking source output to desired power level.

3. Measure test cable and aircraft cable "through" losses.

4. Position the transmit antenna at a desired location, typically near a window or door. Point the antenna to radiate toward a window or door seam.

5. Clear spectrum analyzer's trace. Set spectrum analyzer to "Trace Max Hold" and sweep continuously across the desired measurement band.

6. Scan the transmit antenna slowly along the door seam, while the spectrum analyzer is still set at "Trace Max Hold". No scanning was needed at the windows due to small window sizes.

7. Record trace and the peak marker value. For systems that experience narrowband peaks caused by strong local transmitters such as LOC, position the marker at the peak of the broadband envelope while avoiding the narrowband peaks. Record data at this marker location.

8. Change polarization and repeat from step 2 so that both vertical and horizontal polarizations of the transmit antenna are included.

9. Relocate the transmit antenna to another window/door and repeat from step 4.

Post processing involved removing the measured system "through" loss from the total path loss data. The system loss includes the effects of test cable losses, amplifier gains, and other types of losses/gains in the measurement path. Active GPS pre-amplifier gain is also removed in the final results.

Figure 4.1-4 shows a 1-meter path loss measurement near a B737 VOR/LOC antenna located in the tail. A 1-meter path loss measurement was conducted to check the integrity of the aircraft antenna path. The results were not used to calculate IPL and are not reported in this document. Of all systems considered for IPL measurement, only the VOR/LOC's antenna on the B737-200 is located in the tail. All other systems have their antennas located either on top of the aircraft, such as TCAS, GPS and VHF Comm, or behind the nose radome, such as GS. On a B747, all systems with IPL measurements have their antennas in the nose (GS and LOC), or on top above the upper deck windows (TCAS, VHF-Com, SatCom, GPS).

Figure 4.1-5 shows a measurement being conducted with the transmit antenna at a window, and the computer and software used for data acquisition. Instruments and computers were located within the passenger cabin. Spurious emissions from these equipment were too low to be measurable or to affect the measurement. In contrast, the output signal from the tracking source was 10 dBm or higher depending upon whether an external amplifier was used.

Figure 4.1-4: Conducting 1-meter path loss baseline measurement for the LOC antenna in the B737's tail. The reference transmit antenna is one meter from the receive aircraft antenna. The two VOR/LOC antennas are parallel to each other and are embedded horizontally within the top edge of the aircraft tail.

Figure 4.1-5: IPL measurement at window locations. (a) A dipole was used as transmit antenna for LOC, VOR, GS and VHF-Com. (b) A dual ridge horn antenna was used for TCAS, GPS and SatCom. (c) A computer recorded data from the spectrum analyzer (located underneath the computer).

4.1.2 Measured Interference Path Loss Results

Using the method described in the previous section, IPL was measured for several radio receivers on six B737-200 and four B747-400 aircraft. The specific systems measured are listed in Table 4.1-2 along with the measurement frequencies, and Table 4.1-3 documents the specific aircraft and their nose numbers.

Table 4.1-2: System Measured and Frequency Bands

Aircraft Systems	Aircraft Antenna Location	Measurement Frequency Range (MHz)	Spectrum (MHz)
VHF-Comm 1	Top	116-138	118 – 137
LOC/VOR	Nose (B747) Tail (B737)	108-118	LOC: 108.1 – 111.95 VOR: 108 – 117.95
GS	Nose	325-340	328.6 – 335.4
TCAS	Top	1080 – 1100	1090
GPS (L1)	Top	1565 – 1585	1575.42 ± 2
SatCom	Top	1530 – 1561	1545-1559

Table 4.1-3: B737-200 and B747-400 Aircraft Used for IPL Measurement and Their Nose Numbers

B737-200 Aircraft UAL Nose No.	B747-400 Aircraft UAL Nose No.
1881	8173
1883	8174
1879	8188
1994	8186
1997	
1989	

The following sections report measured IPL data for the aircraft listed. Figures 4.1-6 to 4.1-10 show the IPL results for B737 systems, and Figures 4.1-11 to 4.1-16 show the IPL results for B747 systems. These plots show IPL versus window/door locations where the transmit antenna radiated. It is important to note that the window/door IPL data are similar to the data reported [22], except data in [22] were normalized to the 1-meter path loss measurement. Similar to IPL data in RTCA/DO-199 and RTCA/DO-233, data in this document are not normalized to the 1-meter path loss measurement.

In addition to the window and door locations, IPL measurements were also conducted at each of the seats, including one measurement between two adjacent seats on the left half of two B737 aircraft. As a result, each full aircraft (nose number 1989 and 1997) measurement provided approximately 160 locations (times two for two transmit antenna polarizations) rather than about 36 window and door locations. Only the window and door measurements are shown in Figures 4.1-6 to 4.1-10. Statistics of the IPL data, including the minimum and the average IPL, are shown in Tables 4.2-1 to 4.2-6.

Comparing the window/door data against the full aircraft data for these two B737s (nose number 1989 to 1997), it can be recognized that the window/door measurements capture the *minimum* IPL for the systems on those aircraft. Also, the differences in *average* IPL values are not significant. This comparison validates the common understanding that the minimum IPL occurs at window and door locations, at which most measurements on other aircraft were made.

On these plots, IPL for each receiver system on each aircraft is represented by two traces for the two vertical and horizontal polarizations of the transmit antennas. The window locations are simply labeled as the n^{th} side window starting from the cockpit. The door locations are labeled as "L1" and "L2" for left side doors; "S1" and "S2" for right side doors; and "EE" for emergency exits. At the doors, a sweep was typically conducted with the transmit antenna scanning along the door seam. A door sweep at L1 is labeled as "L1 Dr Swp".

It was observed that the IPL for both B737 and B747 aircraft generally had a dip in magnitude when the transmitter was located in the vicinity of a door. The magnitude of the dip was significant for GS, LOC, VHF Comm and SatCom systems, and it was not observable for TCAS and GPS systems. For GS and LOC, the dip in magnitude near the door location did not affect the minimum IPL. On the other hand, the magnitude of the dip was about 20 dB for VHF, and about 10 dB for SatCom on B747 aircraft. Comparing with SatCom IPL data, GPS IPL data did not show similar behavior, even though both systems operate in a similar frequency range. The main difference was that the SatCom antenna was mounted in the vicinity of a door.

B737-200 IPL Results

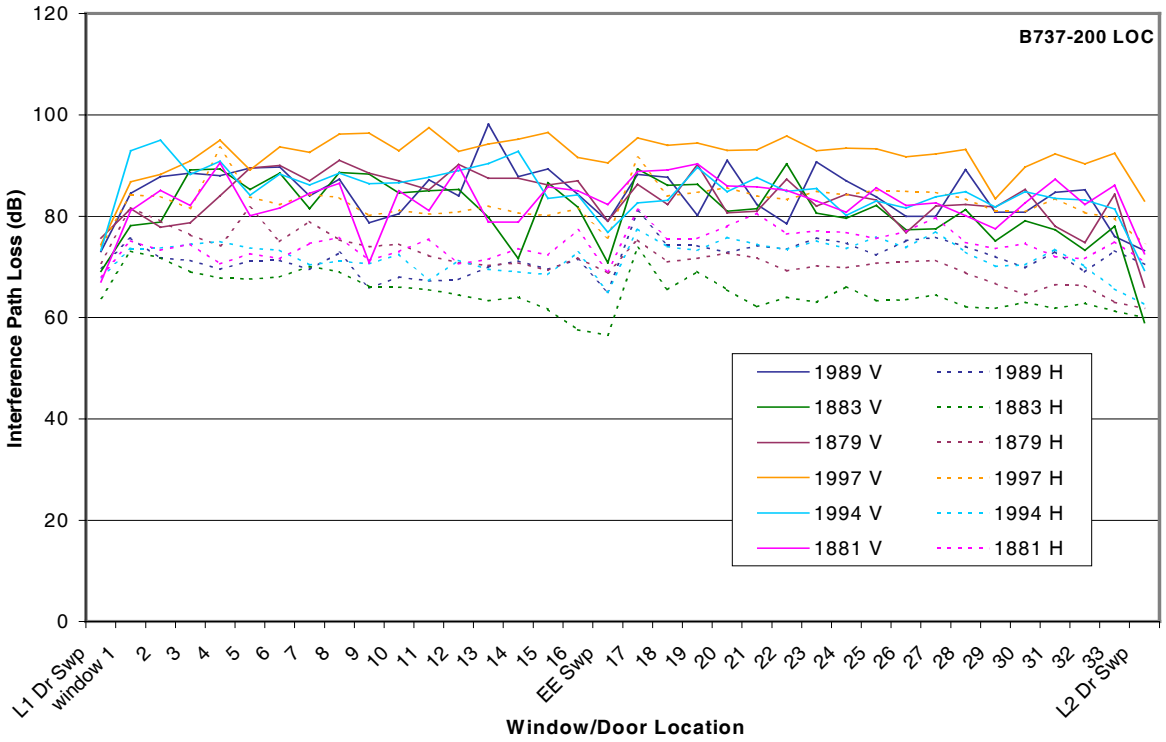

Figure 4.1-6: B737-200 LOC/VOR (Tail) interference path loss. Left windows/doors excitation.

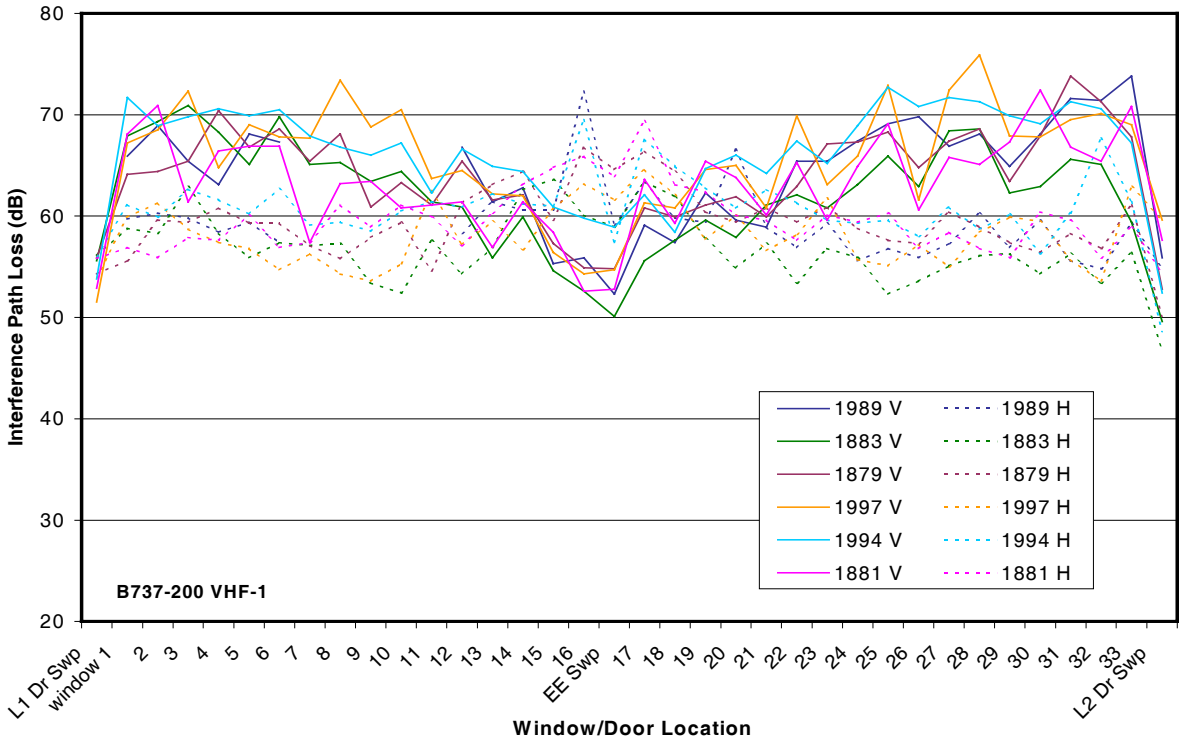

Figure 4.1-7: B737-200 VHF-1 Comm. (Top) interference path loss. Left windows/doors excitation.

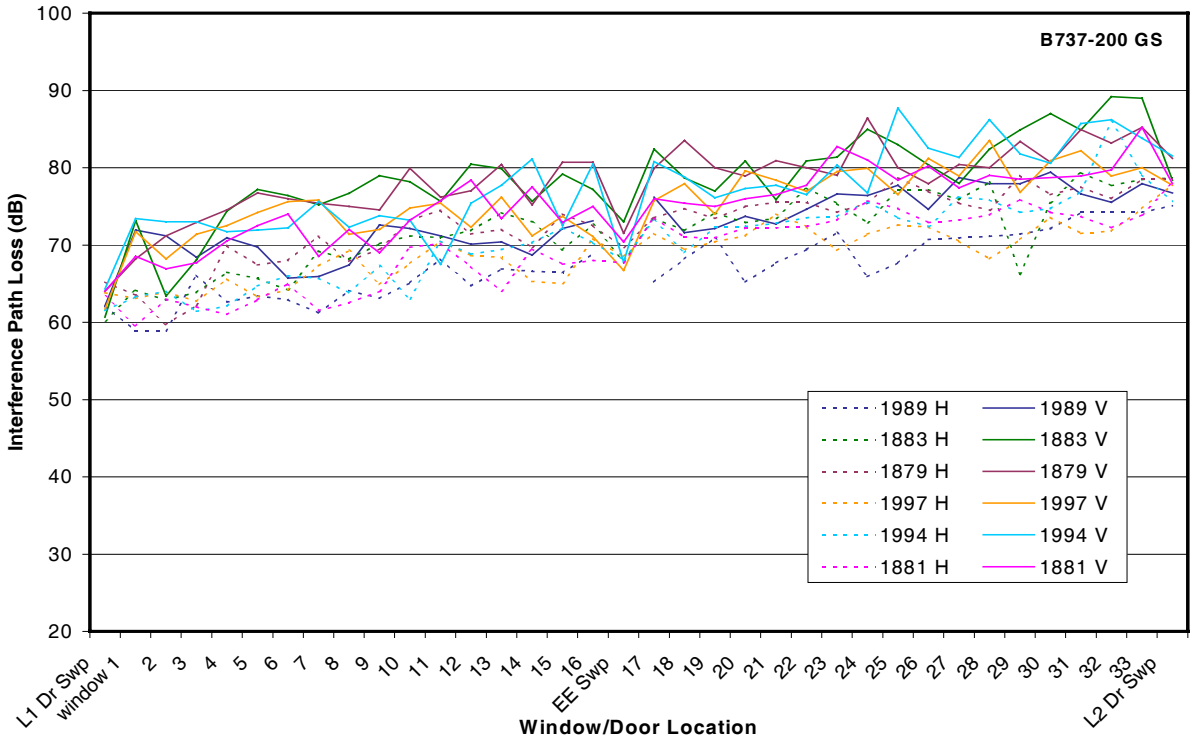

Figure 4.1-8: B737-200 GS (Nose) interference path loss. Left windows/doors excitation.

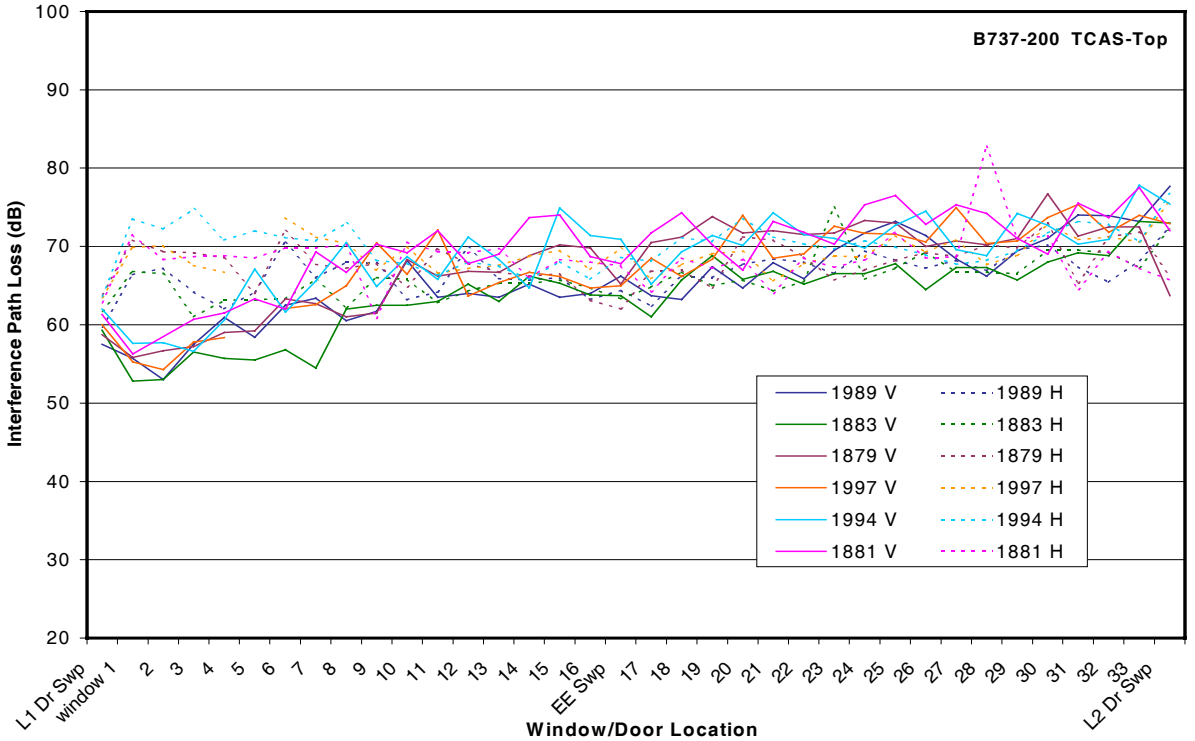

Figure 4.1-9: B737-200 TCAS (Top) interference path loss. Left windows/doors excitation.

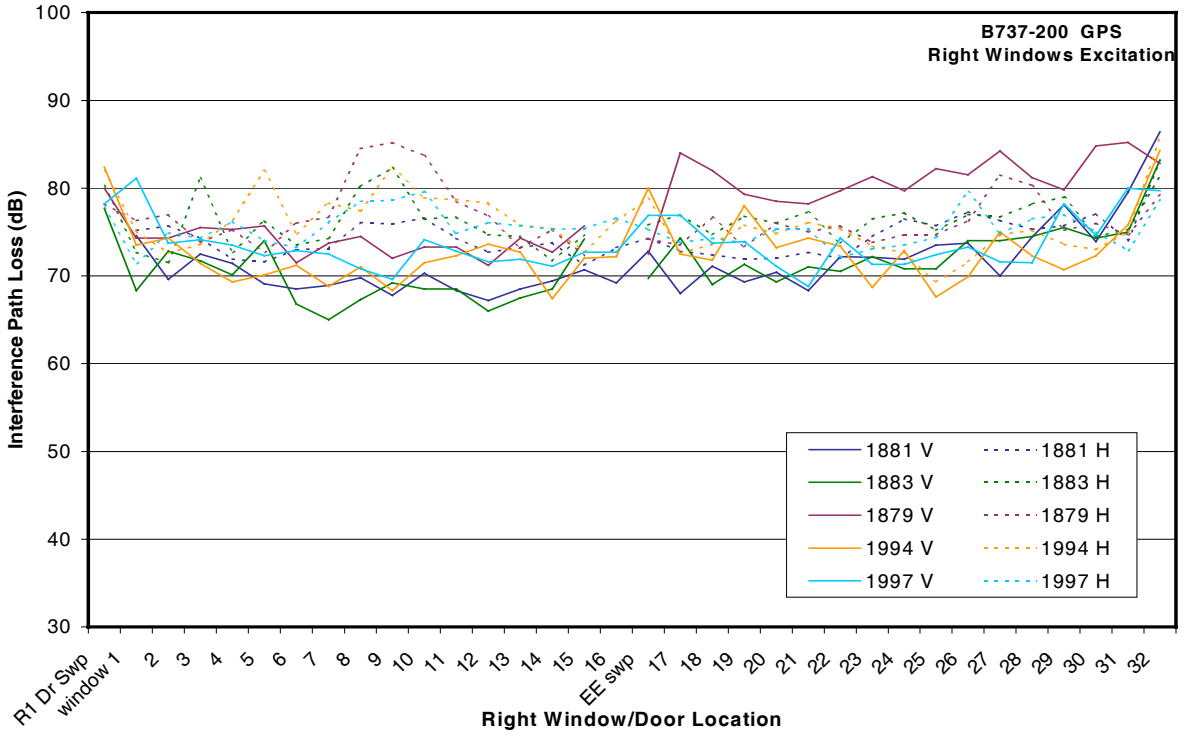

Figure 4.1-10a: B737-200 GPS interference path loss. Right windows/doors excitation.

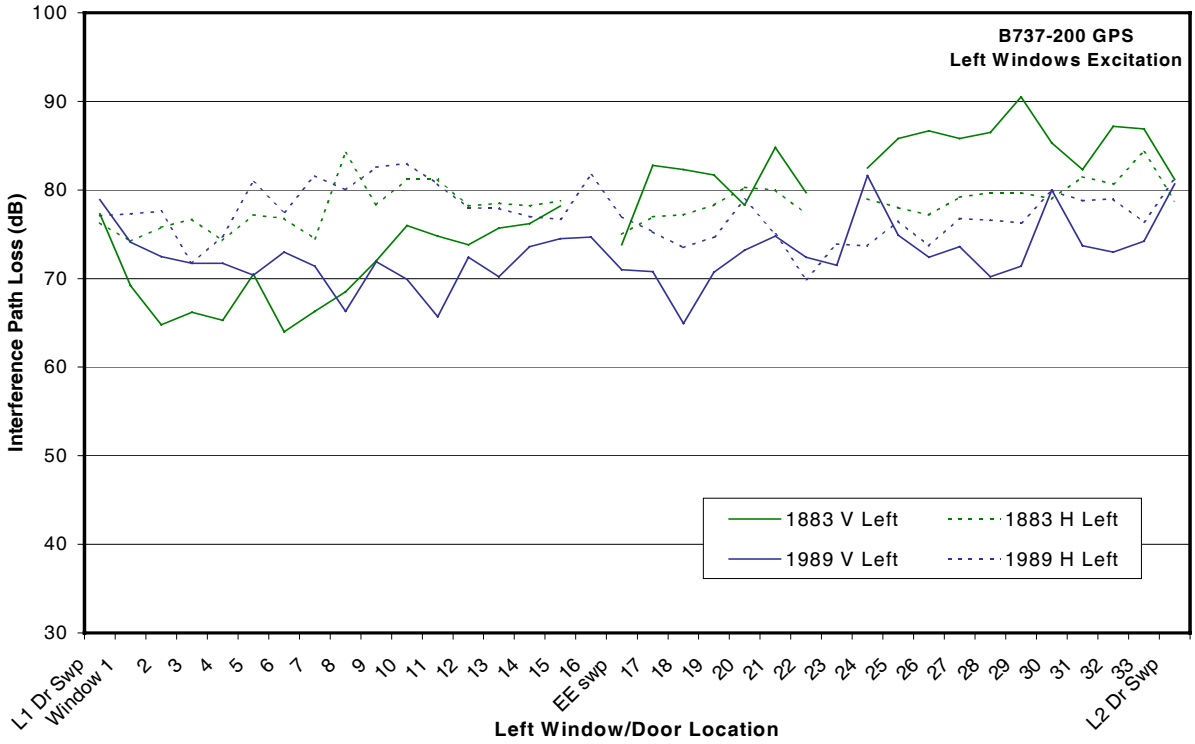

Figure 4.1-10b: B737-200 GPS interference path loss. Left windows/doors excitation.

B747-400 IPL Results

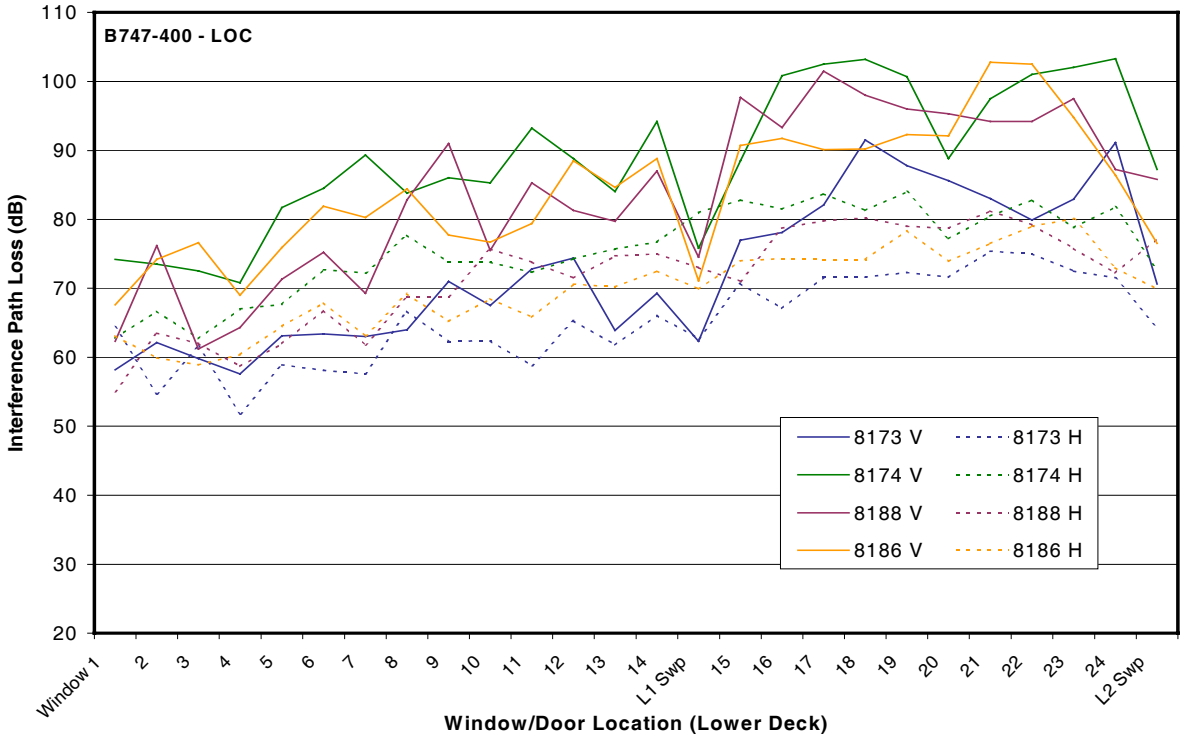

Figure 4.1-11: B747-400 LOC/VOR (Nose) IPL. Lower deck, left windows/doors excitation.

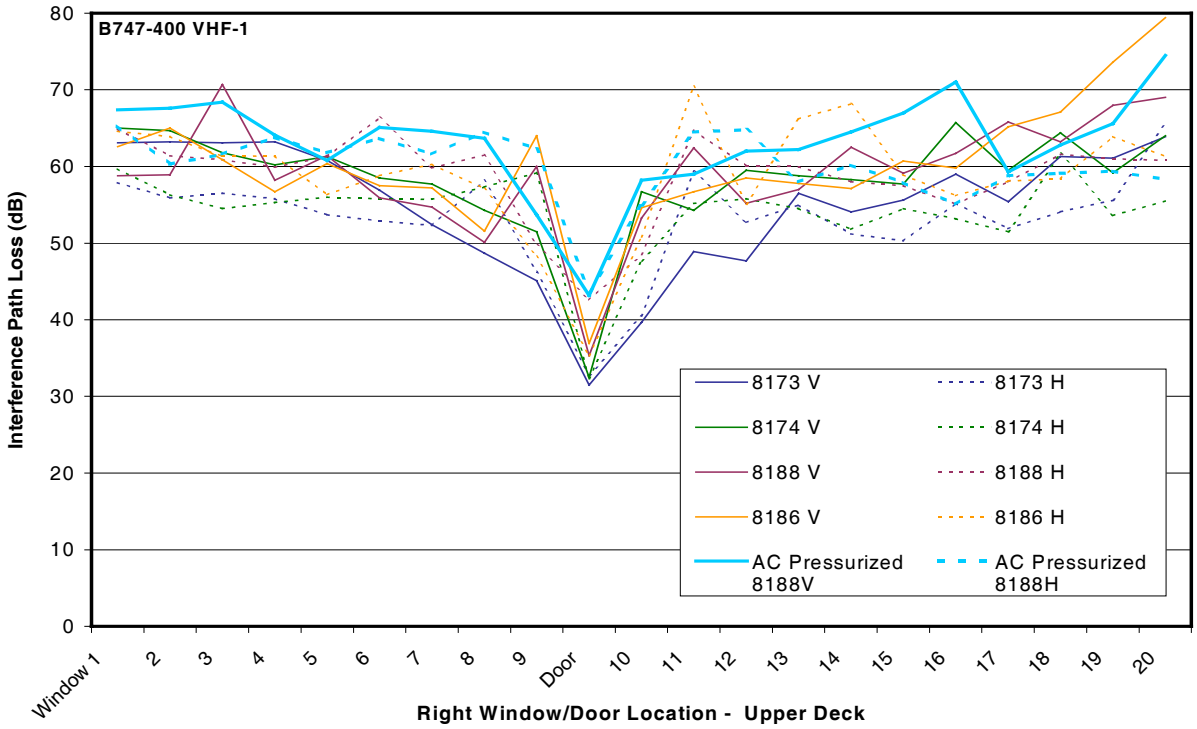

Figure 4.1-12: B747-400 VHF (Top) interference path loss. Upper deck, right windows/doors excitation.

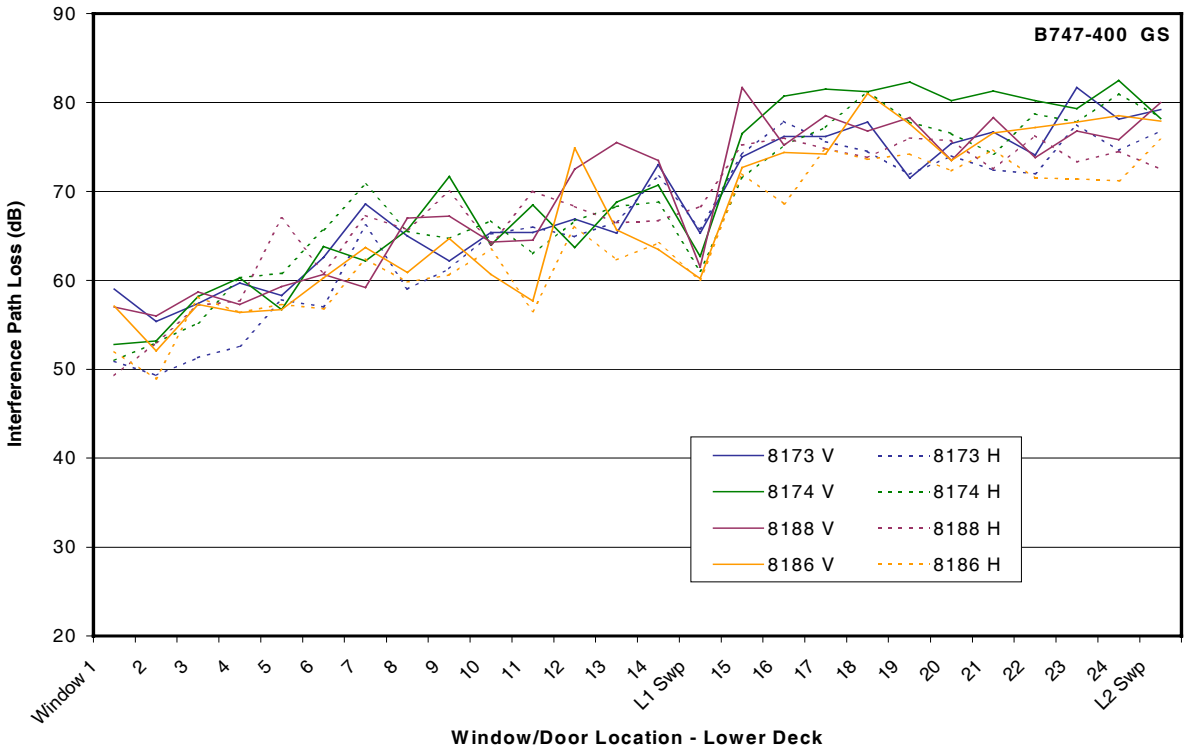

Figure 4.1-13: B747-400 GS (Nose) interference path loss. Lower deck, left windows/doors excitation.

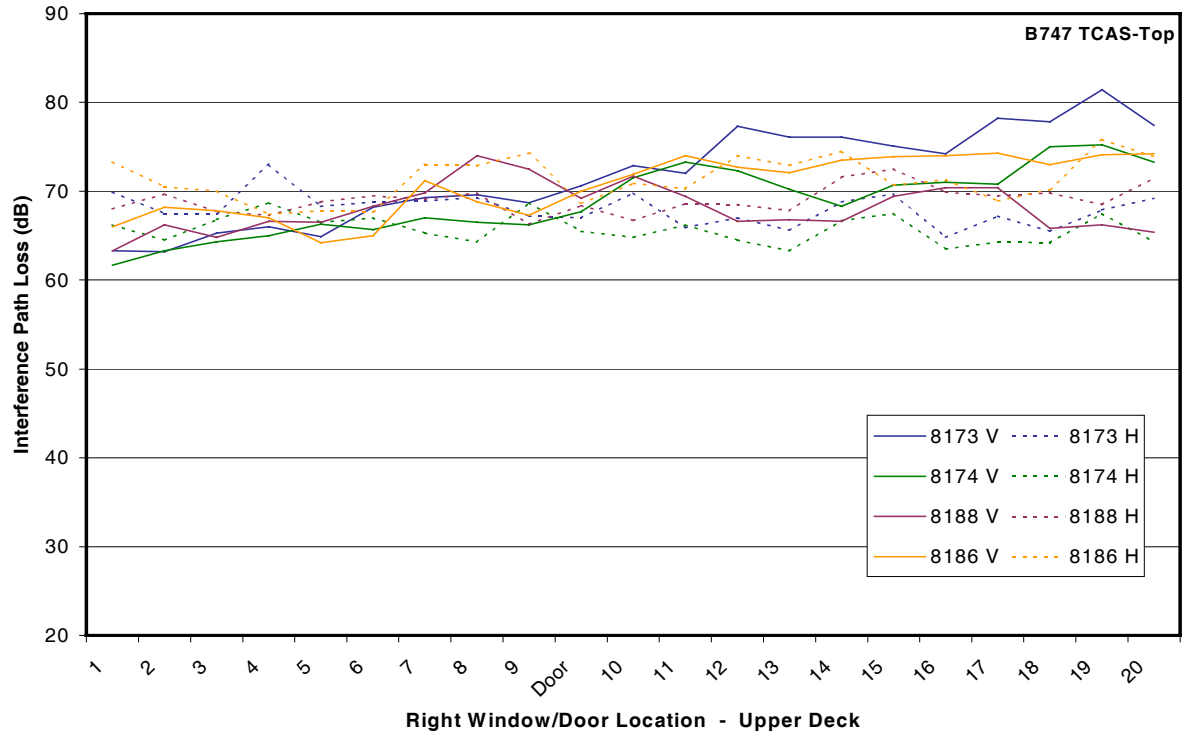

Figure 4.1-14: B747-400 TCAS (Top) interference path loss. Upper deck, right windows/doors excitation.

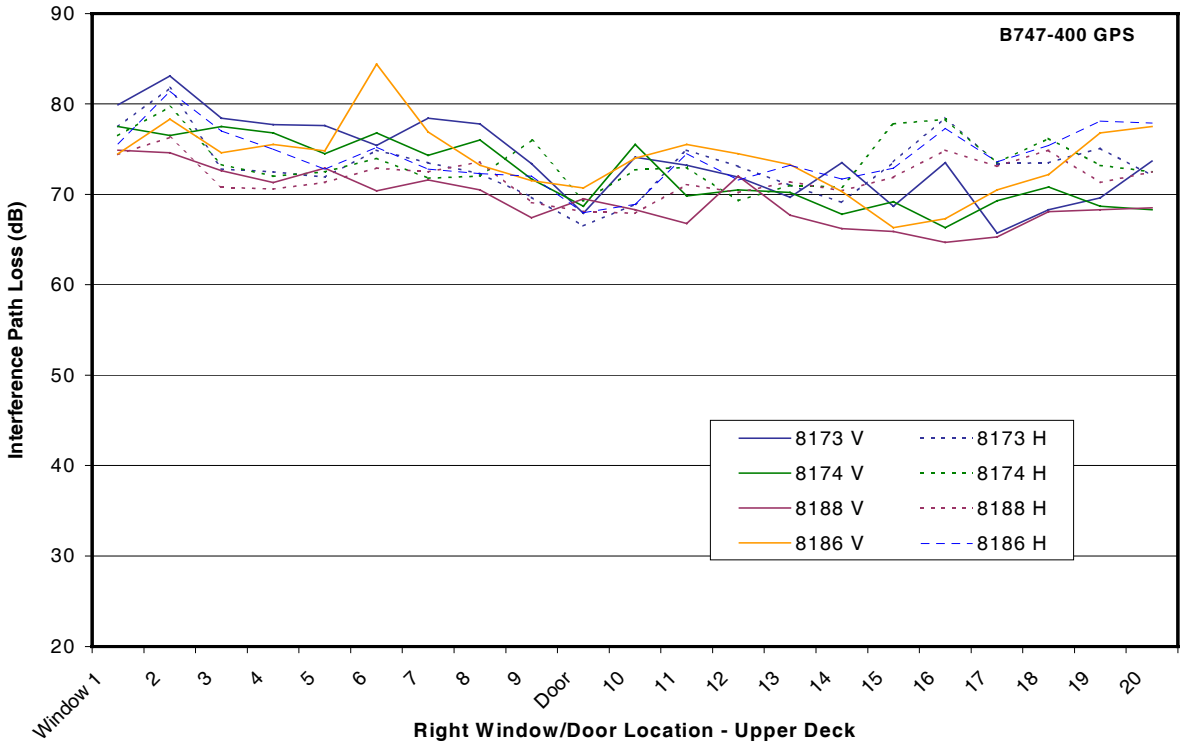

Figure 4.1-15: B747-400 GPS (Top) interference path loss. Upper deck, right windows/doors excitation.

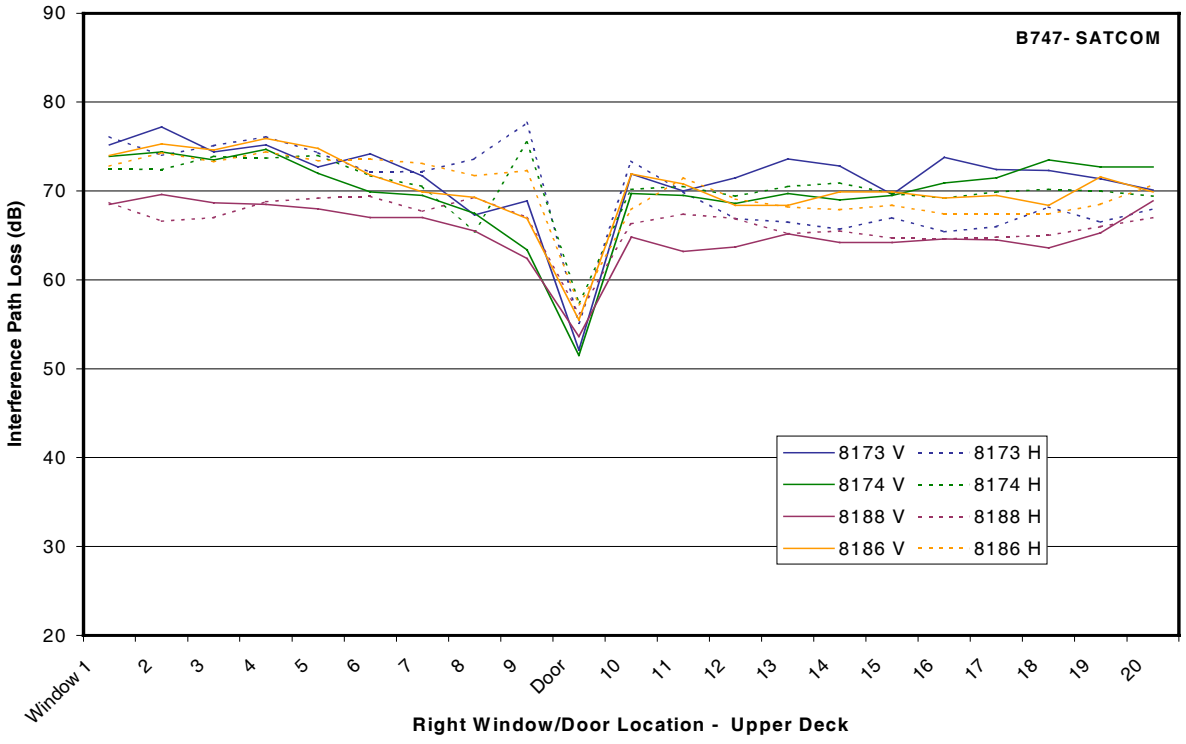

Figure 4.1-16: B747-400 SatCom interference path loss. Upper deck, right windows/doors excitation.

.

This phenomenon indicates that the minimum IPL is strongly influenced by the antenna mounting locations relative to a door. Variations in IPL by 10 or 20 dB due to antenna installation can be expected for any system, not just SatCom and VHF-Comm.

IPL for VHF on a B747 aircraft was also measured with the aircraft partially pressurized. Figure 4.1-12 indicates that by partially pressurizing the passenger cabin, IPL can increase by about 10 dB for a VHF system (with the antenna mounted near a door). Thus, pressurizing an aircraft can have a positive effect by reducing RF leakage through the door, and can increase the IPL.

Effects of Closed Cockpit Windows

In almost all IPL measurements shown in Figures 4.1-6 to 4.1-16, the aircraft cockpit windows were often taped closed with aluminum foil. This condition helped to preserve the aircraft interior while these aircraft were in storage. Due to various reasons, the measurement team did not have authorization to have the foil removed. The concern is whether this configuration could have affected the minimum IPL results, especially for the systems with antennas located close to cockpit windows. The side windows have built-in shades that help to block light when closed, so they were not taped like the cockpit windows. Figure 4.1-16 shows an example of a B737 and B747 aircraft with the cockpit windows previously taped and the proximity of the antenna behind the nose radome relative to the cockpit and side windows for both airplanes.

It is important to assess the impact of taped cockpit windows on the minimum path loss value. The primary systems of concern are those with antennas in the aircraft nose such as LOC and GS on B747 aircraft and GS on B737 aircraft. These antennas are much closer to the cockpit windows than those on top of the aircraft.

To address this concern, data from a previous cooperative effort with Delta Airlines (with the technical support from EWI) were considered [23]. As a result of the cooperative effort, IPL data were available for a B757 aircraft, but without aluminum foil on the cockpit windows. The same procedure used in this effort was also used for the B757 IPL measurement.

In addition to the usual window and door locations, IPL was also measured with a transmit antenna in the cockpit radiating out of the cockpit windows. The transmit antenna was scanned around to illuminate different parts of the cockpit windows to ensure the maximum coupling mechanisms were captured. The results for LOC and GS are shown in Figures 4.1-18 and 4.1-19. Both of these systems have their antennas behind the nose radome close to the cockpit. It is important to note that data shown in Figures 4.1-18 and 4.1-19 are different from the data reported in [23]. Data in [23] have IPL results normalized to 1-meter measurements, whereas data in this report do not.

Figures 4.1-18 and 4.1-19 show that the cockpit IPL data for both LOC and GS were lower than the IPL at *most* other locations. However, they were *not* the lowest in either case. In fact, they were higher than the lowest IPL at the side windows or door by 2-5 dB.

Data shown in Figures 4.1-18 and 4.1-19 provided the assurance that cockpit IPL data do not impact the minimum path loss value for GS and LOC (in the nose) in a significant way. Other window and door locations can result in lower IPL. For *passenger operated* PED interference, cockpit IPL is much less relevant since most devices will be located within the passenger cabin.

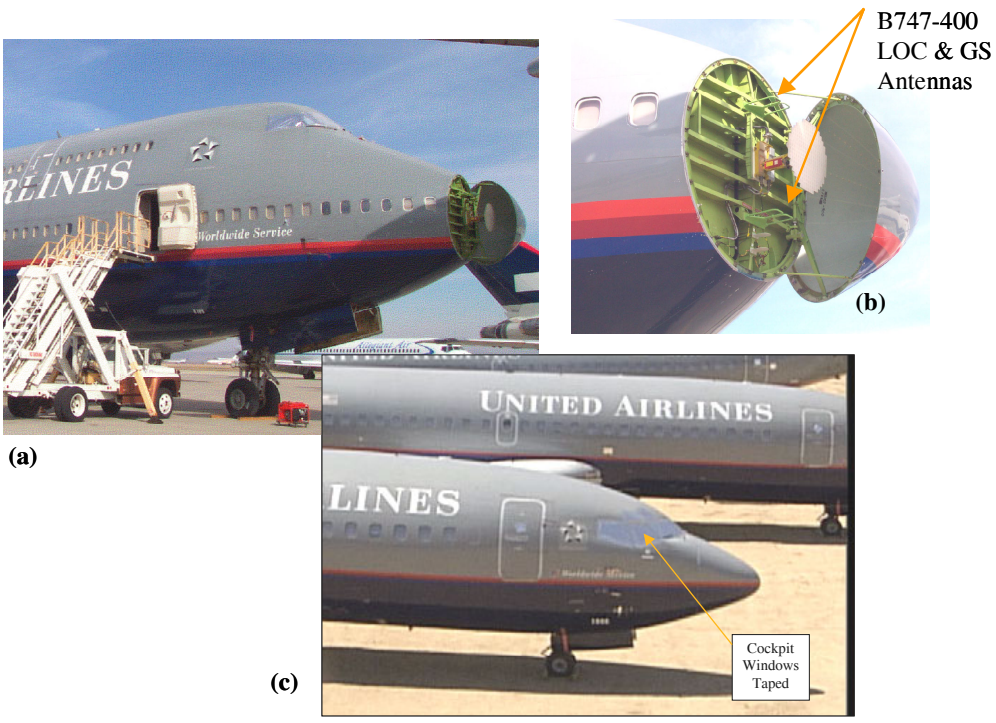

Figure 4.1-17: (a) B747-400 and (c) B737-200 aircraft with cockpit windows taped. Note the cockpit and side window locations relative to the antennas on top and in the nose cone. (b) Horizontally polarized GS and LOC antennas were located behind the nose cone.

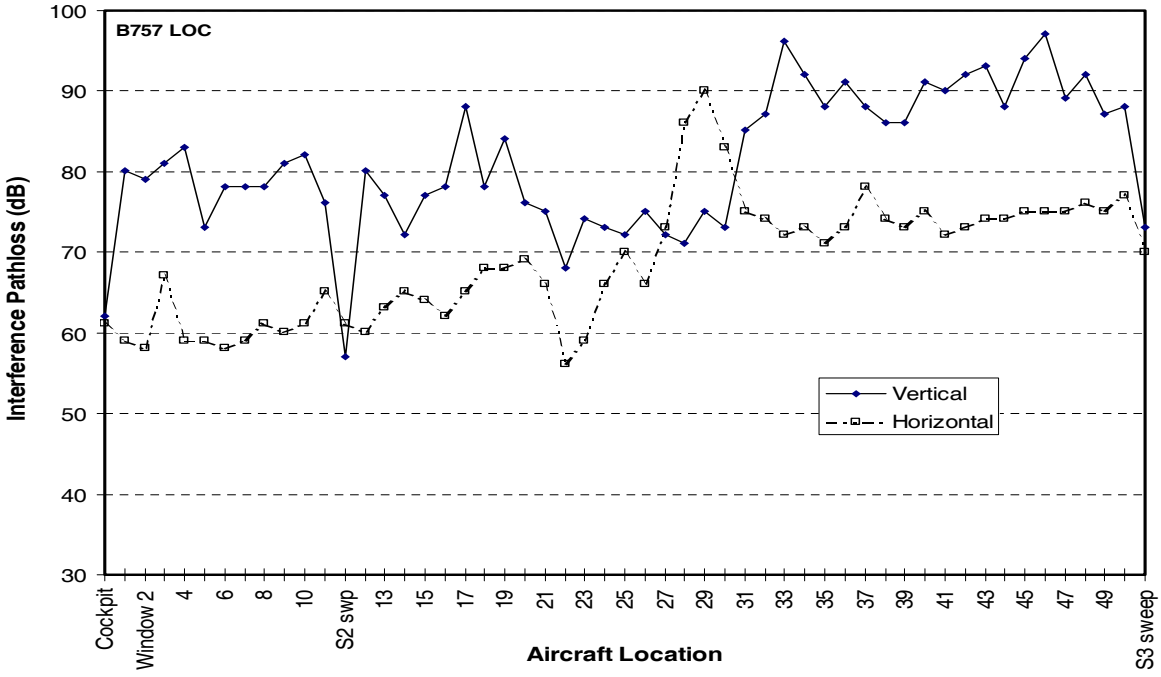

Figure 4.1-18: B757 LOC window/door path loss. Cockpit windows were not taped.

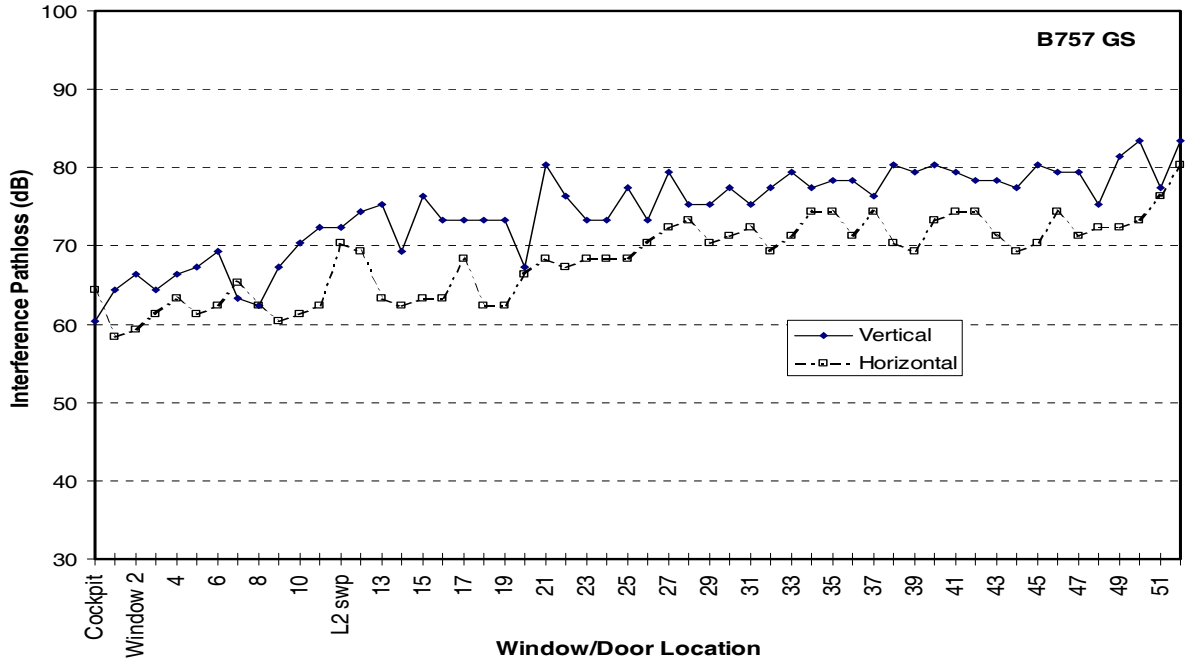

Figure 4.1-19: B757 GS window/door path loss. Cockpit windows were not taped.

For a B747 aircraft, Figure 4.1-17(b) shows that the side windows are much closer to the aircraft antennas behind the radome than the cockpit windows. Comparing the distance from the cockpit windows to the nose or top antennas, Figure 4.1-17 shows that the *upper deck* windows are closer to the top antennas, and the *lower deck* windows are closer to the nose antennas. Based on B757 cockpit data shown in Figures 4.1-18 and 4.1-19, it is expected that B747 cockpit IPL will not affect (lower) the minimum IPL significantly.

4.2 Other Interference Path Loss Data

In addition to the data previously presented, there are other IPL data previously reported in various documents. These documents include RTCA/DO-199 [2], DO-233 [3], a Veda [5] report, including those from the cooperative agreement between NASA and Delta Airlines [23]. Most of these data were previously summarized in the report on interference effects of cellular phones to aircraft radio-navigation receivers [1]. For completeness, they are again reported in Tables 4.2-1 to 4.2-7 along with the recently-measured B747 and B737 IPL data.

In RTCA/DO-199 (Appendix A), most reported papers used the same definition for IPL as shown in Eq. 4.1-1, but with a correction for transmit antenna gain. Namely,

$$PLF = (Tx\ Power\ in\ dBm) - (Rx\ Power\ in\ dBm) + (Tx\ Antenna\ Gain\ in\ dB), \qquad \text{(Eq. 4.2-1)}$$

where

PLF is Path Loss Factor, and

Tx and *Rx* are *Transmit* and *Receive* (Antennas), respectively.

There were also test papers in RTCA/DO-199 with PLF calculated *without* the correction applied (paper SC156-110), and the transmit antenna gain factors were not provided. In these cases, the path loss definition is the same as in Eq. 4.1-1.

Boeing 757 path loss data from papers RTCA/DO-199 SC156-26, -65 and -186 for VOR, LOC, VHF Comm. and GS are not reported in Tables 4.2-1 to 4.2-7. These papers defined transmit power in a way not directly comparable with definitions used in this document, RTCA/DO-233, and the remaining papers in RTCA/DO-199. Data from these papers resulted in unusually low path loss values and are excluded from the minimum IPL estimation in Table 4.3-1 and the interference safety margin calculations in Section 5.

In RTCA/DO-233, *PLF* calculations "may" include *Tx* antenna gain. Antenna factors were given for a dipole antenna used but not for other transmit antennas.

The main difference between the path loss definition in this document and the definition used in parts of RTCA/DO-199 and RTCA/DO-233 is whether the transmit antenna's free-space antenna factors are included in the path loss data provided. In this document, it is assumed that the environment is far from free space and that free-space antenna factors are not valid correction factors. The true transmit antenna factors are not known, and are not included in the path loss calculations. However, free-space antenna factors for the antennas used are provided in Table 4.1-1.

In Tables 4.2-1 to 4.2-7, IPL was reported for LOC, GS, VHF Comm., SatCom, TCAS, and GPS. Data were grouped into large, medium, and small aircraft categories. For each aircraft measured, the minimum IPL (MIPL), the average IPL and the standard deviation (StDev) were reported. The new B747 and B737 data in these tables were computed from Figures 4.1-6 to 4.1-16. They were computed from the combined data for both vertical and horizontal polarizations.

The number of measurement points and measurement frequency range were also reported when available. The number of measurement points was often reported as a *number times 2*, i.e. "*26x2*". This notation indicated that both transmit antenna polarizations, vertical and horizontal, were used at each measurement location, effectively doubling the number of data points. Thus, "26x2" indicated measurements were taken at 26 locations, with vertical and horizontal polarized source antenna, resulting in 52 data points.

The statistics of the MIPL for each large, medium and small aircraft category were also reported. In addition, statistics of the MIPL calculated using ALL available data were shown at the end of each table and again in Table 4.3-1. These statistics include the lowest MIPL and the average MIPL for the safety margin calculations in Section 5.

Table 4.2-1: LOC IPL

New Data	Aircraft & Model	Interference Path Loss (IPL) (dB)			No. of Meas.	Test Freq. Range (MHz)
		Min (MIPL)	Average	StDev		
	Large Aircraft					
✓	B747 8173 (UAL/EWI/NASA)	51.8	68.8	9.4	26x2	108-118
✓	B747 8174 (UAL/EWI/NASA)	62.7	82.3	10.9	26x2	108-118
✓	B747 8188 (UAL/EWI/NASA)	55.0	77.7	11.6	26x2	108-118
✓	B747 8186 (UAL/EWI/NASA)	58.9	77.0	10.6	26x2	108-118
	B747 (DO-233)	64.8	93.9	12.7		
	B747 (EWI/UAL)	55.0	61.0	2.0	38	
	DC10 (DO-199)	82.0	91.0		10	108
	L1011 (DO-233)	60.7	85.2	9.4		
	Column Minimum	***51.8***	***61.0***			
	Column Average	***61.4***	***79.6***			
	Column Maximum	***82.0***	***93.9***			
	Medium Aircraft					
✓	B737 1989 Windows (UAL/EWI/NASA)	65.0	78.1	7.7	36x2	108-118
✓	B737 1989 Full (UAL/EWI/NASA)	65.0	81.7	5.6	156x2	108-118
✓	B737 1883 (UAL/EWI/NASA)	56.5	73.0	9.8	36x2	108-118
✓	B737 1879 (UAL/EWI/NASA)	61.8	77.5	7.7	36x2	108-118
✓	B737 1997 (UAL/EWI/NASA)	74.2	87.3	6.2	36x2	108-118
✓	B737 1994 (UAL/EWI/NASA)	62.6	78.5	7.9	36x2	108-118
✓	B737 1881 (UAL/EWI/NASA)	67.0	78.6	6.0	36x2	108-118
	B737 (DO-233)	72.7	90.7	8.8		
	B757 (DO-233)	51.5	86.1	11.4		
	B757 (Delta/EWI/NASA)	56.1	75.3	10.2	52x2	
	B727 -a (DO-199)	63.0	67.0		6	108-112
	B727 -b (DO-199)	35.0	53.0		86	108-112
	B727 (RTCA/SC-177)	72.0	90.0			
	A320 (DO-233)	48.8	85.7	14.8		
	A320 (Aerospatiale)	54.0	75.0			
	Column Minimum	***35.0***	***53.0***			
	Column Average	***60.3***	***78.5***			
	Column Maximum	***74.2***	***90.7***			
	Small Aircraft					
	Canadair RJ (Delta/EWI/NASA)	57.9	71.6	6.6	14x2	
	Emb 120 (Delta/EWI/NASA)	41.8	56.3	4.5	11x2	
	ATR72 (Delta/EWI/NASA)	63.9	72.1	4.2	25x2	
	Column Minimum	***41.8***	***56.3***			
	Column Average	***54.5***	***66.7***			
	Column Maximum	***63.9***	***72.1***			

Table 4.2-1: Concluded

All Aircraft Column Minimum	**35.0**	**53.0**
All Aircraft Column Average	**60.0**	**77.5**
All Aircraft Column Maximum	**82.0**	**93.9**
All Aircraft Standard Deviation	**10.0**	**10.4**

Table 4.2-2: VHF Comm IPL

New Data	Aircraft & Model	Interference Path Loss (IPL) (dB)			No. of Meas.	Test Freq. Range (MHz)
		Min (MIPL)	Average	StDev		
	Large Aircraft					
✓	B747 8173 (UAL/EWI/NASA)	31.5	53.9	7.7	21x2	116-138
✓	B747 8174 (UAL/EWI/NASA)	32.3	56.3	6.7	21x2	116-138
✓	B747 8188 (UAL/EWI/NASA)	35.3	58.9	6.6	21x2	116-138
✓	B747 8186 (UAL/EWI/NASA)	35.3	59.5	7.9	21x2	116-138
✓	B747 8188 (UAL/EWI/NASA) (AC Pressurized)	43.2	61.5	5.9	21x2	116-138
	B747 -VHF1 (DO-233)	40.5	79.2	12.0		
	B747 -VHF2 (DO-233)	63.2	86.2	10.8		
	B747 -VHF3 (DO-233)	71.5	92.9	7.4		
	DC 10 (DO-199)	63.0	80.0		45	117-137
	L1011 -VHF1 (DO-233)	56.2	72.9	6.1		
	L1011 -VHF2 (DO-233)					
	L1011 -VHF3 (DO-233)	62.2	77.2	4.2		
	Column Minimum	***31.5***	***53.9***			
	Column Average	***48.6***	***70.8***			
	Column Maximum	***71.5***	***92.9***			
	Medium Aircraft					
✓	B737 1989 (UAL/EWI/NASA)	52.3	61.9	5.2	36x2	116-138
✓	B737 1883 (UAL/EWI/NASA)	46.8	59.3	5.2	36x2	116-138
✓	B737 1879 (UAL/EWI/NASA)	50.1	61.6	4.7	36x2	116-138
✓	B737 1997 Windows (UAL/EWI/NASA)	51.5	61.9	5.8	36x2	116-138
✓	B737 1997 Full (UAL/EWI/NASA)	51.5	65.8	4.3	173x2	116-138
✓	B737 1994 (UAL/EWI/NASA)	48.6	63.5	5.1	36x2	116-138
✓	B737 1881 (UAL/EWI/NASA)	52.6	61.2	4.5	36x2	116-138
	B737 -VHF1 (DO-233)	52.9	69.0	7.6		
	B737 -VHF2 (DO-233)	58.4	74.2	9.3		
	B737 -VHF3 (DO-233)	53.2	76.2	9.6		
	B757 -VHF1 (DO-233)	49.7	72.9	9.8		
	B757 -VHF2 (DO-233)	38.0	64.7	8.7		
	B757 -VHF3 (DO-233)	53.0	79.3	8.7		
	B757-VHF-Left (Delta/EWI/NASA)	36.3	52.8	7.4	56x2	
	B757-VHF-Right (Delta/EWI/NASA)	49.3	60.6	6.2	38x2	
	B757-VHF-Center (Delta/EWI/NASA)	50.3	64.0	6.7	55x2	
	B727 N40 -a (DO-199)	67.0	71.0		6	118-135
	B727 N40 -b (DO-199)	44.0	53.0		49	118-135
	B727 N40 -c (DO-199)	76.0	80.0		6	109

Table 4.2-2: Concluded

MD80-VHF1 (DO-233)	57.2	74.5	9.2	
MD80-VHF2 (DO-233)	64.9	81.7	10.0	
MD80-VHF3 (DO-233)	55.2	81.7	13.3	
A320 -VHF1 (DO-233)	51.5	70.0	8.4	
A320 -VHF2 (DO-233)	62.1	77.6	6.7	
A320 -VHF3 (DO-233)	55.6	76.2	7.4	
Column Minimum	***36.3***	***52.8***		
Column Average	***53.1***	***68.6***		
Column Maximum	***76.0***	***81.7***		
Small Aircraft				
CRJ VHF-L (Delta/EWI/NASA)	36.7	53.7	7.6	14x2
CRJ VHF-R (Delta/EWI/NASA)	50.9	62.3	6.0	14x2
Emb 120 -VHF-L (Delta/EWI/NASA)	28.7	47.0	7.3	12x2
Emb 120 -VHF-R (Delta/EWI/NASA)	45.0	53.5	3.7	11x2
ATR72- VHF-L (Delta/EWI/NASA)	48.4	61.3	8.2	13x2
ATR72- VHF-R (Delta/EWI/NASA)	43.5	60.0	6.3	26x2
Column Minimum	***28.7***	***47.0***		
Column Average	***42.2***	***56.3***		
Column Maximum	***50.9***	***62.3***		
All Aircraft Column Minimum	**28.7**	**47.0**		
All Aircraft Column Average	**50.4**	**67.4**		
All Aircraft Column Maximum	**76.0**	**92.9**		
All Aircraft Standard Deviation	**10.9**	**10.6**		

Table 4.2-3: VOR IPL

New Data	Aircraft & Model	Interference Path Loss (IPL) (dB)			No. of Meas.	Test Freq. Range (MHz)
		Min (MIPL)	Average	StDev		
	Large Aircraft					
✓	B747 8173 (UAL/EWI/NASA)	51.8	68.8	9.4	26x2	108-118
✓	B747 8174 (UAL/EWI/NASA)	62.7	82.3	10.9	26x2	108-118
✓	B747 8188 (UAL/EWI/NASA)	55.0	77.7	11.6	26x2	108-118
✓	B747 8186 (UAL/EWI/NASA)	58.9	77.0	10.6	26x2	108-118
	B747 (DO-233)	84.7	105.0	5.1		
	B747 (EWI/UAL)	76.0	80.0	3.0	8	
	DC 10 (DO-199)	80.0	89.0		20	113-117
	L1011 (DO-233)	70.3	79.0	2.0		
	Column Minimum	***51.8***	***68.8***			
	Column Average	***67.4***	***82.4***			
	Column Maximum	***84.7***	***105.0***			
	Medium Aircraft					
✓	B737 1989 Windows (UAL/EWI/NASA)	65.0	78.1	7.7	36x2	108-118
✓	B737 1989 Full (UAL/EWI/NASA)	65.0	81.7	5.6	156x2	108-118
✓	B737 1883 (UAL/EWI/NASA)	56.5	73.0	9.8	36x2	108-118
✓	B737 1879 (UAL/EWI/NASA)	61.8	77.5	7.7	36x2	108-118
✓	B737 1997 (UAL/EWI/NASA)	74.2	87.3	6.2	36x2	108-118
✓	B737 1994 (UAL/EWI/NASA)	62.6	78.5	7.9	36x2	108-118
✓	B737 1881 (UAL/EWI/NASA)	67.0	78.6	6.0	36x2	108-118
	B737 (DO-233)	76.0	90.0	5.0		
	B757 (DO-233)	49.9	90.7	9.9		
	B757 (Delta/EWI/NASA)	46.7	65.8	6.8	56x2	
	B727-a (DO-199)	70.0	74.0		6	112-117
	B727 -b (DO-199)	30.0	56.0		86	112-117
	B727-c (DO-199)	71.0	76.0		6	109-120
	B727 (RTCA/SC-177)	75.0	90.0			
	CV-580 (Veda/FAA)	45.0				
	MD80 (DO-233)	66.2	87.8	9.4		
	A320 (DO-233)	65.0	91.9	8.7		
	A320 (Aerospatiale)	59.0	84.0			
	Column Minimum	***30.0***	***56.0***			
	Column Average	***61.4***	***80.1***			
	Column Maximum	***76.0***	***91.9***			

Table 4.2-3: Concluded

Small Aircraft				
Canadair RJ (Delta/EWI/NASA)	57.9	71.6	6.6	14x2
Emb 120 (Delta/EWI/NASA)	41.8	56.3	4.5	11x2
ATR72 (Delta/EWI/NASA)	63.9	72.1	4.2	25x2
Column Minimum	***41.8***	***56.3***		
Column Average	***54.5***	***66.7***		
Column Maximum	***63.9***	***72.1***		
All Aircraft Column Minimum	**30.0**	**56.0**		
All Aircraft Column Average	**62.4**	**79.3**		
All Aircraft Column Maximum	**84.7**	**105.0**		
All Aircraft Standard Deviation	**12.2**	**10.6**		

Table 4.2-4: GS IPL

New Data	Aircraft & Model	Interference Path Loss (IPL) (dB)			No. of Meas.	Test Freq. Range (MHz)
		Min (MIPL)	Average	StDev		
	Large Aircraft					
✓	B747 8173 (UAL/EWI/NASA)	49.3	67.6	8.4	26x2	325-340
✓	B747 8174 (UAL/EWI/NASA)	51.0	69.6	9.3	26x2	325-340
✓	B747 8188 (UAL/EWI/NASA)	49.3	68.8	7.9	26x2	325-340
✓	B747 8186 (UAL/EWI/NASA)	48.9	66.1	8.5	26x2	325-340
	B747 (DO-233)	54.6	86.2	14.1		
	B747 (EWI/UAL)	53.0	71.0	8.0	36	
	DC10 (DO-199)	77.0	91.0		24	329-335
	L1011 (DO-233)	64.4	82.6	8.1		
	Column Minimum	***48.9***	***66.1***			
	Column Average	***55.9***	***75.4***			
	Column Maximum	***77.0***	***91.0***			
	Medium Aircraft					
✓	B737 1989 (UAL/EWI/NASA)	58.9	70.1	5.0	36x2	325-340
✓	B737 1883 (UAL/EWI/NASA)	60.2	75.1	6.5	36x2	325-340
✓	B737 1879 (UAL/EWI/NASA)	59.7	75.4	5.5	36x2	325-340
✓	B737 1997 Windows (UAL/EWI/NASA)	61.7	72.2	5.2	36x2	325-340
✓	B737 1997 Full (UAL/EWI/NASA)	61.7	73.3	4.3	169x2	325-340
✓	B737 1994 (UAL/EWI/NASA)	61.4	73.9	6.5	36x2	325-340
✓	B737 1881 (UAL/EWI/NASA)	59.5	72.2	5.7	36x2	325-340
	B737 (DO-233)	68.8	83.1	4.9		
	B757 (DO-233)	57.5	83.0	9.9		
	B757 (Delta/EWI/NASA)	58.9	72.1	6.0	53x2	
	B727 (RTCA/SC-177)	68.0	83.0			
	B727 (DO-199)	68.0	76.0		12	328
	CV-580 (Veda/FAA)	64.0				
	MD80 (DO-233)	63.5	85.4	11.0		
	A320 (DO-233)	64.6	84.2	10.0		
	A320 (Aerospatiale)	*56.0*	70.0			
	Column Minimum	***56.0***	***70.0***			
	Column Average	***62.0***	***76.6***			
	Column Maximum	***68.8***	***85.4***			
	Small Aircraft					
	Canadair RJ (Delta/EWI/NASA)	51.6	59.7	3.2	14x2	
	Emb 120 (Delta/EWI/NASA)	46.2	51.5	2.3	10x2	
	ATR72	57.5	68.0	5.4	26x2	
	Column Minimum	***46.2***	***51.5***			
	Column Average	***51.8***	***59.7***			
	Column Maximum	***57.5***	***68.0***			

Table 4.2-4: Concluded

All Aircraft Column Minimum	**46.2**	**51.5**
All Aircraft Column Average	**59.1**	**74.3**
All Aircraft Column Maximum	**77.0**	**91.0**
All Aircraft Standard Deviation	**7.2**	**8.8**

Table 4.2-5: TCAS IPL

New Data	Aircraft & Model	Interference Path Loss (IPL) (dB)			No. of Meas.	Test Freq. Range (MHz)
		Min (MIPL)	Average	StDev		
	Large Aircraft					
✓	B747 8173 (UAL/EWI/NASA)	63.2	69.9	4.4	21x2	1080-1100
✓	B747 8174 (UAL/EWI /NASA)	61.7	67.3	3.3	21x2	1080-1100
✓	B747 8188 (UAL/EWI /NASA)	63.3	68.6	2.3	21x2	1080-1100
✓	B747 8186 (UAL/EWI /NASA)	64.2	71.0	3	21x2	1080-1100
	Column Minimum	***61.7***	***67.3***			
	Column Average	***63.1***	***69.2***			
	Column Maximum	***64.2***	***71.0***			
	Medium Aircraft					
✓	B737 1989 (UAL/EWI /NASA)	53.0	66.1	4.4	36x2	1080-1100
✓	B737 1883 (UAL/EWI /NASA)	52.8	64.8	4.3	36x2	1080-1100
✓	B737 1879 (UAL/EWI /NASA)	55.8	67.6	4.4	36x2	1080-1100
✓	B737 1997 Windows (UAL/EWI /NASA)	54.3	68.3	4.4	36x2	1080-1100
✓	B737 1997 Full (UAL/EWI /NASA)	54.3	70.9	3.8	179x2	1080-1100
✓	B737 1994 (UAL/EWI /NASA)	56.6	69.3	4.2	36x2	1080-1100
✓	B737 1881 (UAL/EWI /NASA)	56.3	69.0	4.5	36x2	1080-1100
	B757 (DO-233)	69.1	83.3	7.3		
	B757-TCAS-Top (Delta/EWI /NASA)	58.6	71.5	6.9	55x2	
	B757-TCAS-Bottom (Delta/EWI /NASA)	57.6	75.0	7.7	53x2	
	A320 -TCAS-T (DO-233)	54.8	74.6	11.3		
	A320 -TCAS-B (DO-233)	63.0	78.5	7.1		
	A320 (Aerospatiale)					
	Column Minimum	***52.8***	***64.8***			
	Column Average	***57.2***	***71.6***			
	Column Maximum	***69.1***	***83.3***			
	Small Aircraft					
	CRJ TCAS-Top(Delta/EWI /NASA)	53.1	59.2	4	14x2	
	CRJ TCAS-Bottom(Delta/EWI /NASA)	54.7	61.5	3.3	14x2	
	Emb 120 -TCAS-Top (Delta/EWI /NASA)	50.7	57.6	4.5	11x2	
	Emb 120 -TCAS-Bottom (Delta/EWI /NASA)	48.2	59.7	5.8	11x2	
	ATR72- TCAS-Top(Delta/EWI /NASA)					
	ATR72- TCAS-Bottom(Delta/EWI /NASA)					
	Column Minimum	***48.2***	***57.6***			
	Column Average	***51.7***	***59.5***			
	Column Maximum	***54.7***	***61.5***			
	All Aircraft Column Minimum	**48.2**	**57.6**			
	All Aircraft Column Average	**57.3**	**68.7**			
	All Aircraft Column Maximum	**69.1**	**83.3**			
	All Aircraft Standard Deviation	**5.3**	**6.4**			

Table 4.2-6: SatCom IPL

New Data	Aircraft & Model	Interference Path Loss (IPL) (dB)			No. of Meas.	Test Freq. Range (MHz)
		Min (MIPL)	Average	StDev		
	Large Aircraft					
✓	B747 8173 (UAL/EWI/NASA)	52.1	70.7	18.6	21x2	
✓	B747 8174 (UAL/EWI/NASA)	51.5	70.1	18.6	21x2	
✓	B747 8188 (UAL/EWI/NASA)	53.6	65.8	12.2	21x2	
✓	B747 8186 (UAL/EWI/NASA)	55.5	70.2	14.7	21x2	
	B747 (DO-233)	87.0	96.8	5.0		
	Column Minimum	**51.5**	***65.8***			
	Column Average	**59.9**	***74.7***			
	Column Maximum	***87.0***	***96.8***			
	Column Standard Deviation	***15.2***	***12.5***			

Table 4.2-7: GPS IPL

New Data	Aircraft & Model	Interference Path Loss (IPL) (dB)			No. of Meas.	Test Freq. Range (MHz)
		Min (MIPL)	Average	StDev		
	Large Aicraft					
✓	B747 8173 (UAL/EWI/NASA)	65.7	73.5	4.0	21x2	1565-1585
✓	B747 8174 (UAL/EWI/NASA)	66.3	72.9	3.3	21x2	1565-1585
✓	B747 8188 (UAL/EWI/NASA)	64.7	70.6	2.9	21x2	1565-1585
✓	B747 8186 (UAL/EWI/NASA)	66.3	74.0	3.5	21x2	1565-1585
	Column Minimum	***64.7***	***70.6***			
	Column Average	***65.8***	***72.8***			
	Column Maximum	***66.3***	***74.0***			
	Medium Aircraft					
✓	B737 1989 (UAL/EWI/NASA)	64.9	75.0	4.0	36x2	1565-1585
✓	B737 1883 (UAL/EWI/NASA)	64.0	76.0	5.3	76x2	1565-1585
✓	B737 1879 (UAL/EWI/NASA)	71.2	77.1	3.9	33x2	1565-1585
✓	B737 1997 (UAL/EWI/NASA)	68.8	74.5	2.7	34x2	1565-1585
✓	B737 1994 (UAL/EWI/NASA)	67.4	74.4	3.9	34x2	1565-1585
✓	B737 1881 (UAL/EWI/NASA)	67.2	73.0	3.5	33x2	1565-1585
	CV-580 (Veda/FAA)	41.0				
	B727 N40 (DO-199)	71.0	77.0		12	1575
	Column Minimum	***41.0***	***73.0***			
	Column Average	***64.4***	***75.3***			
	Column Maximum	***71.2***	***77.1***			
	Small Aircraft					
	Gulf G4 (DO-233)	82.4	91.4	5.7		
	CRJ (Delta/EWI/NASA)	43.2	53.5	6.1	14x2	
	Column Minimum	***43.2***	***53.5***			
	Column Average	***62.8***	***72.5***			
	Column Maximum	***82.4***	***91.4***			
	All Aircraft Column Minimum	**41.0**	**53.5**			
	All Aircraft Column Average	**64.6**	**74.1**			
	All Aircraft Column Maximum	**82.4**	**91.4**			
	All Aircraft Standard Deviation	**10.6**	**8.0**			

4.3 Summary of Minimum Interference Path Loss Data

Table 4.3-1 summarizes the MIPL shown in the tables in Section 4.2. Data in this table were taken from the "All Aircraft" summary rows at the end of each table. In this table, the *minimum MIPL* values displayed are the *lowest* MIPL of all aircraft. Likewise, the *average MIPL* values displayed are the *average* of the MIPL of all aircraft. The minimum MIPL and the average MIPL will be used in the later calculations for interference safety margins. The maximum MIPL and the StDev of the MIPL of all aircraft are also shown. The standard deviations were calculated without assigning additional weight to any specific aircraft model or number of measurement points.

As observed from the table, there can be a large difference in dB between the maximum MIPL and the minimum MIPL. MIPL can vary between 35 dB to 82 dB for LOC and between 30 dB to 84.7 dB for VOR. TCAS system has the smallest MIPL range, 48.2 dB to 69.1 dB, and the lowest MIPL standard deviation value of 5.3 dB.

Table 4.3-1: Summary of Aircraft Minimum IPL (MIPL)

	Min MIPL (dB)	Ave MIPL (dB)	Max MIPL (dB)	StDev (dB)
LOC	35.0	60.0	82.0	10.0
VOR	30.0	62.4	84.7	12.2
VHF	28.7	50.4	76.0	10.9
GS	46.2	59.1	77.0	7.2
TCAS	48.2	57.3	69.1	5.3
SatCom	51.5	59.9	87.0	15.2
GPS	41.0	64.6	82.4	10.6

5 Interference Analysis

In this section, receiver susceptibility thresholds are discussed, and the measured interference thresholds are summarized from RTCA/DO-199. In addition, safety margins are calculated from the interference susceptibility thresholds, the path loss data in Section 4, and the emissions from WLAN devices and two-way radios.

5.1 Published Receiver Susceptibility

Of the three elements required for risk assessment (WLAN/PED/two-way radio emission; aircraft IPL; and receiver interference threshold), receiver interference threshold (to PED interfering signal) is the one

element with the least amount of available data. RTCA/DO-199 and RTCA/DO-233 provide the most information on the subject. However, the amount of data available is far from enough to provide confidence in the figures provided. Except for GPS, the ICAO Annex 10, Vol.1 [24] and receiver MOPS did not properly address the in-band, on-channel interference. Spurious signals from PEDs and WLAN devices were too low to cause other interference, such as desensitization, addressed in these documents.

5.1.1 RTCA/DO-233

For LOC, RTCA/DO-233 sets four different interference thresholds for in-band, on-channel interference. Signal-to-Interference (*S/I*) ratio for the four interference types can vary between 7 dB to as much as 46 dB depending upon the frequency spacing between the CW interference signal from the 90 Hz or 150 Hz ILS sidebands of the LOC carrier. In addition, a modulated interference signal may result in a different interference threshold than CW interference. Additional information is documented in [3] and in [1].

RTCA/DO-233 did not provide similar guidance for other systems such as VOR or GS. And unlike RTCA/DO-199, RTCA/DO-233 did not provide data to support their findings and recommendations concerning receiver interference thresholds.

5.1.2 RTCA/DO-199

RTCA/DO-199 is the only publicly available document that provided results from testing of receiver interference thresholds. In RTCA/DO-199, receiver interference levels along with test signal strengths were documented in the form of tables and charts, from which relevant threshold data for LOC, GS, VOR, TCAS, VHF-Com and SatCom were extracted. For a CW interference signal, the official *S/I* ratios were chosen from the typical values, which were valid across most of the channel bandwidth. However, when the interfering signal was such that it mixed with the local carrier to produce a frequency close to the receiver's side band, susceptibility notches could occur. Test results show the *S/I* ratio can be as high as 38 dB for LOC, 35 dB for GS and 46 dB for VOR. Theoretical analysis was also conducted and presented for LOC and VOR.

For CW interference, the disruption threshold tends to vary along with the signal level in such a way that the S/I ratio stays constant. As a result, the disruption threshold can only be determined if the test signal is known. In RTCA/DO-199, the test signals were set equal to the minimum desired signals at the receivers. These signals were calculated from the minimum desired external field environments within the coverage airspace assuming an isotropic, lossless antenna, and fixed values of cable losses. The minimum desired external field environments were taken from several sources. The sources included the ICAO Annex 10, Vol.1, and FAA National Orders, and others depending on the system under consideration. Additional details on the desired signal strength calculations and the interference criteria unique to each system can be found in RTCA/DO-199.

According to RTCA/DO-199, it was very difficult to maintain signal lock at the susceptibility notches to cause undetected interference even if it was intended. The official thresholds were selected, therefore, by ignoring narrowband notches. Table 5.1-1 summarizes the test signal level used, the official disruption threshold, along with the unofficial disruption threshold at the susceptibility notches. The underlined data in this table were used in the safety margin calculations in Section 5.2.

Table 5.1-1: RTCA/DO-199 Interference Thresholds

	LOC	VOR	GS	VHF	GPS	MLS
Desired Signal at Receiver (dBm)	**-88**	**-97**	**-78**	**-89**		
Typical Interference Level (dBm)	**-104**	**-110**	**-93**	**-107**	**-126.5***	**-62**
Signal/Inteference (S/I) Ratio (dB)	16	13	15	18		
Minimum Interference Level (dBm) (at notches)	**-127**	**-143**	**-113**	**-107**		
Signal/Interference ratio (dB)	39	46	35	18		
Theoretical Thresholds (dBm)	**-130**	**-148**	**-120**			
Theoretical S/I Ratio (dB)	42	51	42			

* For GPS, -126.5 dBm minimum interference level is required in GPS receiver MOPS such as DO-208 and DO-229B. DO-199 provides –130 dBm interference level for GPS.

For GPS, the interference threshold was very well defined and was consistent across various standards, Technical Standard Orders (TSOs) and receiver MOPS for airborne navigation equipment. These documents provided the minimum performance standards for stand-alone, satellite-based and ground-based GPS systems and sensors. A few of these documents include: ITU-R M.1477 [25], RTCA/DO-235A [26], RTCA/DO-229B [27], RTCA/DO-253A [28], RTCA/DO-228 [29], and RTCA/DO-208 [30].

These documents show that the lowest interference threshold is **–126.5 dBm** for a GPS system in acquisition mode with CW interference or signals with bandwidth up to 700 Hz. This threshold was specified at the output of a passive antenna, or at the output of an active antenna, but before the pre-amplifier stage. Thus, the active GPS antenna pre-amplification gain must be accounted for in the path loss value in order to use the –126.5 dBm threshold value.

5.2 Safety Margin Calculations

Knowing device emission “A”, aircraft minimum path loss “-B”, and receiver susceptibility threshold “C”, safety margin can be computed using

$$Safety\ Margin = C - (A + B)$$

This section first calculates the interference signal strength at the receiver’s antenna port (A +B). Safety margin can then be computed with the knowledge of “C”.

Applying the minimum and the average values of MIPL (“-B”) in Table 4.3-1 to the emission data (“A”) in Table 3.6-1, the resulting interference signals at the receiver (“A+B”) are shown in Table 5.2-1. Due to the large range of IPL “-B” values, the results of the calculation (A+B) are presented with only the maximum and the average values that are calculated from the minimum and the average path loss “-B” values.

Table 5.2-1: Interference Signal Strength at Receiver's Antenna Port (A+B). Maximum and Average values in dBm

	802.11b	**Bluetooth**	**802.11a**	**FRS/GMRS Radio**	**Laptops/ PDA**
LOC (Max/Ave)	-113.2/-138.2	-101.8/-126.8	-109.2/-134.2	-114.3/-139.3	-103/-128
VOR (Max/Ave)	-108.2/-140.6	-96.8/-129.2	-104.2/-136.6	-109.3/-141.7	-98.0/-130.4
VHF(*) (Max/Ave)	-106.9/-128.6	-95.5/-117.2	-102.9/-124.6	-108/-129.7	-96.7/-118.4
GS (Max/Ave)	-121.9/-134.8	-123.4/-136.3	-118/-130.9	-74.7/-87.6	-104.9/-117.8
TCAS (Max/Ave)	-113.5/-122.6	-97.9/-107	-105.9/-115	-91.7/-100.8	-93.9/-103
GPS (Max/Ave)	-108.7/-132.3	-122.7/-146.3	-106.2/-129.8	-98.0/-121.6	-96.8/-120.4
MLS (Max/Ave)	-155.7/-161.7	-156.2/-162.2	-130/-136	-111/-117	-155/-161

(*) Emission data were not collected in the VHF band (118 – 137 MHz). For this calculation, the VHF band maximum emission was assumed to be the same as in Band 1 (105 – 120 MHz), which covered LOC and VOR bands.

Comparing the maximum and the average signal strength at the receivers, (A+B), in Table 5.2-1 to the typical and the minimum susceptibility thresholds in Table 5.1-1, safety margins can be calculated. The result for each system is a 2x2 matrix. Deciding which element of the safety margin matrix to use depends upon whether the maximum or the average value for (A+B) was used, and on whether the typical or the minimum interference threshold was used. In the cases where there was only one value for interference threshold, such as GPS, the safety margin results are 2x1 matrices.

Tables 5.2-2 to 5.2-7 report the results of the calculation with the safety margin results highlighted in **bold** for each combination of WLAN/radio device, MIPL, and interference threshold values. The calculations were conducted for LOC, VOR, VHF Comm, GS, GPS and MLS. To determine safety margin using the tables, one simply locates the right combinations of WLAN/PED/Radio devices, MIPL values, and interference thresholds on the tables. Thus, for LOC, the combination of a 802.11b WLAN device, a minimum MIPL (resulting in the interference signal at receiver of –113.2 dB), and a minimum LOC interference threshold (-127 dBm) results in –13.8 dB safety margin. A large positive safety margin is desirable, whereas a large negative safety margin indicates a possibility of interference.

Safety margin calculations for TCAS and SatCom were not possible due to lack of interference threshold data. However, IPL and WLAN/radio device emissions reported can be used in future calculations once the interference thresholds are defined.

Table 5.2-2: LOC Safety Margin (in dB) for Different Combinations of WLAN/Radio Devices, MIPL and Interference Thresholds

	802.11b &		**BlueTooth &**		**802.11a &**		**FRS/GMRS &**		**Laptops/PDAs &**	
	Min MIPL	Ave MIPL	Min MIPL	Ave MIPL	Min MIPL	Ave MIPL	Min MIPL	Ave MIPL	Min MIPL	Ave MIPL
Interference Signal at Receiver (dBm) =	*-113.2*	*-138.2*	*-101.8*	*-126.8*	*-109.2*	*-134.2*	*-114.3*	*-139.3*	*-103.0*	*-128.0*
LOC Interference Threshold										
Minimum (dBm) *-127*	**-13.8**	**11.2**	**-25.2**	**-0.2**	**-17.8**	**7.2**	**-12.7**	**12.3**	**-24.0**	**1.0**
Typical (dBm) *-104*	**9.2**	**34.2**	**-2.2**	**22.8**	**5.2**	**30.2**	**10.3**	**35.3**	**-1.0**	**24.0**

Table 5.2-3: VOR Safety Margin (in dB) for Different Combinations of WLAN/Radio Devices, MIPL and Interference Thresholds

	802.11b &		**BlueTooth &**		**802.11a &**		**FRS/GMRS &**		**Laptops/PDAs &**	
	Min MIPL	Ave MIPL	Min MIPL	Ave MIPL	Min MIPL	Ave MIPL	Min MIPL	Ave MIPL	Min MIPL	Ave MIPL
Interference Signal at Receiver (dBm) =	*-108.2*	*-140.6*	*-96.8*	*-129.2*	*-104.2*	*-136.6*	*-109.3*	*-141.7*	*-98.0*	*-130.4*
VOR Interference Threshold										
Minimum (dBm) *-143*	**-34.8**	**-2.4**	**-46.2**	**-13.8**	**-38.8**	**-6.4**	**-33.7**	**-1.3**	**-45.0**	**-12.6**
Typical (dBm) *-110*	**-1.8**	**30.6**	**-13.2**	**19.2**	**-5.8**	**26.6**	**-0.7**	**31.7**	**-12.0**	**20.4**

Table 5.2-4: VHF Safety Margin (in dB) for Different Combinations of WLAN/Radio Devices, MIPL and Interference Thresholds (see note below table)

	802.11b &		**BlueTooth &**		**802.11a &**		**FRS/GMRS &**		**Laptops/PDAs &**	
	Min MIPL	Ave MIPL	Min MIPL	Ave MIPL	Min MIPL	Ave MIPL	Min MIPL	Ave MIPL	Min MIPL	Ave MIPL
Interference Signal at Receiver (dBm) =	*-106.9*	*-128.6*	*-95.5*	*-117.2*	*-102.9*	*-124.6*	*-108.0*	*-129.7*	*-96.7*	*-118.4*
VHF Interference Threshold (dBm) *-107*	**-0.1**	**21.6**	**-11.5**	**10.2**	**-4.1**	**17.6**	**1.0**	**22.7**	**-10.3**	**11.4**

Note: RF emission data were not collected in the VHF band (Band 1 does not cover the VHF band). Since the frequency band are close (105 – 120 MHz for Band 1 and 118 – 137 MHz for VHF band), it is assumed for this calculation that the emission in the VHF band is equal to the emissions in the Band 1.

Table 5.2-5: GS Safety Margin (in dB) for Different Combinations of WLAN/Radio Devices, MIPL and Interference Thresholds

		802.11b &		**BlueTooth &**		**802.11a &**		**FRS/GMRS &**		**Laptops/PDAs &**	
		Min MIPL	Ave MIPL	Min MIPL	Ave MIPL	Min MIPL	Ave MIPL	Min MIPL	Ave MIPL	Min MIPL	Ave MIPL
Interference Signal at Receiver (dBm) =		*-121.9*	*-134.8*	*-123.4*	*-136.3*	*-118.0*	*-130.9*	*-74.7*	*-87.6*	*-104.9*	*-117.8*
GS Interference Threshold											
Minimum (dBm)	*-113*	**8.9**	**21.8**	**10.4**	**23.3**	**5.0**	**17.9**	**-38.3**	**-25.4**	**-8.1**	**4.8**
Typical (dBm)	*-93*	**28.9**	**41.8**	**30.4**	**43.3**	**25.0**	**37.9**	**-18.3**	**-5.4**	**11.9**	**24.8**

Table 5.2-6: GPS Safety Margin (in dB) for Different Combinations of WLAN/Radio Devices, MIPL and Interference Thresholds

		802.11b &		**BlueTooth &**		**802.11a &**		**FRS/GMRS &**		**Laptops/PDAs &**	
		Min MIPL	Ave MIPL	Min MIPL	Ave MIPL	Min MIPL	Ave MIPL	Min MIPL	Ave MIPL	Min MIPL	Ave MIPL
Interference Signal at Passive Antenna Output (dBm) =		*-108.7*	*-132.3*	*-122.7*	*-146.3*	*-106.2*	*-129.8*	*-98.0*	*-121.6*	*-96.8*	*-120.4*
GPS Interference Threshold (dBm)	*-126.5*	**-17.8**	**5.8**	**-3.8**	**19.8**	**-20.3**	**3.3**	**-28.5**	**-4.9**	**-29.7**	**-6.1**

Table 5.2-7: MLS Safety Margin (in dB) for Different Combinations of WLAN/Radio Devices, MIPL and Interference Thresholds

		802.11b &		**BlueTooth &**		**802.11a &**		**FRS/GMRS &**		**Laptops/PDAs &**	
		Min MIPL	Ave MIPL	Min MIPL	Ave MIPL	Min MIPL	Ave MIPL	Min MIPL	Ave MIPL	Min MIPL	Ave MIPL
Interference Signal at Receiver (dBm) =		*-155.7*	*-161.7*	*-156.2*	*-162.2*	*-130.0*	*-136.0*	*-111.0*	*-117.0*	*-155.0*	*-161.0*
MLS Interference Threshold (dBm)	*-62*	**93.7**	**99.7**	**94.2**	**100.2**	**68.0**	**74.0**	**49.0**	**55.0**	**93.0**	**99.0**

* For MLS both path loss and receiver susceptibility thresholds came from DO-199.

As observed from the tables, interference safety margins can be positive or negative depending upon the combination of MIPL and receiver interference thresholds used. WLAN devices generally have better safety margin than standard laptops and PDAs based on test data in this effort.

The exception is 802.11a devices in MLS band where emissions from most other WLAN devices were low and not measurable. Emissions from 802.11a devices became the highest in this band. Due to large positive safety margin associated with MLS interference, there appears to be no concern in this band. However, the safety margin for MLS seems unusually large. In addition, there was lack of data to validate either the interference threshold or the MIPL data provided in RTCA/DO-199 and used in this analysis. Additional data in this MLS band would be highly desirable.

6 Summary and Conclusions

Emission measurements were conducted on WLAN devices and two-way radios. These observations were made:

a. WLAN device spurious emissions are not any worse (not higher) than spurious emissions from computer laptops/PDAs in the aircraft communication and navigation bands considered. The exception is in the MLS band with emissions from 802.11a devices higher than emissions from the laptops/PDAs. High emissions from 802.11a devices in Band 5 is not a concern due to a very large positive safety margin.

b. The emission levels from WLAN devices and laptops/PDAs are lower than the FCC limits, but they can be higher than RTCA/DO-160D Category M limits.

c. Spurious emissions in GS band from FRS and GMRS two-way radios can be 23 dB higher than RTCA/DO-160D Category M limit, and 30 dB higher than the maximum laptop/PDA emissions in the same band.

Aircraft IPL measurements were made on four Boeing B747-400 and six Boeing B737-200 aircraft. The additional data greatly supplements the low volume of existing IPL data. In addition, the following observations were made:

a. Measurements conducted at window and door locations capture the same minimum IPL value as if a full aircraft IPL measurement were conducted. This finding was observed for all systems on a B737 aircraft (nose No. 1989) where IPL data were collected at all aircraft seats, windows, doors, and locations between seats on one side of the aircraft.

b. Path loss is greatly affected by the proximity of the aircraft antennas relative to an aircraft door. This observation indicates that antenna installation location can affect the minimum IPL even for the same aircraft.

c. The range of lowest and highest minimum IPL can be very large (59 dB for LOC) if all past and current data are considered.

Interference threshold data are inadequate to thoroughly assess the threat from PED-type EMI. Based on the limited interference threshold data, safety margin calculations were conducted for many aircraft systems. The results show that the safety margins can be negative or positive depending upon the interference thresholds (minimum or typical) and the minimum IPL data (the lowest or the average) used.

7 References

[1] Ely, J. J.; Nguyen T. X.; Koppen, S. V.; Salud, M. T.; and Beggs J. H.: *Wireless Phone Threat Assessment and New Wireless Technology Concerns for Aircraft Navigation Radios*, Final Report to the FAA, under FAA/NASA Interagency Agreement DFTA03-96-X-90001, Revision 9, April 2002.

[2] RTCA/DO-199, *Potential Interference to Aircraft Electronic Equipment from Devices Carried Aboard*, September 16, 1988.

[3] RTCA DO-233, *Portable Electronic Devices Carried On Board Aircraft*, Prepared by SC-177, August 20, 1996.

[4] Hill, David A.: *Electromagnetic Theory of Reverberation Chambers*, Chapter 4, Technical Note 1506, National Institute of Standards and Technology, December 1998.

[5] Veda Inc., *CV-580 RF Coupling Validation Experiment Report*, Report #79689-96U/P30041, 11/15/1996.

[6] IEEE Computer Society, LAN/MAN Standards Committee, *Part 11: Wireless LAN Medium Access Control (MAC) and Physical Layer (PHY) Specifications: High-speed Physical Layer in the 5 GHZ Band*, September 16, 1999.

[7] Bluetooth SIG, *Bluetooth Specification Version 1.1*, February 22, 2001.

[8] MIL-STD-462D, *Measurement of Electromagnetic Interference Characteristics*, January 11, 1993.

[9] RTCA DO-160D, Change No. 1, Section 20, "Radio Frequency Susceptibility (Radiated and Conducted)", *Environmental Conditions and Test Procedures for Airborne Equipment*", Prepared by SC-135, December 14, 2000.

[10] ANSI C63.4-2000, *Interim Standard for Methods of Measurement of Radio-Noise Emissions from Low-Voltage Electrical and Electronic Equipment in the Range of 9 kHz to 40 GHz*, published by the IEEE, December 8, 2000.

[11] Draft ETSI EN 301 908-7 V1.1.1, *Electromagnetic Compatibility and Radio Spectrum Matters; Base Stations and User Equipment for IMT-2000 Third Generation Cellular Networks: Part7: Harmonized Standard for IMT-2000, CDMA TDD Covering Essential Requirements of Article 3.2 of the R&TTE Directive*, April, 2001.

[12] Koppen, S. V.: *A Description of the Software Element of the NASA Portable Electronic Device Radiated Emissions Investigation*, NASA Contractor Report CR-2002-211675, May 2002.

[13] Crawford, M. L.; and Koepke, G. H.: *Design, Evaluation, and Use of a Reverberation Chamber for Performing Electromagnetic Susceptibility/Vulnerability Measurements*, NBS Technical Note 1092, U. S. Department of Commerce/National Bureau of Standards, April 1986.

[14] Ladbury, J.; Koepke, G.; and Camell, D.: *Evaluation of the NASA Langley Research Center Mode-Stirred Chamber Facility*, NIST Technical Note 1508, January 1998.

[15] International Electrotechnical Commission (IEC) 61000-4-21, 2003 (Draft)

[16] 47CFR Ch. 1, Part 15.109, "Radiated Emission Limits", *US Code of Federal Regulations,* Federal Register dated December 19, 2001.

[17] 47CFR Ch. 1, Part 15.209, "Radiated Emission Limits; General Requirements", *US Code of Federal Regulations*, Federal Register dated December 19, 2001.

[18] 47CFR Ch. 1, Part 95.635, "Personal Radio Service – Unwanted Radiation", *US Code of Federal Regulations*, Federal Register dated 10-01-98.

[19] Koepke, G.; Hill, D.; and Ladbury, J.: "Directivity of the Test Device in EMC Measurements", *2000 IEEE International Symposium on Electromagnetic Compatibility*, Aug. 21-25, 2000.

[20] *World Jet Inventory Report Year-End 2002*, Jet Information Service, Inc.

[21] Ely, Jay J.; Shaver, T.W.; and Fuller, G. L.: *Ultrawideband Electromagnetic Interference to Aircraft Radios, results of Limited Functional Testing with United Airlines and Eagles Wings Incorporated, in Victorville, California*, NASA/TM-2002-211949, October 2002.

[22] Fuller, G.: *B737-200 and B747-400 Path Loss Tests, Victorville, California*. Eagles Wings Inc., Prepared for NASA LaRC under NASA PO# L-16099, Task 1, 2 and 3, 2002.

[23] Delta Airlines Engineering, *ENGINEERING REPORT Delta/NASA Cooperative Agreement NCC-1-381 Deliverable Reports*, Report No. 10-76052-20, December 8, 2000.

[24] International Civil Aviation Organization (ICAO), Aeronautical Telecommunications, Annex 10, Vol. 1 (Fifth Edition – July 1996).

[25] International Telecommunication Union (ITU), Recommendations ITU-R M.1477 (2000).

[26] RTCA/DO-235A, *Assessment of Radio Frequency Interference Relevant to the GNSS*, Dec. 5, 2002.

[27] RTCA/DO-229B, *Min. Operational Perf. Standards for Global Positioning System (GPS)/ Wide Area Augmentation System*, Oct. 6, 1999.

[28] RTCA/DO-253A, *Min. Operational Perf. Standards for GPS Local Area Augmentation System Airborne Equipment*, Nov. 28, 2001.

[29] RTCA/DO-228, *Min. Operational Perf. Standards for Global Navitgation Satellite Systems (GNSS) Airborne Antenna Equipment*, Oct. 10, 1995.

[30] RTCA/DO-208, *Min. Operational Perf. Standards for GPS Airborne Supplemental Navigation Equipment using Global Positioning System (GPS)*, July 12, 199, Change 1, Sept. 21, 1993.

Appendix A: Measurement and Results of Intentional Transmitters Including WLAN Devices and Two-Way Radios

The following charts illustrate WLAN device idle, ping storm envelope, and file transfer (Xfer) envelope compared to the baseline (idle and file Xfer) of the host laptop. An equivalent measurement noise floor is included in each chart for each band to represent the instrument noise floor, but with calibration factors applied as had been done with the emission data. These charts were used to further reduce the data to the forms that are found in Sections 3.3 and 3.5 of this report. Table A-1 has details on the organization of data charts produced from each wireless communication device tested. Every device tested in a wireless technology category was grouped together by measurement bands, so that each device may be easily compared with each other.

The legends in each chart list the data plots by host laptop computer number and WLAN device designation. For instance, Figure A1 displays emission data plots acquired from Laptop 4 with 802.11a WLAN device 11A-1 installed. Tables 3.2-14 to 3.2-16 list the WLAN device designations and associated manufacturers. Table 3.2-4 provides the host laptop designations and manufacturers.

Table A-1: Organization of Charts in this Section

Wireless Technology	Band 1 Figure	Band 2 Figure	Band 3 Figure	Band 4 Figure	Band 5 Figure
802.11A	A1-A5	A6-A10	A11-A15	A16-A20	A21-A25
802.11B	A26-A32	A33-A39	A40-A46	A47-A53	A54-A60
Bluetooth	A61-A65	A66-A71	A72-A77	A78-A83	A84-A89
FRS	A90-A93	A94-A99	A98-A101	A102-A105	A106-A109
GMRS	A110-A112	A113-A115	A116-A118	A119-121	A122-A125

A.1 802.11a WLAN Devices

A.1.1 Band 1

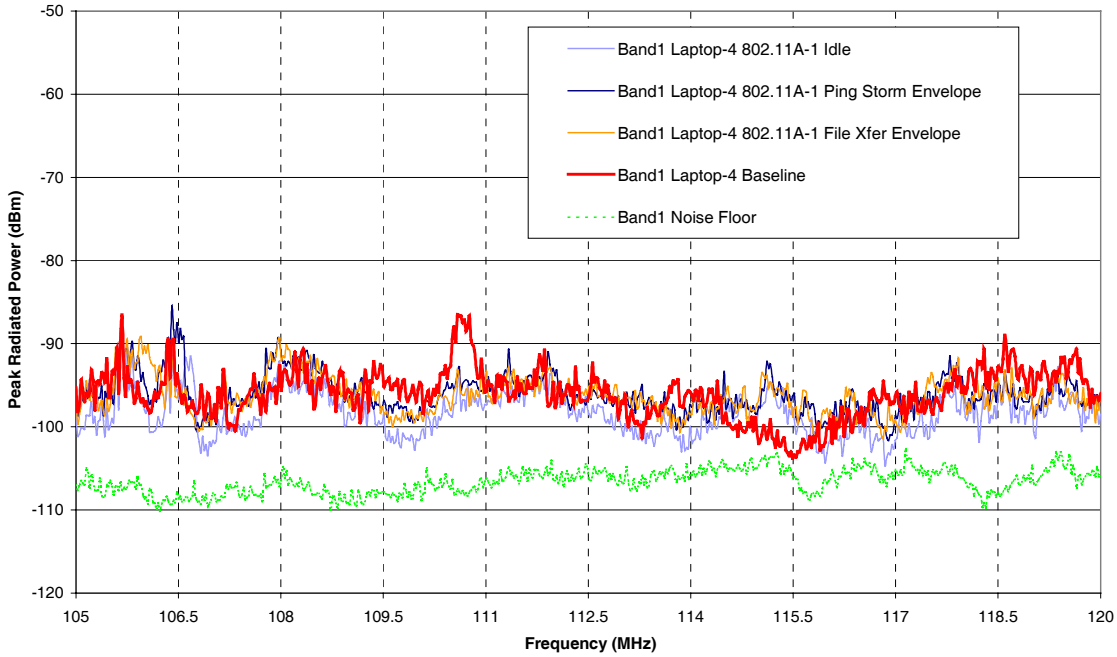

Figure A1: Laptop 4 and 802.11A-1, Band 1.

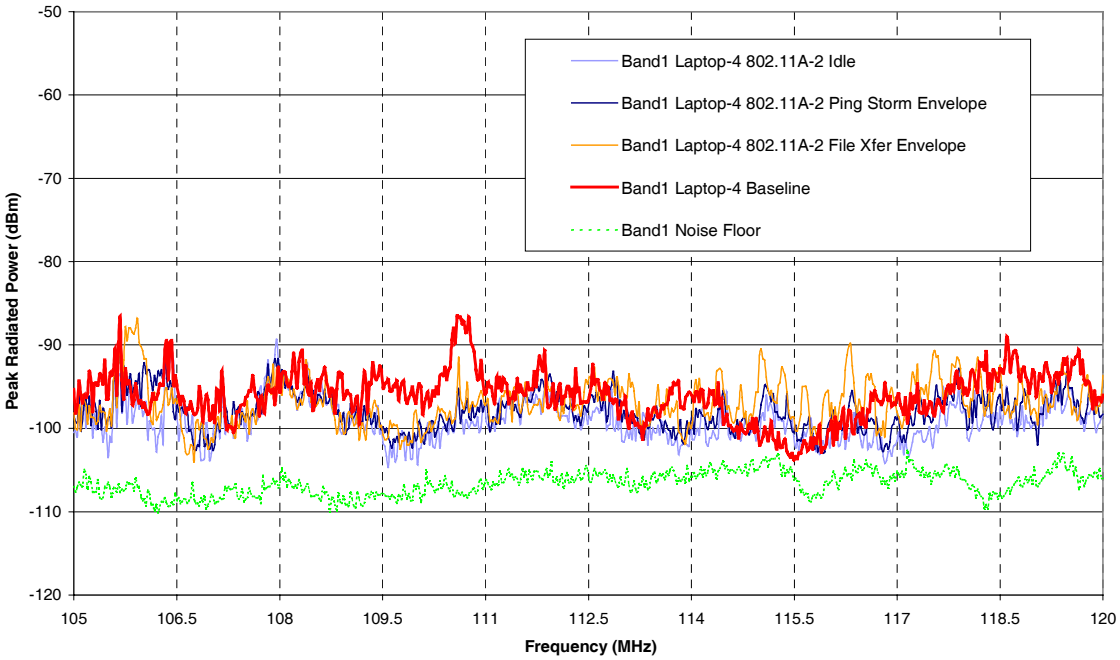

Figure A2: Laptop 4 and 802.11A-2, Band 1.

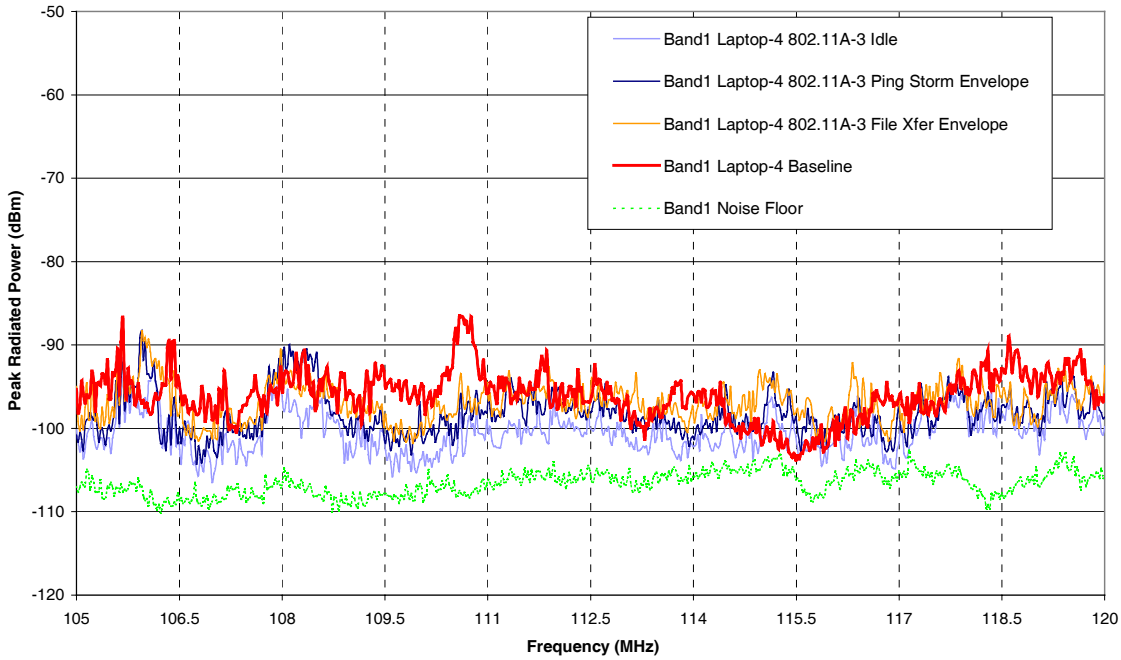

Figure A3: Laptop 4 and 802.11A-3, Band 1.

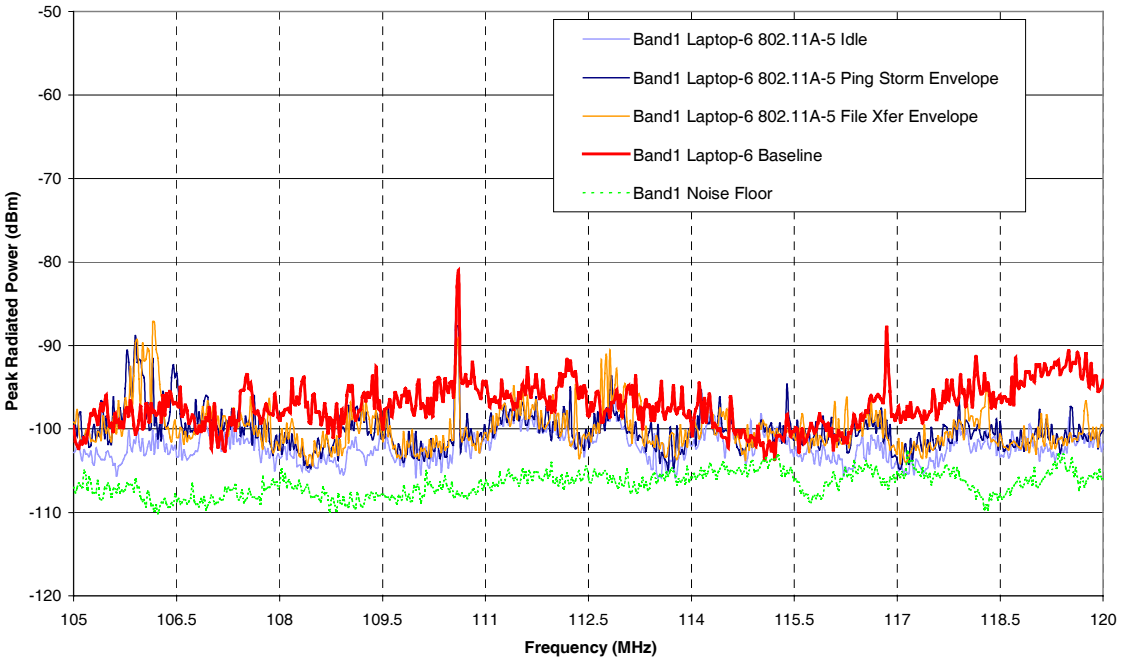

Figure A4: Laptop 6 and 802.11A-5, Band 1.

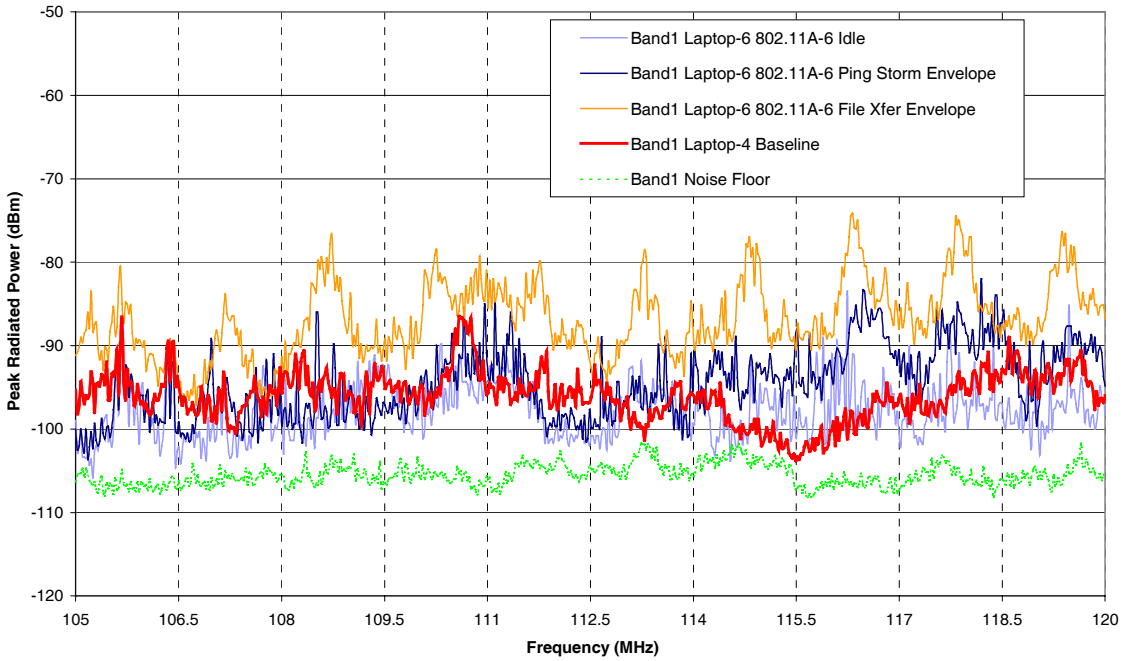

Figure A5: Laptop 6 and 802.11A-6, Band 1.

A.1.2 Band 2

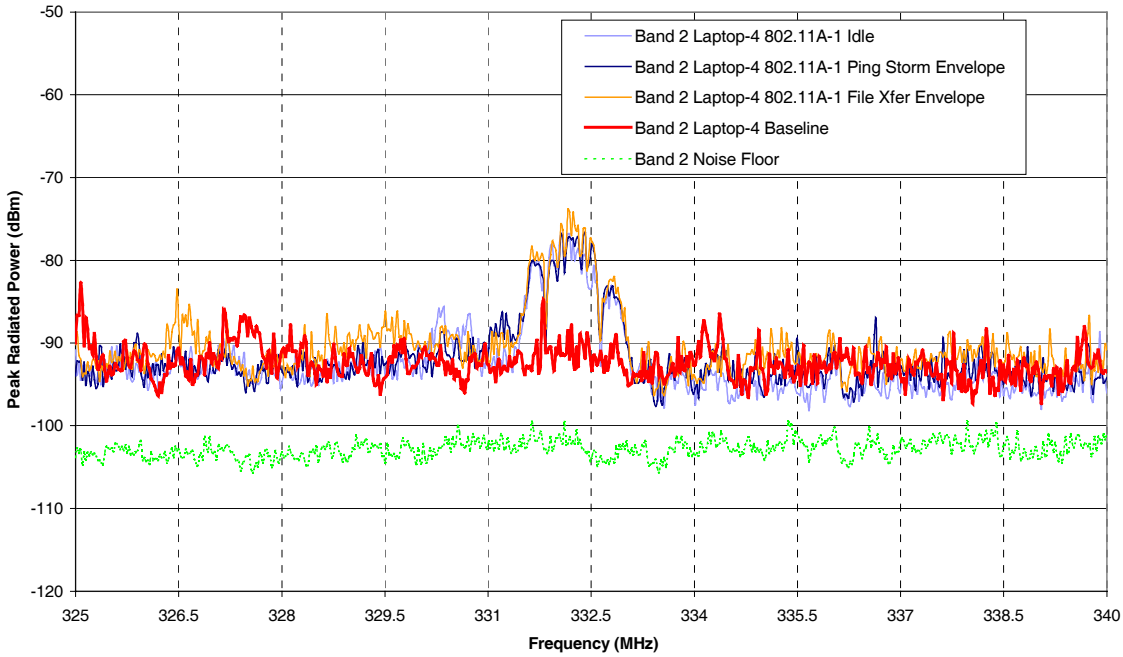

Figure A6: Laptop 4 and 802.11A-1, Band 2.

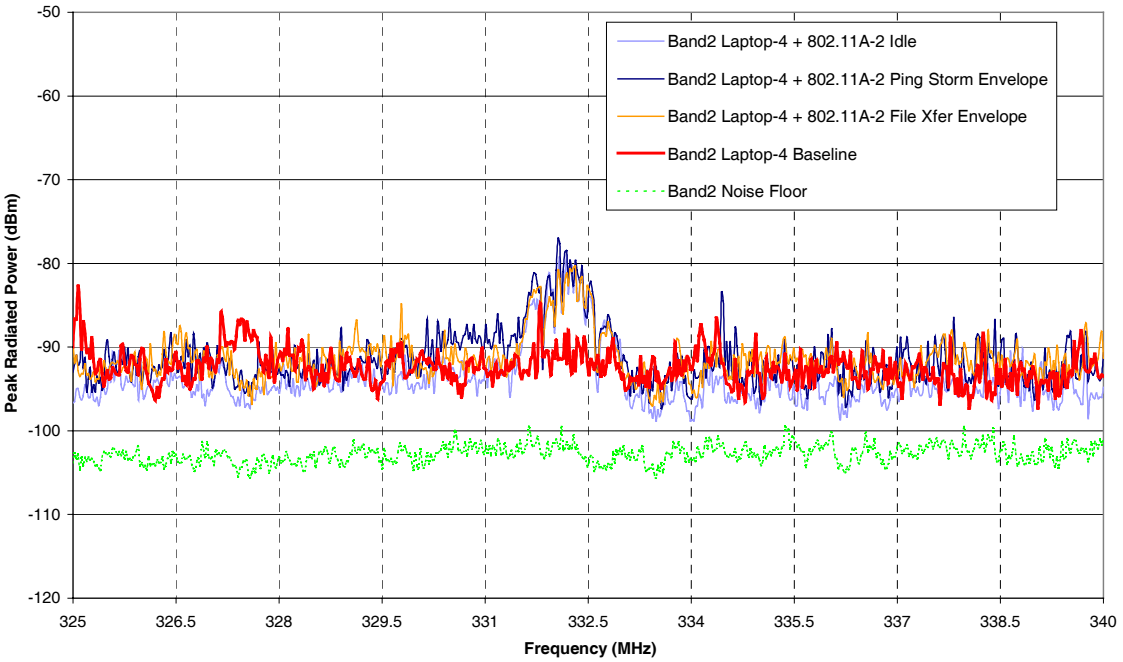

Figure A7: Laptop 4 and 802.11A-2, Band 2.

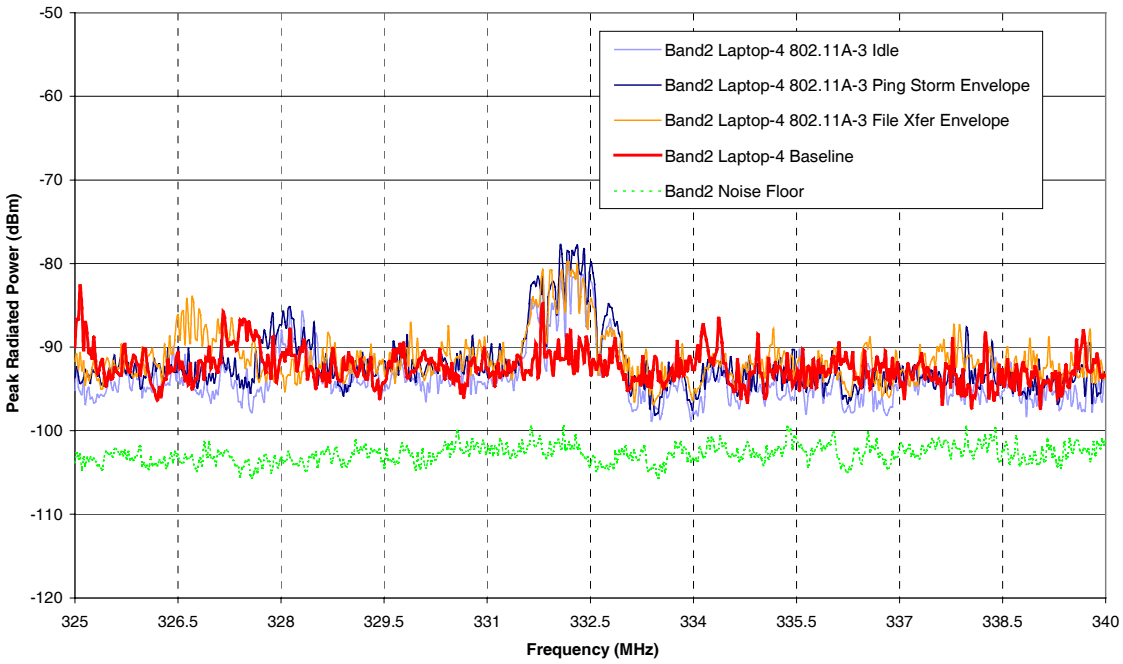

Figure A8: Laptop 4 and 802.11A-3, Band 2.

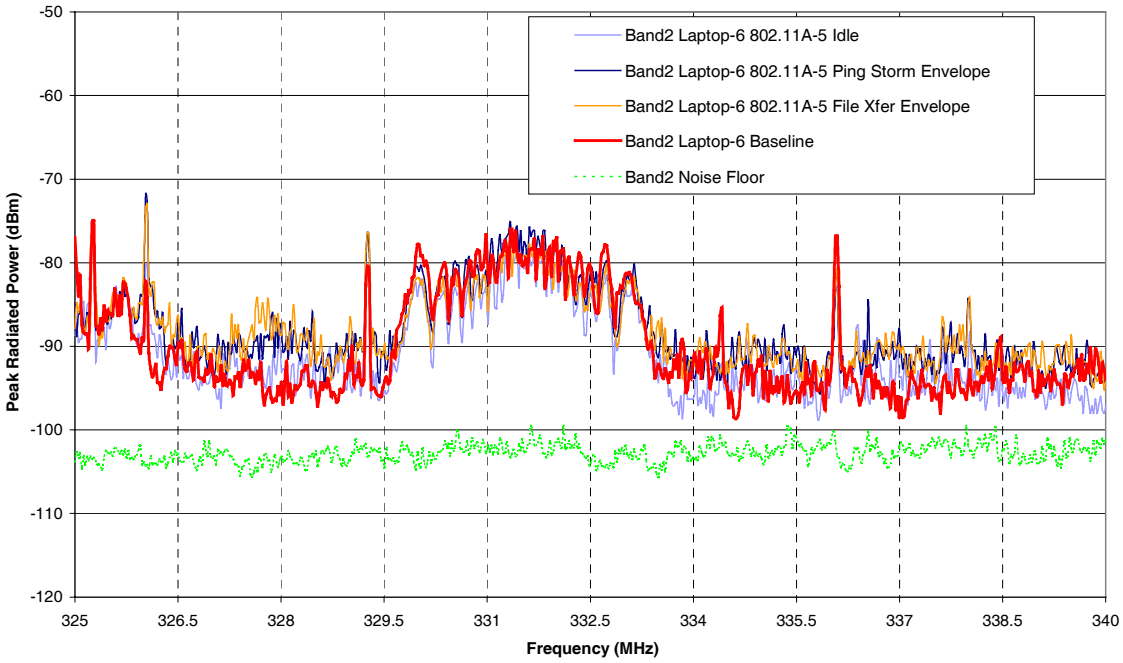

Figure A9: Laptop 4 and 802.11A-5, Band 2.

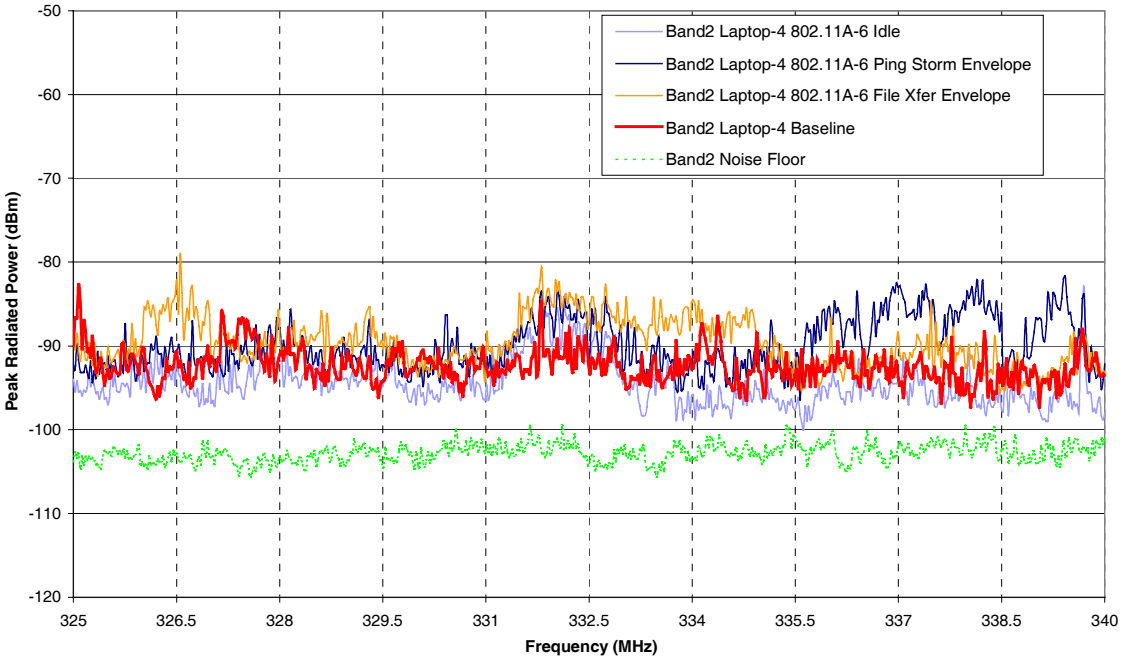

Figure A10: Laptop 4 and 802.11A-6, Band 2.

A.1.3 Band 3

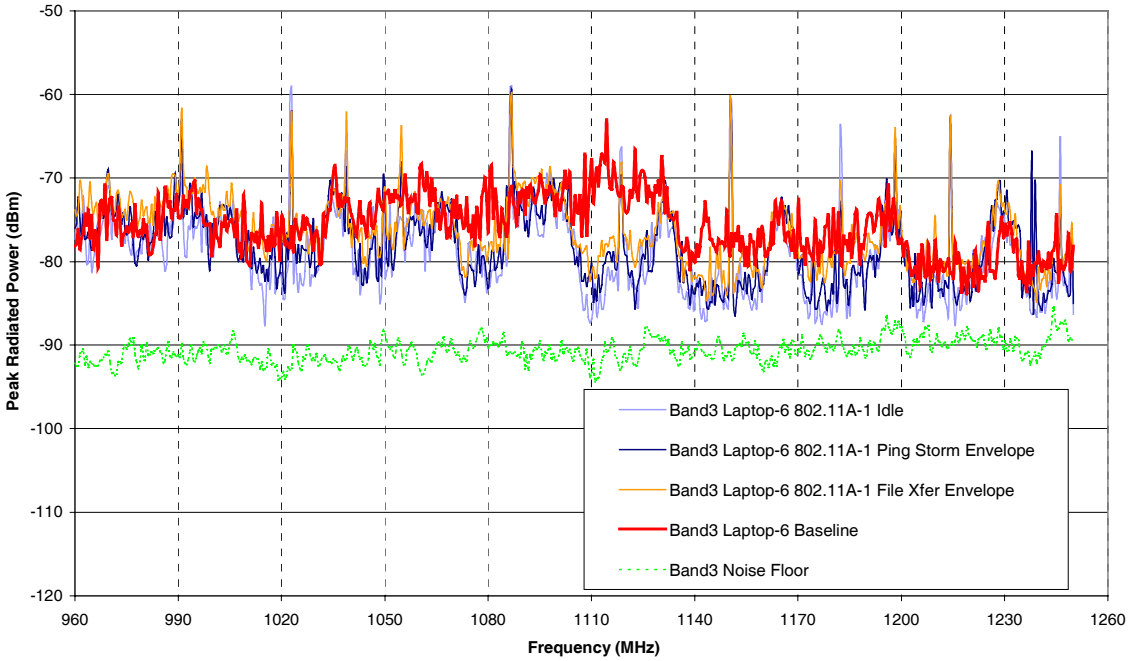

Figure A11: Laptop 6 and 802.11A-1, Band 3.

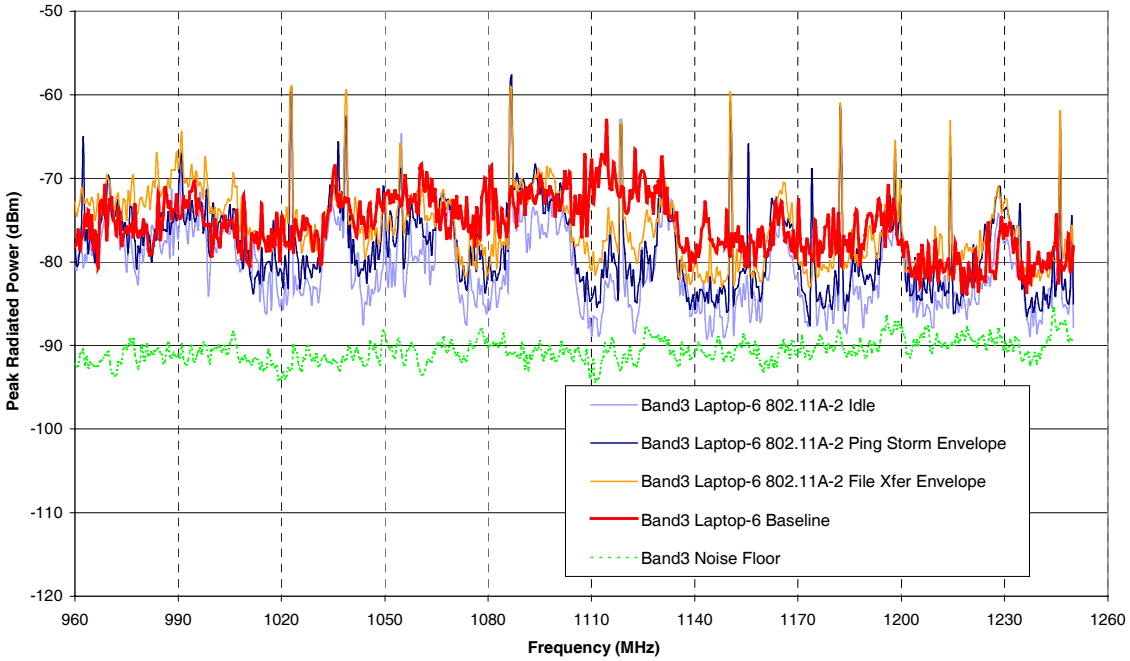

Figure A12: Laptop 6 and 802.11A-2, Band 3.

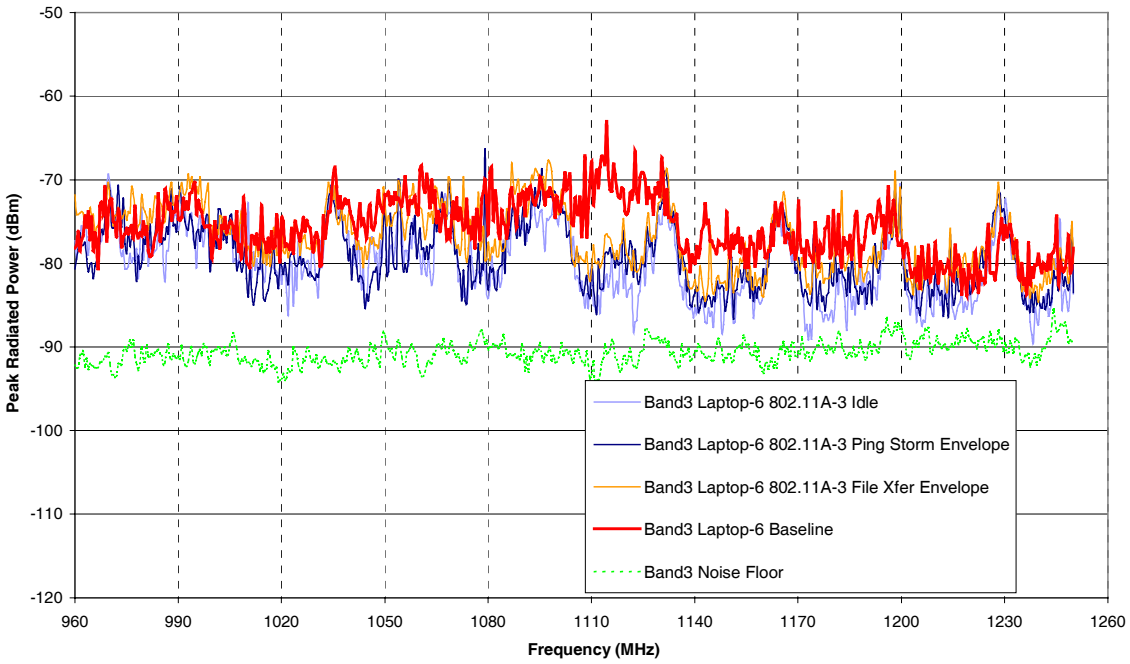

Figure A13: Laptop 6 and 802.11A-3, Band 3.

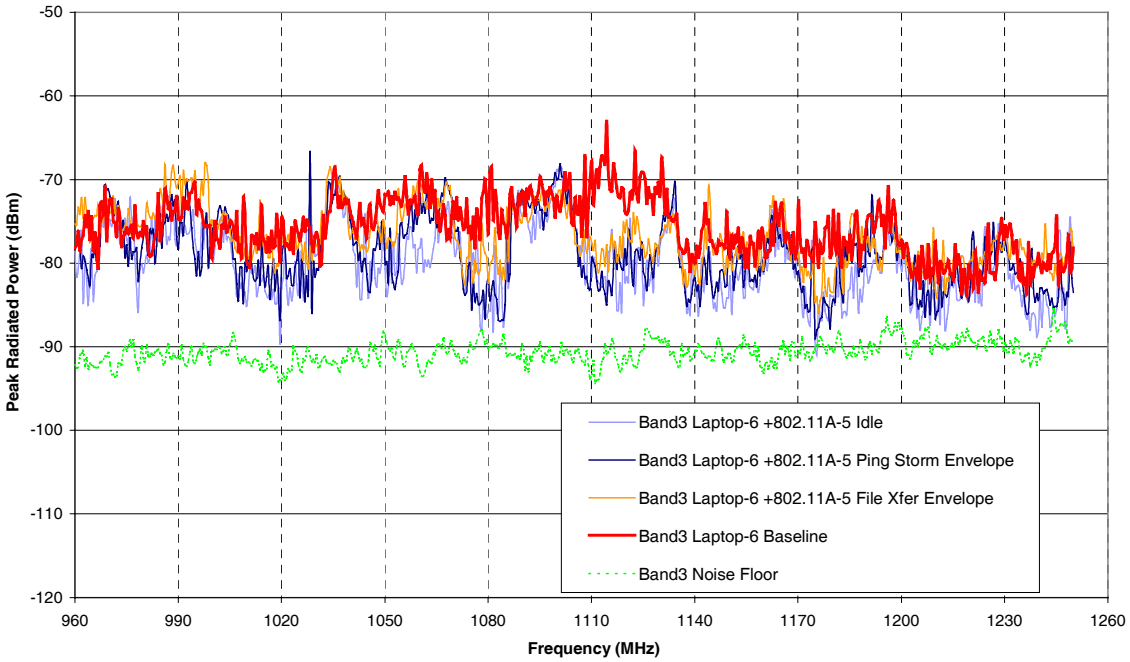

Figure A14: Laptop 6 and 802.11A-5, Band 3.

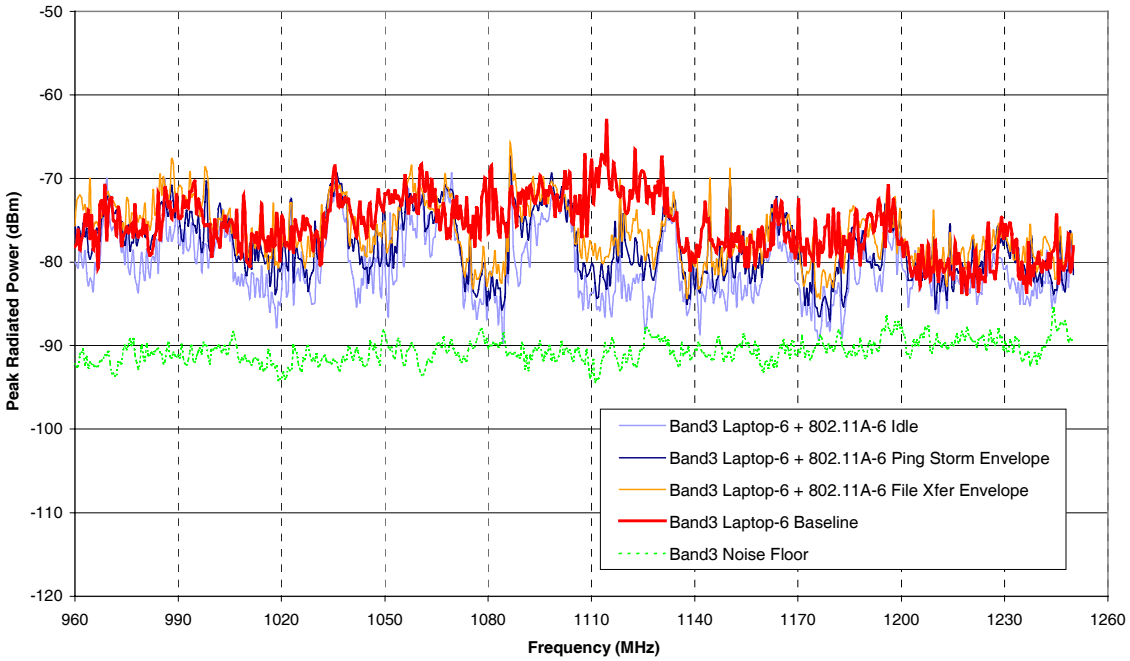

Figure A15: Laptop 6 and 802.11A, Band 3.

A.1.4 Band 4

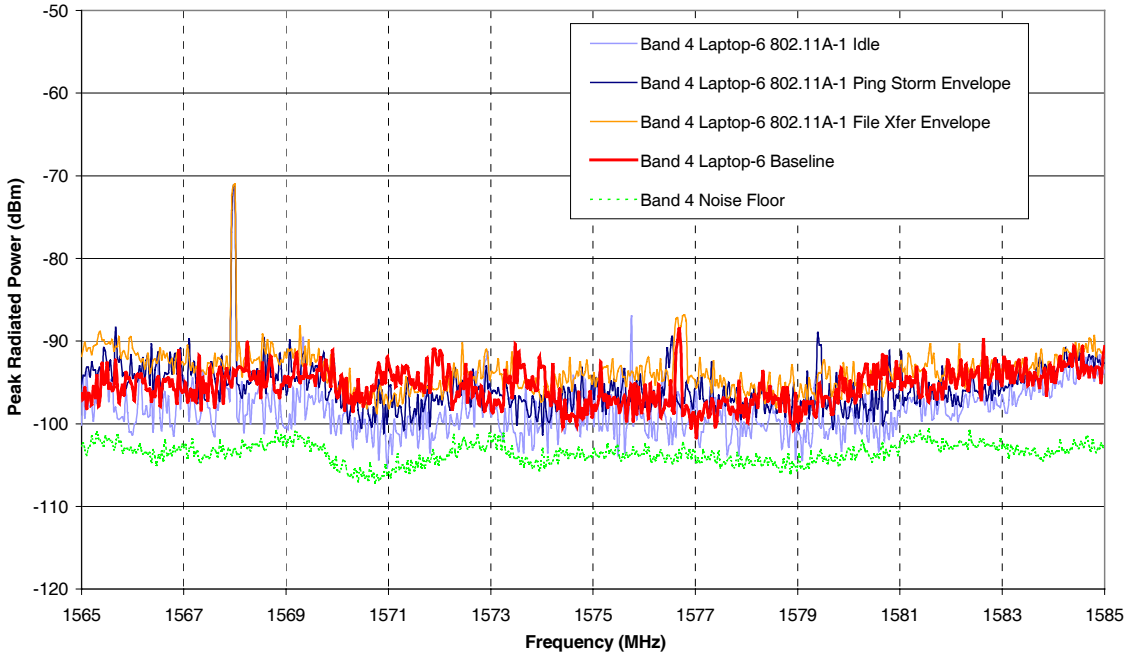

Figure A16: Laptop 6 and 802.11A-1, Band 4.

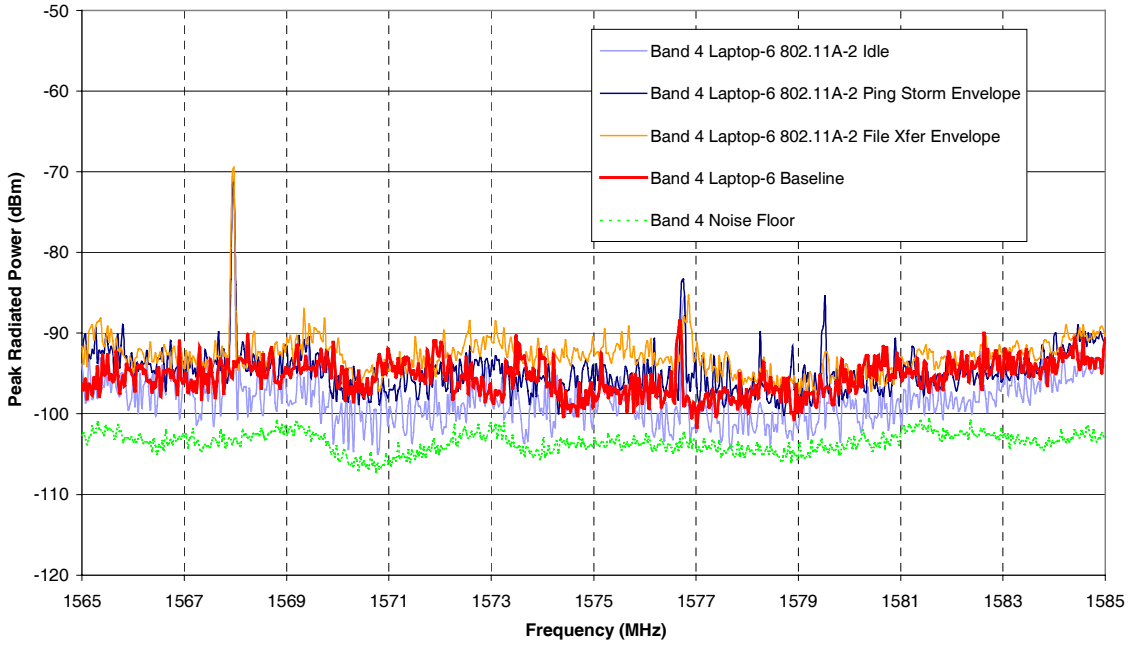

Figure A17: Laptop 6 and 802.11A-2, Band 4.

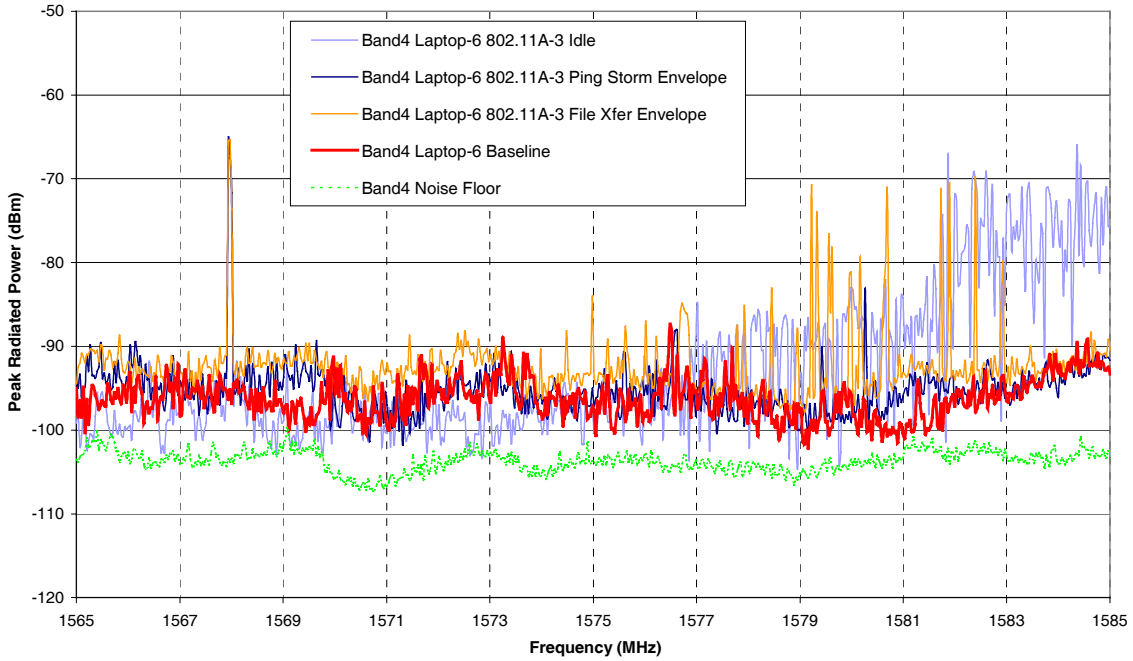

Figure A18: Laptop 6 and 802.11A-3, Band 4.

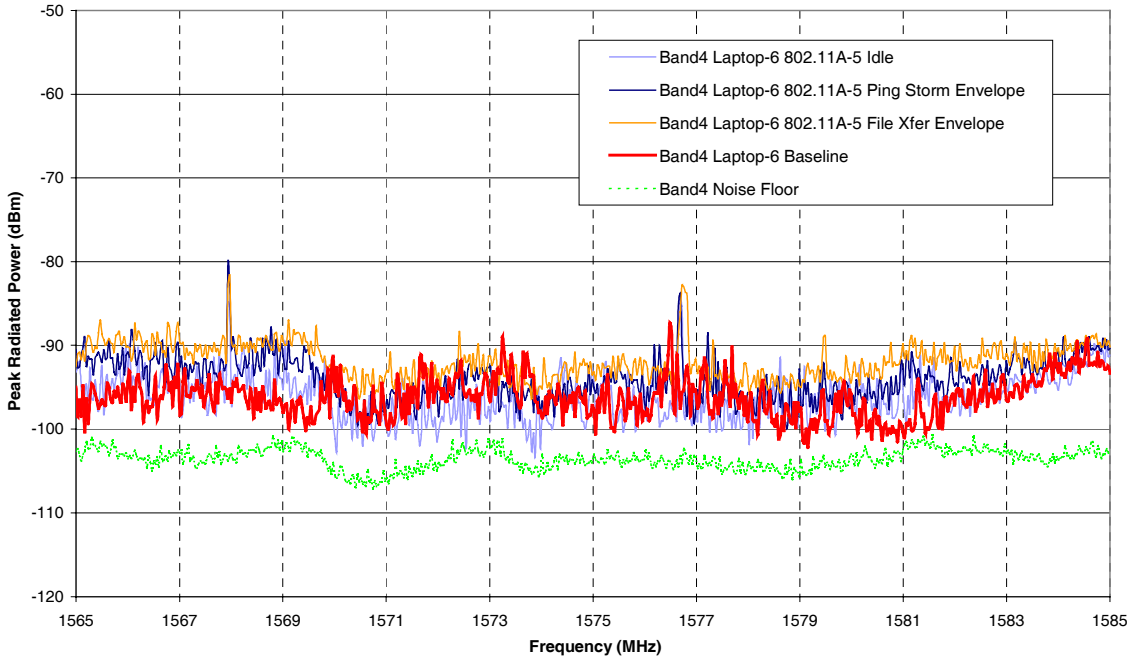

Figure A19: Laptop 6 and 802.11A-5, Band 4.

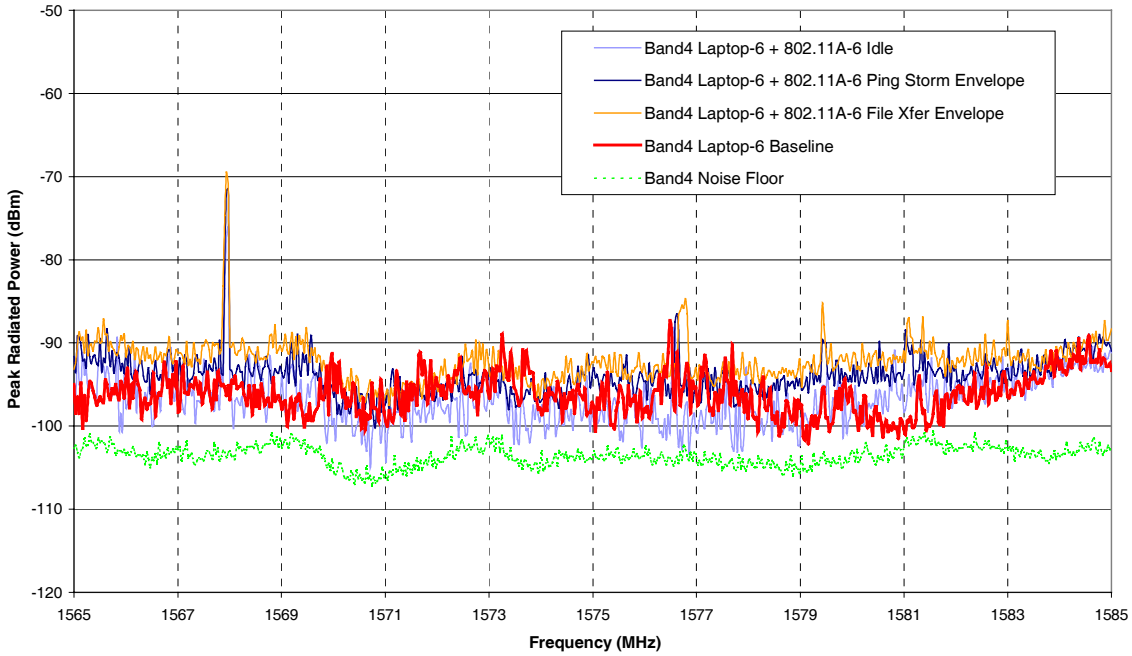

Figure A20: Laptop 6 and 802.11A-6, Band 4.

A.1.5 Band 5

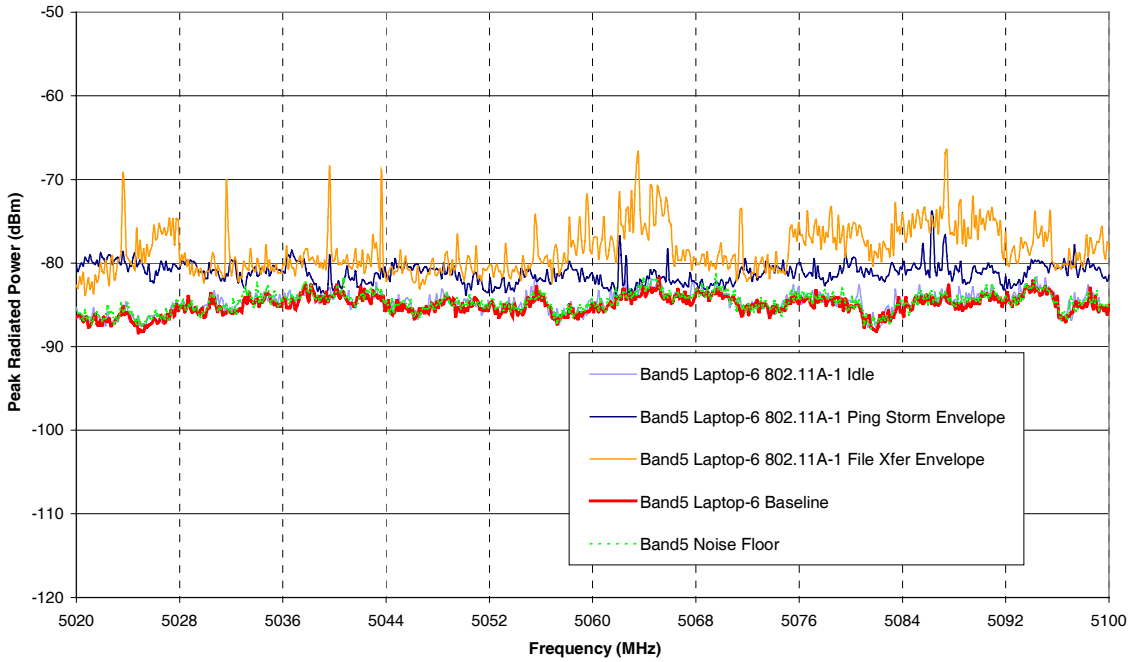

Figure A21: Laptop 6 and 802.11A-1, Band 5.

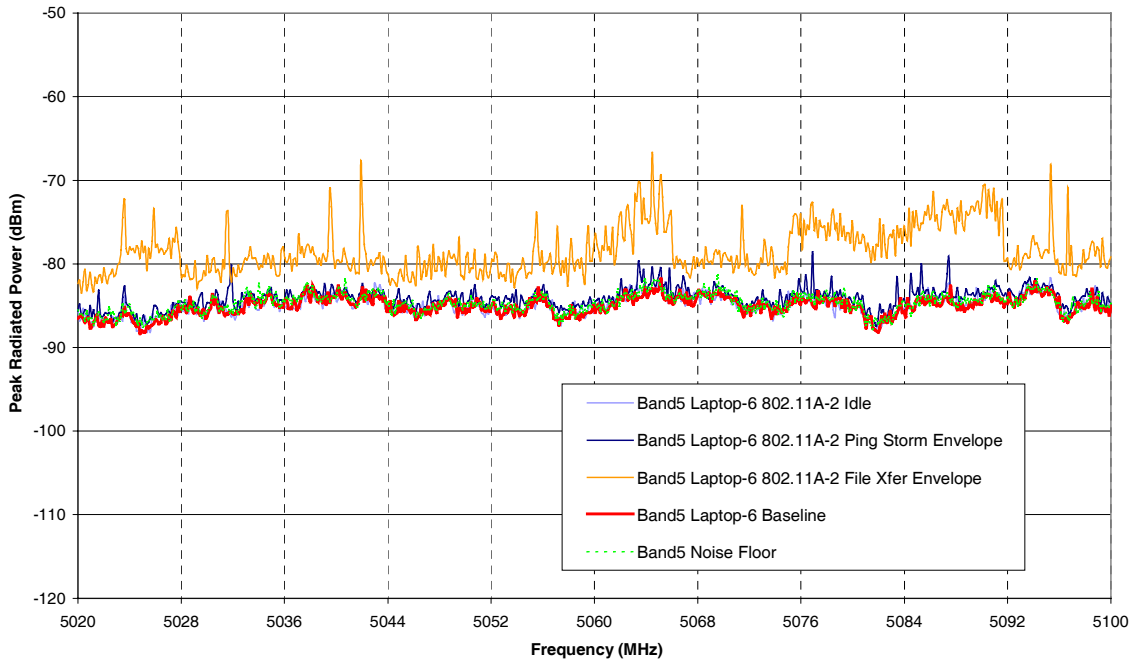

Figure A22: Laptop 6 and 802.11A-2, Band 5.

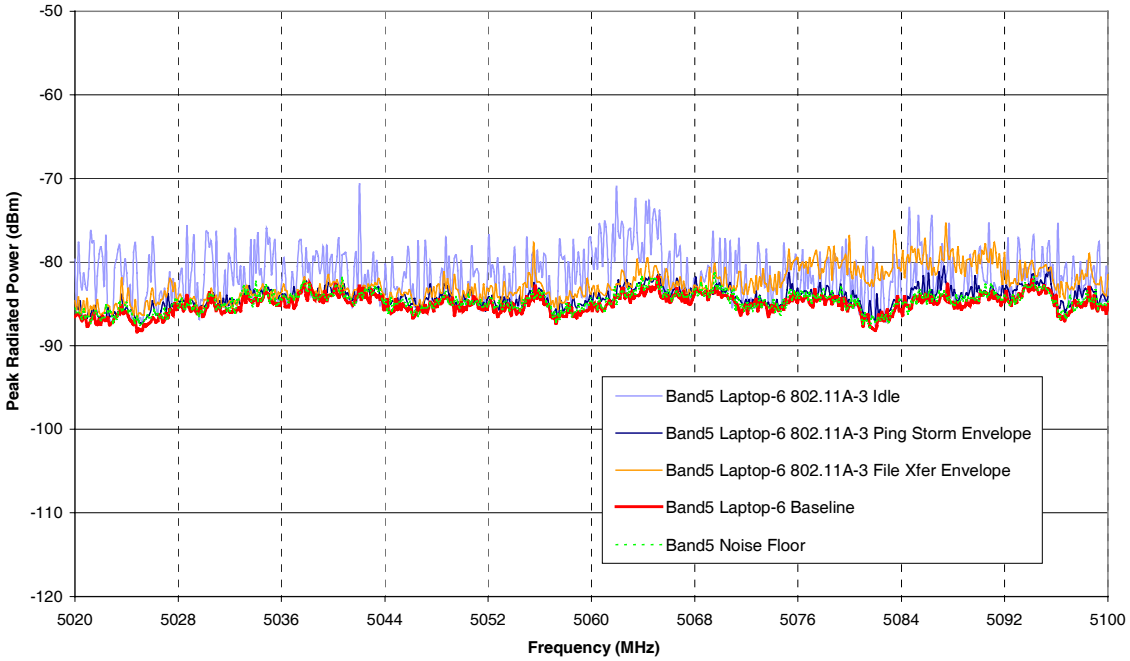

Figure A23: Laptop 6 and 802.11A-3, Band 5.

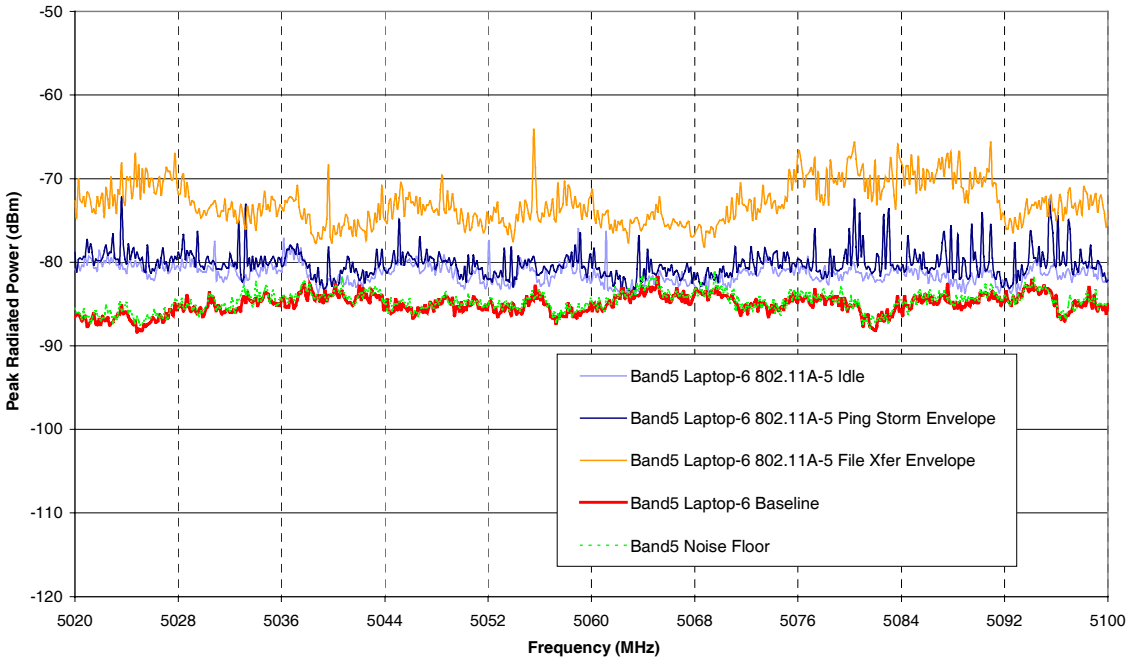

Figure A24: Laptop 6 and 802.11A-5, Band 5.

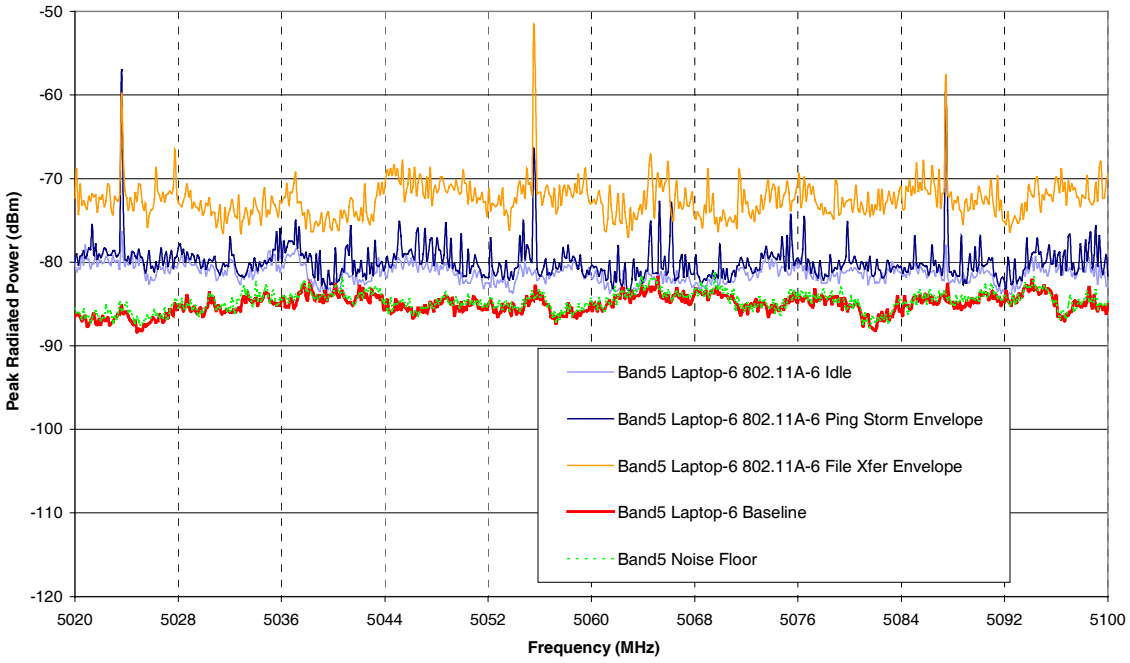

Figure A25: Laptop 6 and 802.11A-6, Band 5.

A.2 802.11b WLAN Devices

A.2.1 Band 1

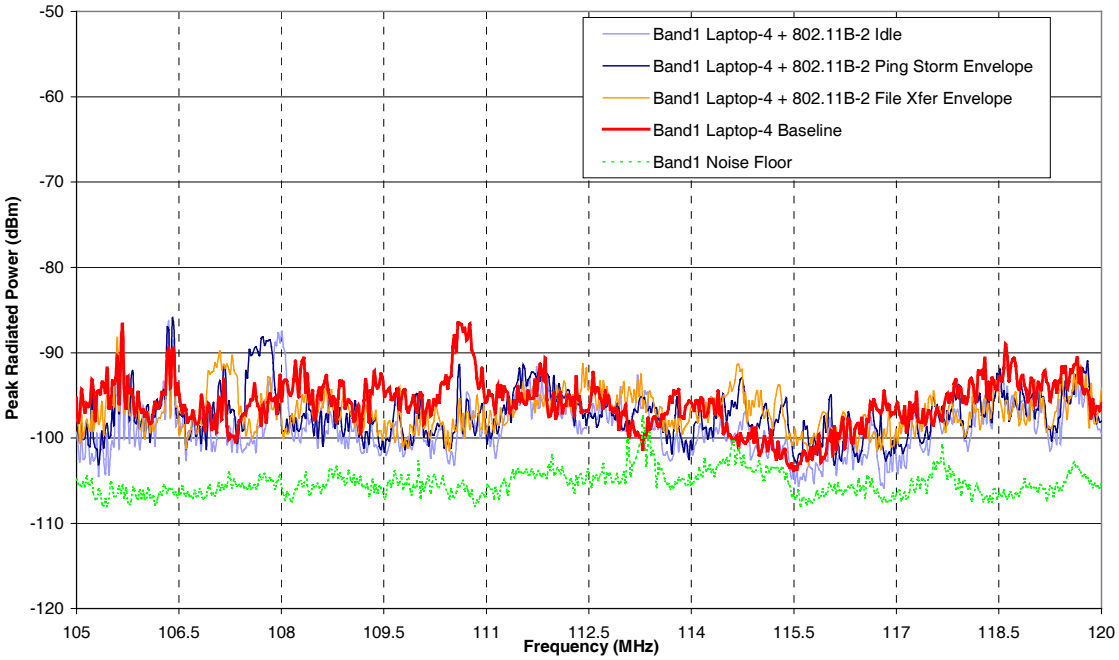

Figure A26: Laptop 4 and 802.11B-2, Band 1.

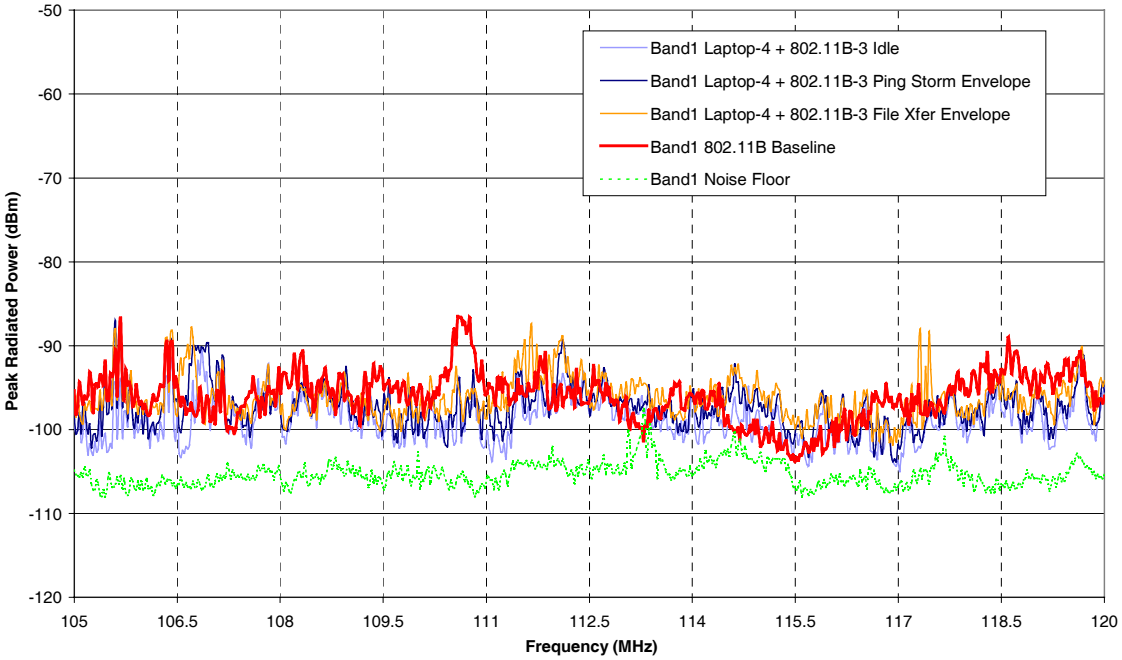

Figure A27: Laptop 4 and 802.11B-3, Band 1.

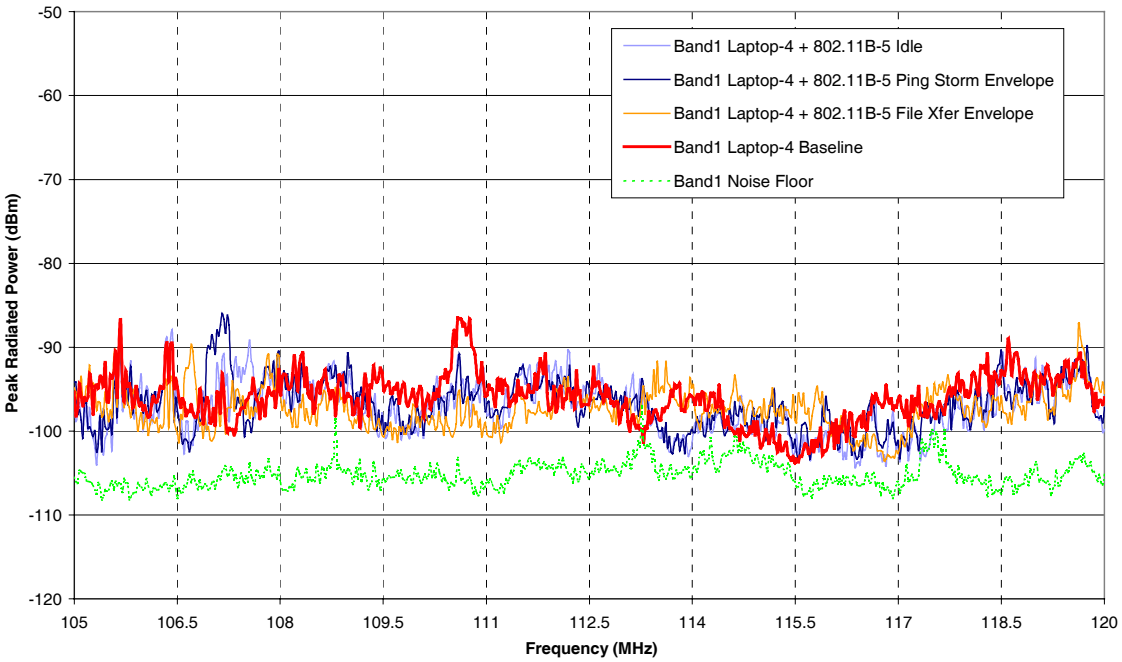

Figure A28: Laptop 4 and 802.11B-5, Band 1.

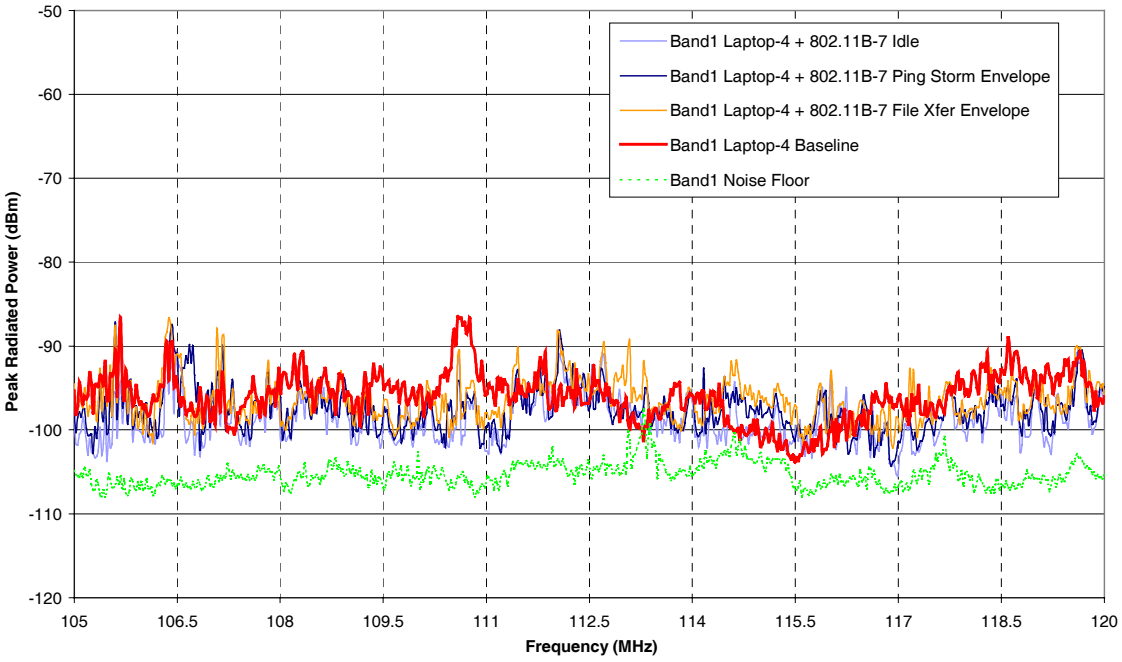

Figure A29: Laptop 4 and 802.11B-7, Band 1.

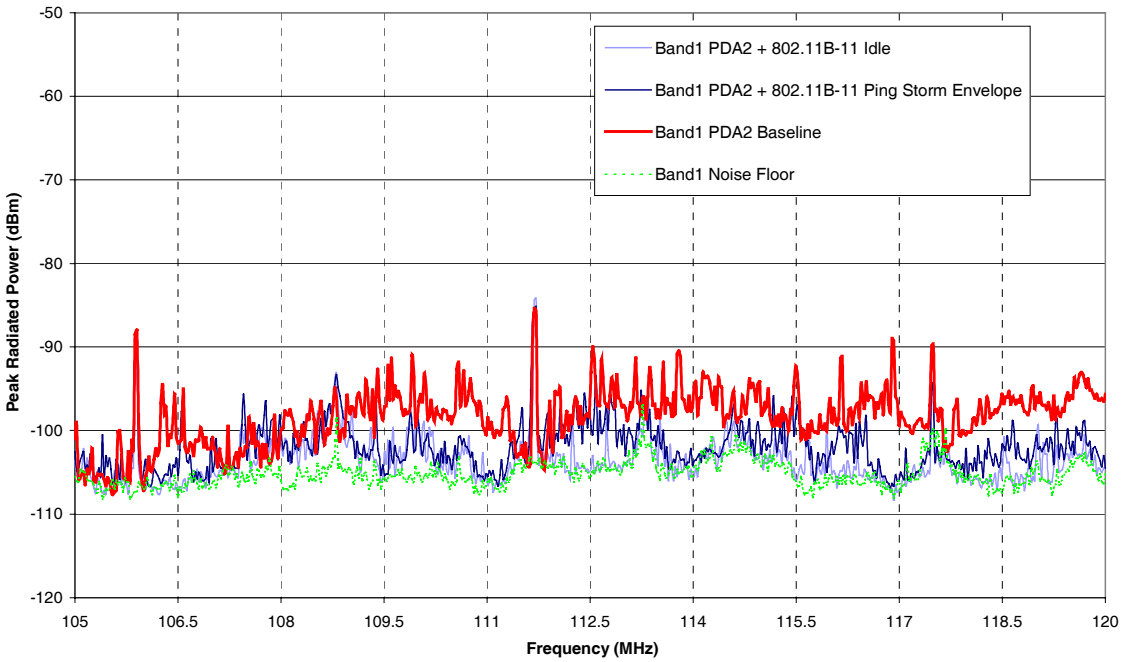

Figure A30: PDA2 802.11B-11, Band 1.

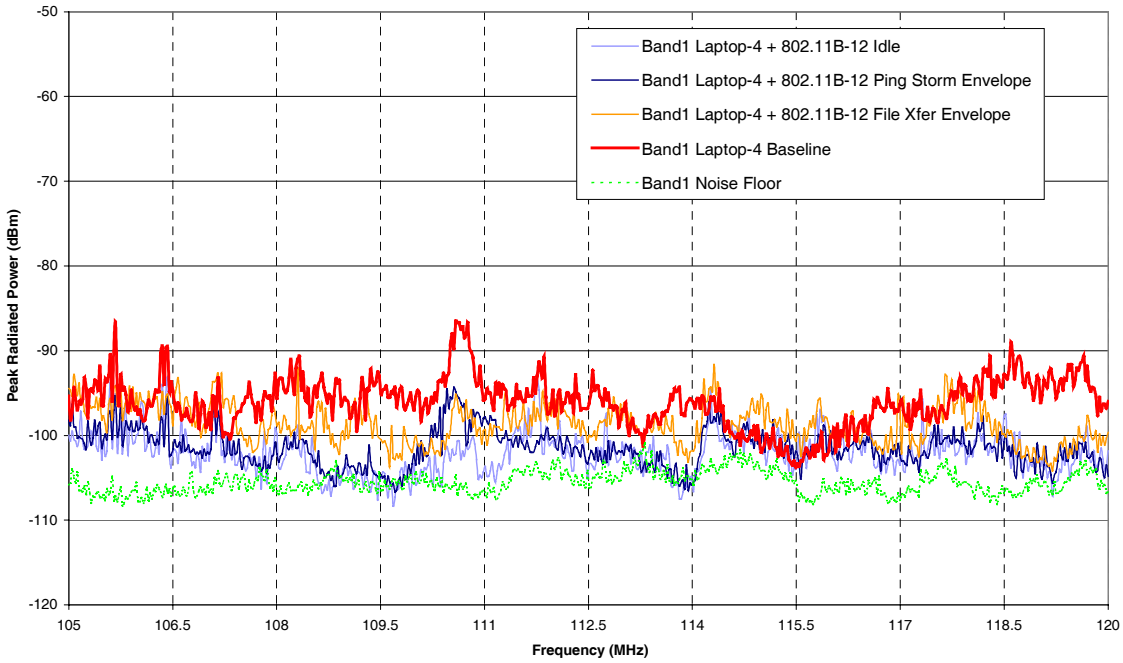

Figure A31: Laptop 4 and 802.11B-12, Band 1.

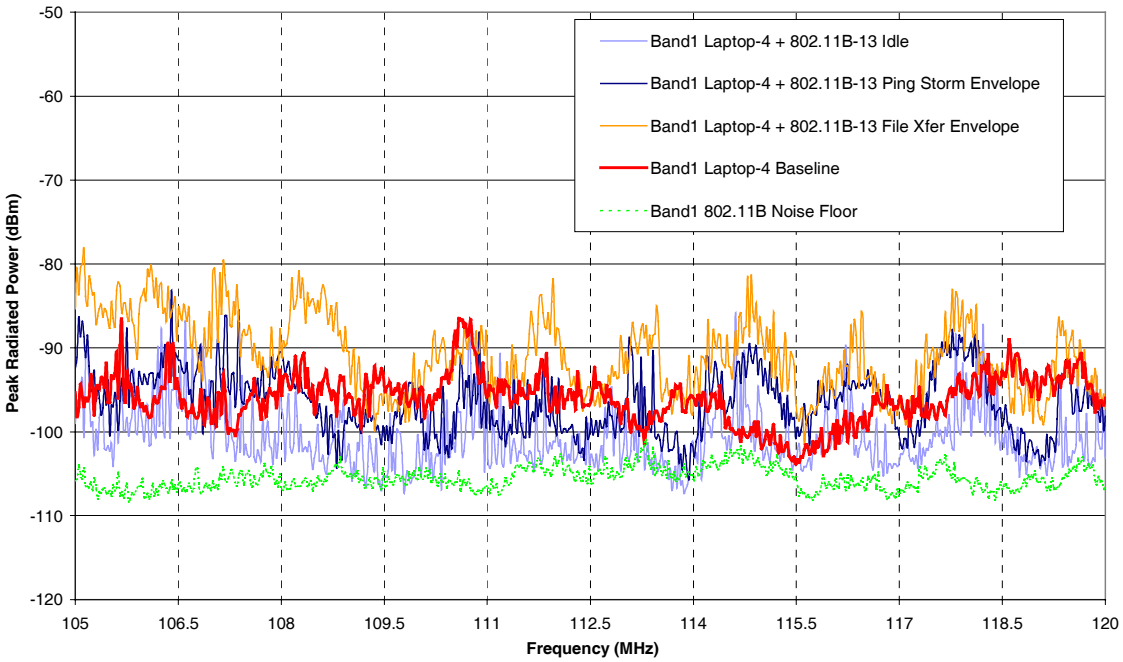

Figure A32: Laptop 4 and 802.11B-13, Band 1.

A.2.2 Band 2

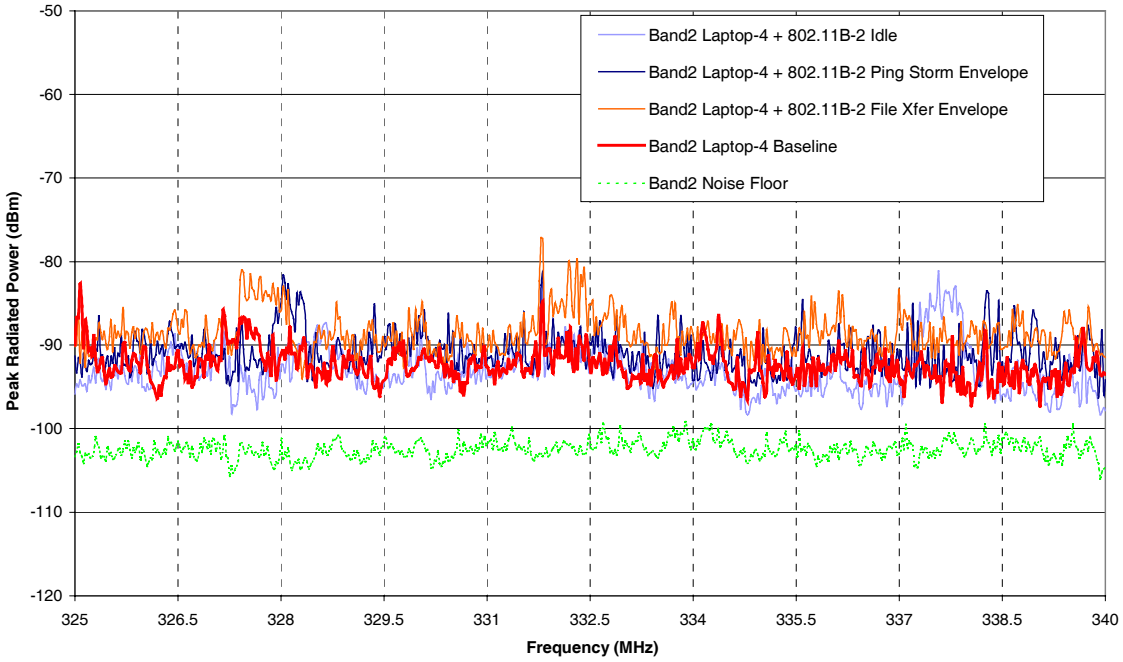

Figure A33: Laptop 4 and 802.11B-2, Band 2.

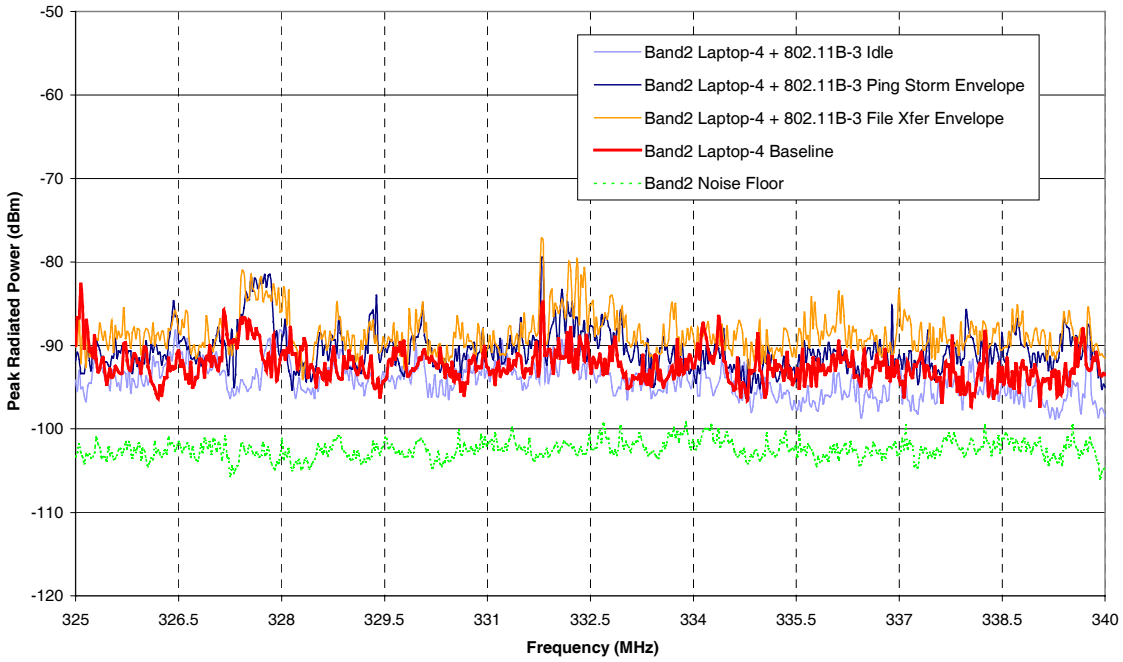

Figure A34: Laptop 4 and 802.11B-3, Band 2.

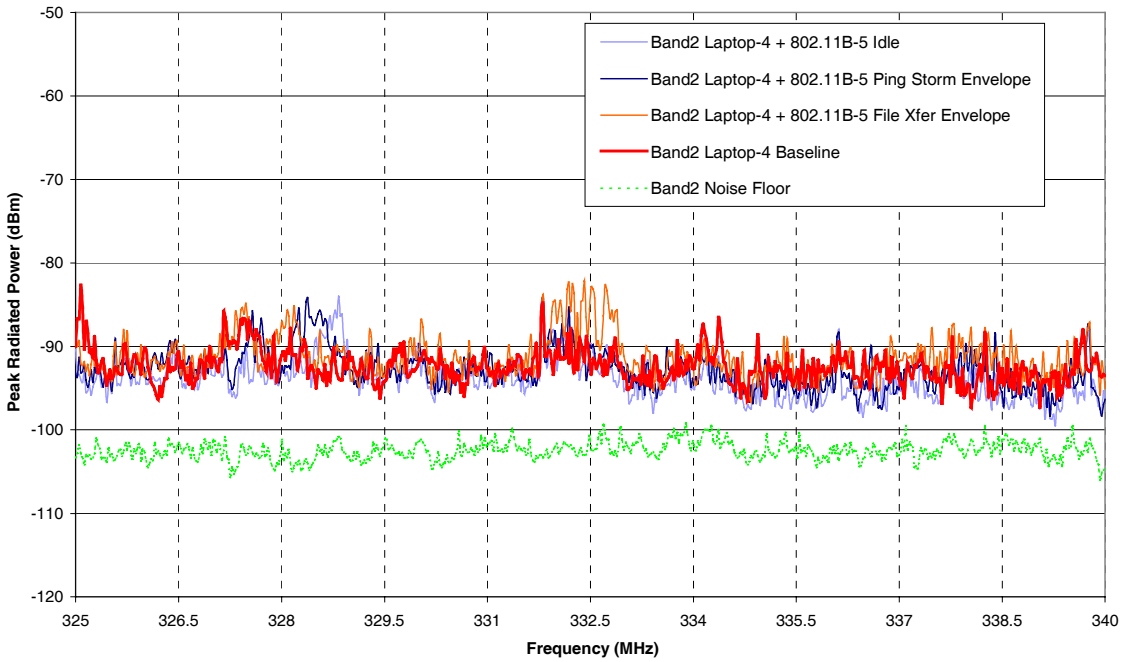

Figure A35: Laptop 4 and 802.11B-5, Band 2.

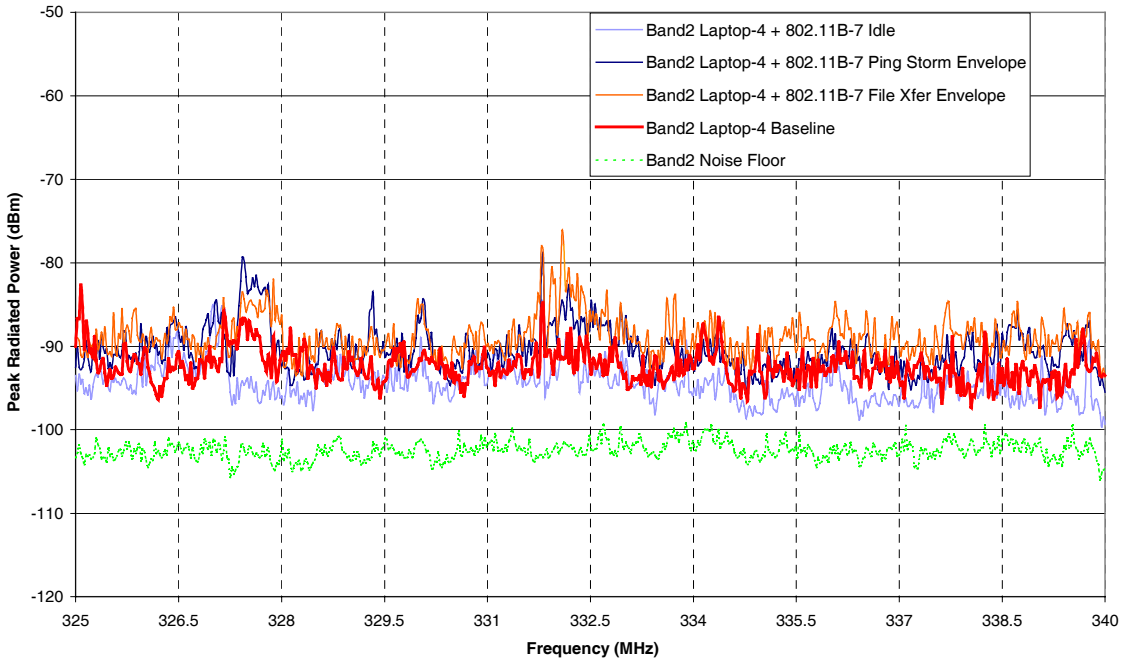

Figure A36: Laptop 4 and 802.11B-7, Band 2.

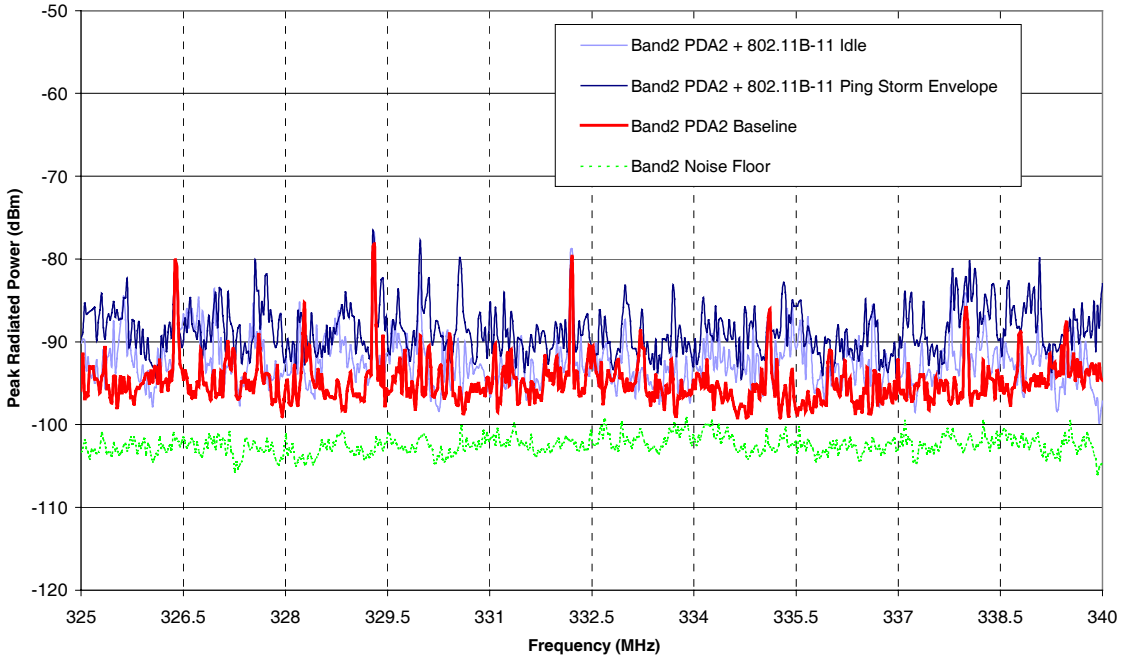

Figure A37: PDA2 and 802.11B-11, Band 2.

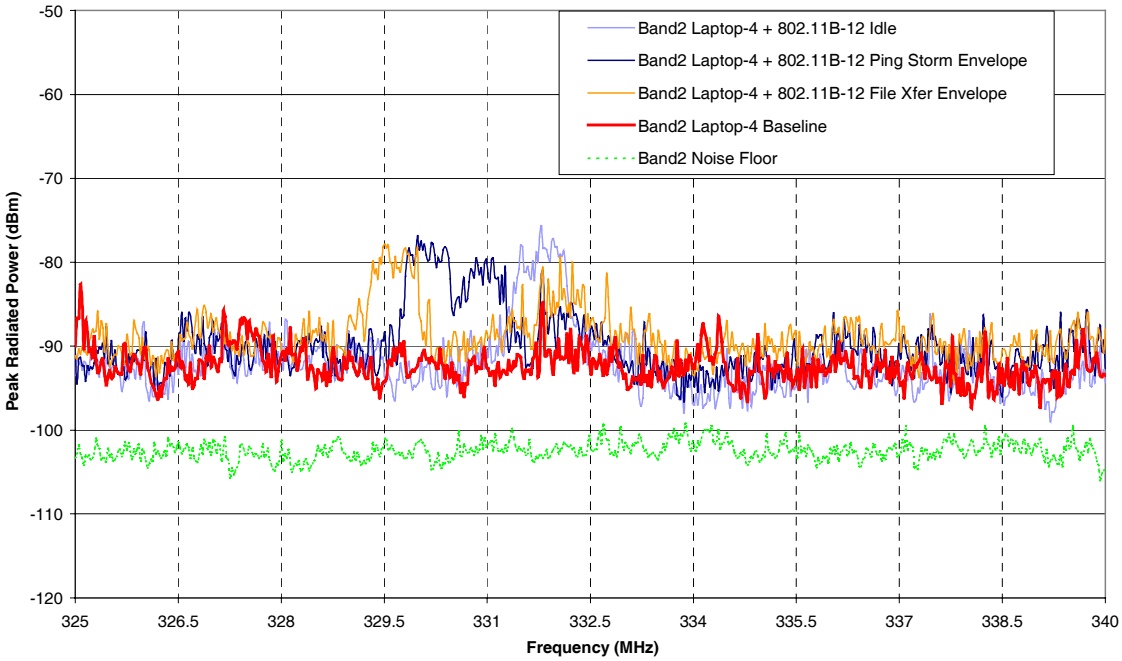

Figure A38: Laptop 4 and 802.11B-12, Band 2.

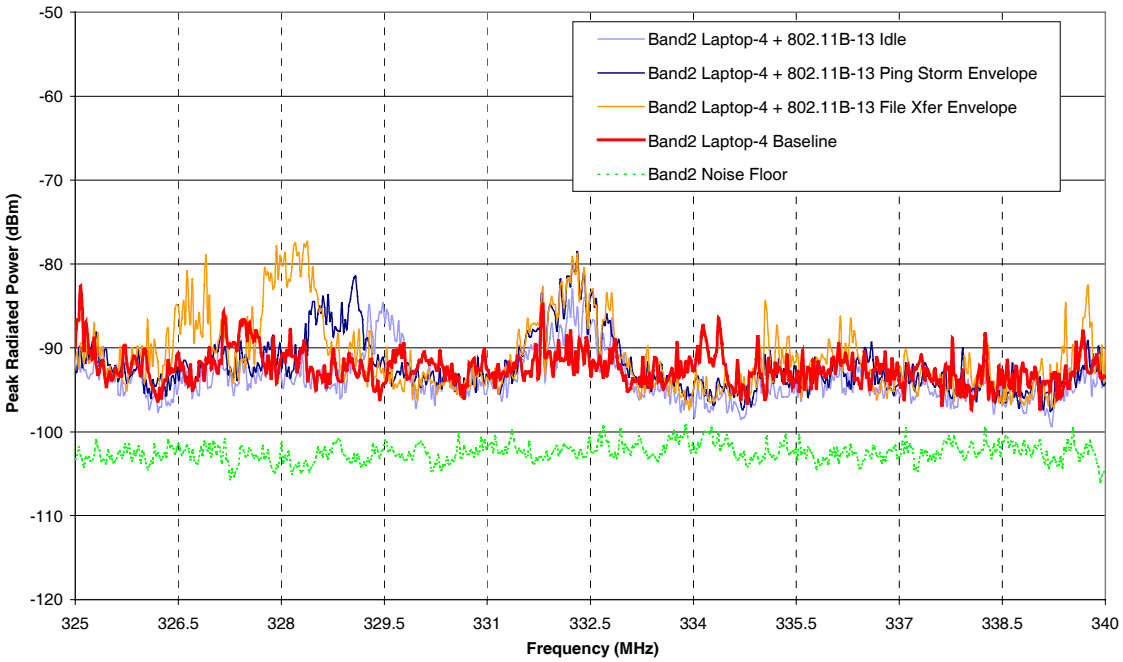

Figure A39: Laptop 4 and 802.11B-13, Band 2.

A.2.3 Band 3

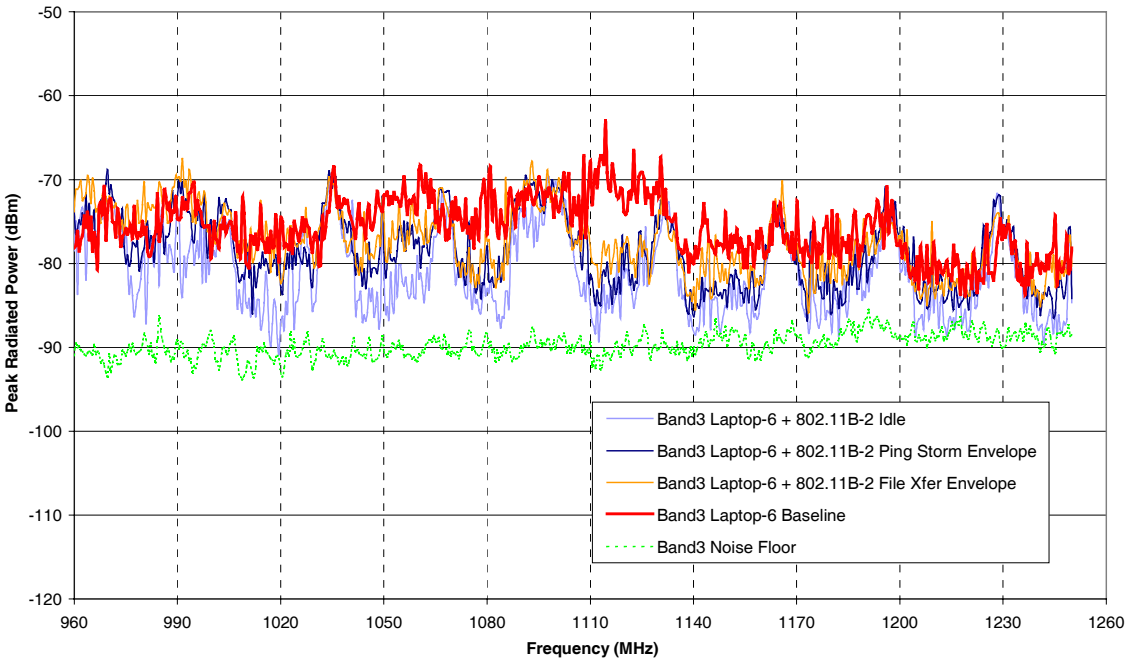

Figure A40: Laptop 6 and 802.11B-2, Band 3.

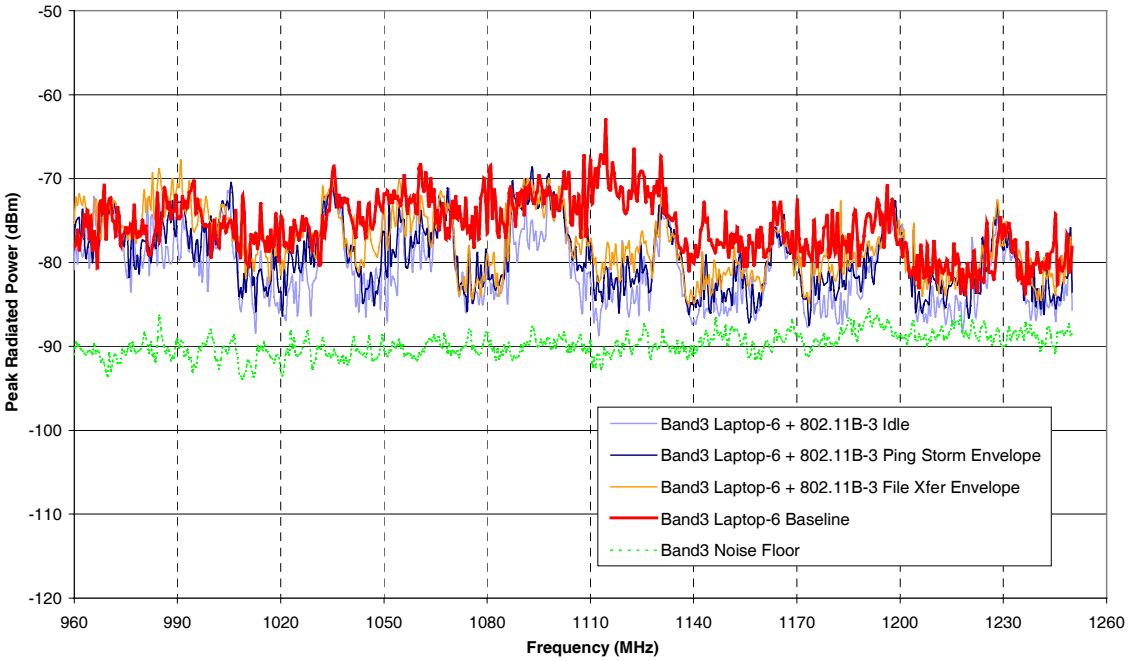

Figure A41: Laptop 6 and 802.11B-3, Band 3.

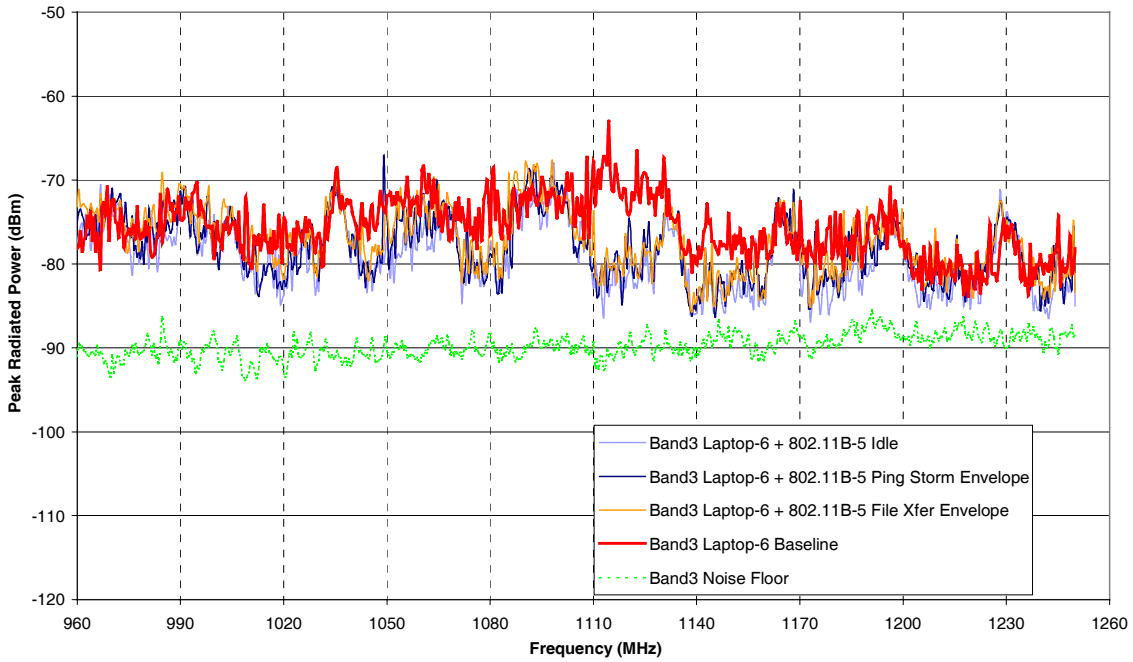

Figure A42: Laptop 6 and 802.11B-5, Band 3.

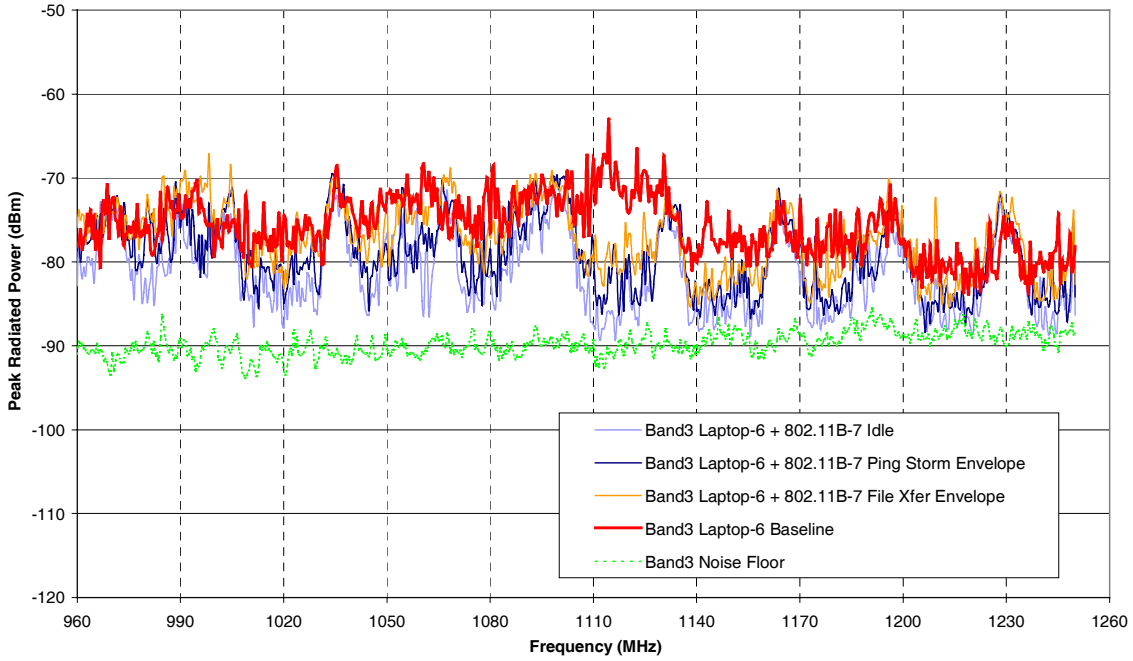

Figure A43: Laptop 6 and 802.11B-7, Band 3.

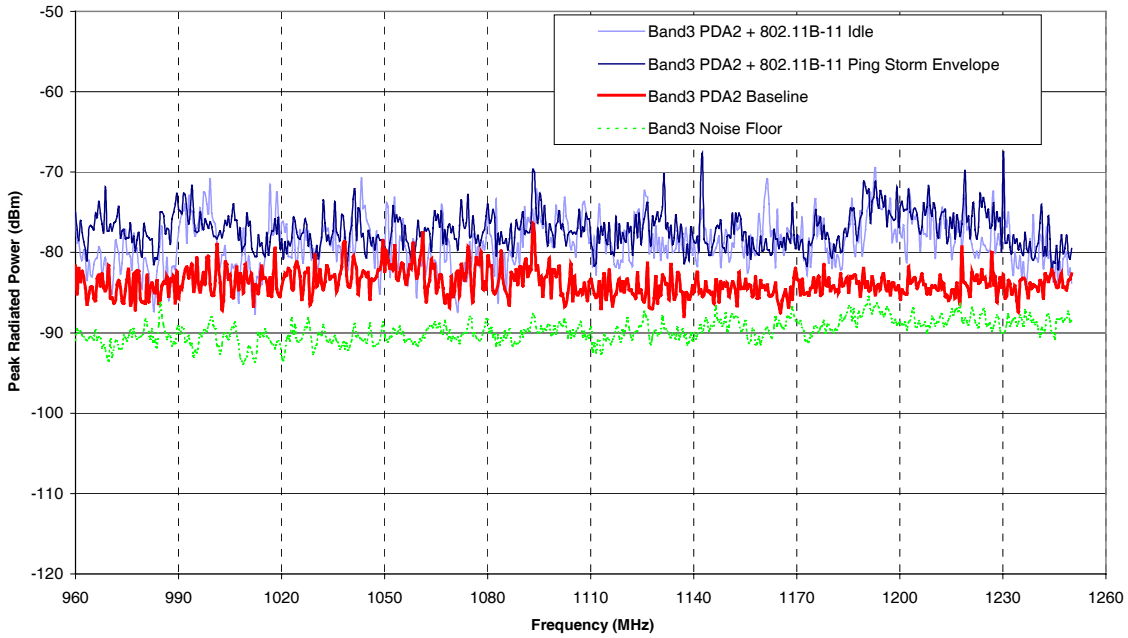

Figure A44: PDA2 and 802.11B-11, Band 3.

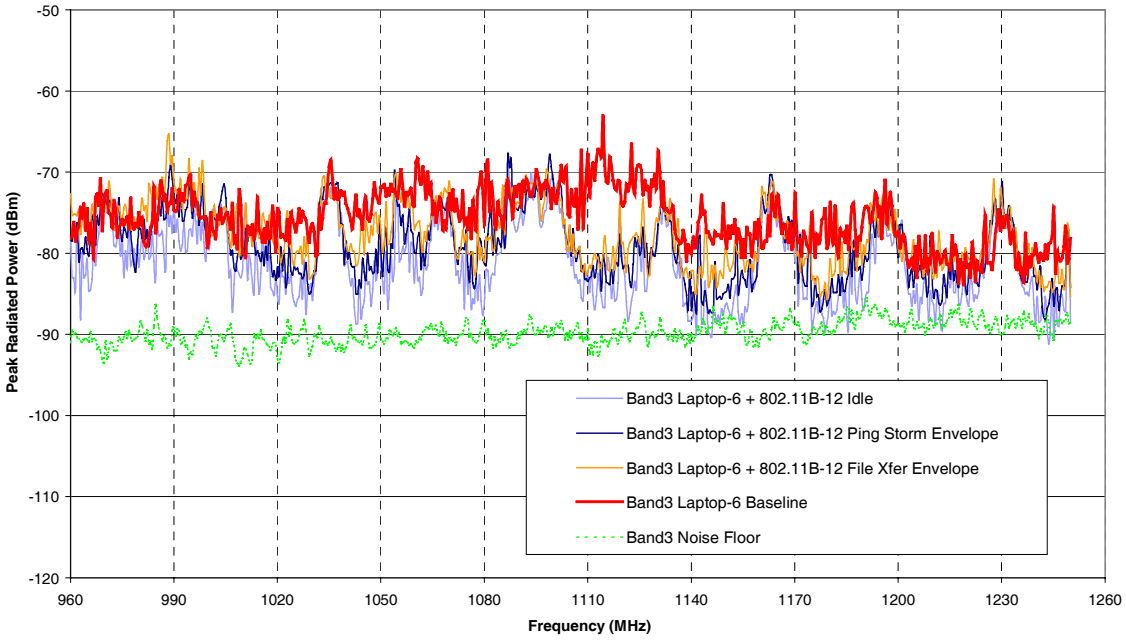

Figure A45: Laptop 6 and 802.11B-12, Band 3.

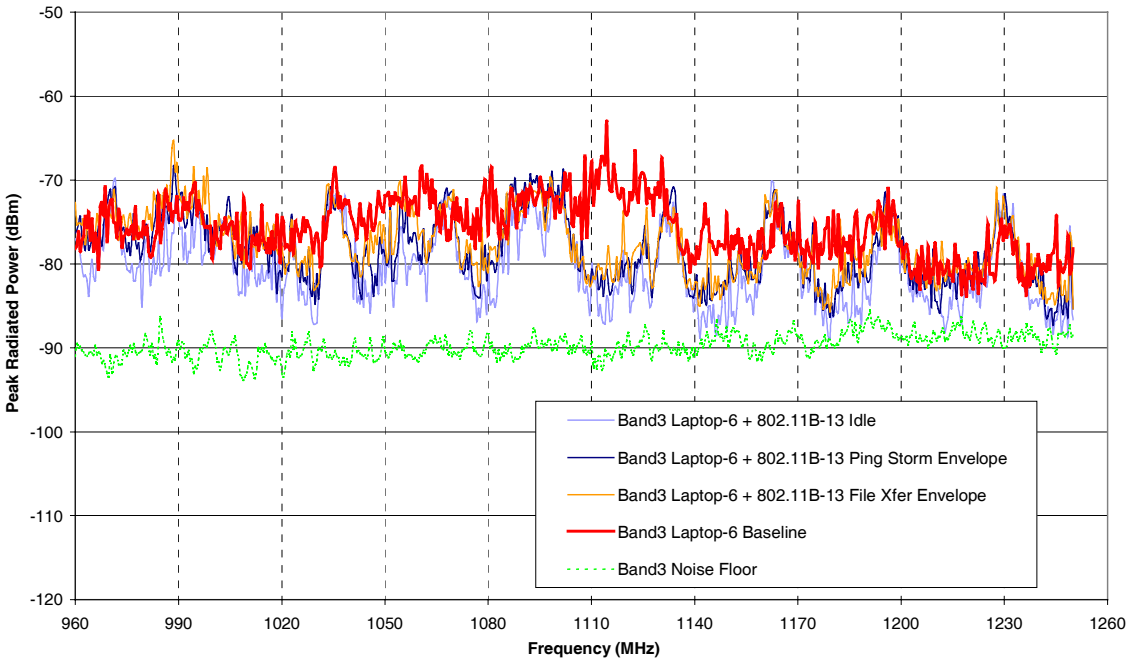

Figure A46: Laptop 6 and 802.11B-13, Band 3.

A.2.4 Band 4

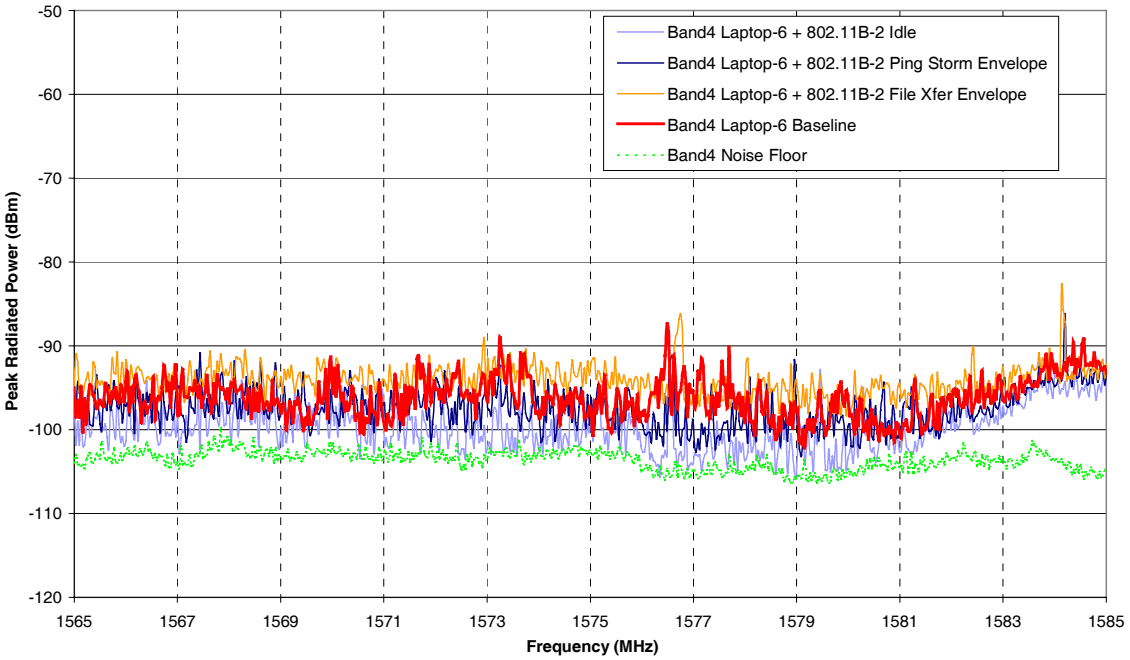

Figure A47: Laptop 6 and 802.11B-2, Band 4.

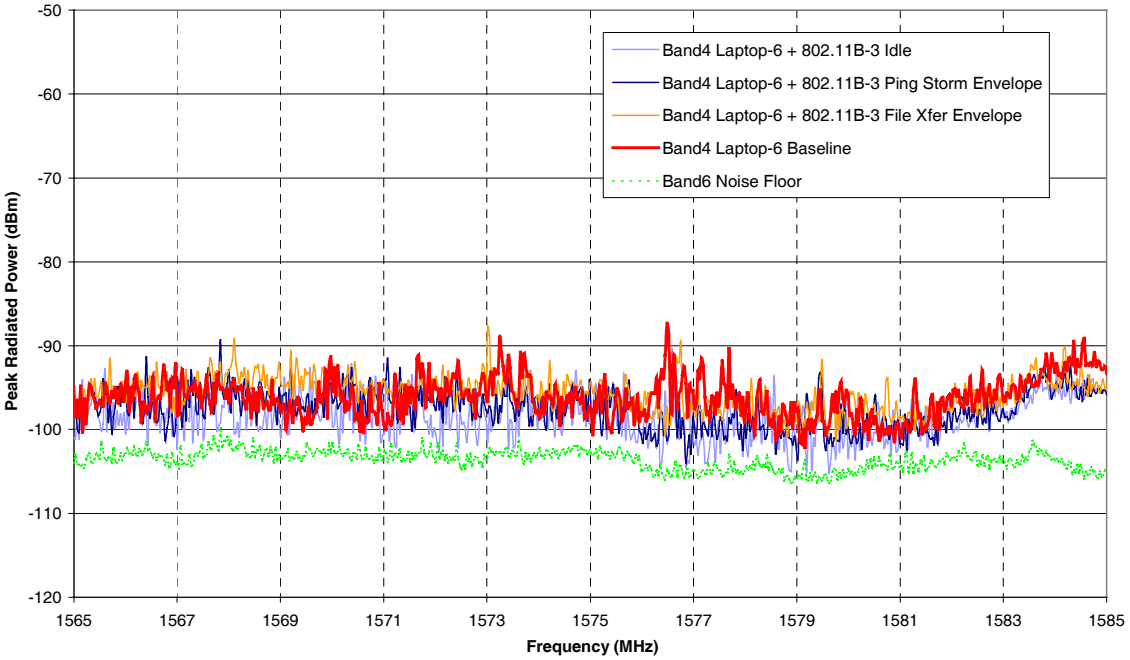

Figure A48: Laptop 6 and 802.11B-3, Band 4.

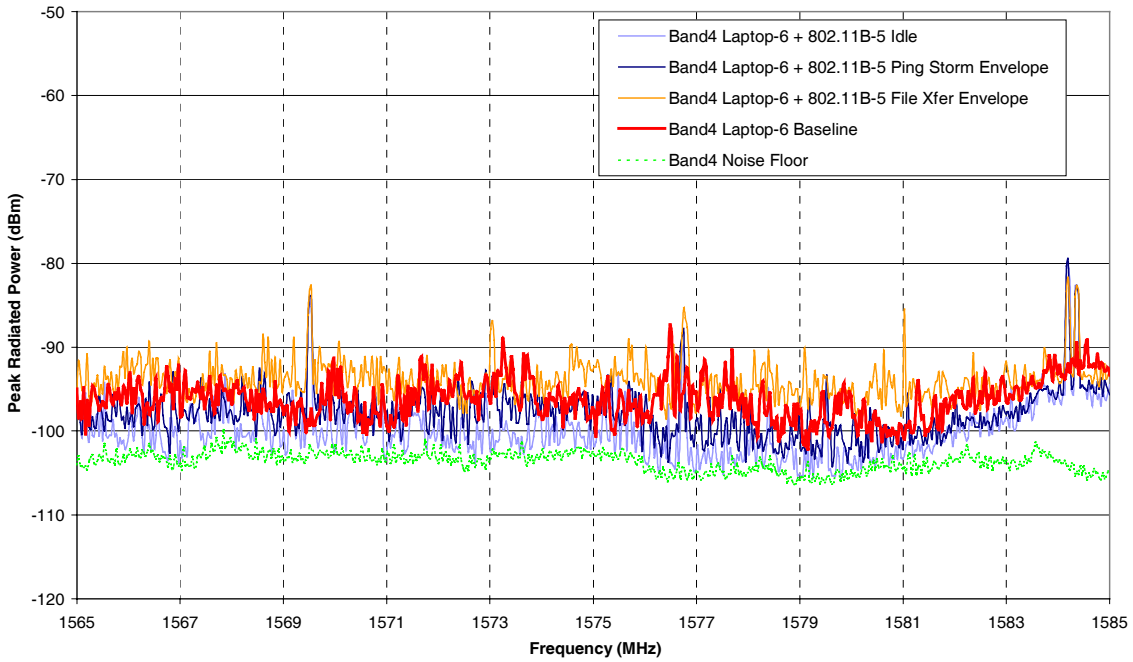

Figure A49: Laptop 6 and 802.11B-5, Band 4.

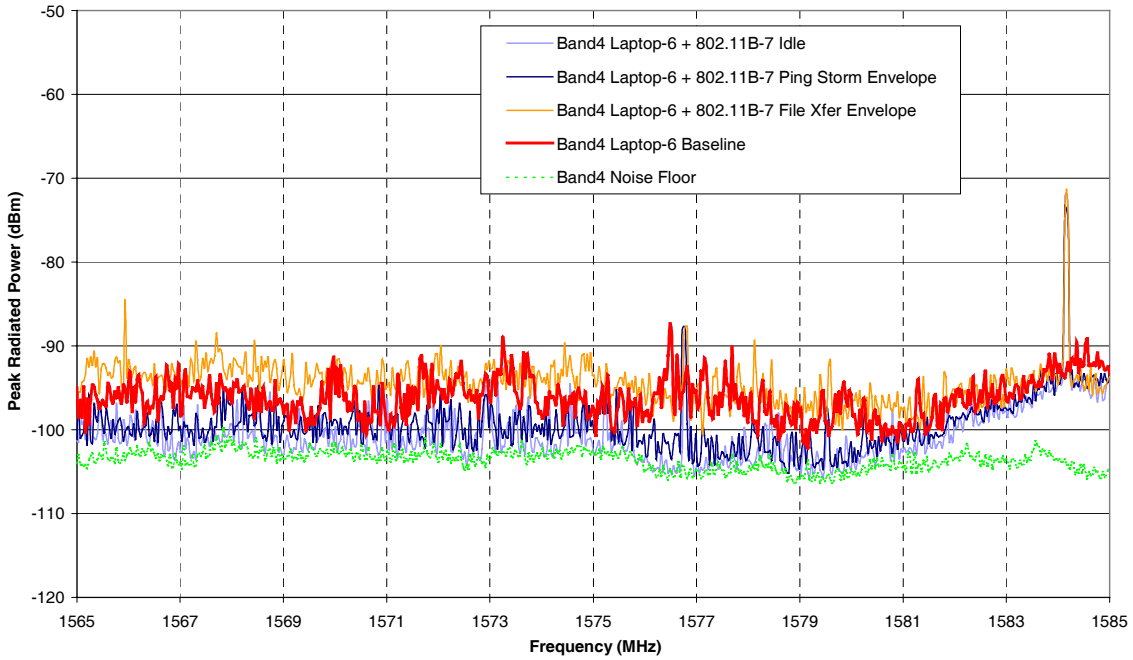

Figure A50: Laptop 6 and 802.11B-7, Band 4.

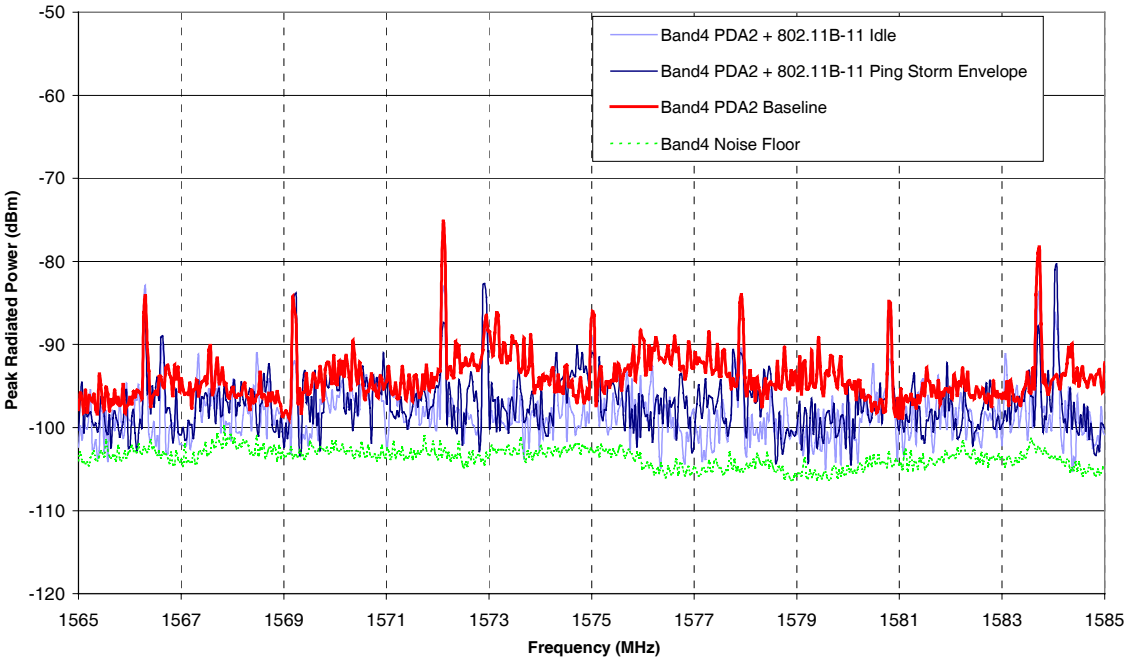

Figure A51: PDA2 and 802.11B-11, Band 4.

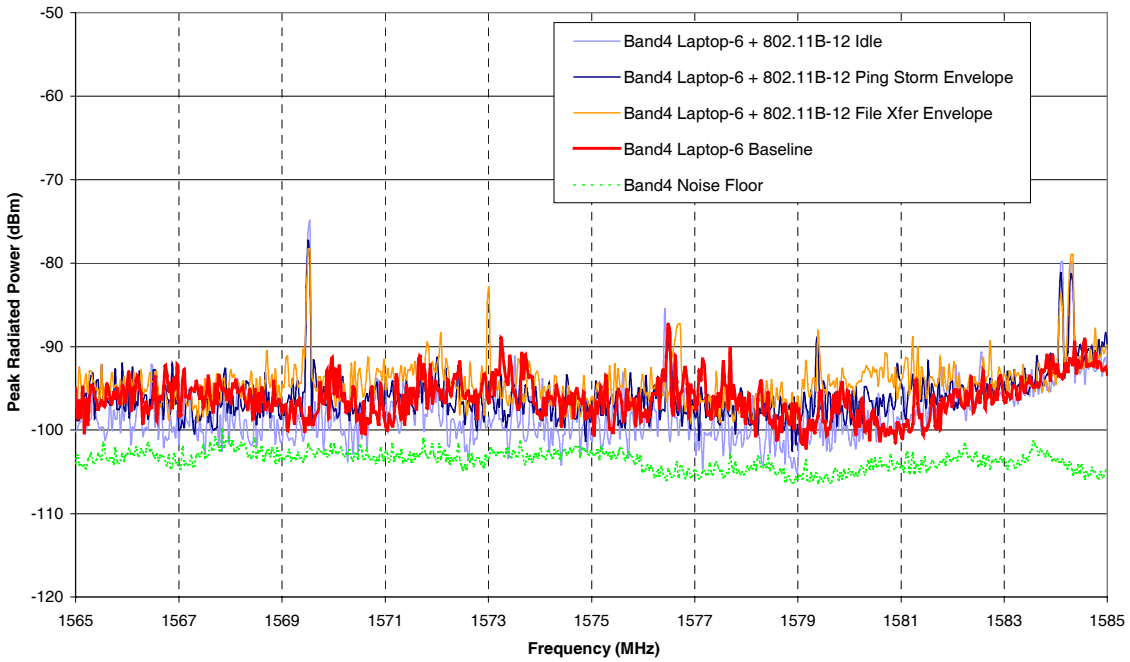

Figure A52: Laptop 6 and 802.11B-12, Band 4.

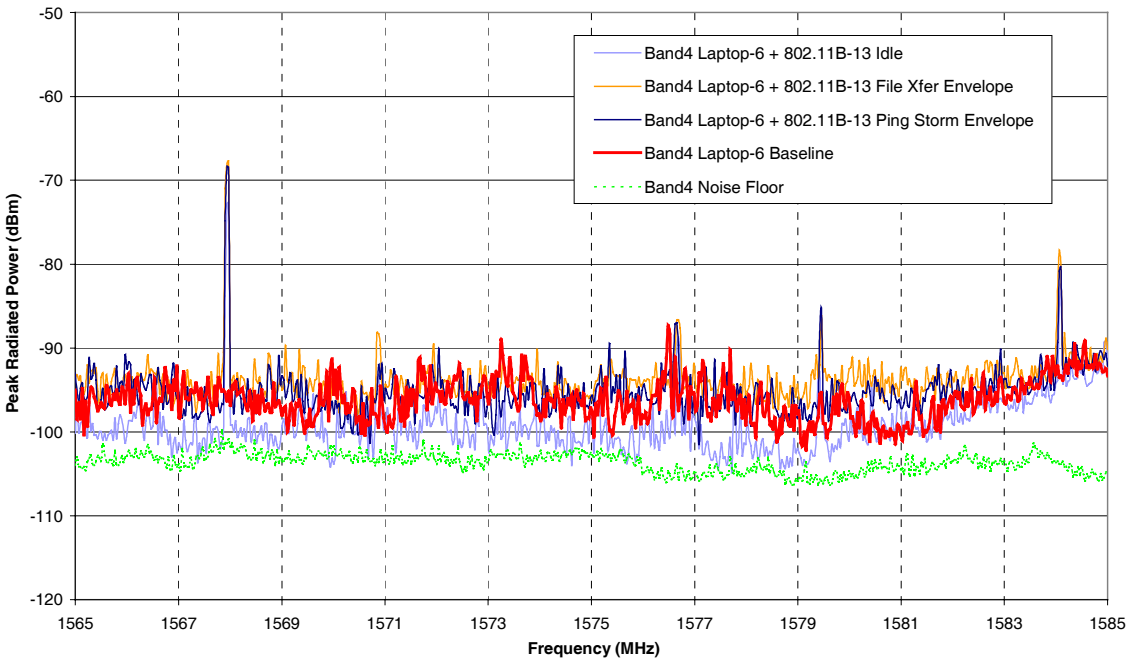

Figure A53: Laptop 6 and 802.11B-13, Band 4.

A.2.5 Band 5

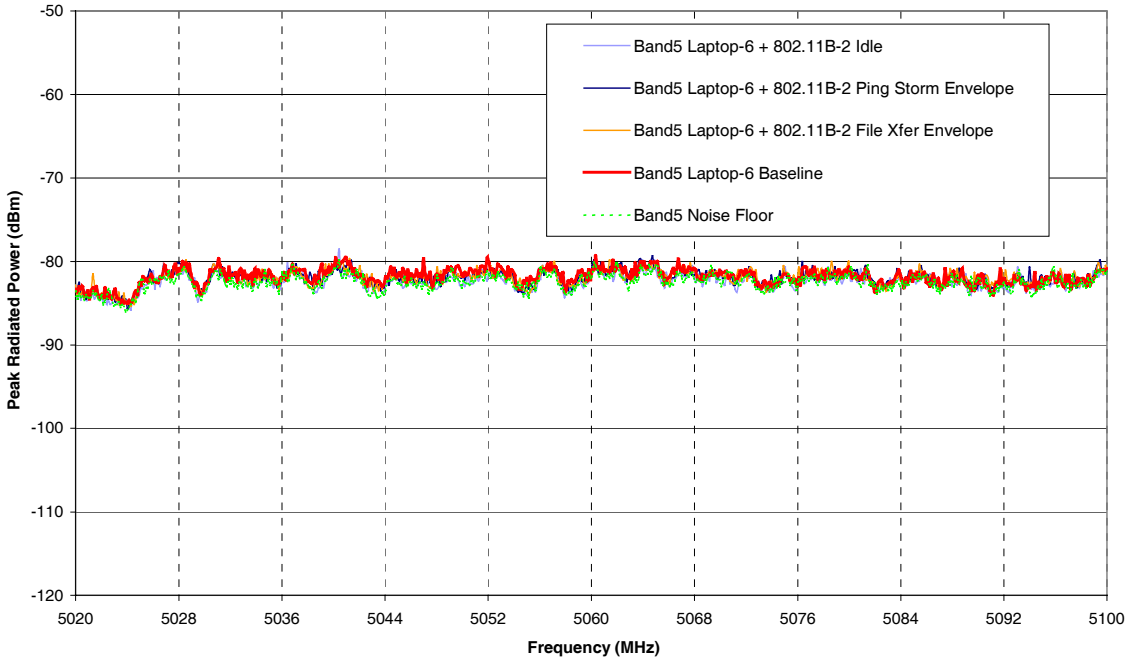

Figure A54: Laptop 6 and 802.11B-2, Band 5.

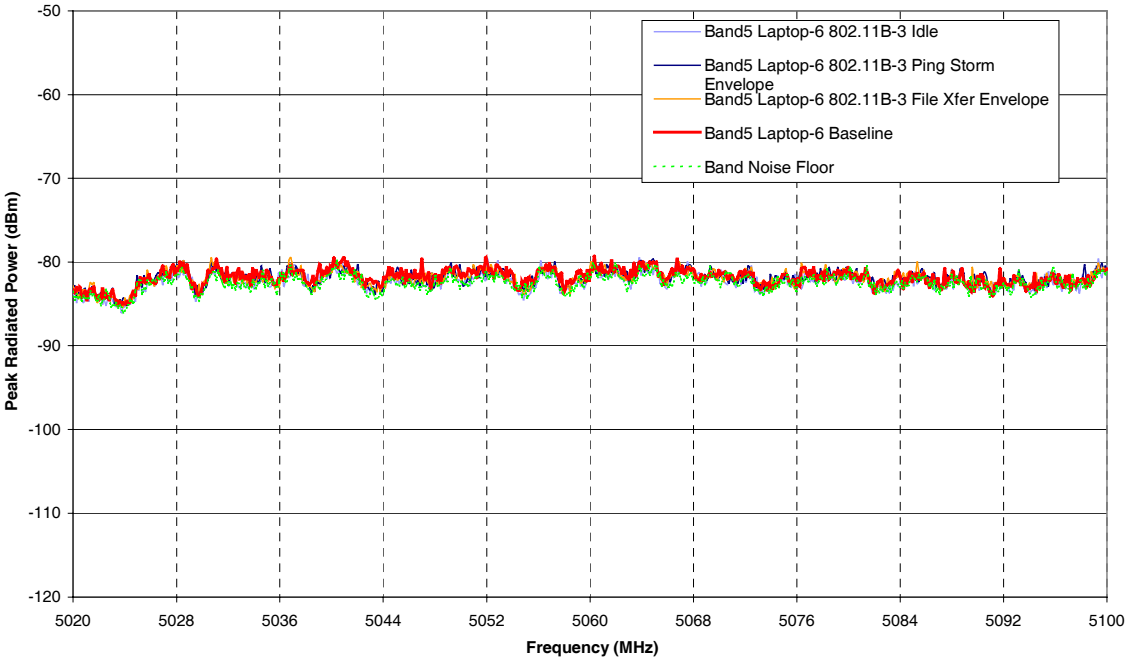

Figure A55: Laptop 6 and 802.11B-3, Band 5.

Figure A56: Laptop 6 and 802.11B-5, Band 5.

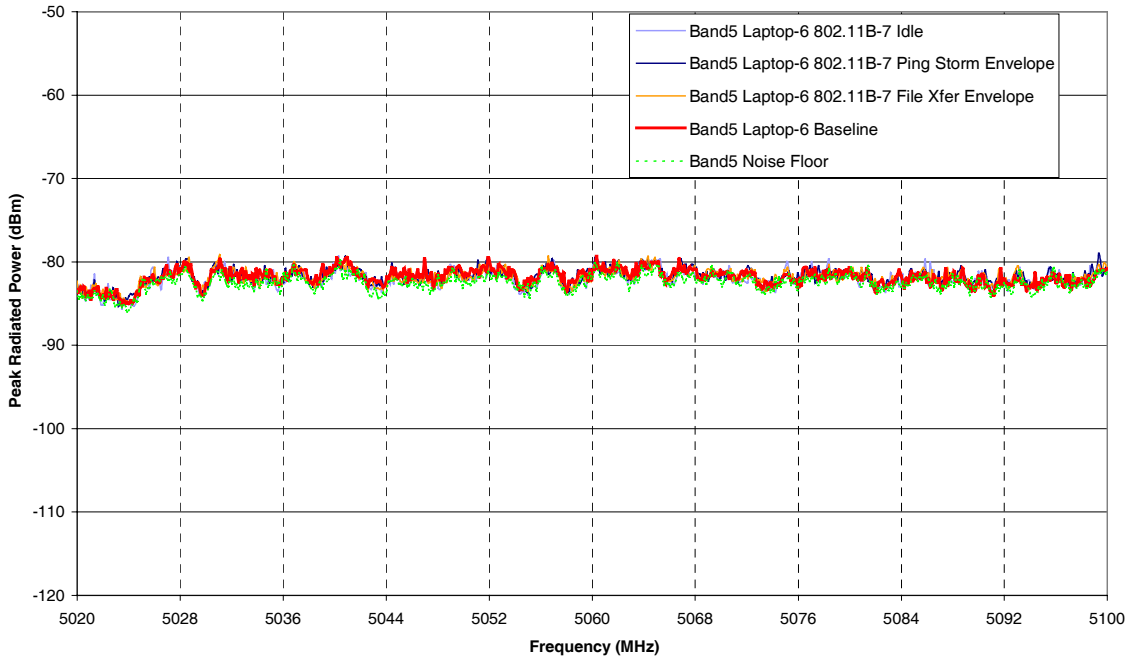

Figure A57: Laptop 6 and 802.11B-7, Band 5.

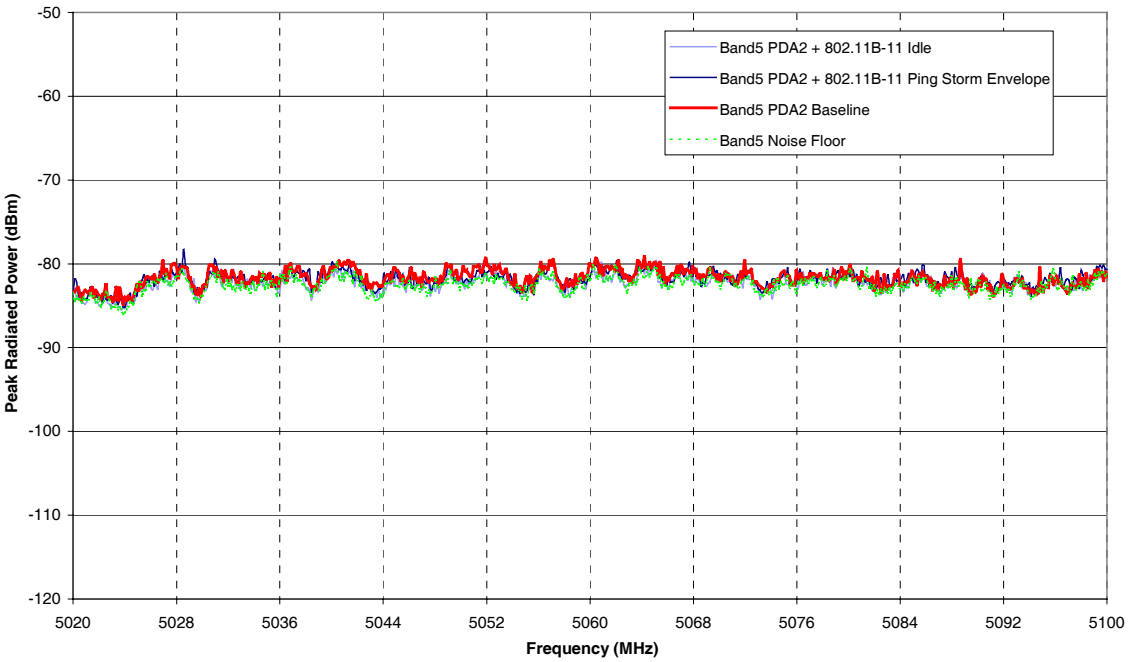

Figure A58: PDA2 and 802.11B-11, Band 5.

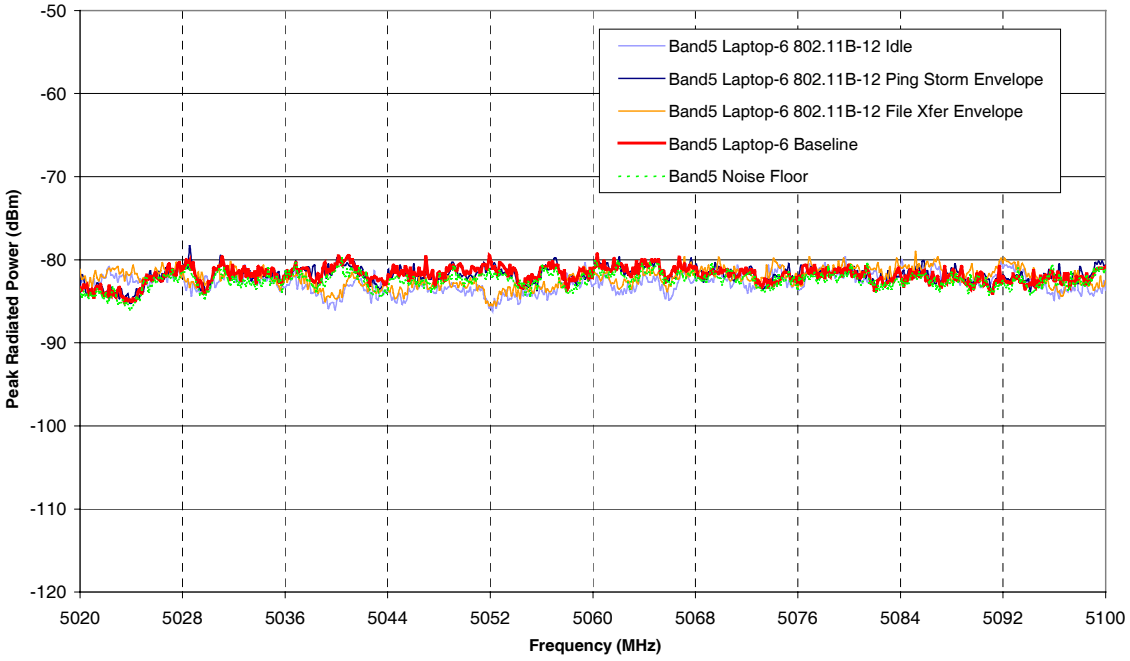

Figure A59: Laptop 6 and 802.11B-12, Band 5.

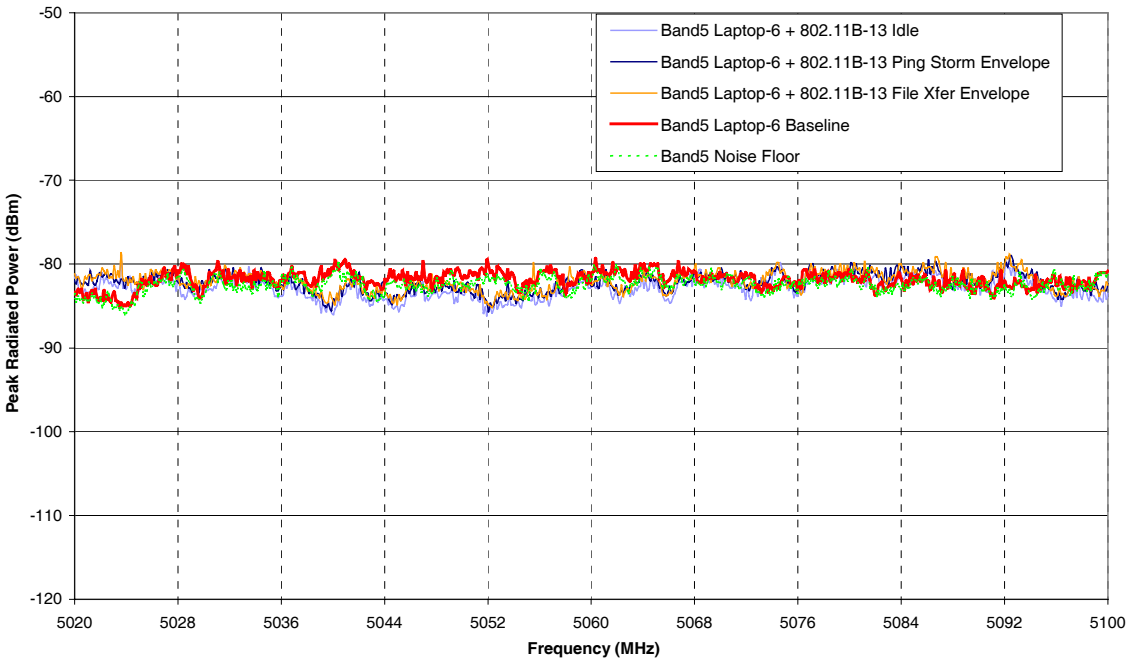

Figure A60: Laptop 6 and 802.11B-13, Band 5.

A.3 Bluetooth Devices

A.3.1 Band 1

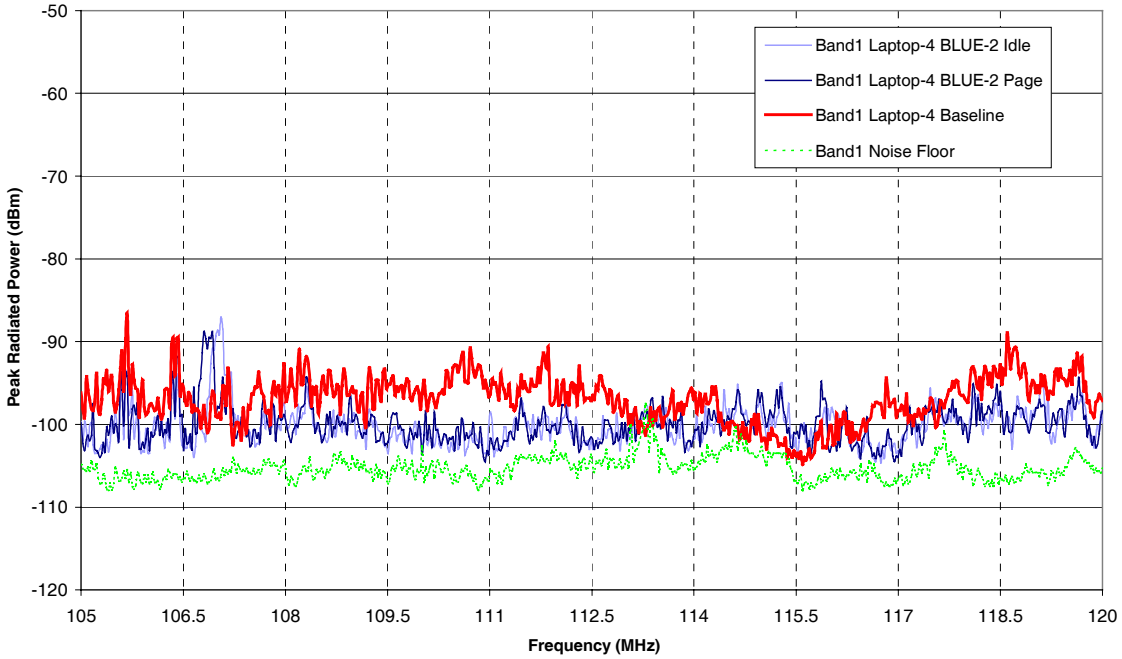

Figure A61: Laptop 4 and BLUE-2, Band 1.

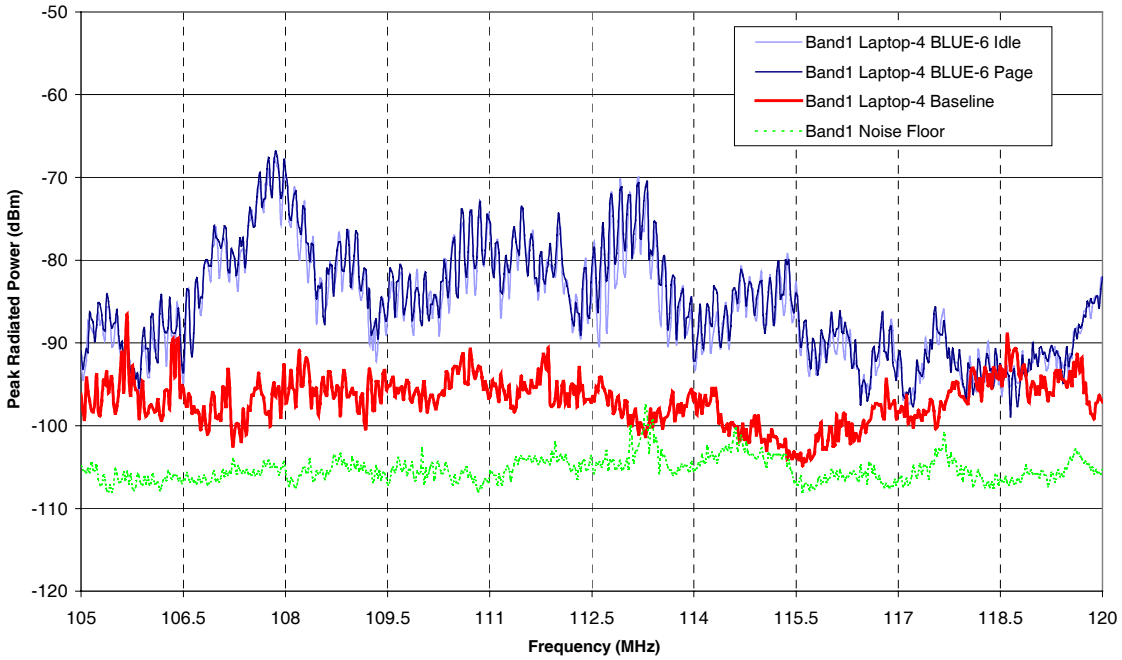

Figure A62: Laptop 4 and BLUE-6, Band 1.

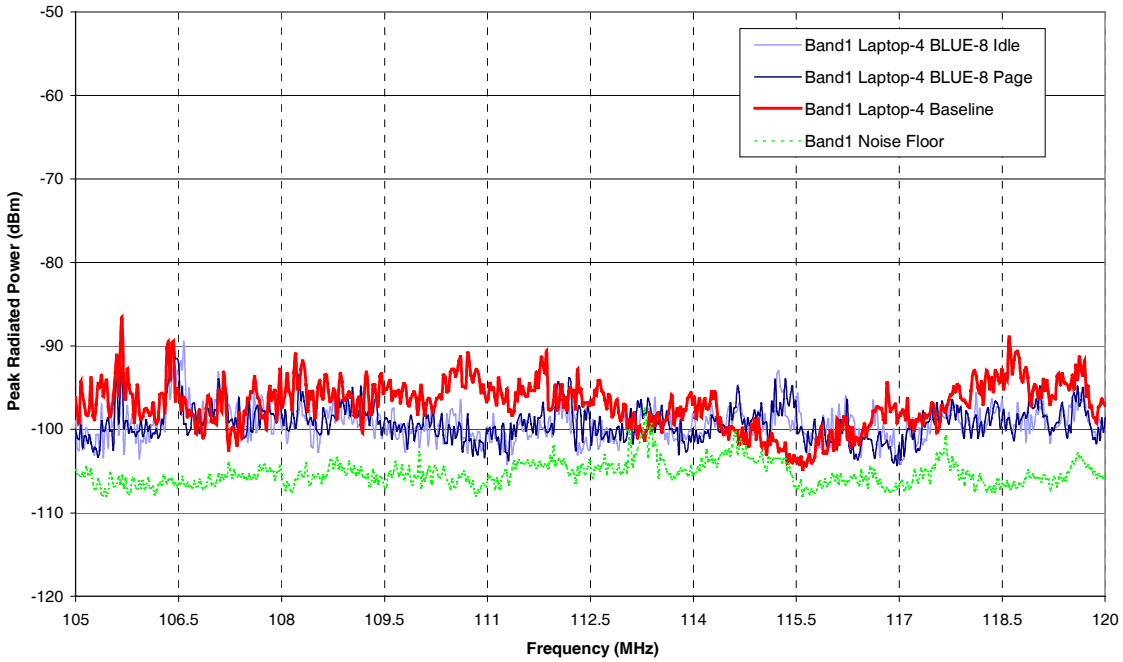

Figure A63: Laptop 4 and BLUE-8, Band 1.

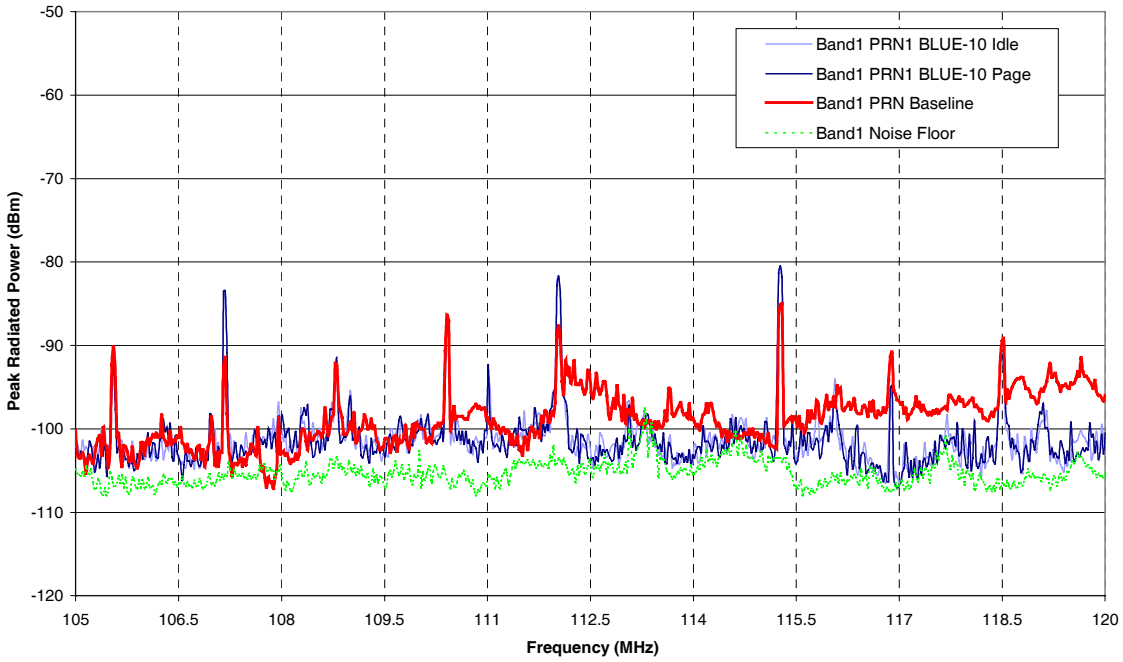

Figure A64: PRN1 and BLUE-10, Band 1.

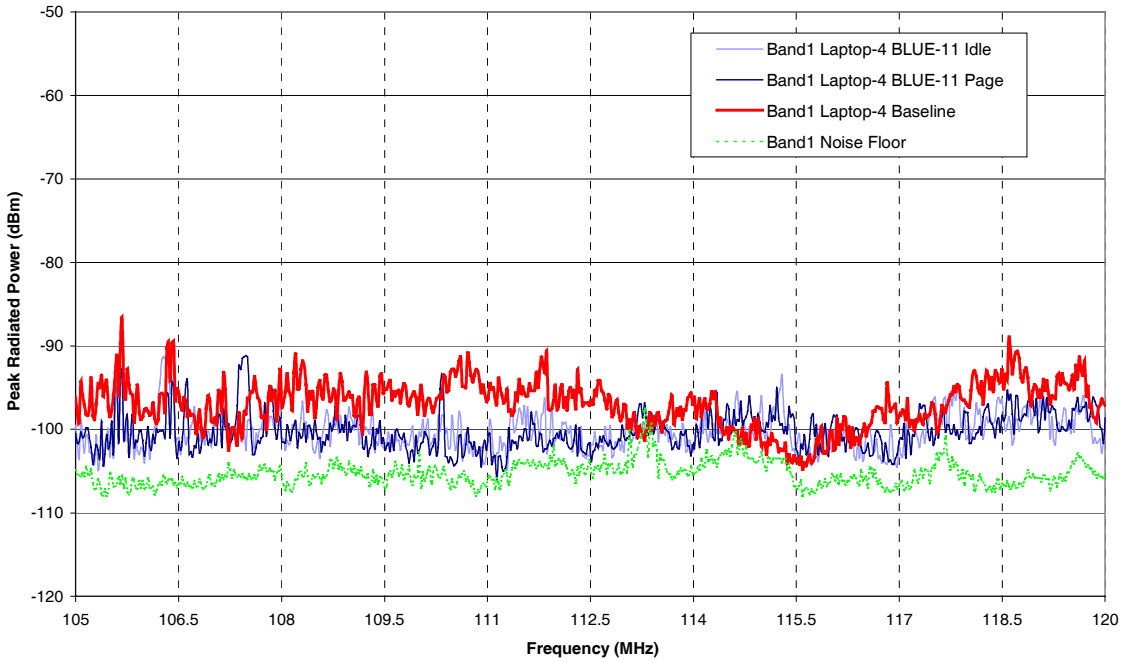

Figure A65: Laptop 4 and BLUE-11, Band 1.

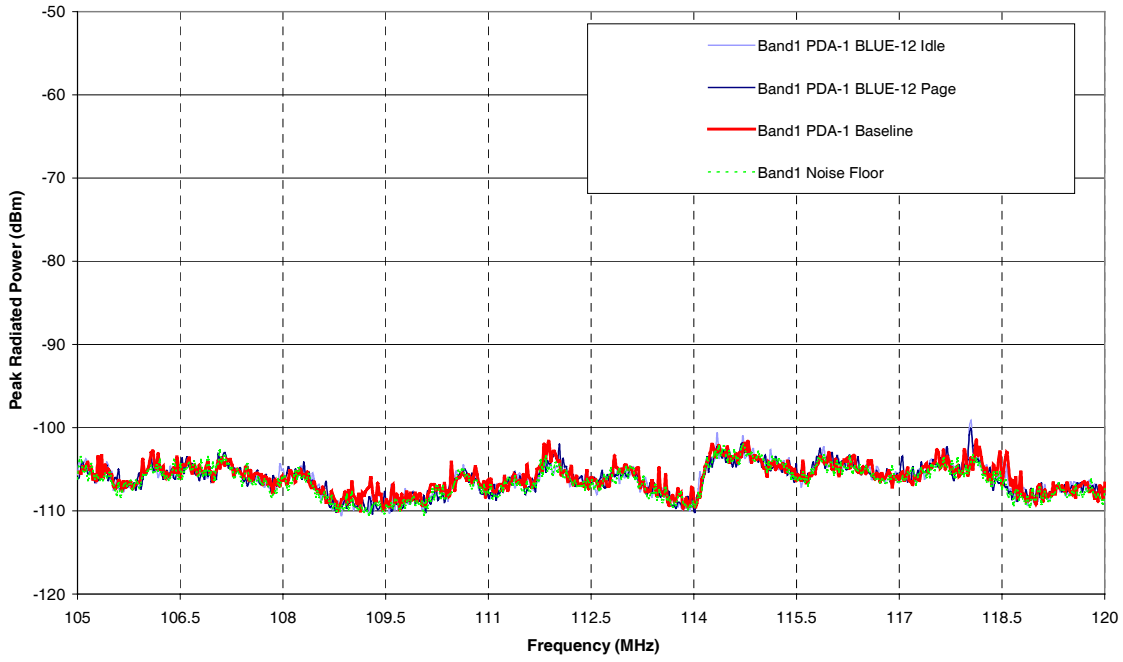

Figure A66: PDA1 and BLUE-12, Band 1.

A.3.2 Band 2

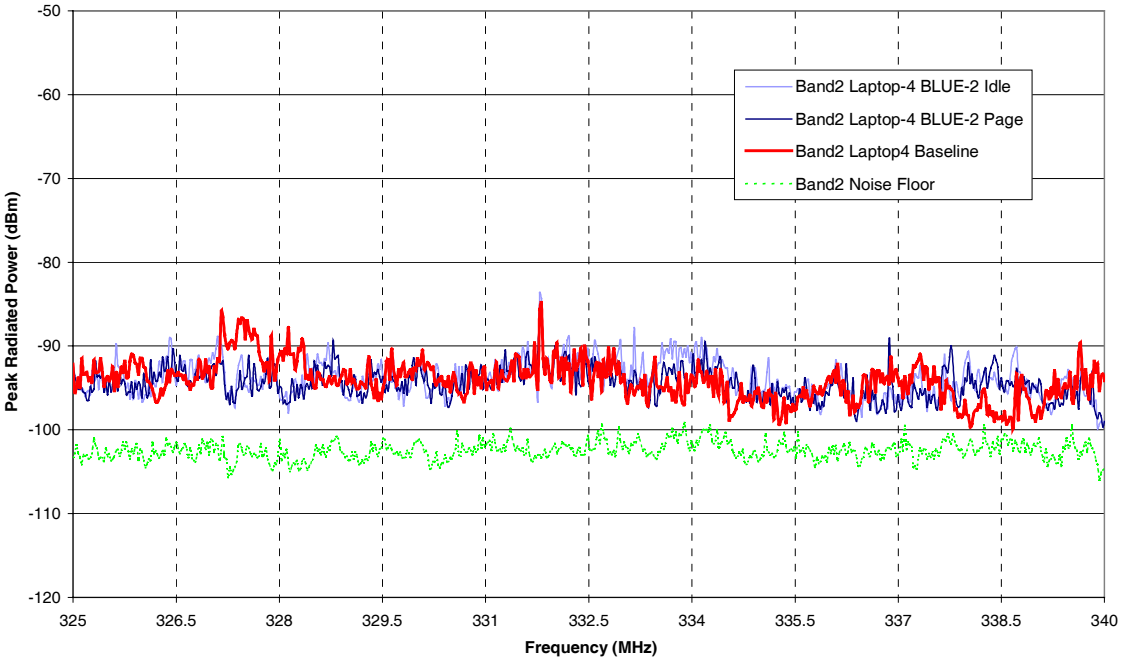

Figure A67: Laptop 4 and BLUE-2, Band 2.

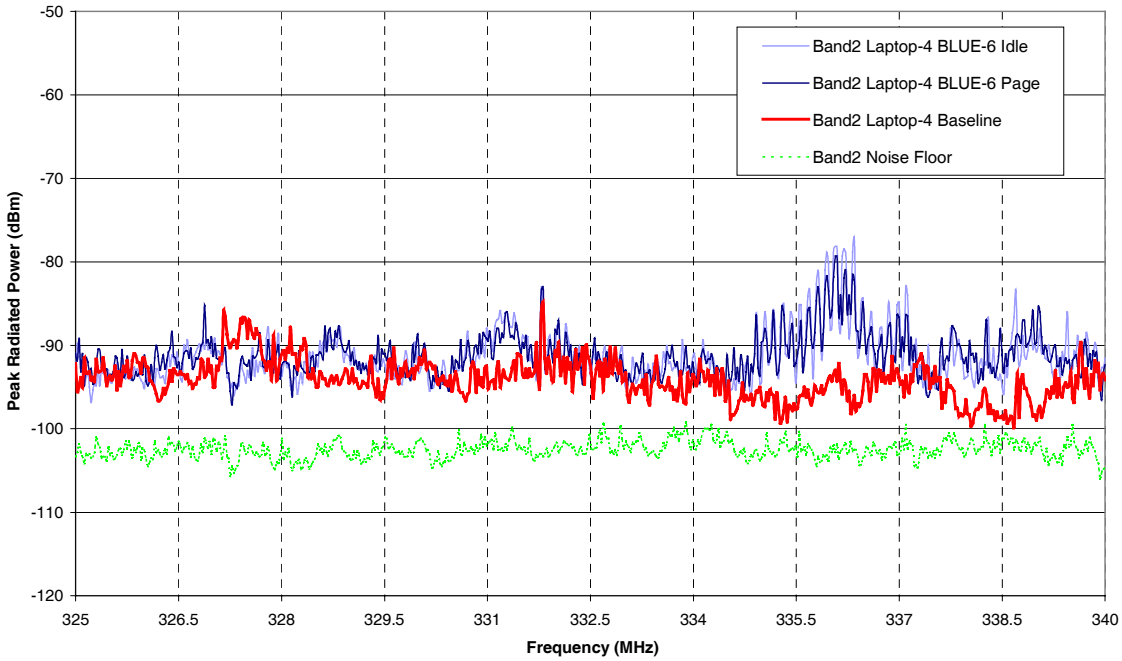

Figure A68: Laptop 4 and BLUE-6, Band 2.

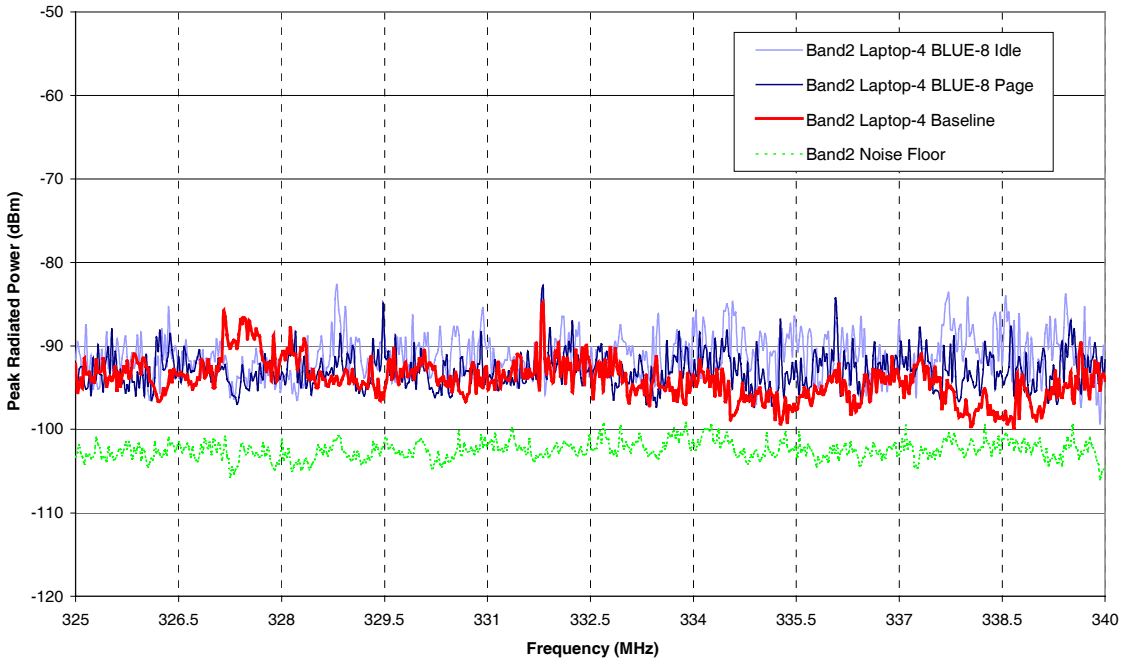

Figure A69: Laptop 4 and BLUE-8, Band 2.

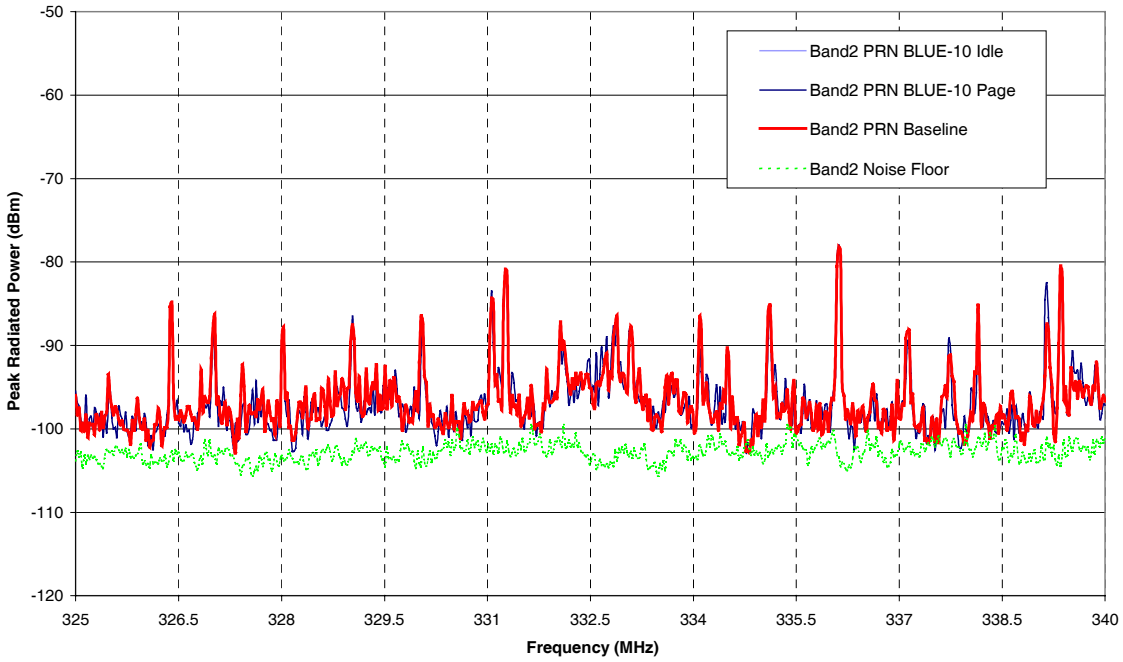

Figure A70: PRN1 and BLUE-10, Band 2.

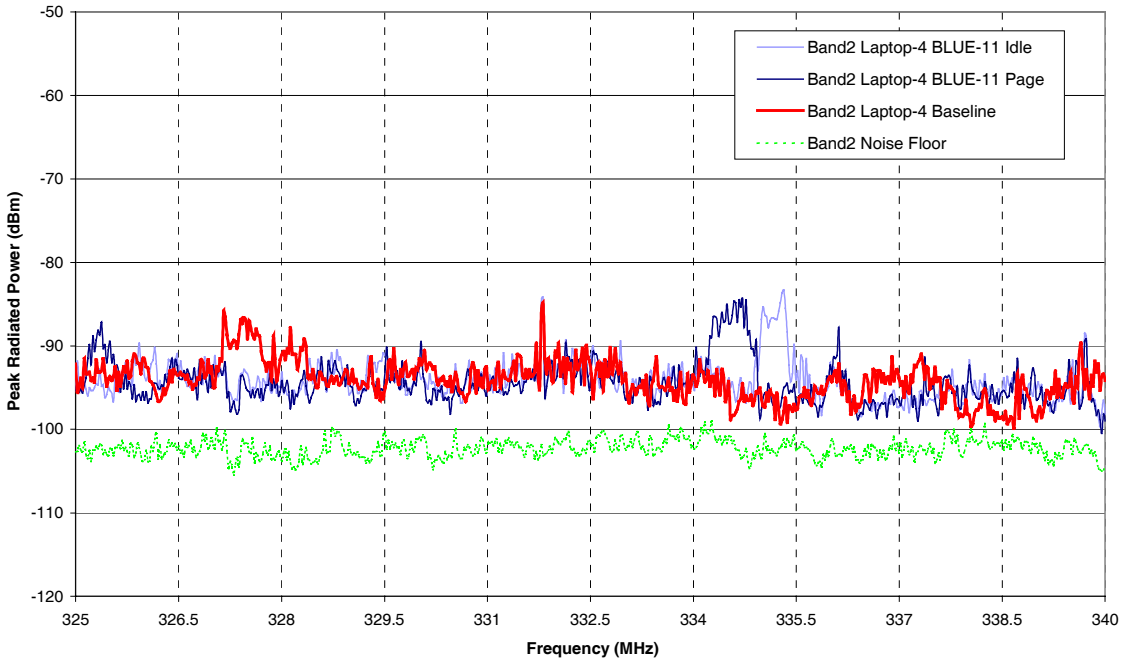

Figure A71: Laptop 4 and BLUE-11, Band 2.

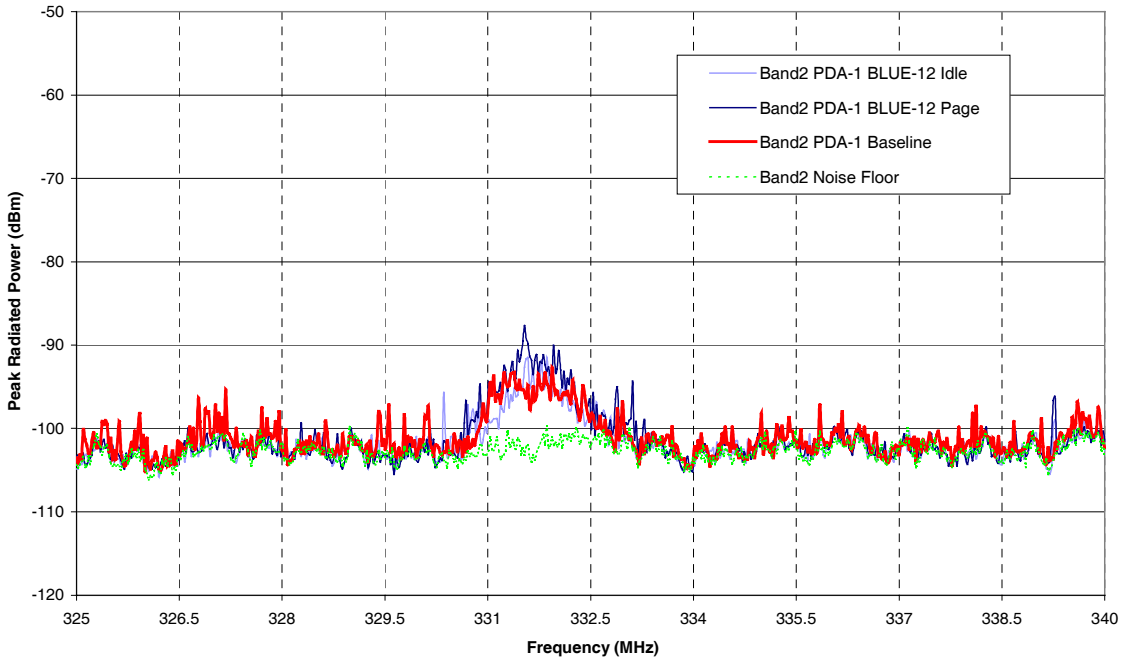

Figure A72: PDA1 and BLUE-12, Band 2.

A.3.3 Band 3

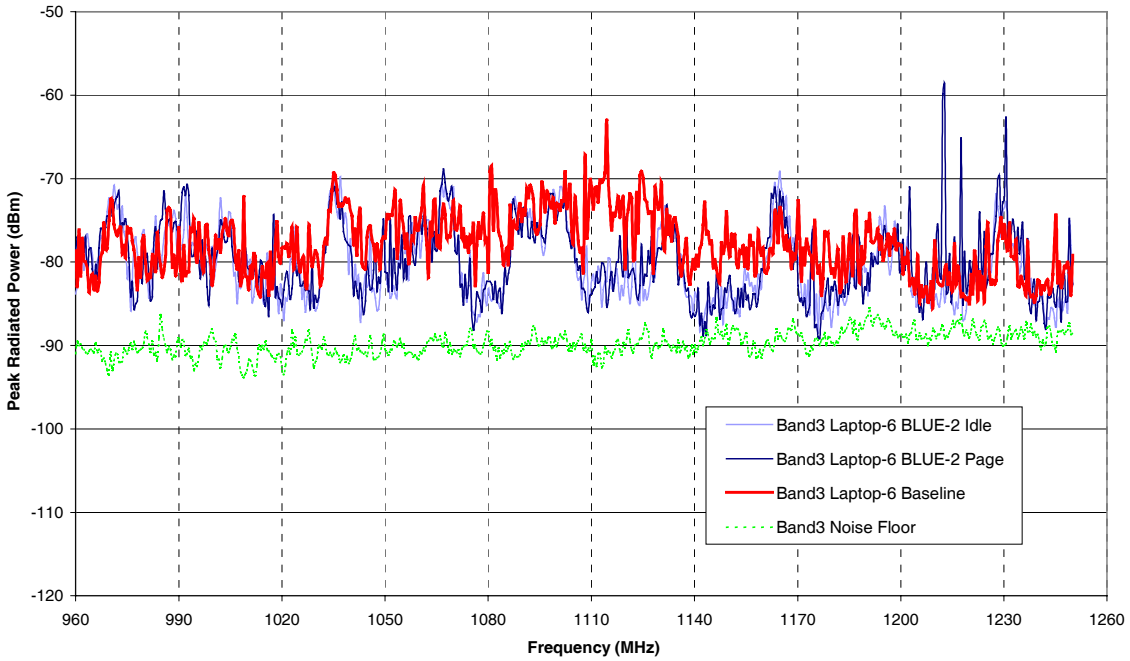

Figure A73: Laptop 6 and BLUE-2, Band 3.

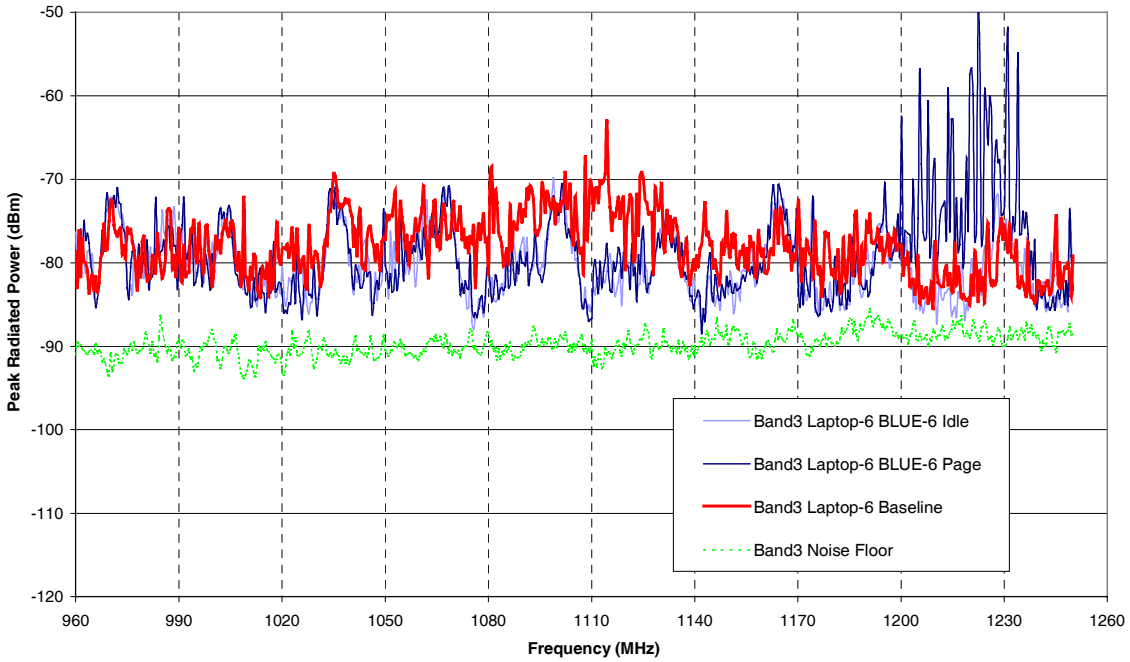

Figure A74: Laptop 6 and BLUE-6, Band 3.

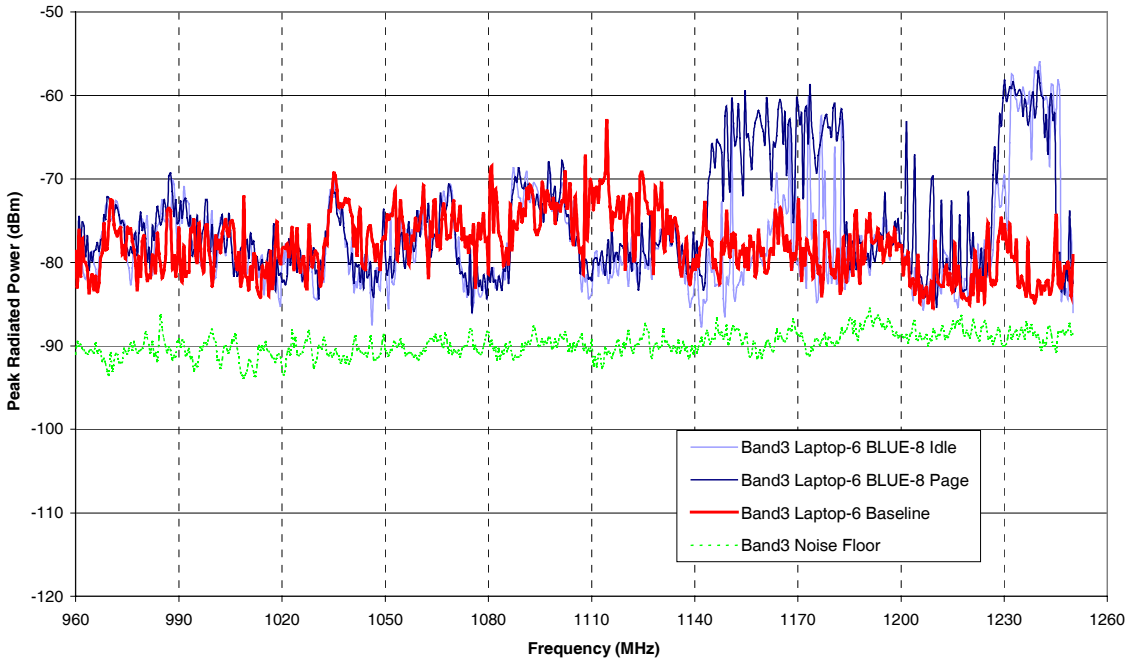

Figure A75: Laptop 6 and BLUE-8, Band 3.

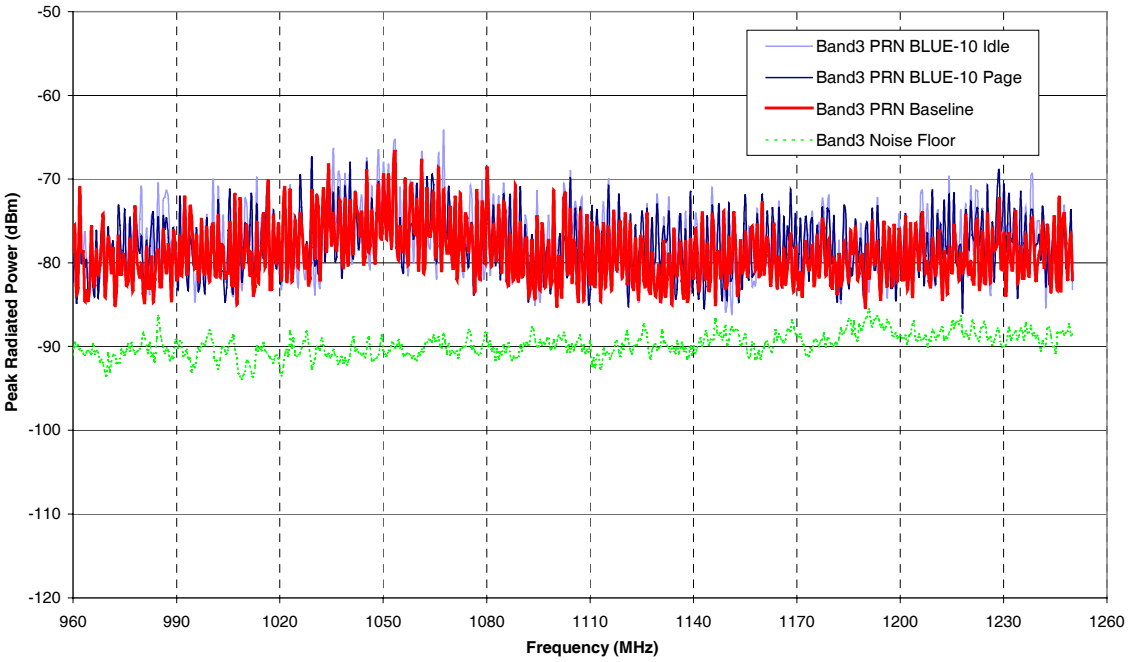

Figure A76: PRN and BLUE-10, Band 3.

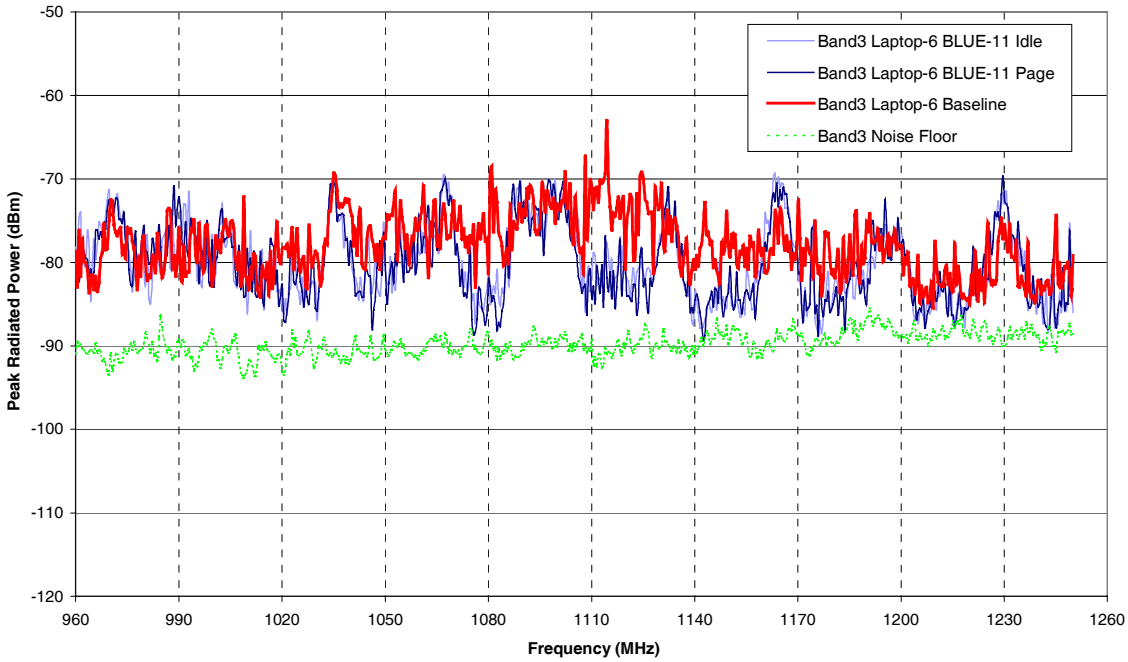

Figure A77: Laptop 6 and BLUE-11, Band 3.

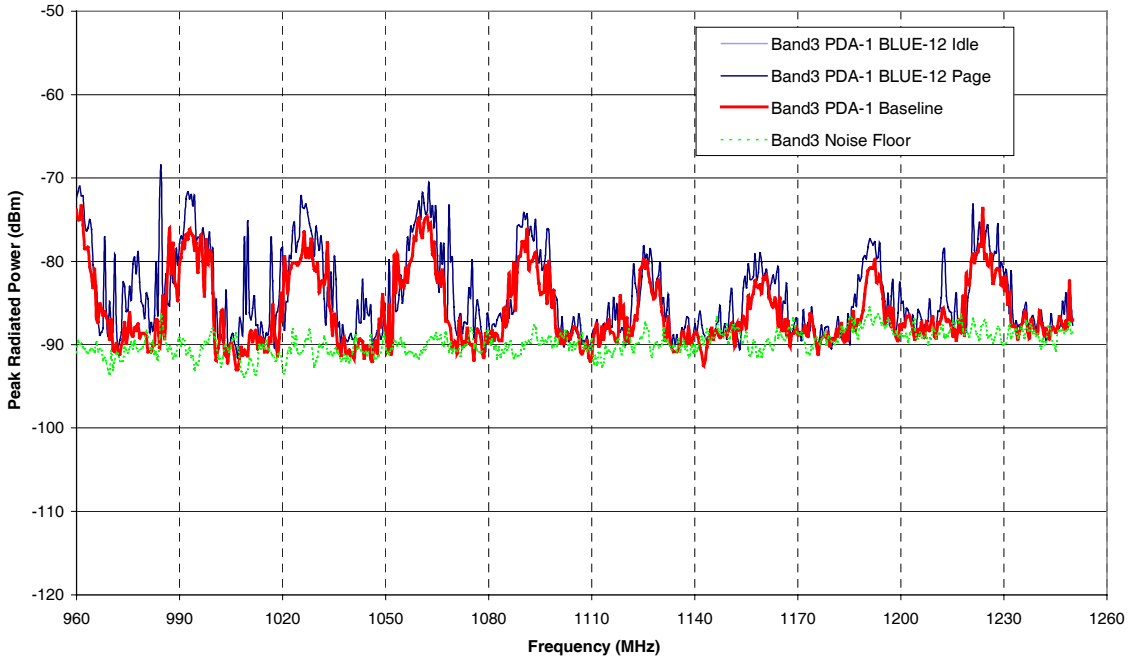

Figure A78: PDA1 and BLUE-12, Band 3.

A.3.4 Band 4

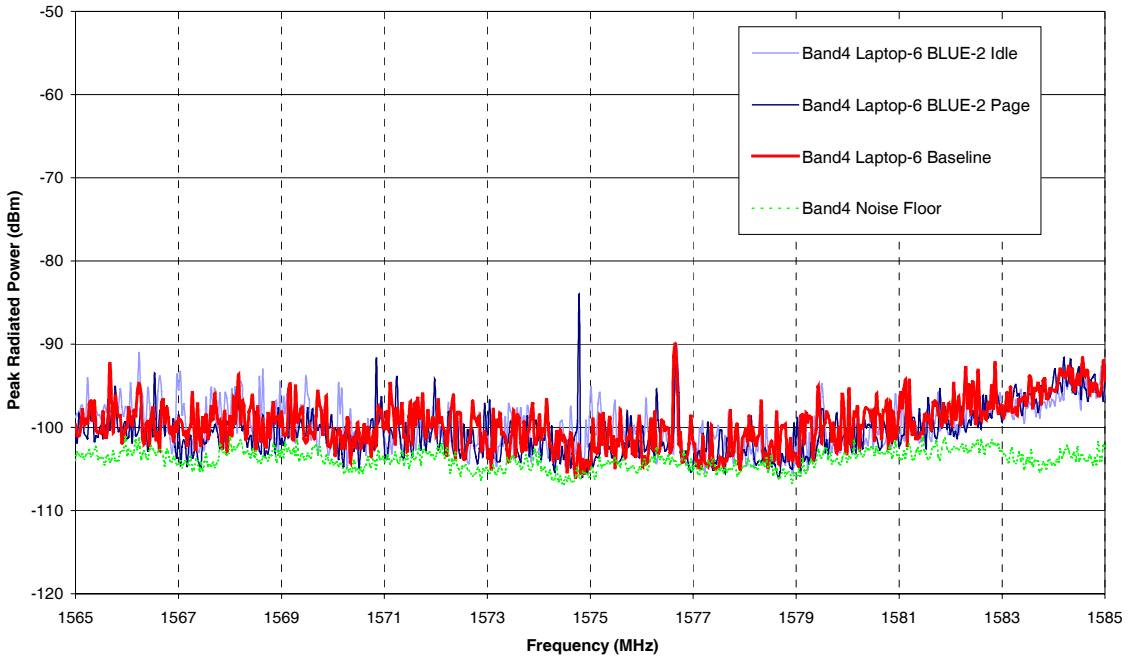

Figure A79: Laptop 6 and BLUE-2, Band 4.

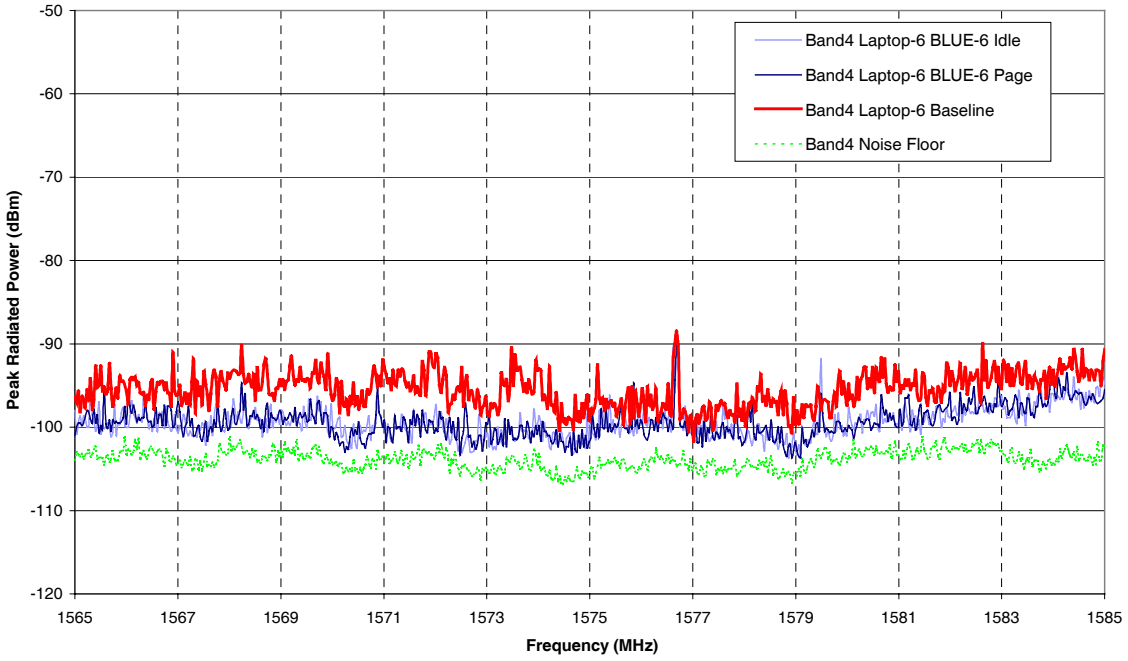

Figure A80: Laptop 6 and BLUE-6, Band 4.

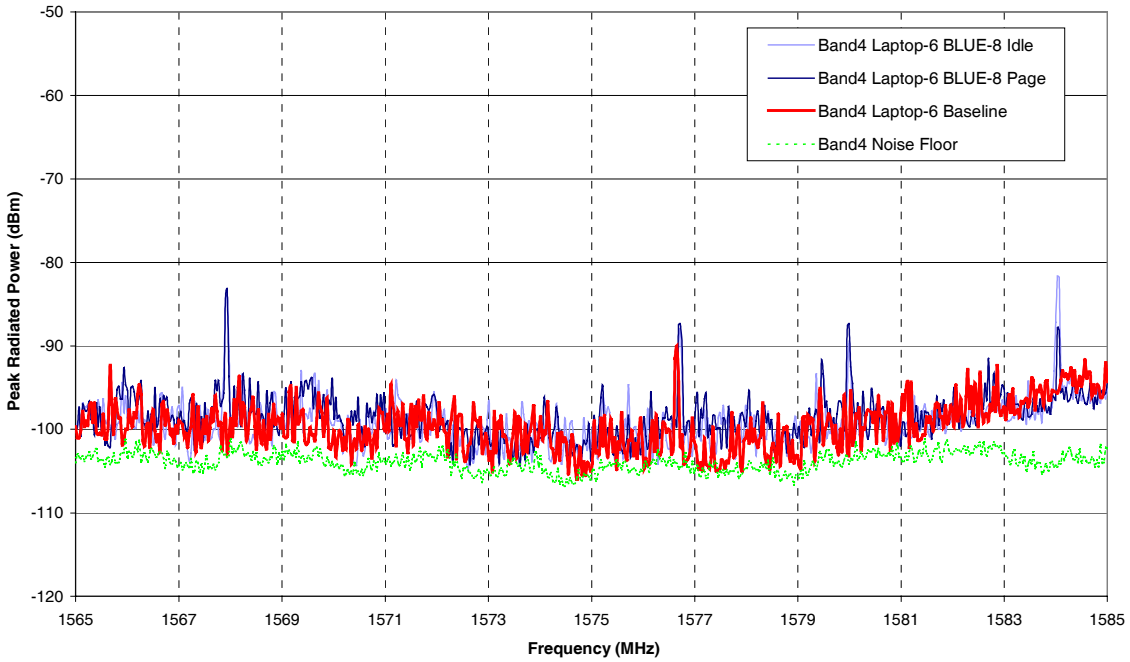

Figure A81: Laptop 6 and BLUE-8, Band 4.

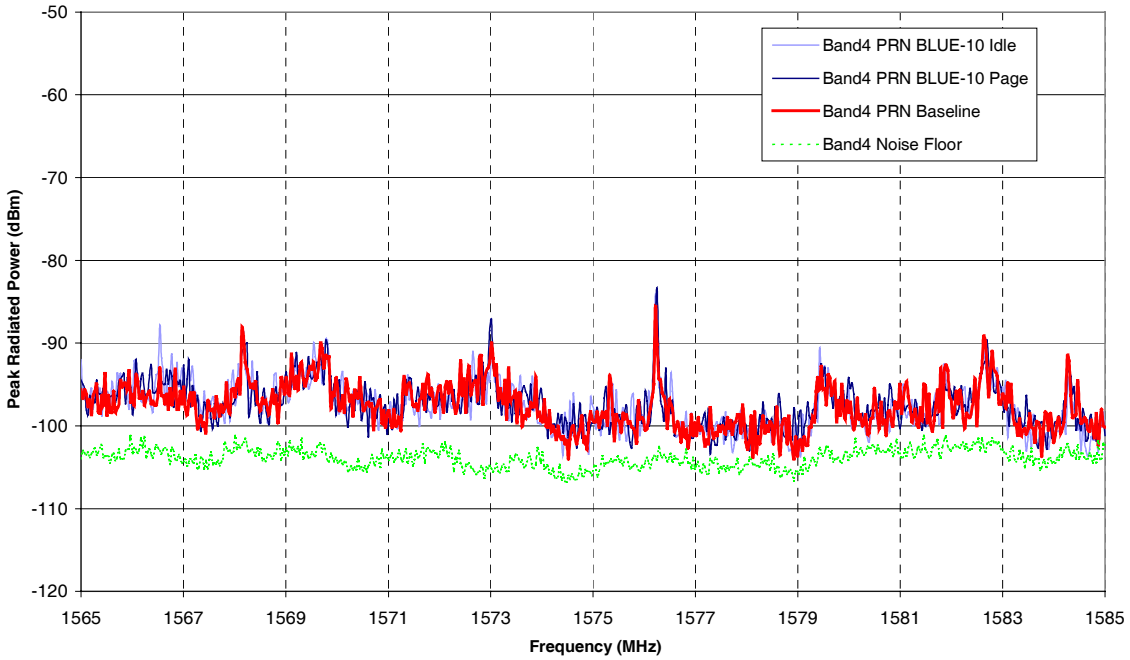

Figure A82: PRN and BLUE-10, Band 4.

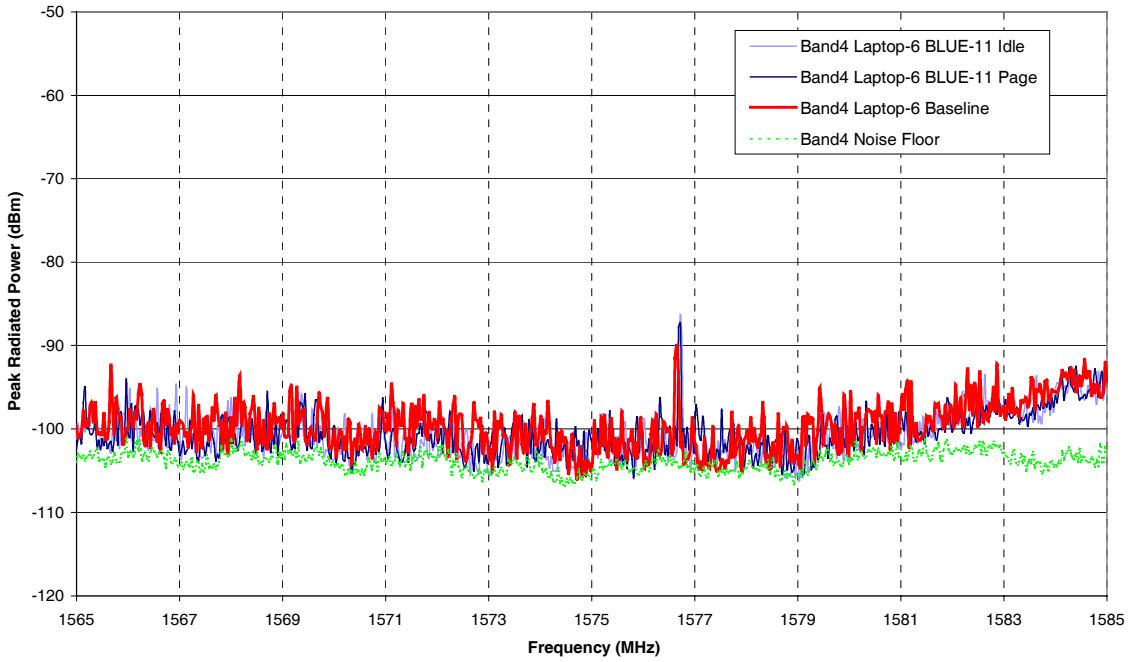

Figure A83: Laptop 6 and BLUE-11, Band 4.

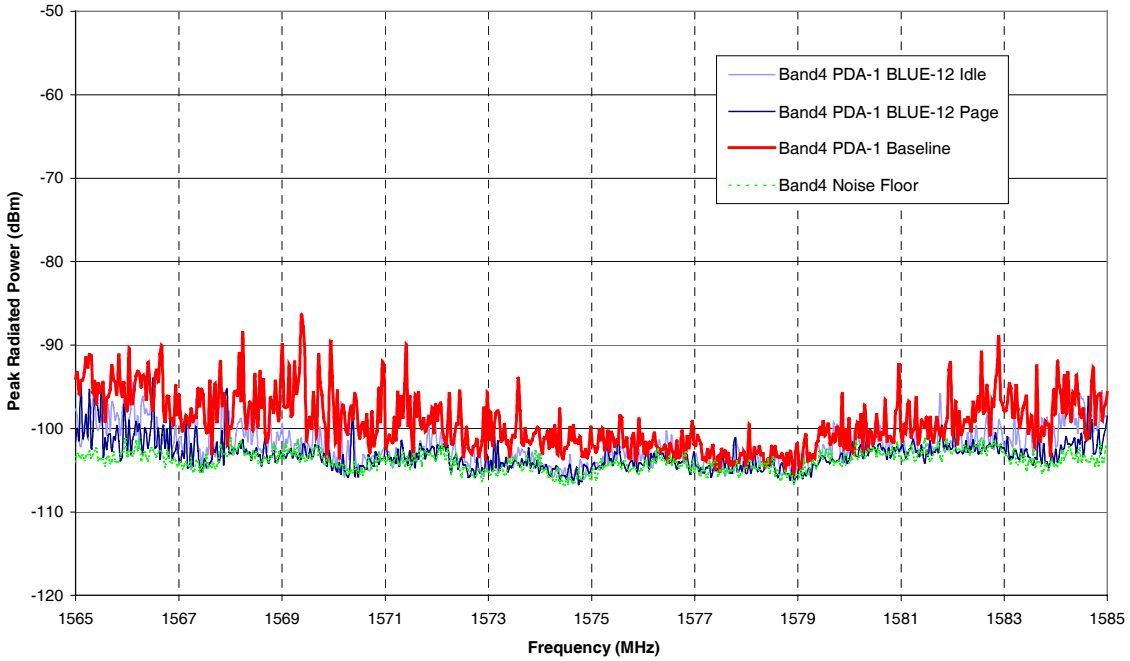

Figure A84: PDA1 and BLUE-12, Band 4.

A.3.5 Band 5

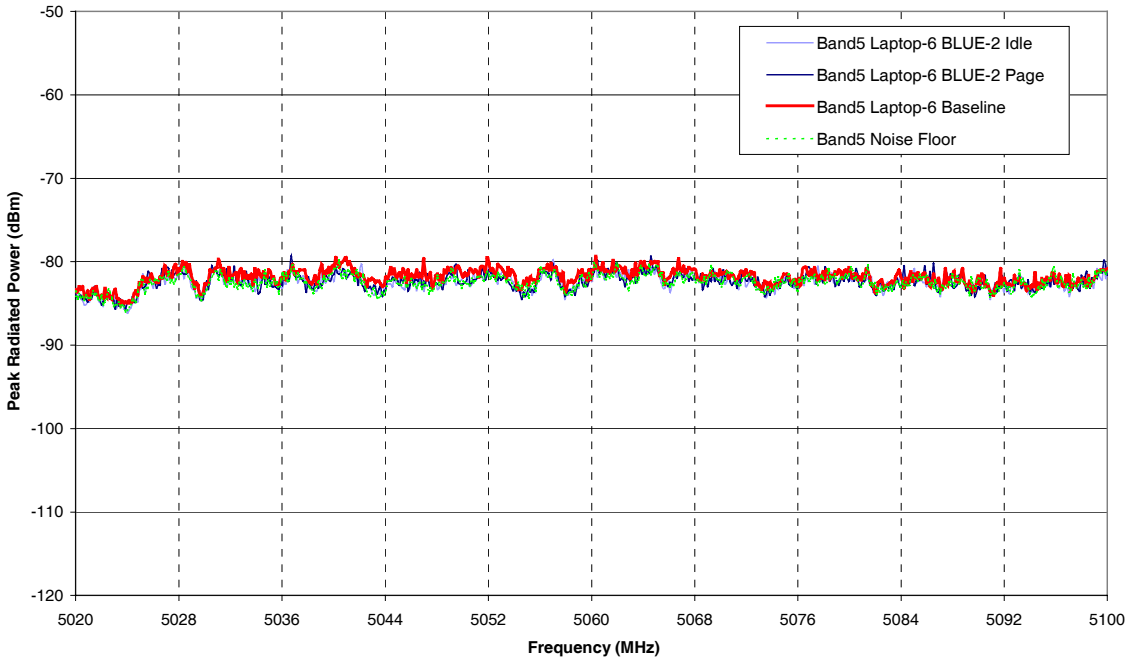

Figure A85: Laptop 6 and BLUE-2, Band 5.

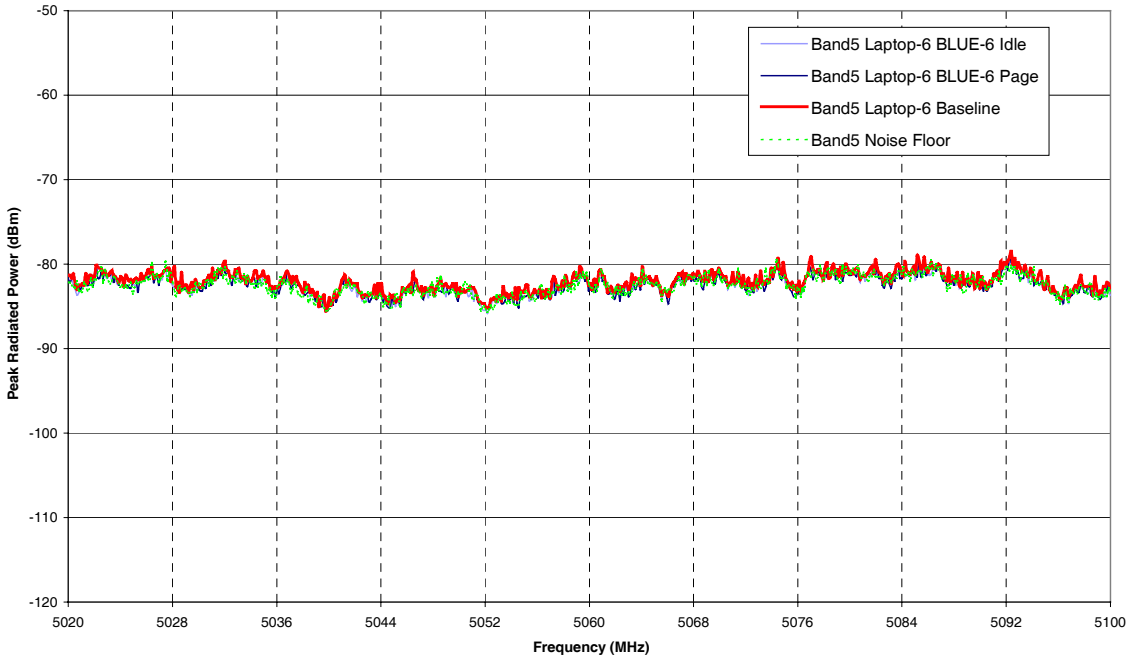

Figure A86: Laptop 6 and BLUE-6, Band 5.

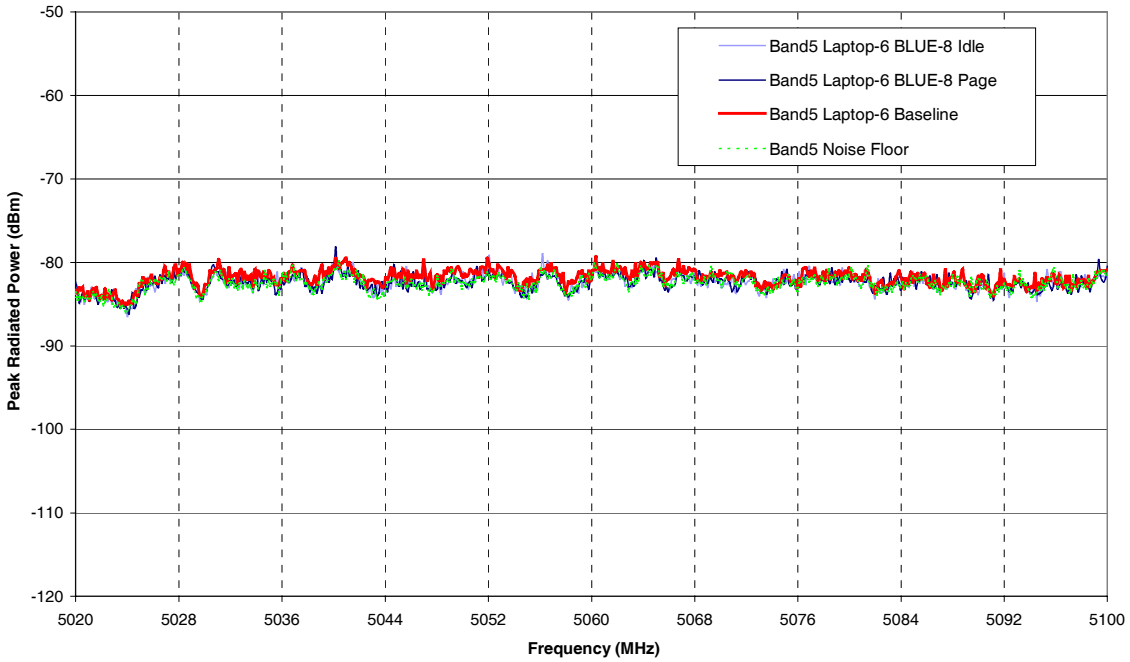

Figure A87: Laptop 6 and BLUE-8, Band 5.

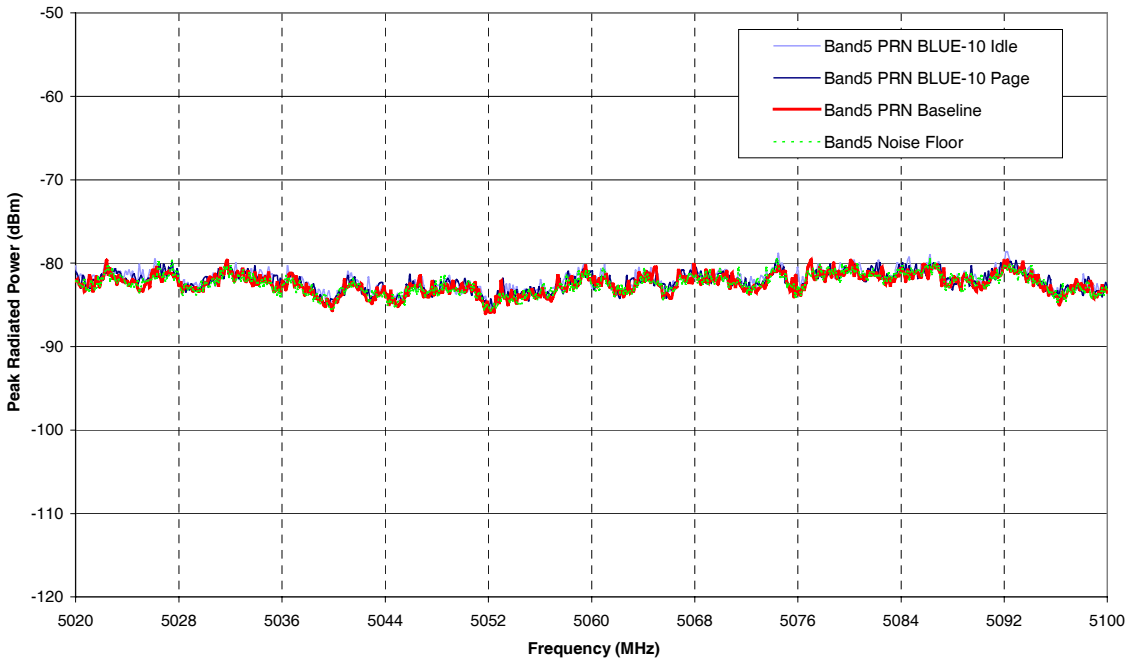

Figure A88: PRN and BLUE-10, Band 5.

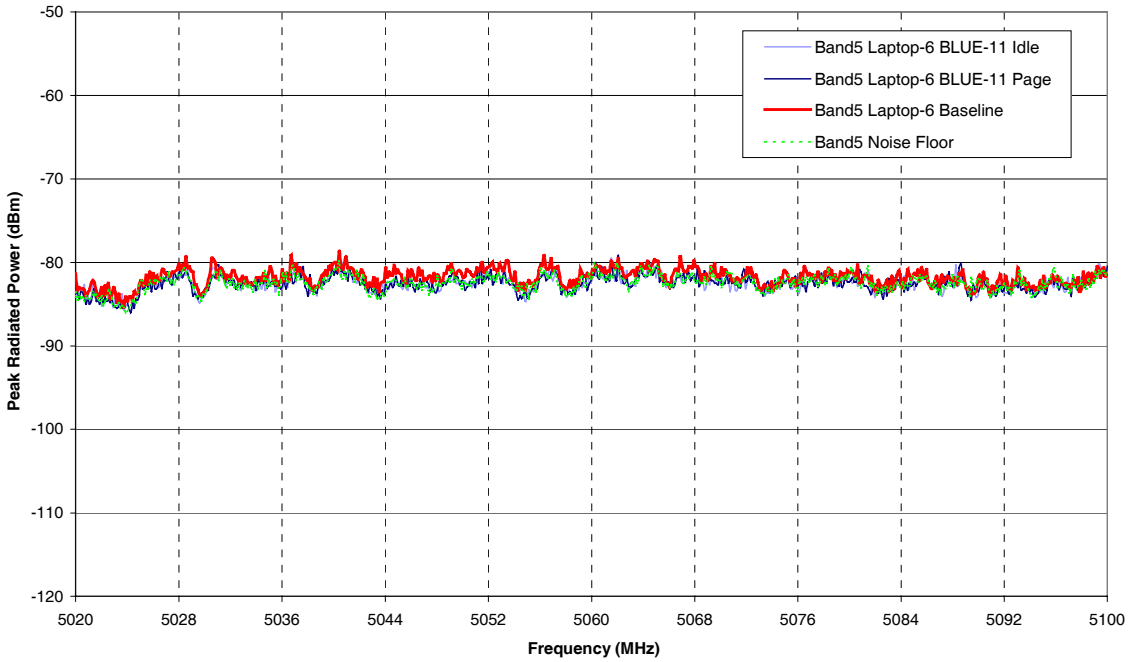

Figure A89: Laptop 6 and BLUE-11, Band 5.

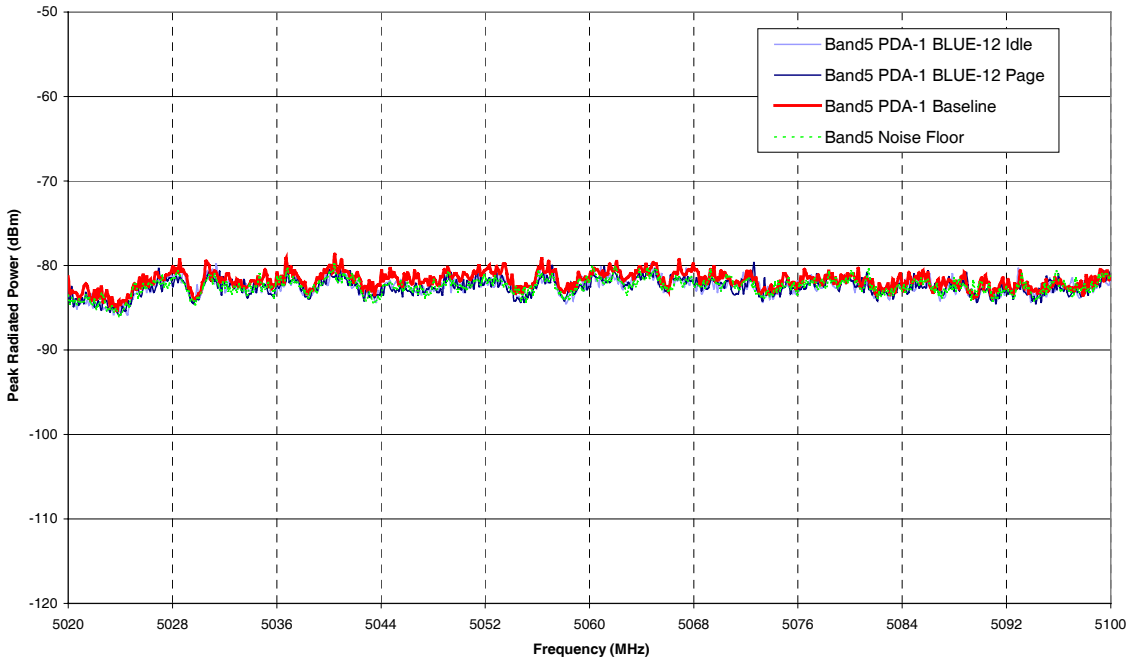

Figure A90: PDA1 and BLUE-12, Band 5.

A.4 FRS Radios

A.4.1 Band 1

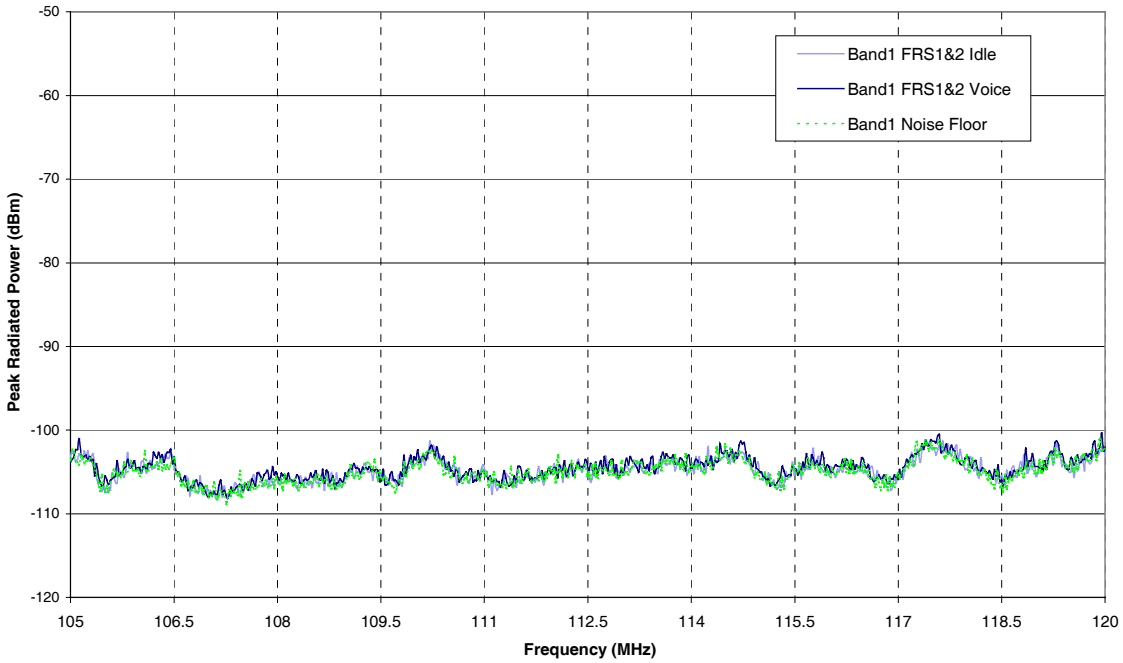

Figure A91: FRS 1&2, Band 1.

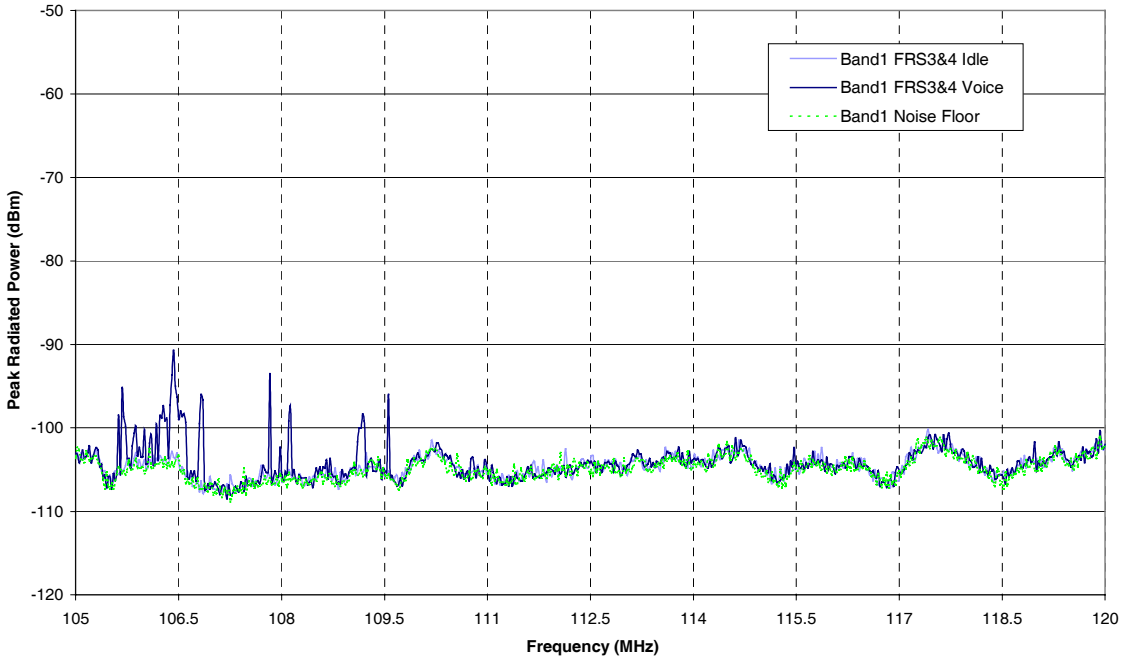

Figure A92: FRS 3&4, Band 1.

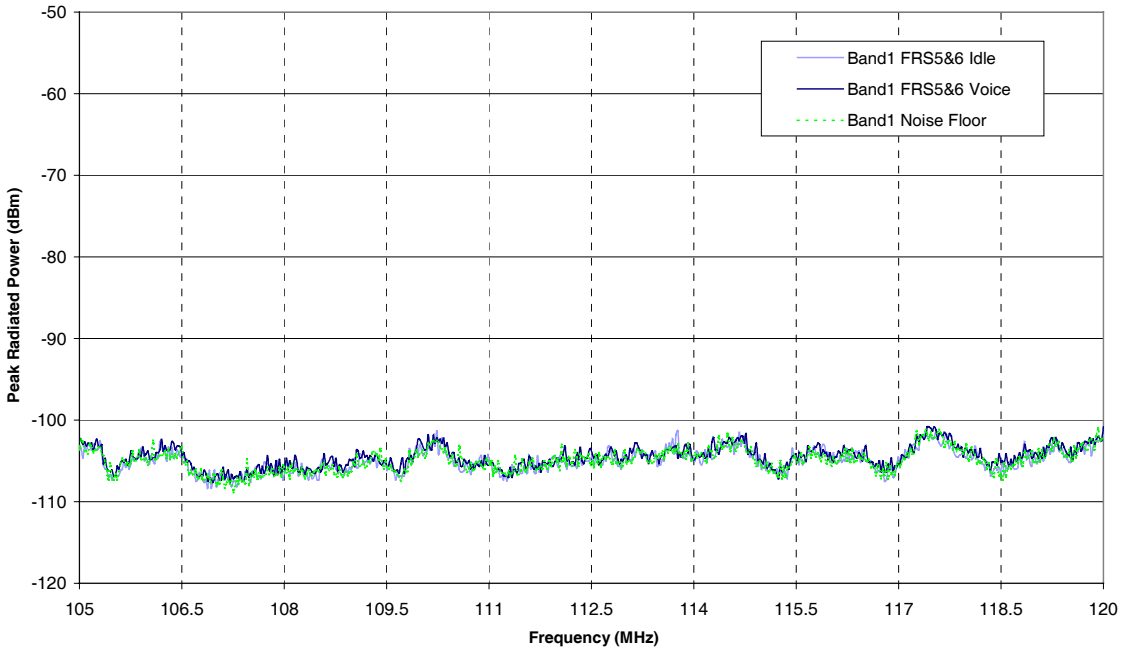

Figure A93: FRS 5&6, Band 1.

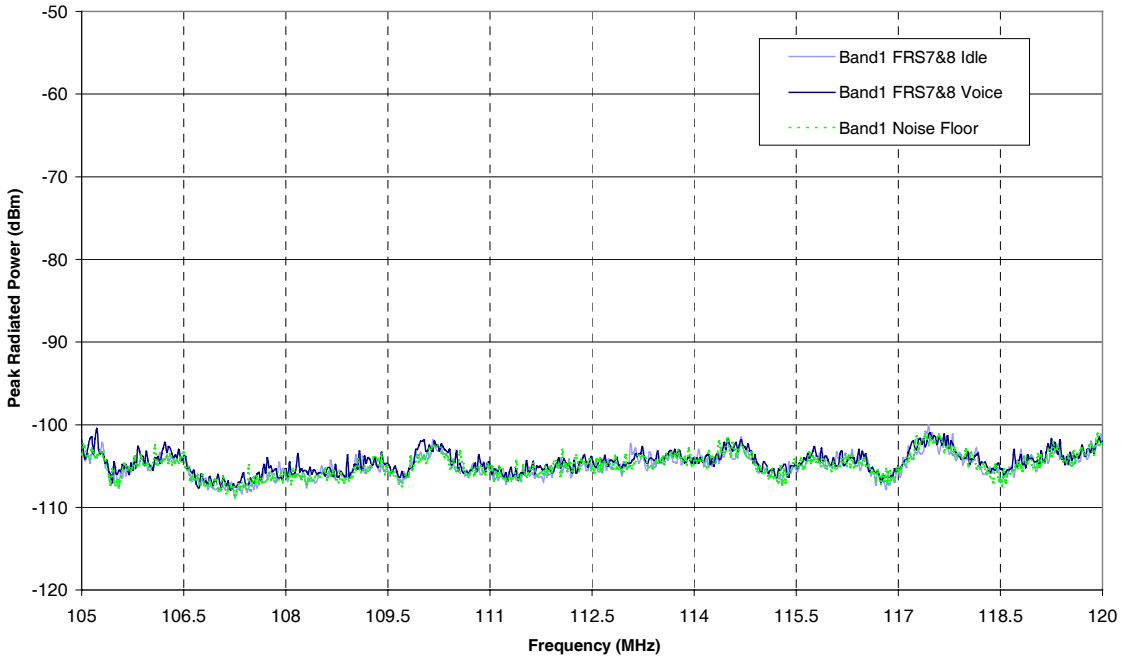

Figure A94: FRS 7&8, Band 1.

A.4.2 Band 2

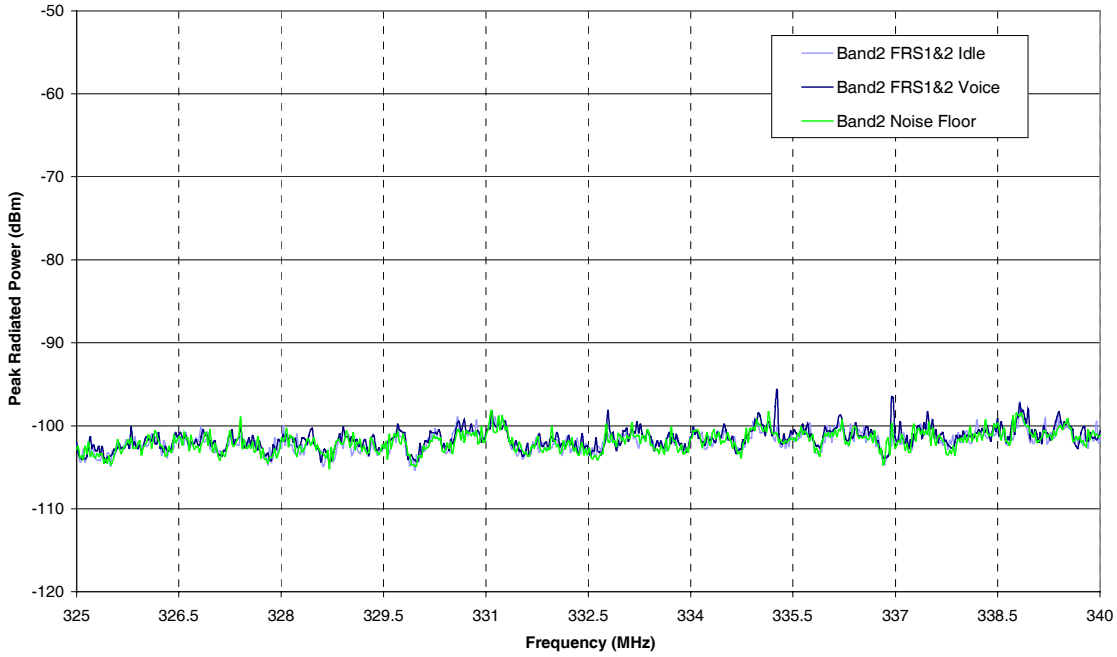

Figure A95: FRS 1&2, Band 2.

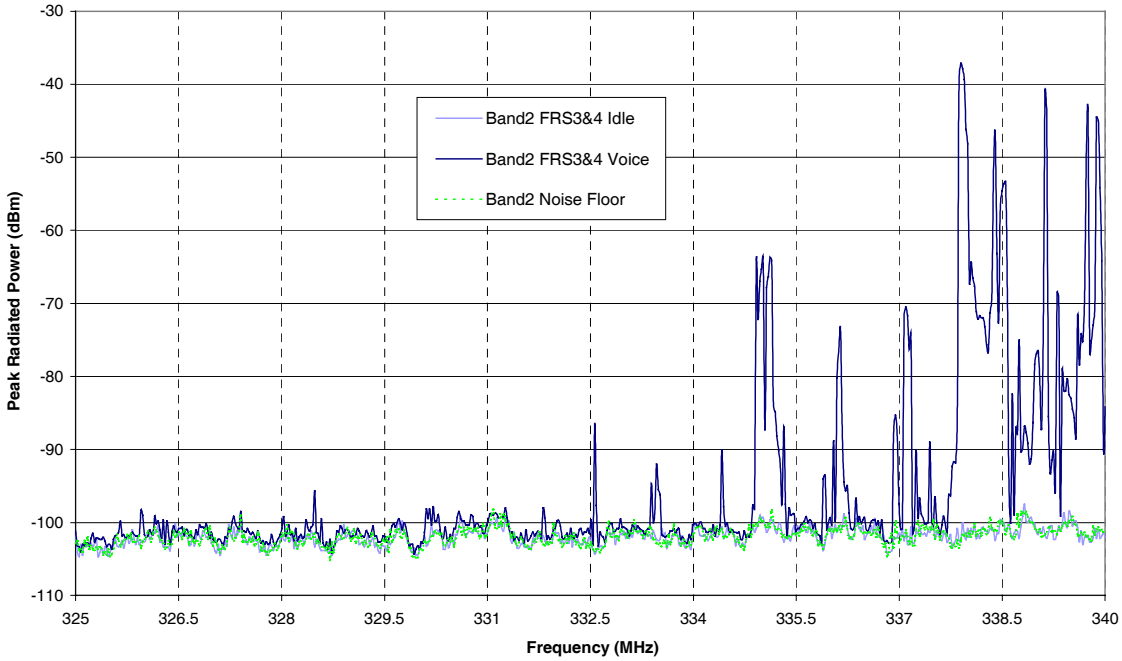

Figure A96: FRS 3&4, Band 2.

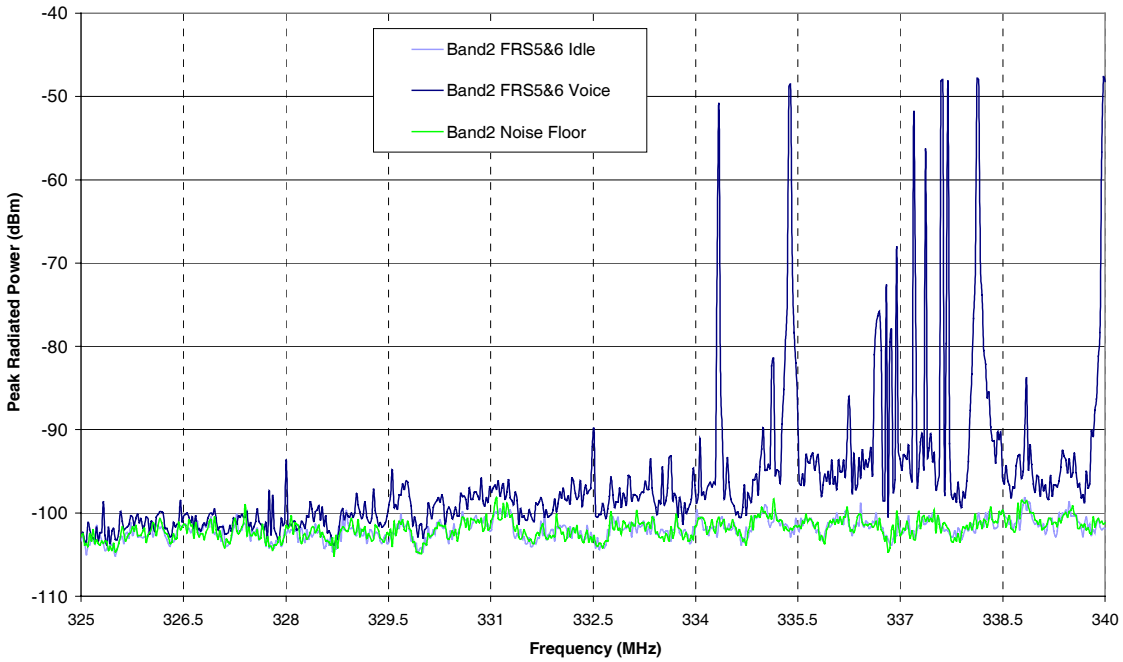

Figure A97: FRS 5&6, Band 2.

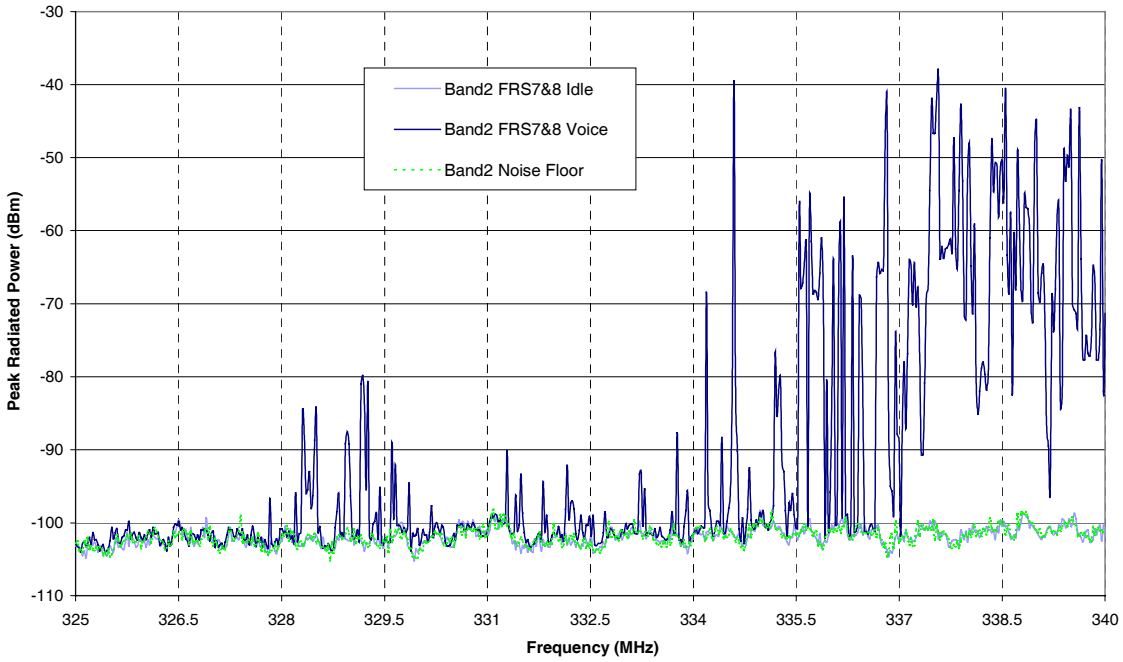

Figure A98: FRS 7&8, Band 2.

A.4.3 Band 3

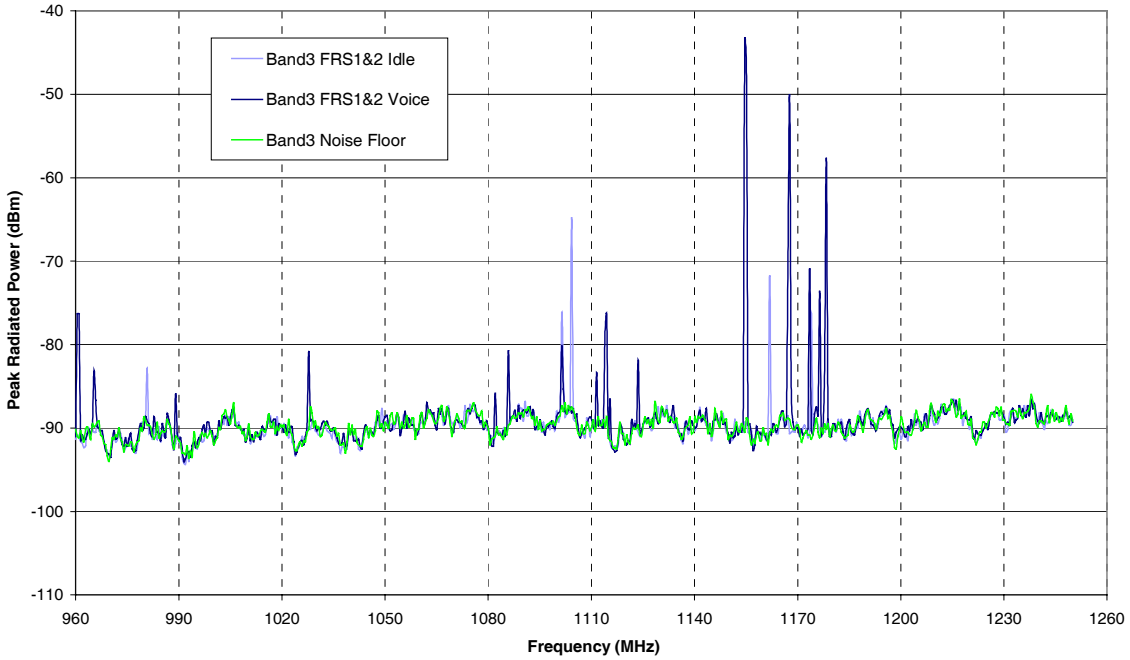

Figure A99: FRS 1&2, Band 3.

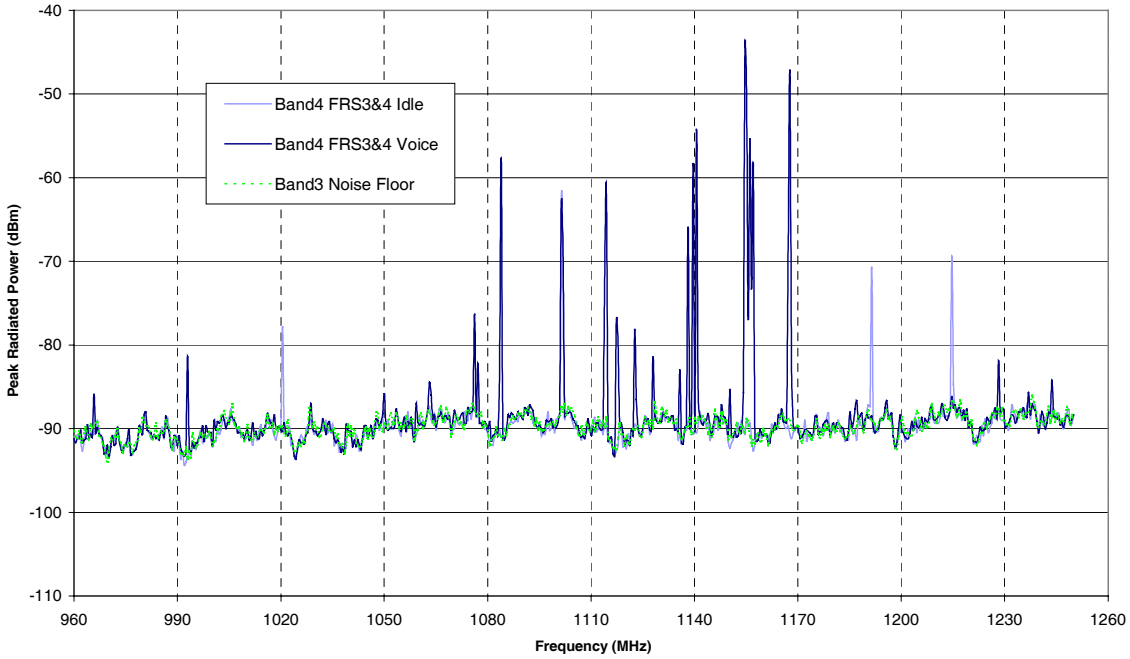

Figure A100: FRS 3&4, Band 3.

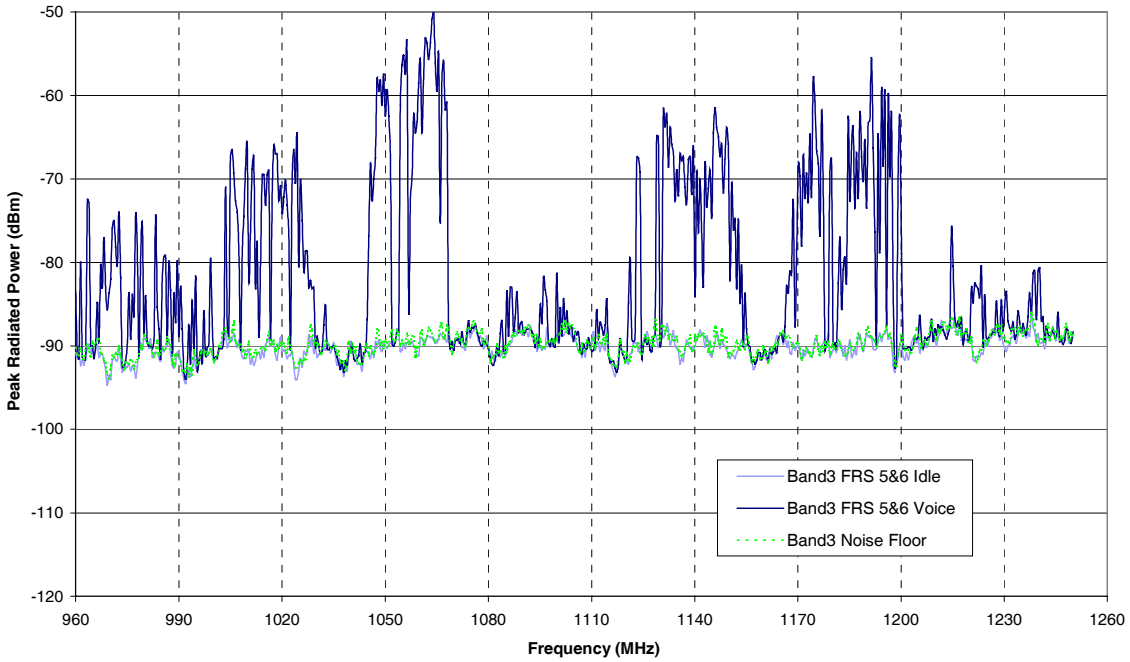

Figure A101: FRS 5&6, Band 3.

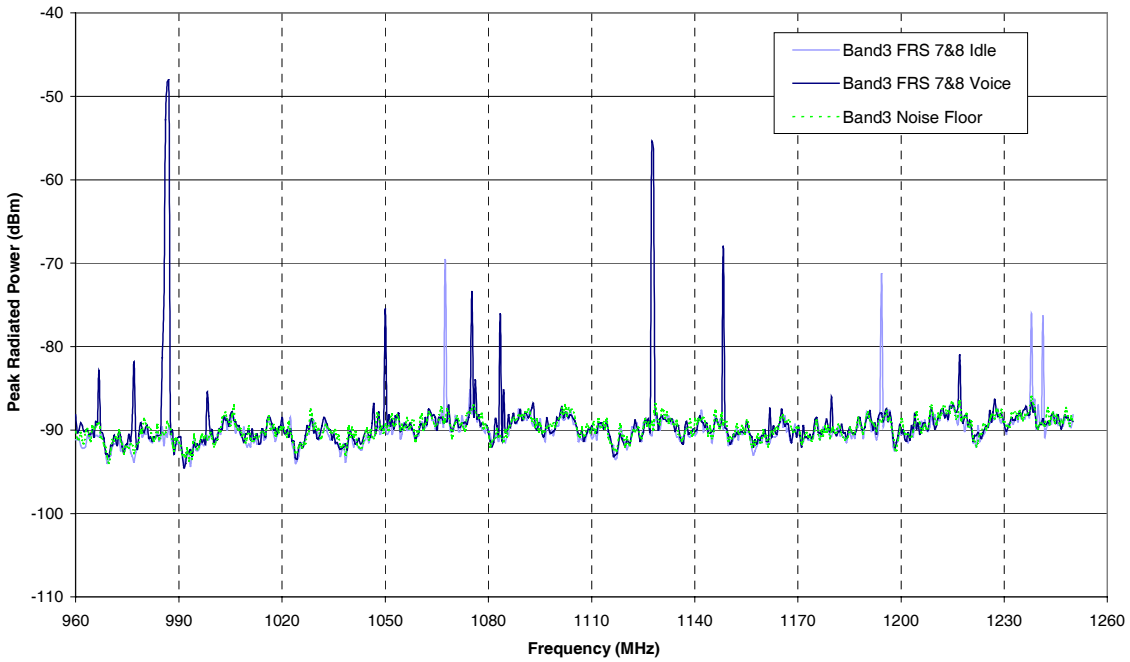

Figure A102: FRS 7&8, Band 3.

A.4.4 Band 4

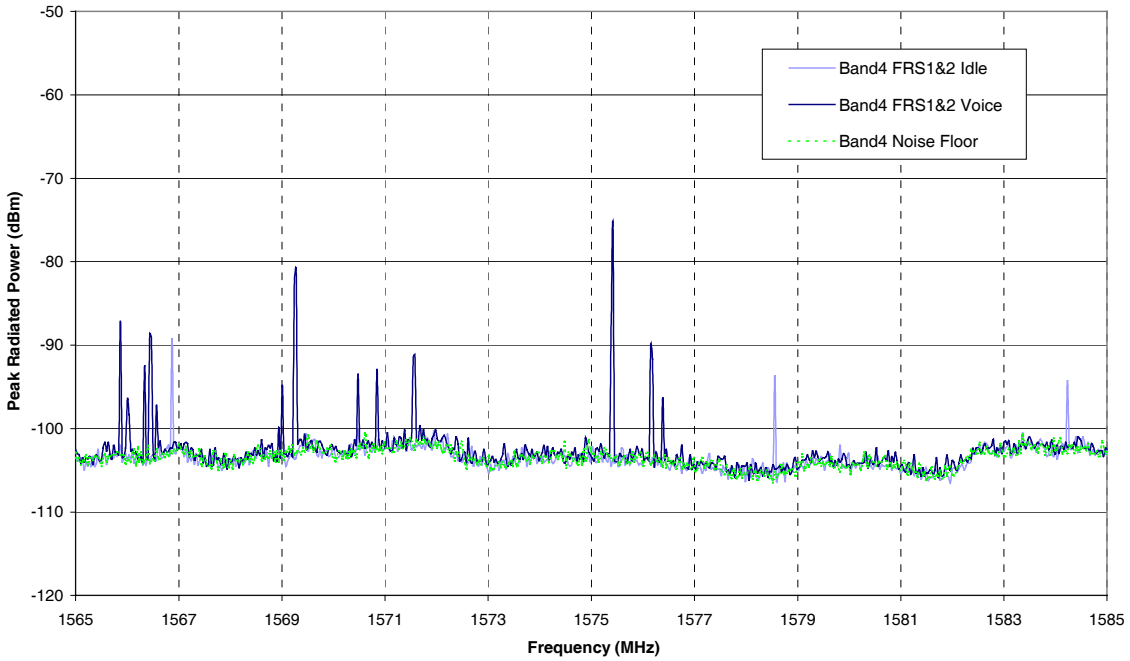

Figure A103: FRS 1&2, Band 4.

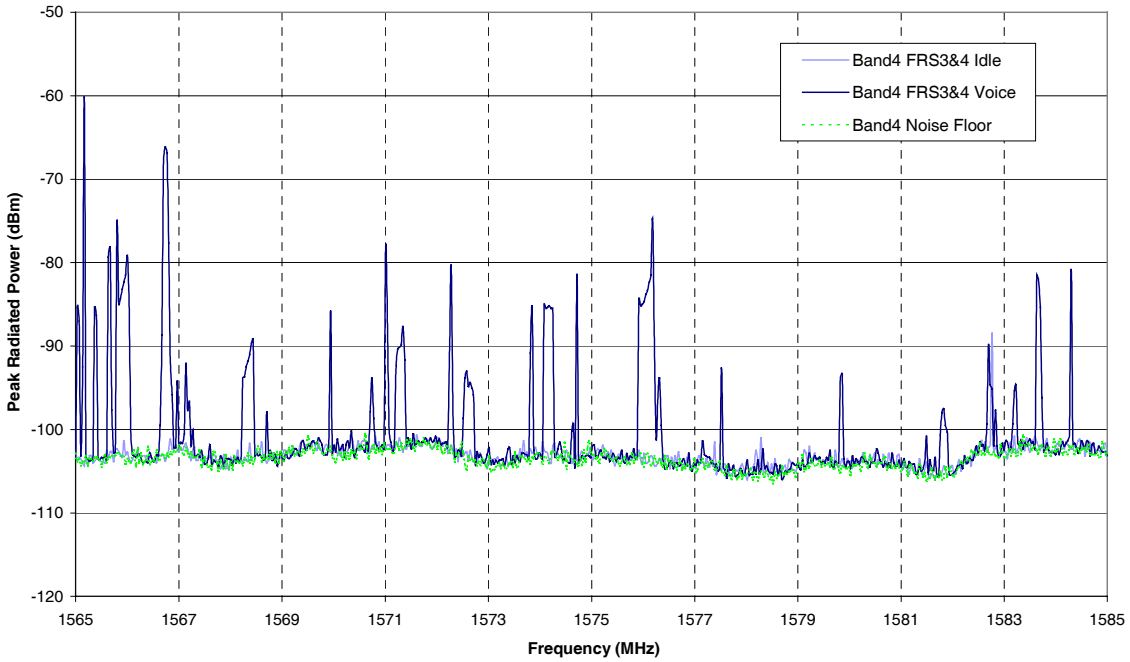

Figure A104: FRS 3&4, Band 4.

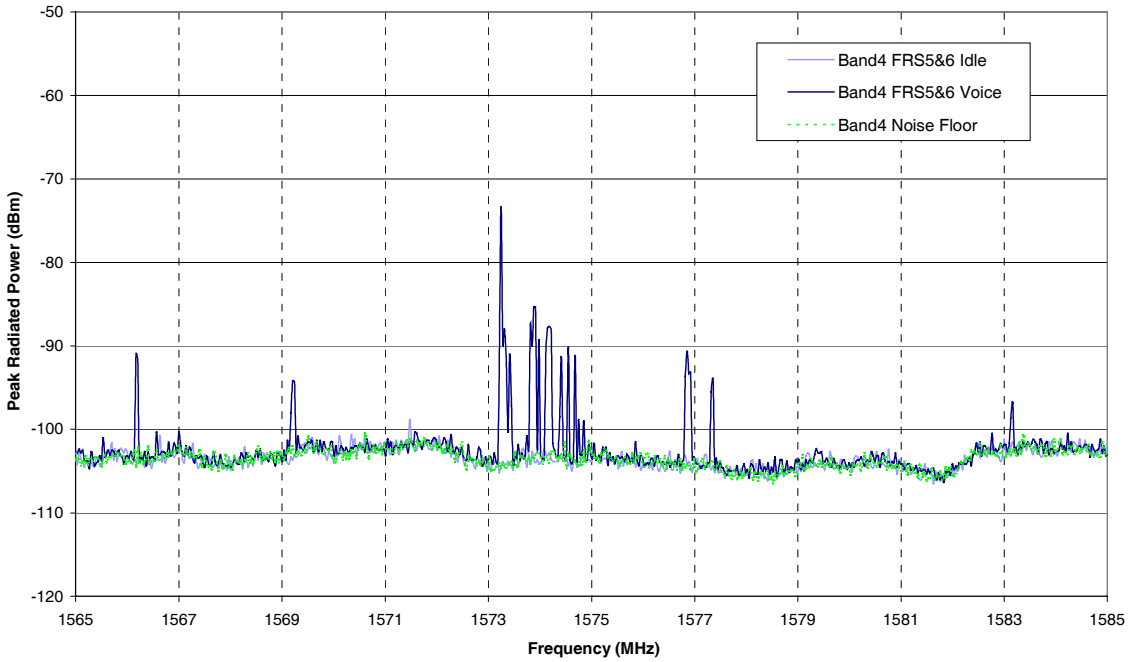

Figure A105: FRS 5&6, Band 4.

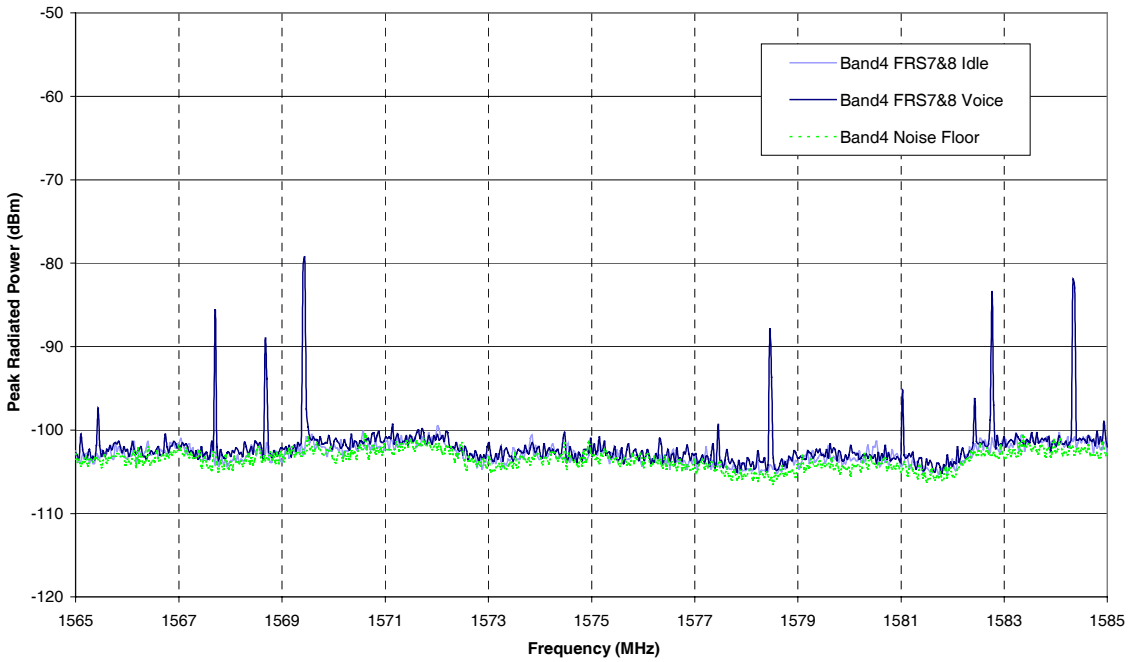

Figure A106: FRS 7&8, Band 4.

A.4.5 Band 5

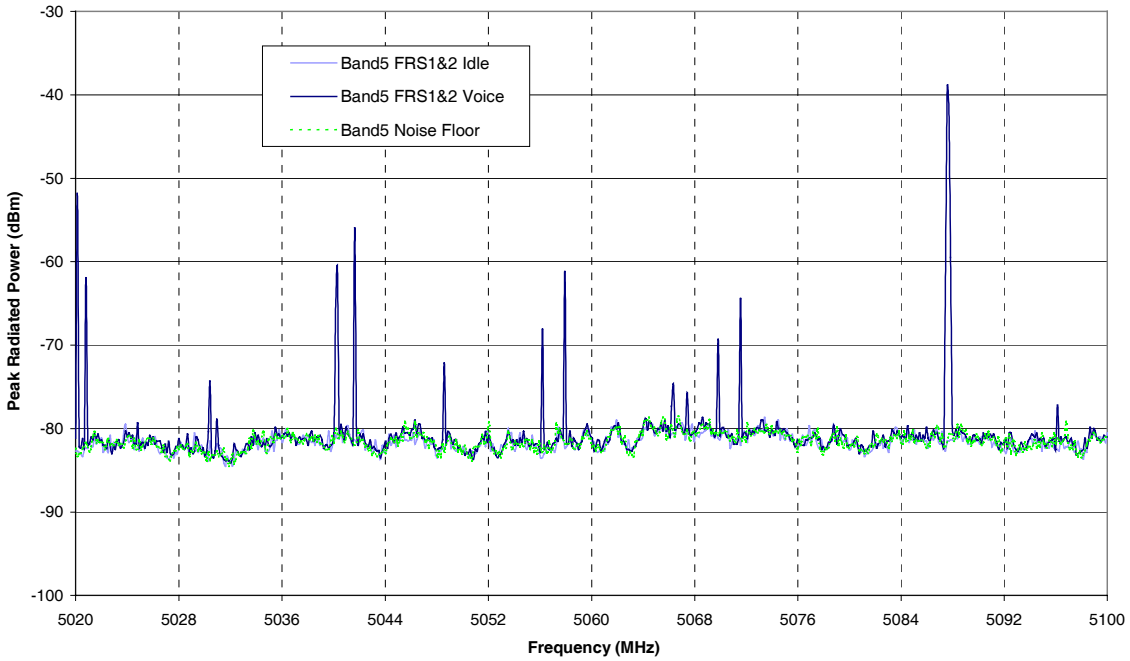

Figure A107: FRS 1&2, Band 5.

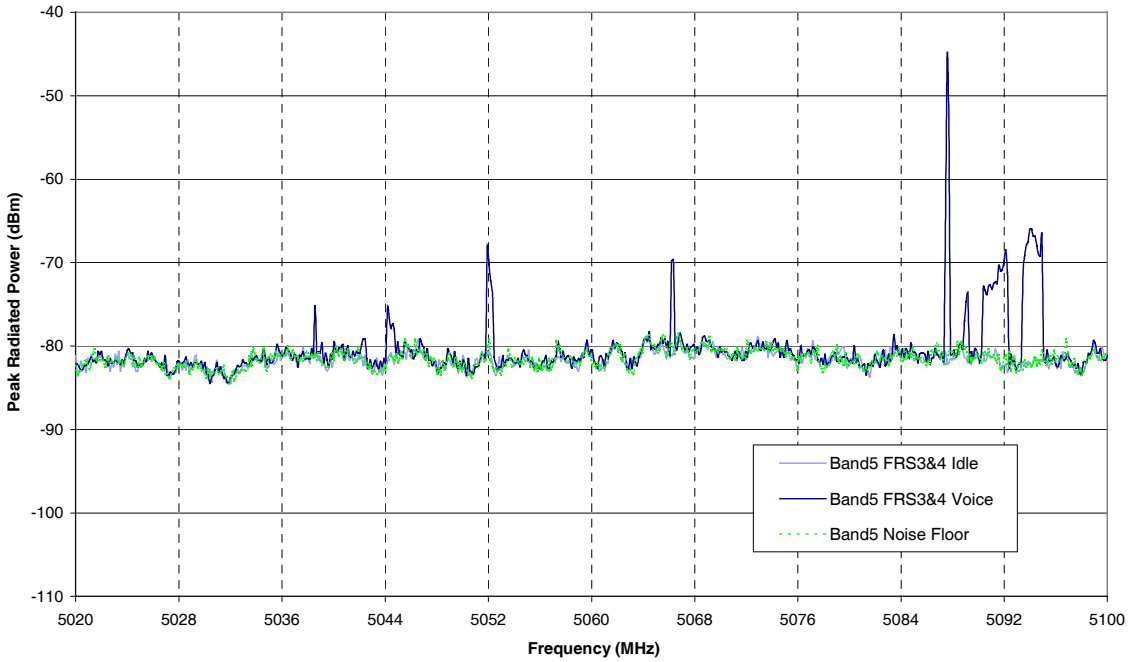

Figure A108: FRS 3&4, Band 5.

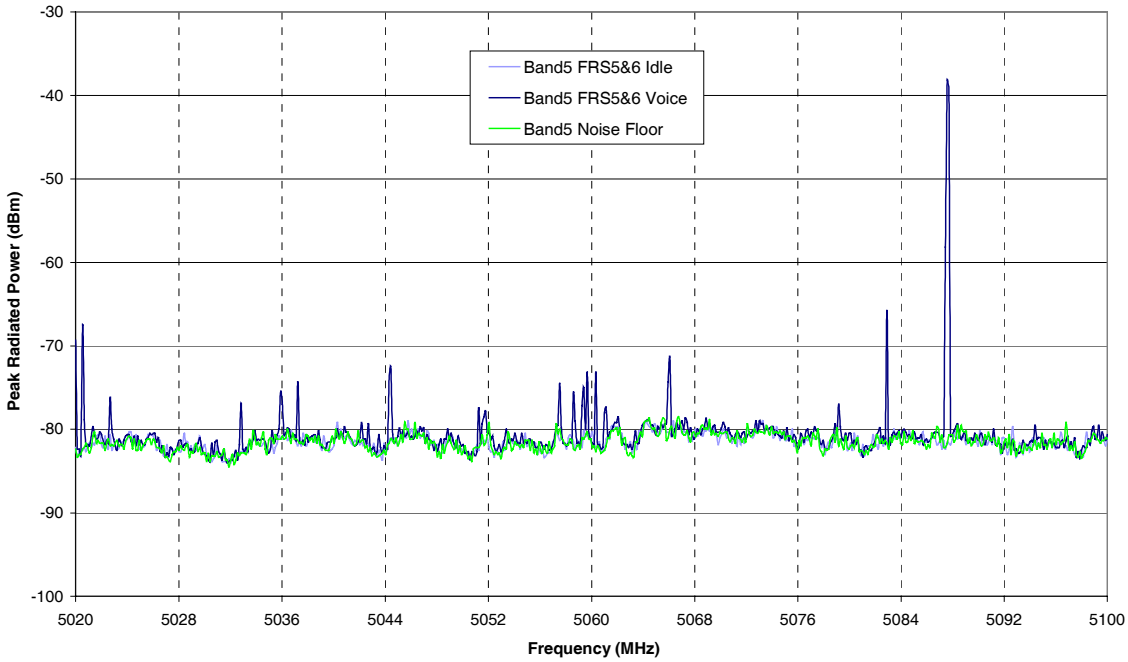

Figure A109: FRS 5&6, Band 5.

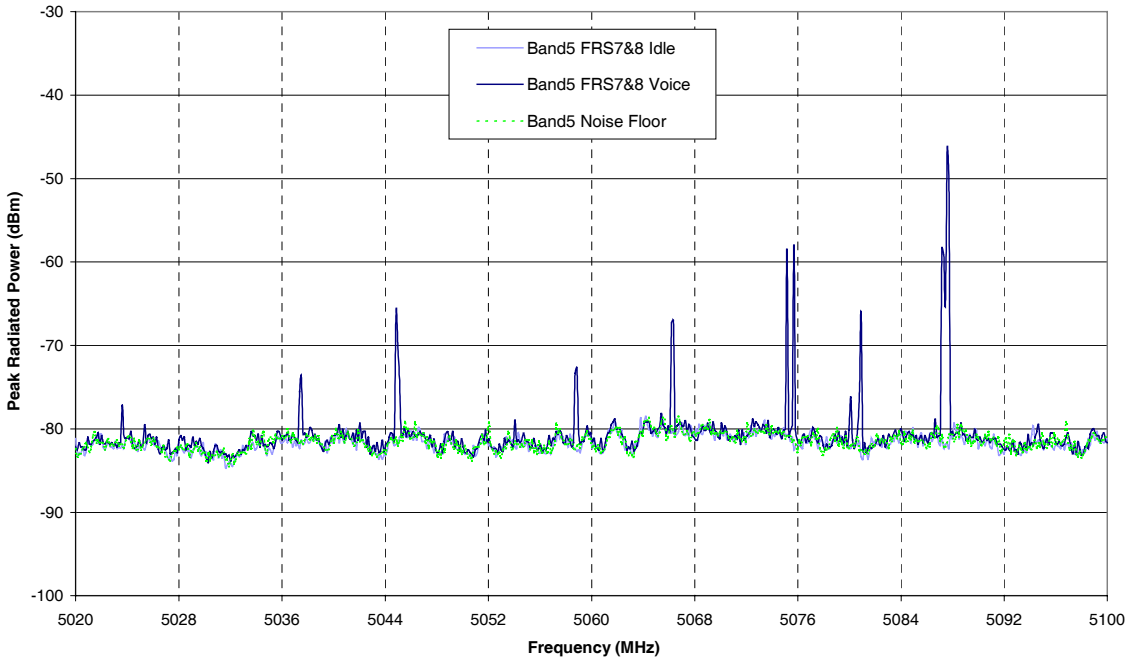

Figure A110: FRS 7&8, Band 5.

A.5 GMRS Radios

A.5.1 Band 1

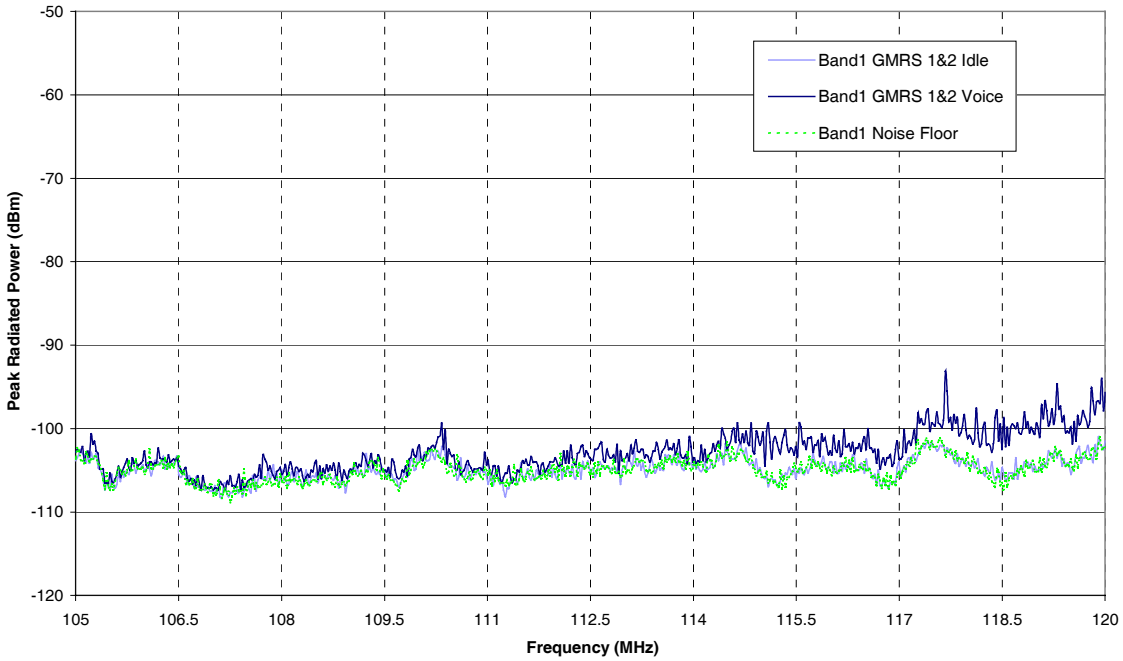

Figure A111: GMRS 1&2, Band 1.

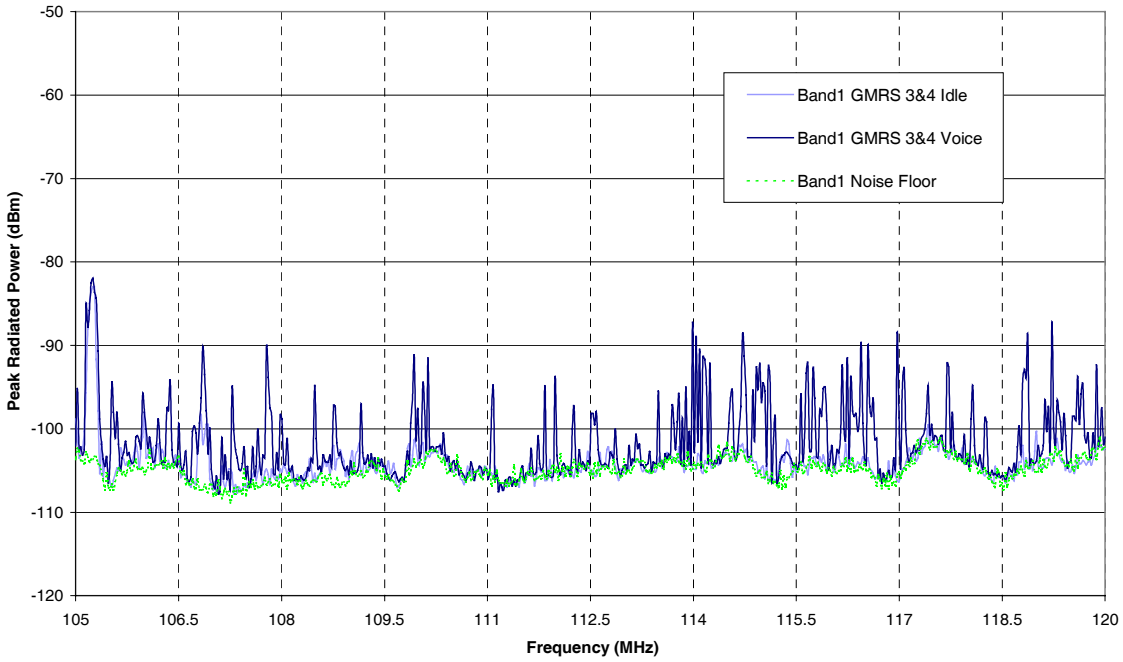

Figure A112: GMRS 3&4, Band 1.

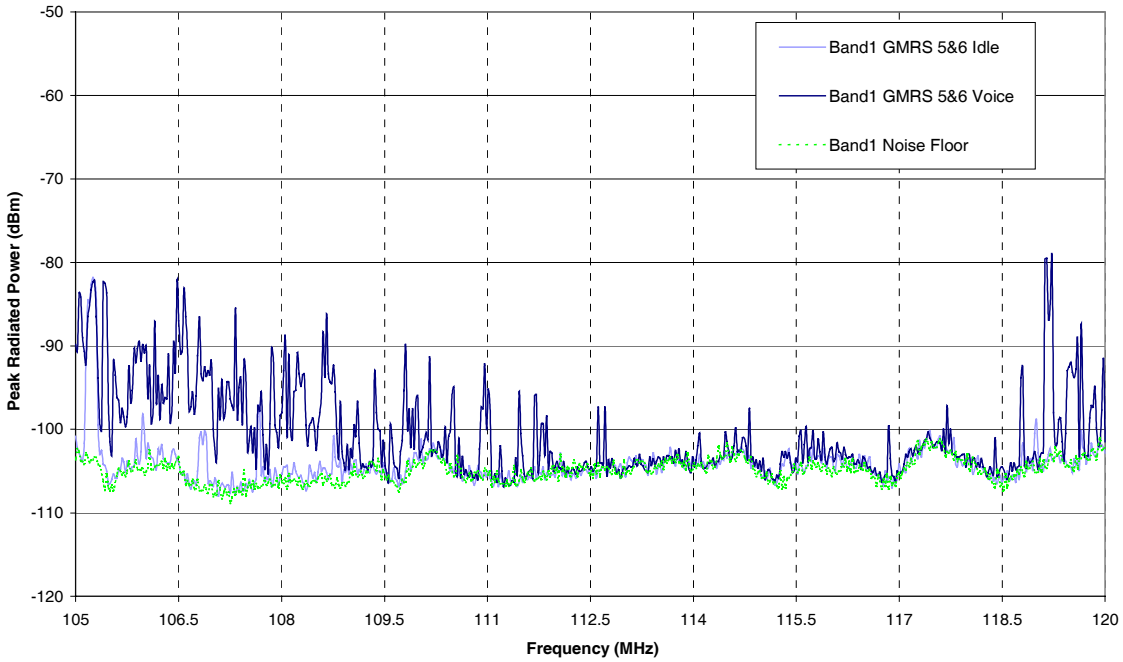

Figure A113: GMRS 5&6, Band 1.

A.5.2 Band 2

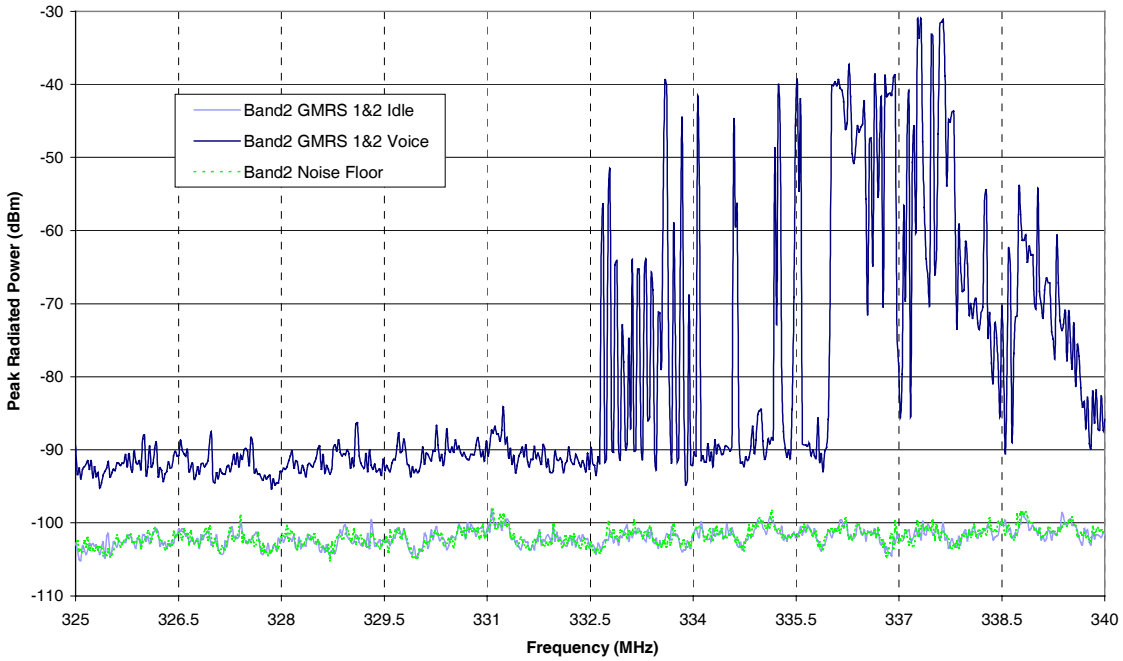

Figure A114: GMRS 1&2, Band 2.

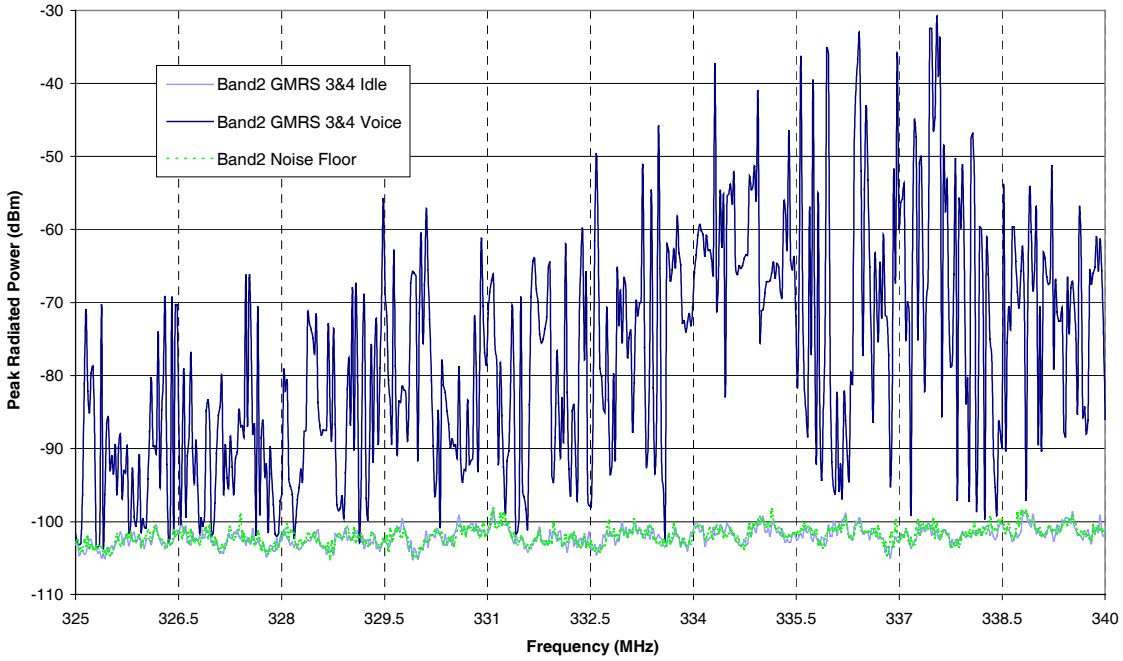

Figure A115: GMRS 3&4, Band 2.

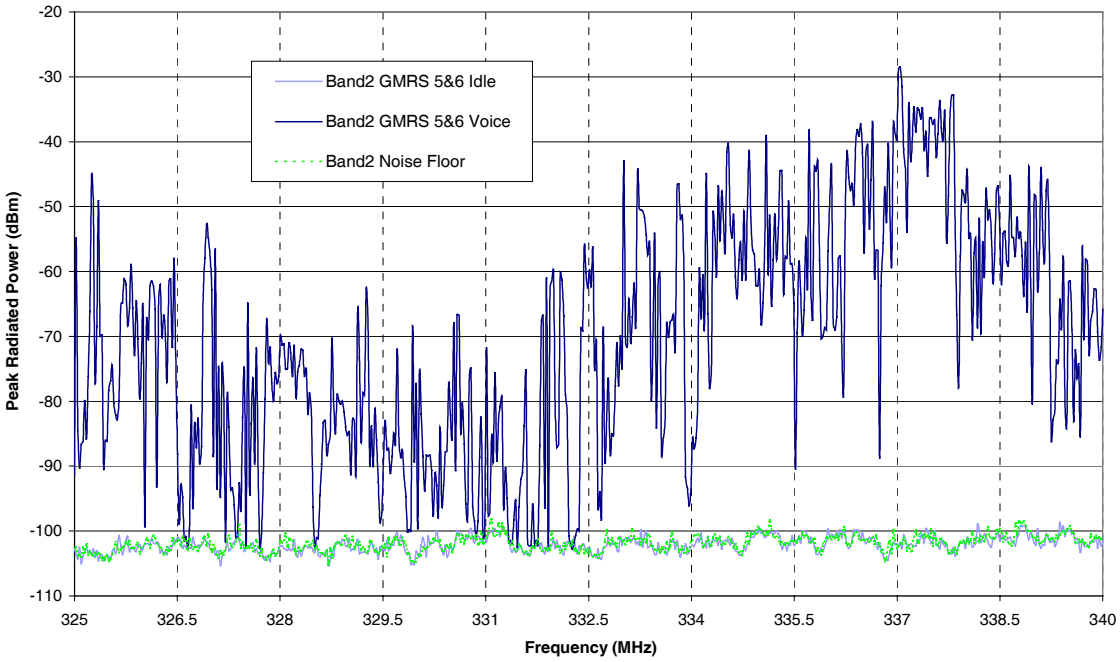

Figure A116: GMRS 5&6, Band 2.

A.5.3 Band 3

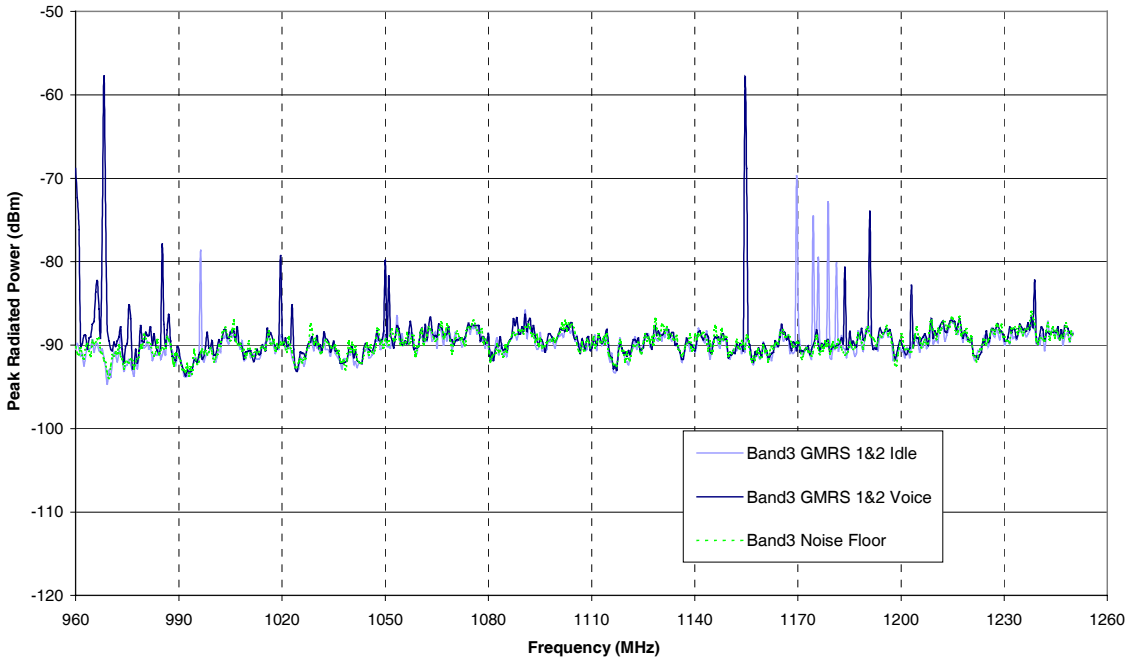

Figure A117: GMRS 1&2, Band 3.

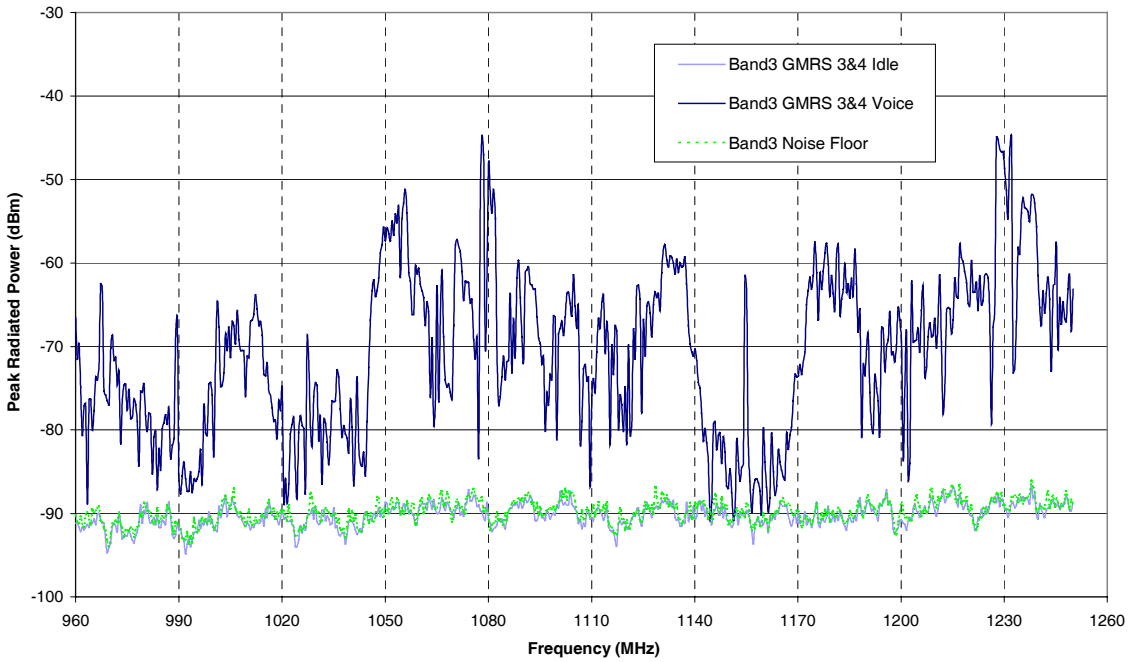

Figure A118: GMRS 3&4, Band 3.

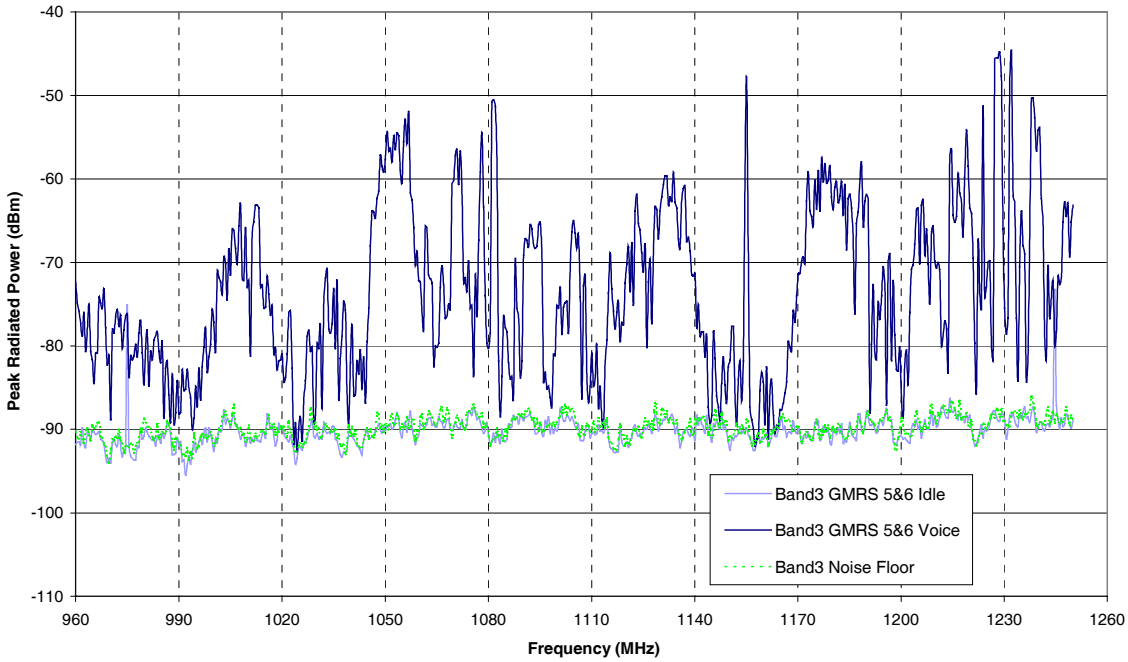

Figure A119: GMRS 5&6, Band 3.

A.5.4 Band 4

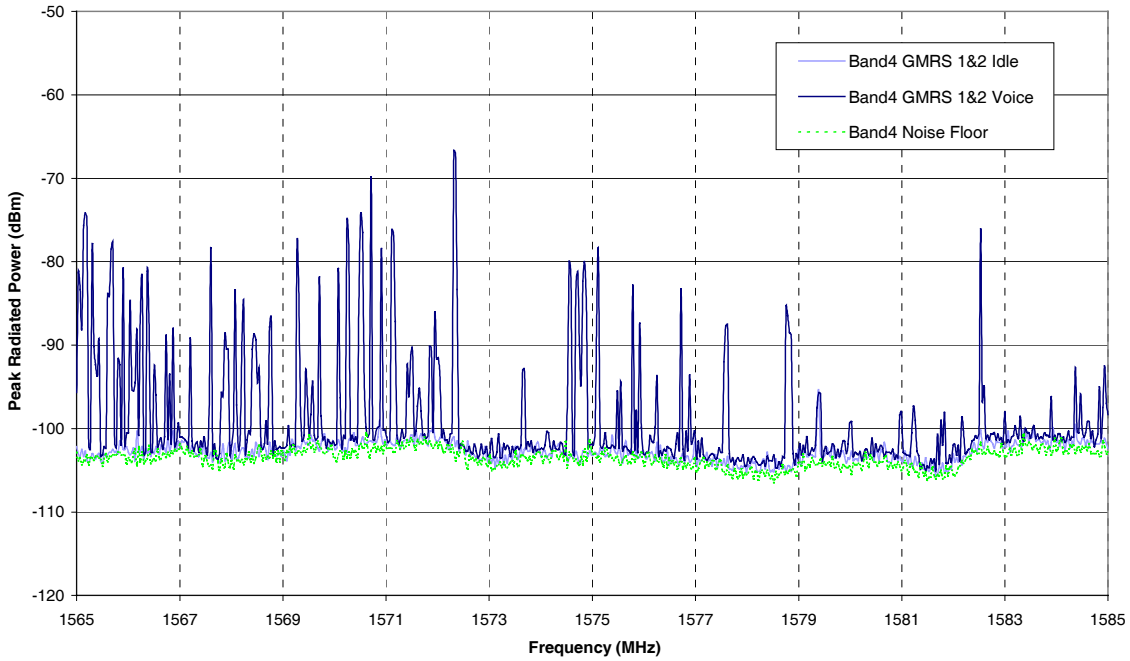

Figure A120: GMRS 1&2, Band 4.

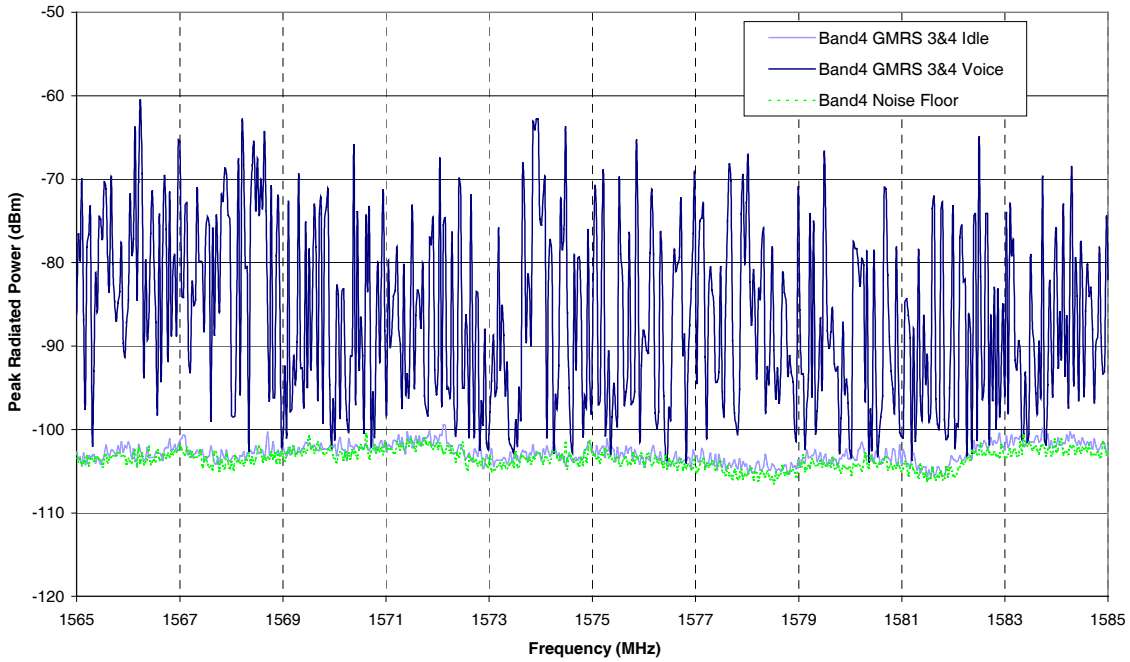

Figure A121: GMRS 3&4, Band 4.

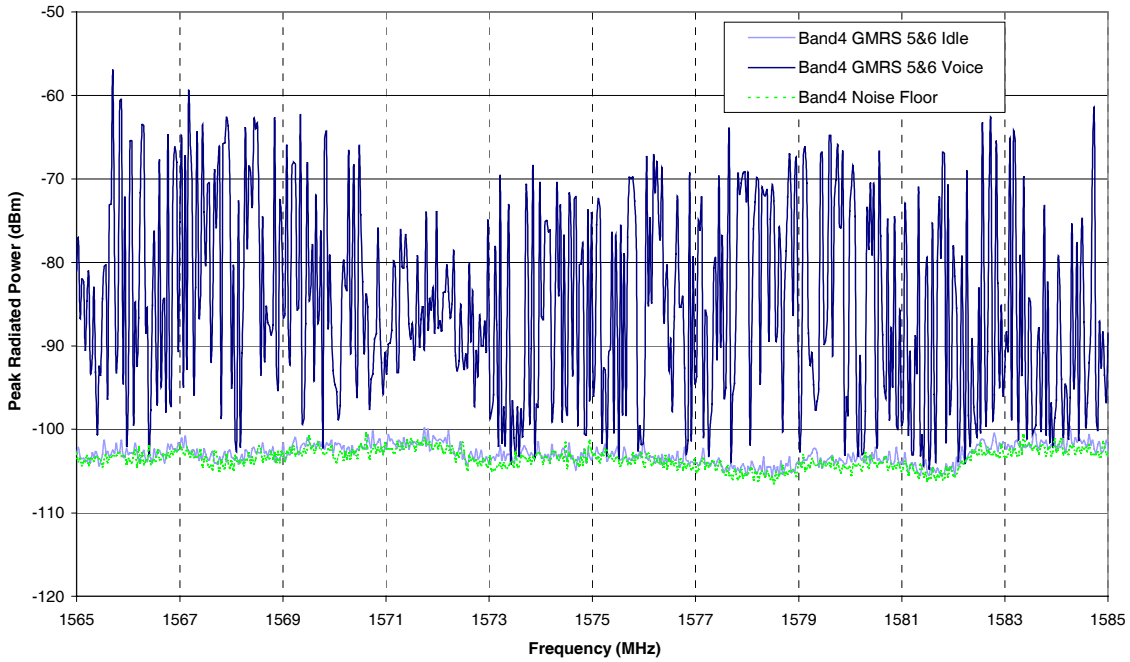

Figure A122: GMRS 5&6, Band 4.

A.5.5 Band 5

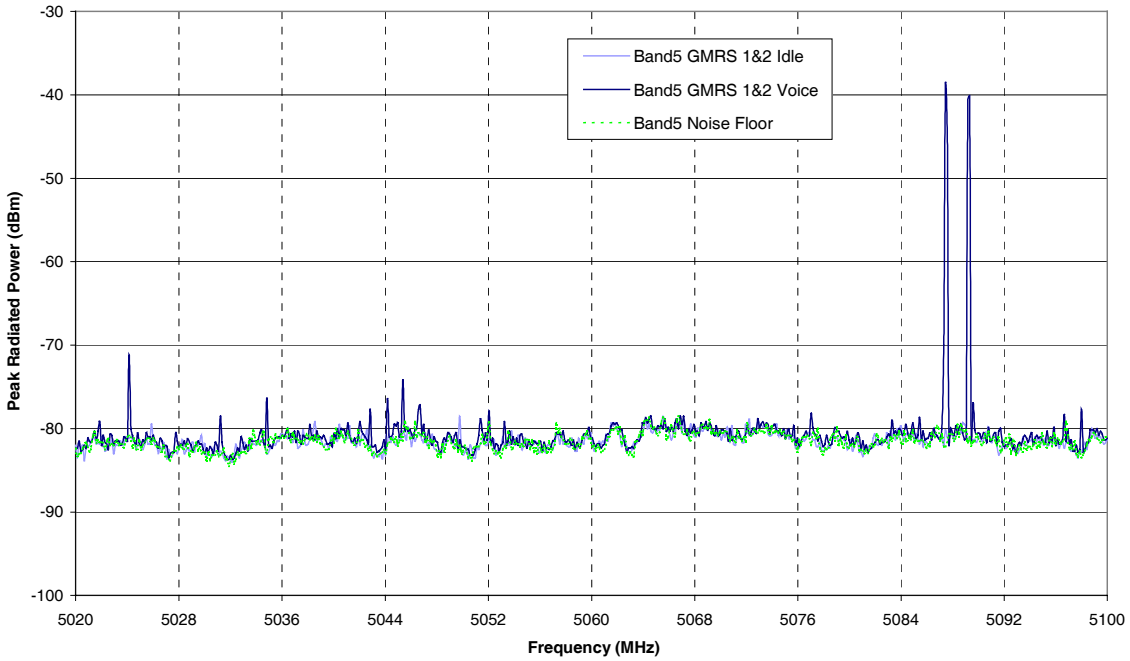

Figure A123: GMRS 1&2, Band 5.

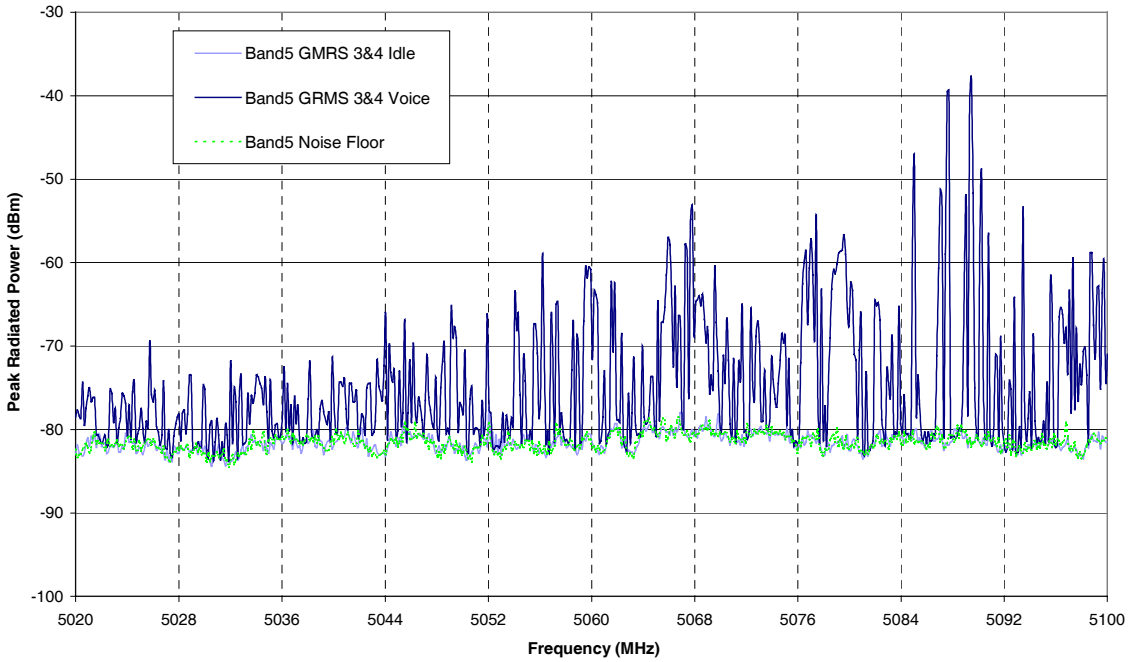

Figure A124: GMRS 3&4, Band 5.

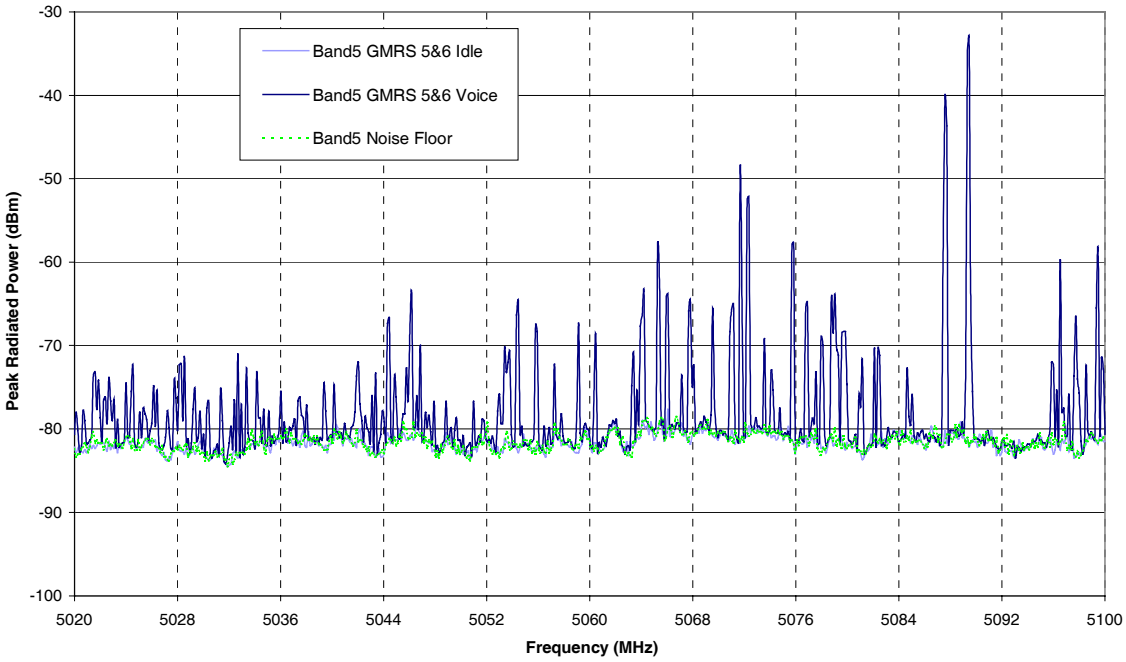

Figure A125: GMRS 5&6, Band 5.

Appendix B: Measurements and Results of Non-Intentional Transmitters Including Computer Laptops and Personal-Digital-Assistants

The following charts show the results of individual modes tested for each non-intentional transmitter, which revealed the best host for each measurement frequency band. These charts were reduced further to achieve the maximum radiated emissions envelope for each host device, as discussed and seen in Section 3.4. Once again the equivalent noise floor was added to the charts to show emissions from the devices were above the calibrated noise floor from the measuring instrument. The organization is such that each host device is grouped together according to the measurement frequency band.

B.1 Band 1

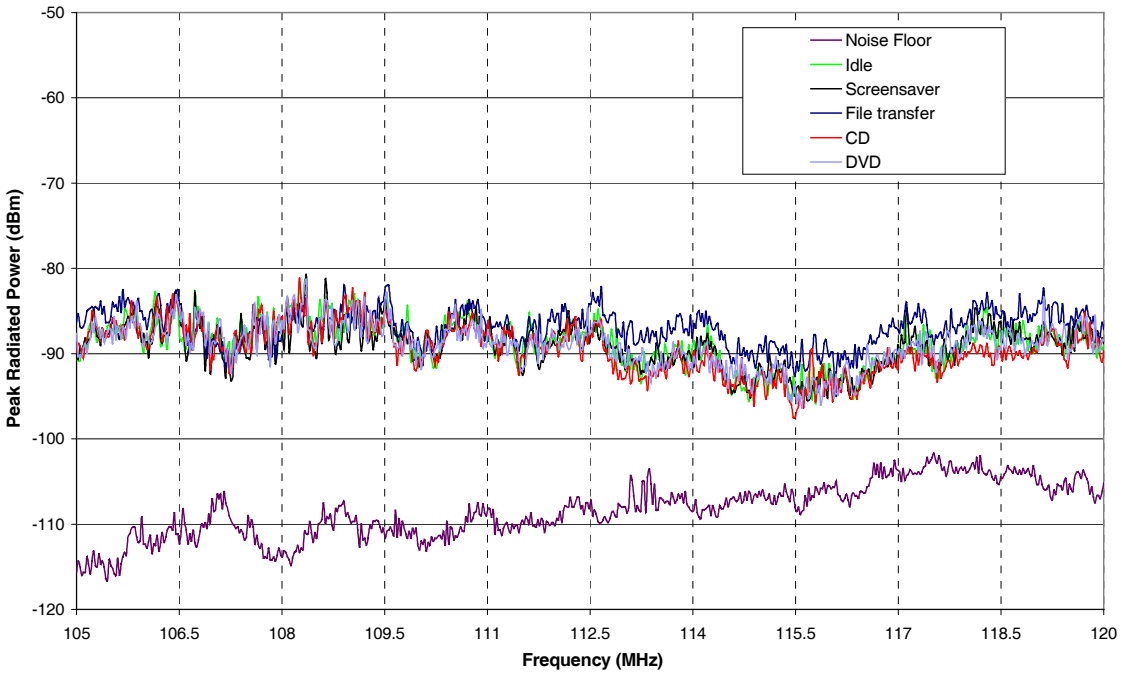

Figure B1: Laptop 1, Band 1.

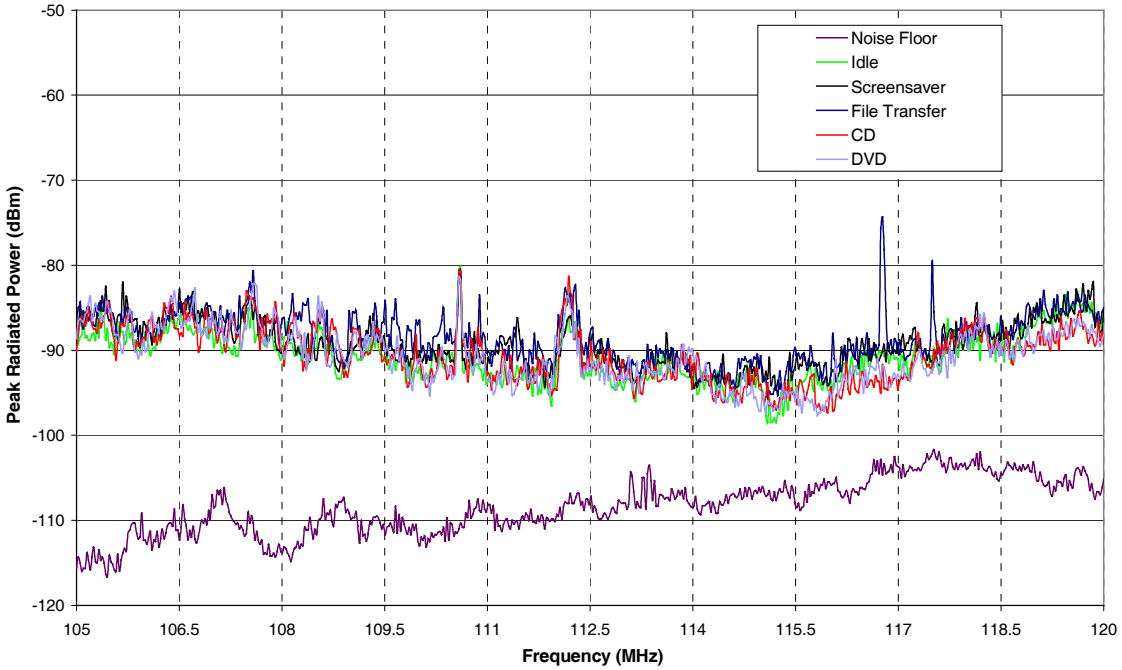

Figure B2: Laptop 2, Band 1.

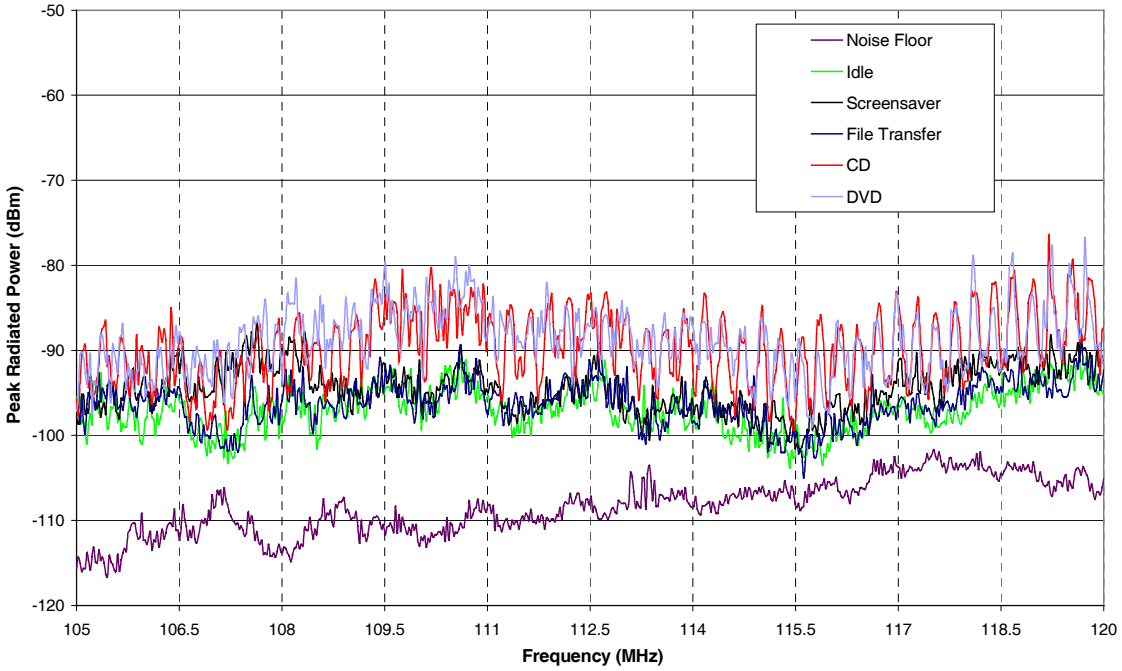

Figure B3: Laptop 3, Band 1.

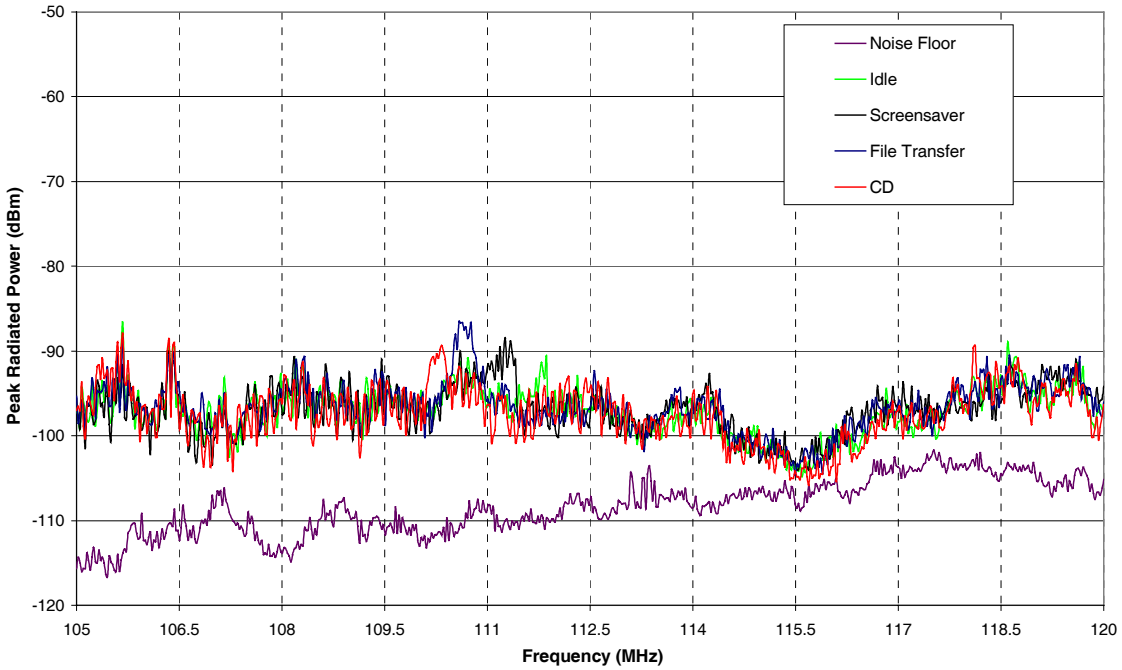

Figure B4: Laptop 4, Band 1.

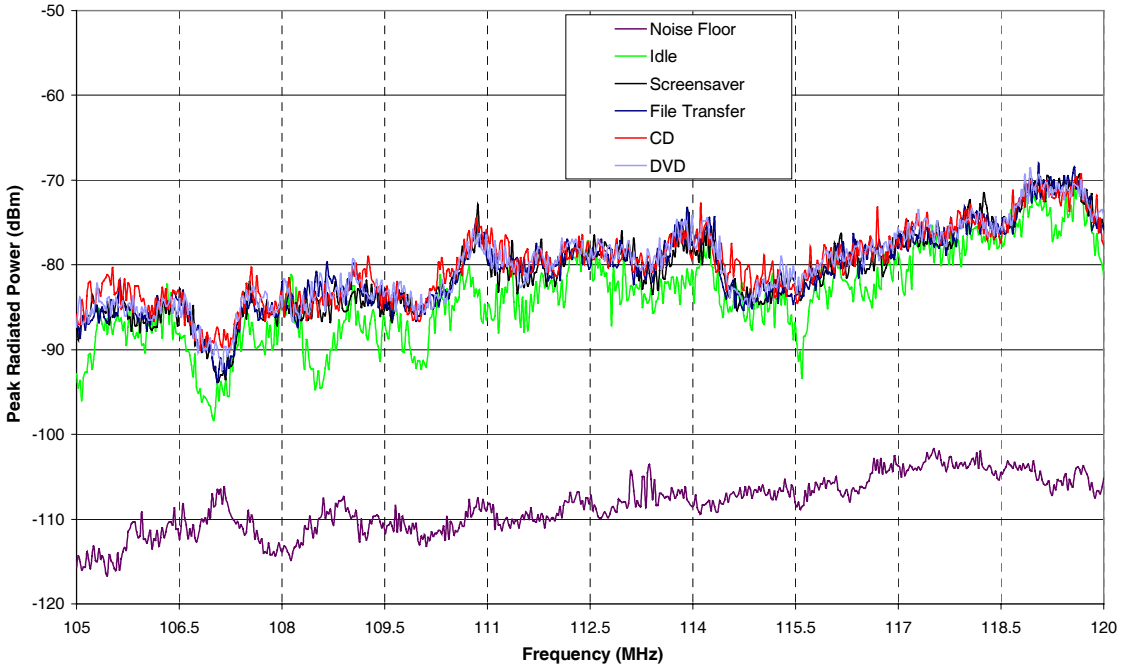

Figure B5: Laptop 5, Band 1.

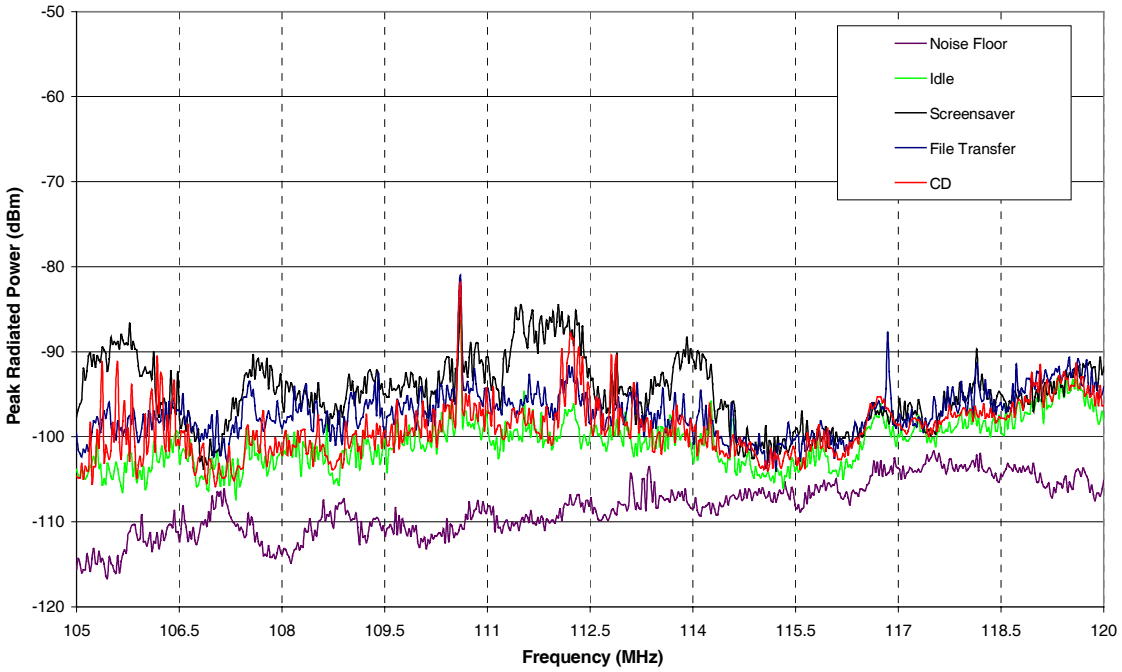

Figure B6: Laptop 6, Band 1.

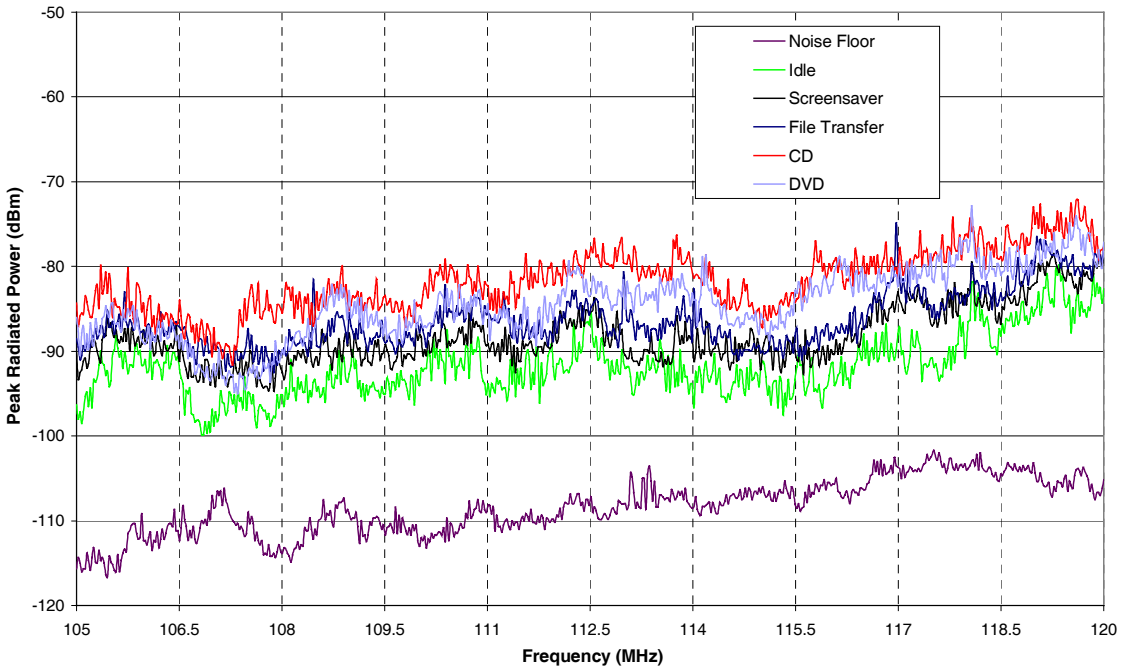

Figure B7: Laptop 7, Band 1.

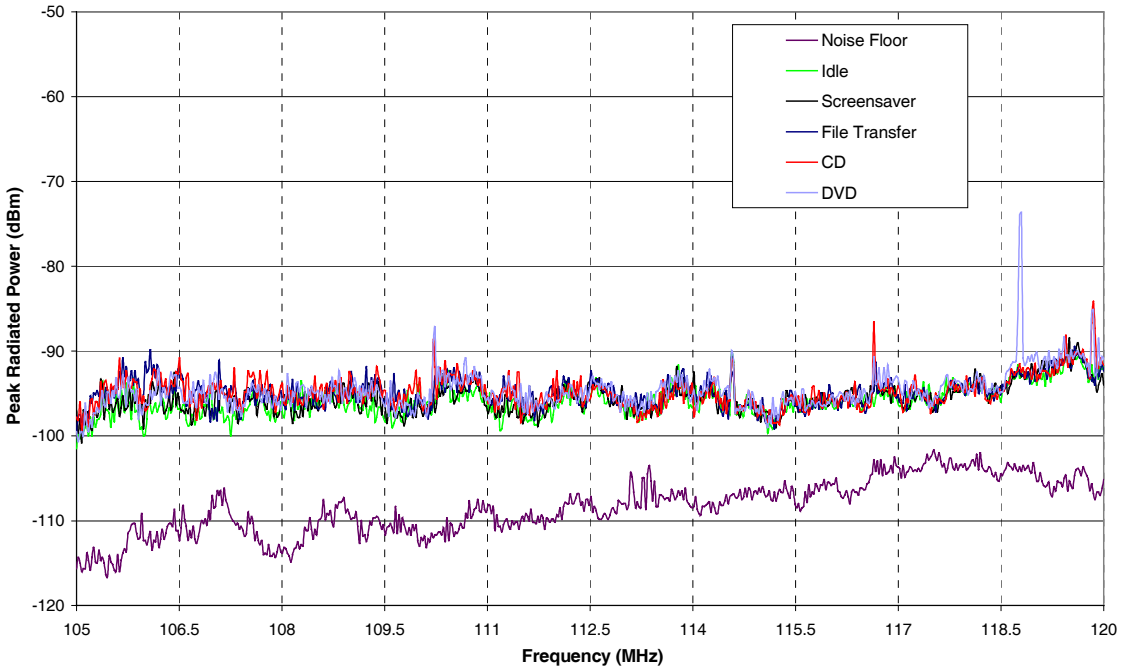

Figure B8: Laptop 8, Band 1.

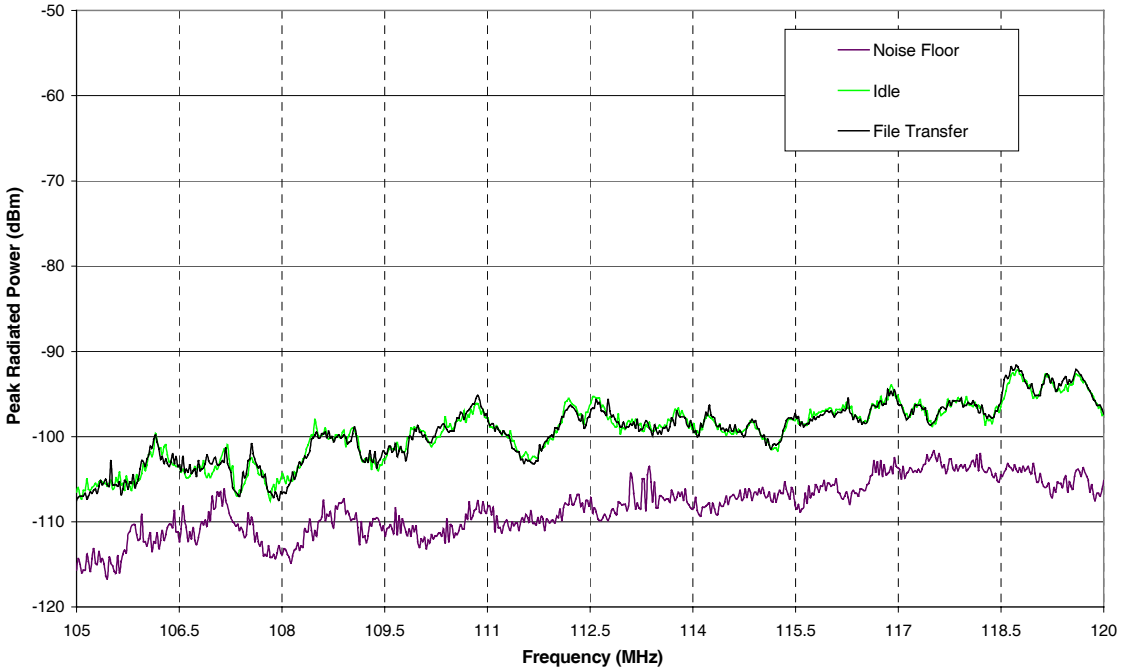

Figure B9: PDA 1, Band 1.

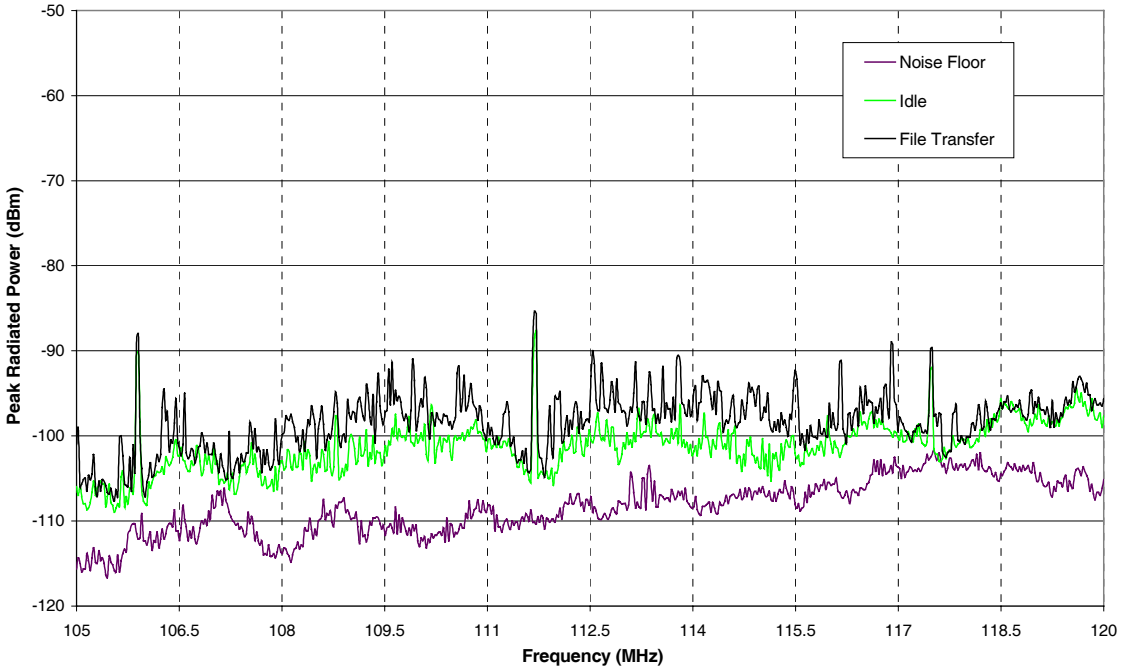

Figure B10: PDA 2, Band 1.

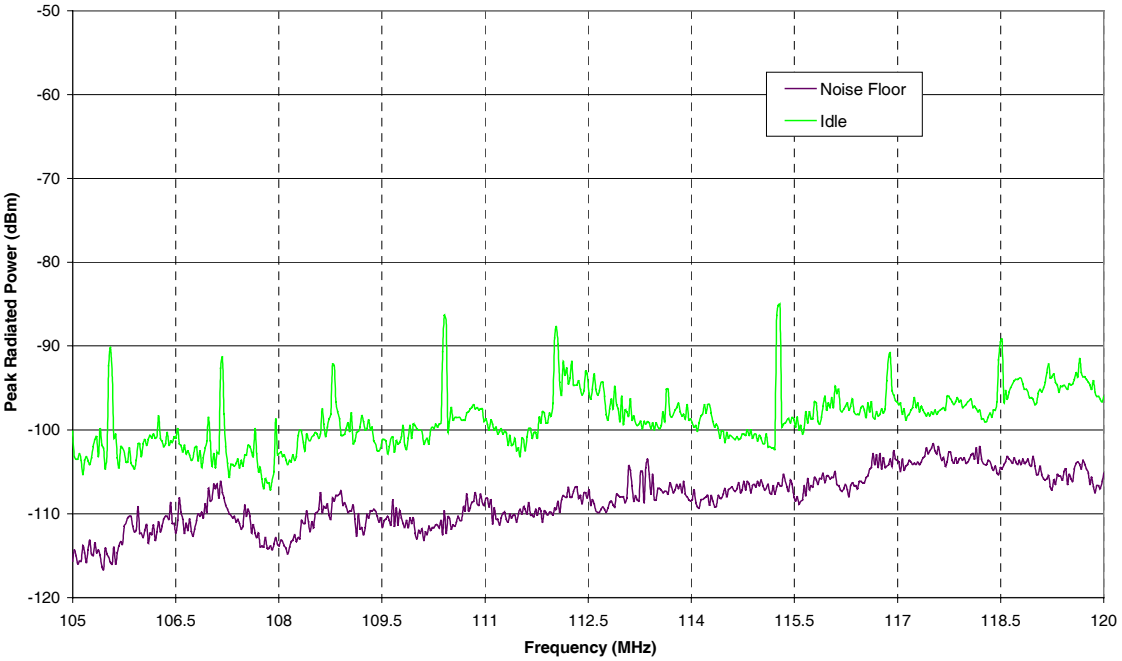

Figure B11: PRN, Band 1

B.2 Band 2

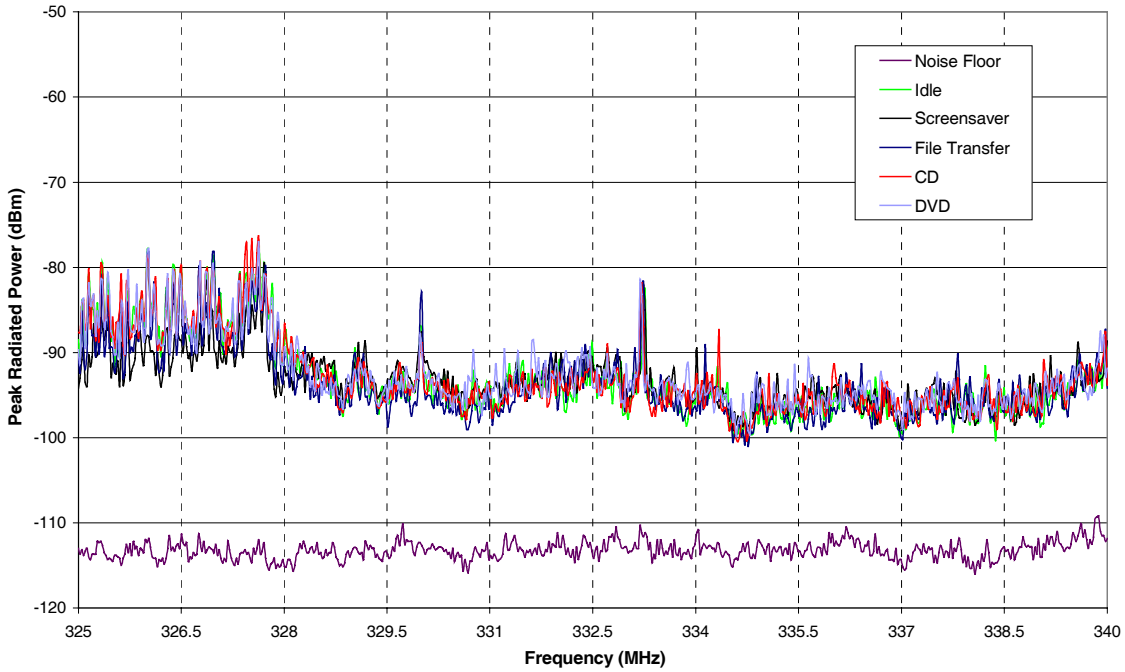

Figure B12: Laptop 1, Band 2.

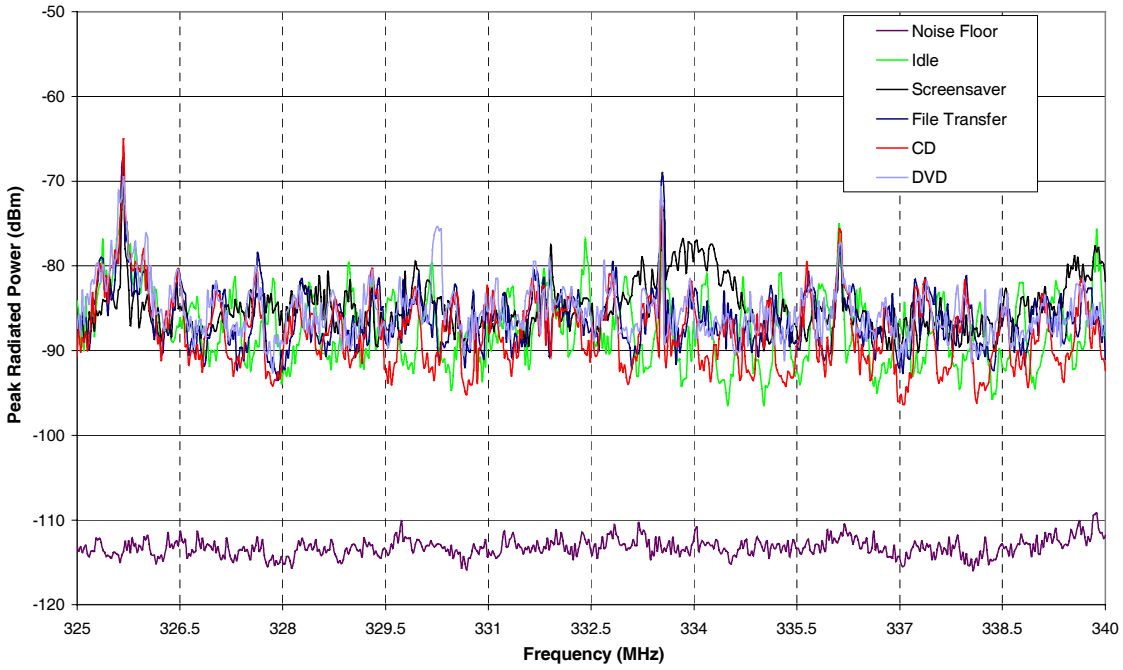

Figure B13: Laptop 2, Band 2.

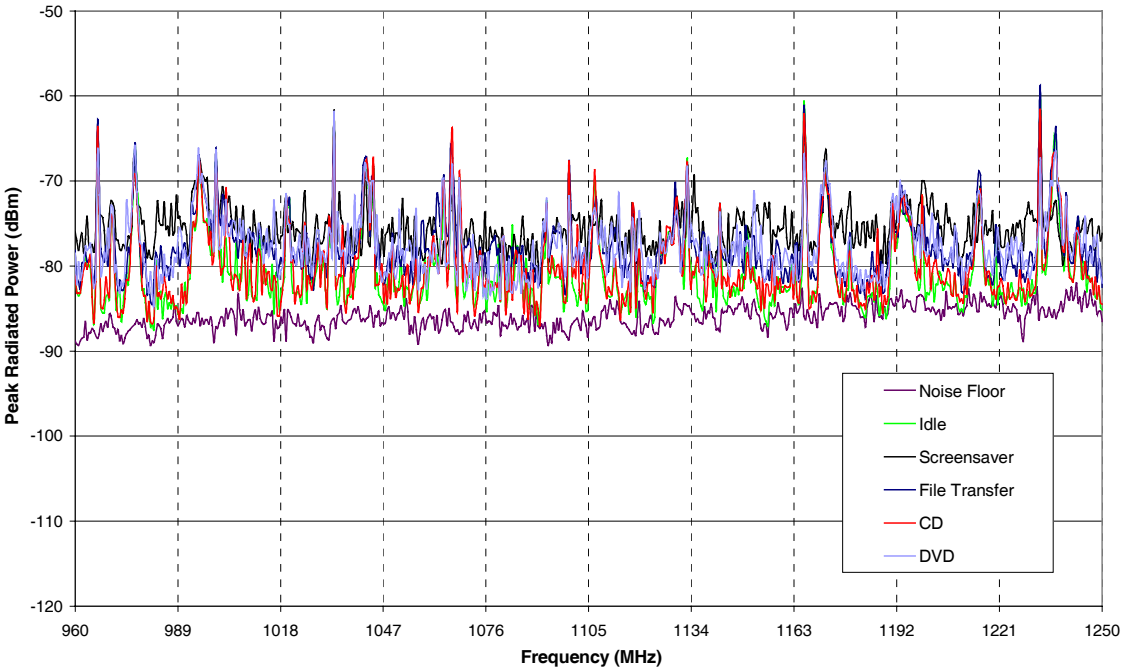

Figure B14: Laptop 3, Band 2.

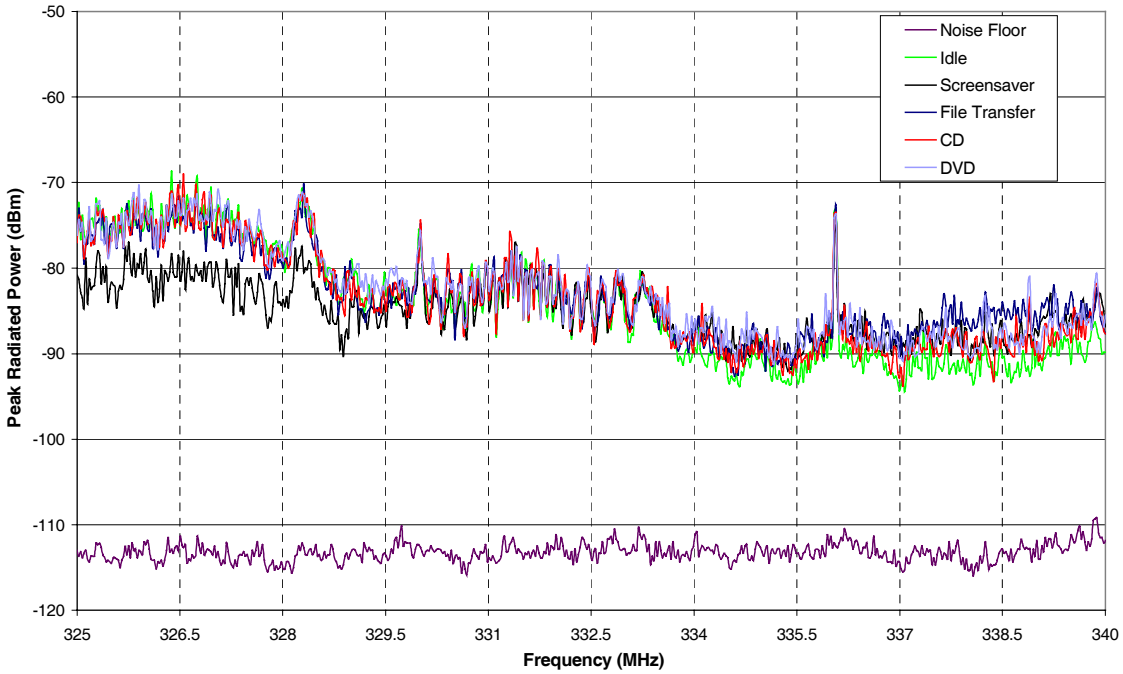

Figure B15: Laptop 4, Band 2.

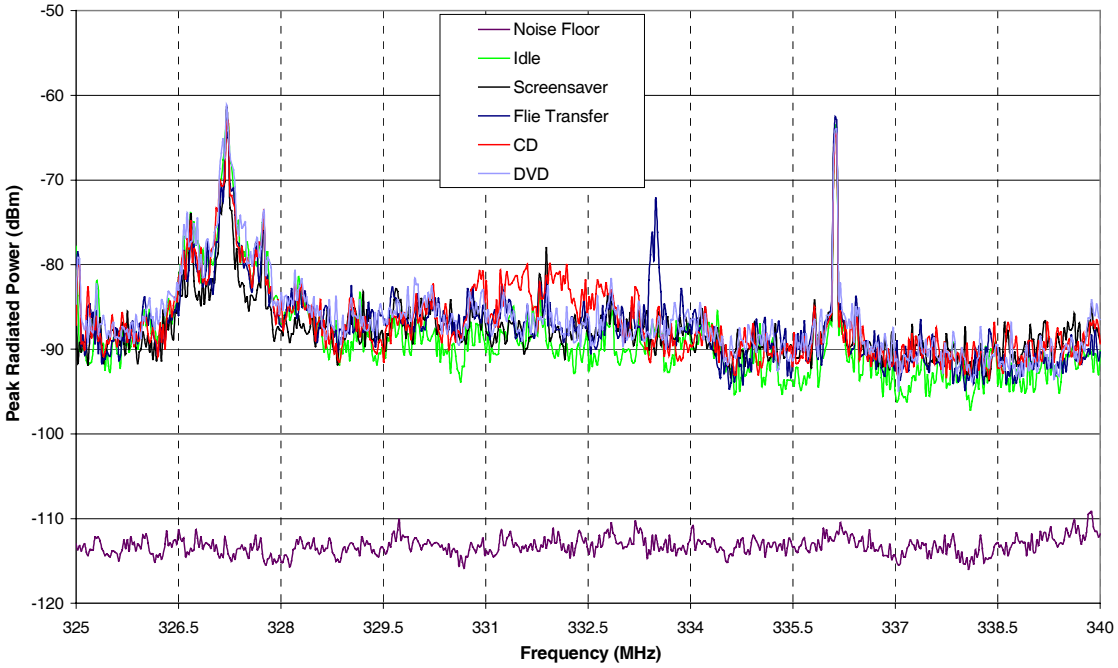

Figure B16: Laptop 5, Band 2.

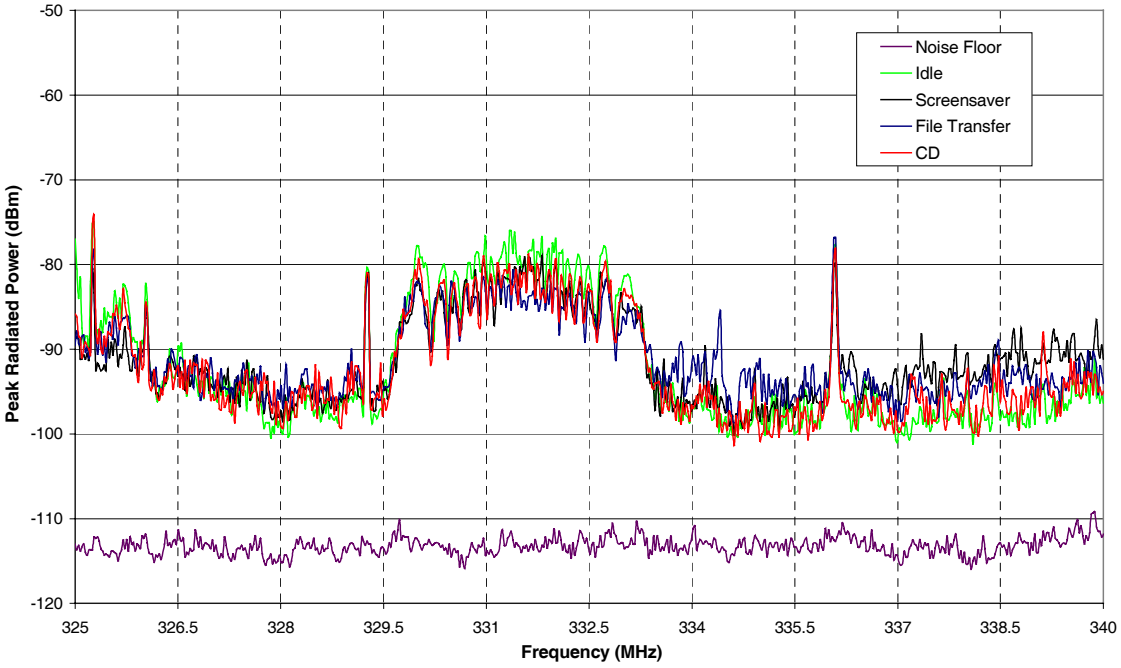

Figure B17: Laptop 6, Band 2.

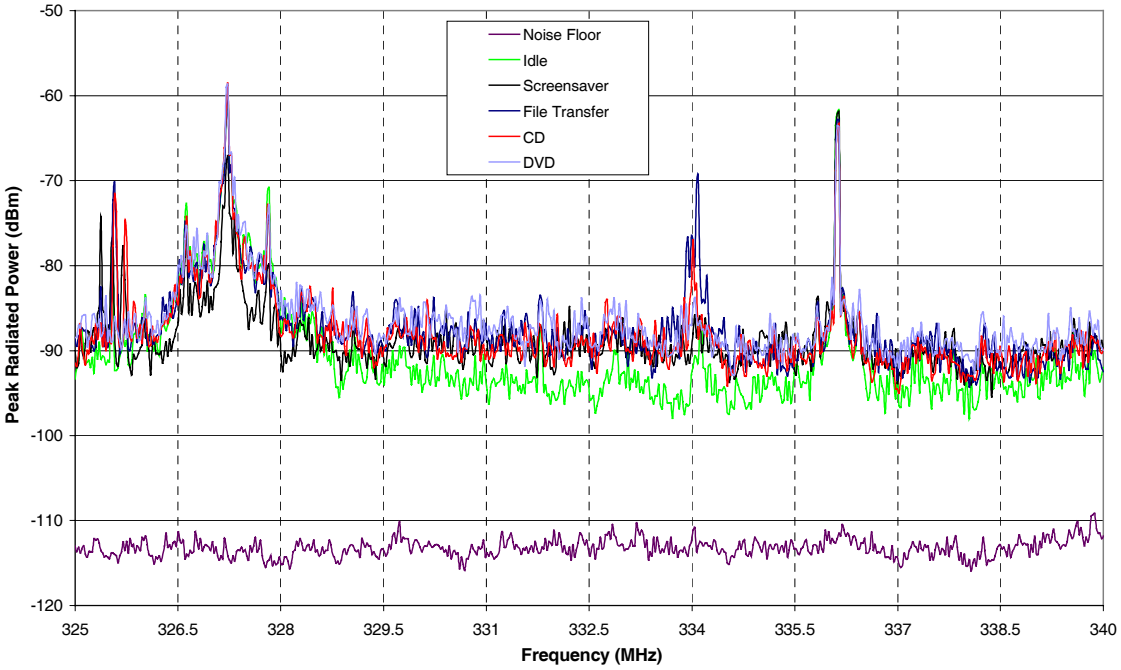

Figure B18: Laptop 7, Band 2.

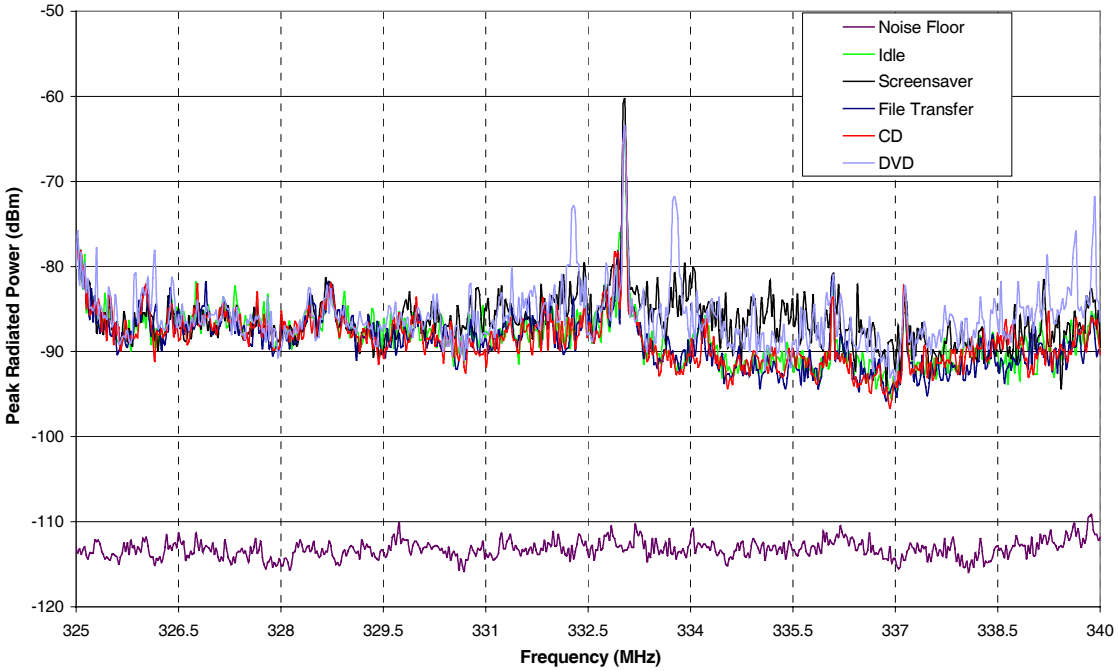

Figure B19: Laptop 8, Band 2.

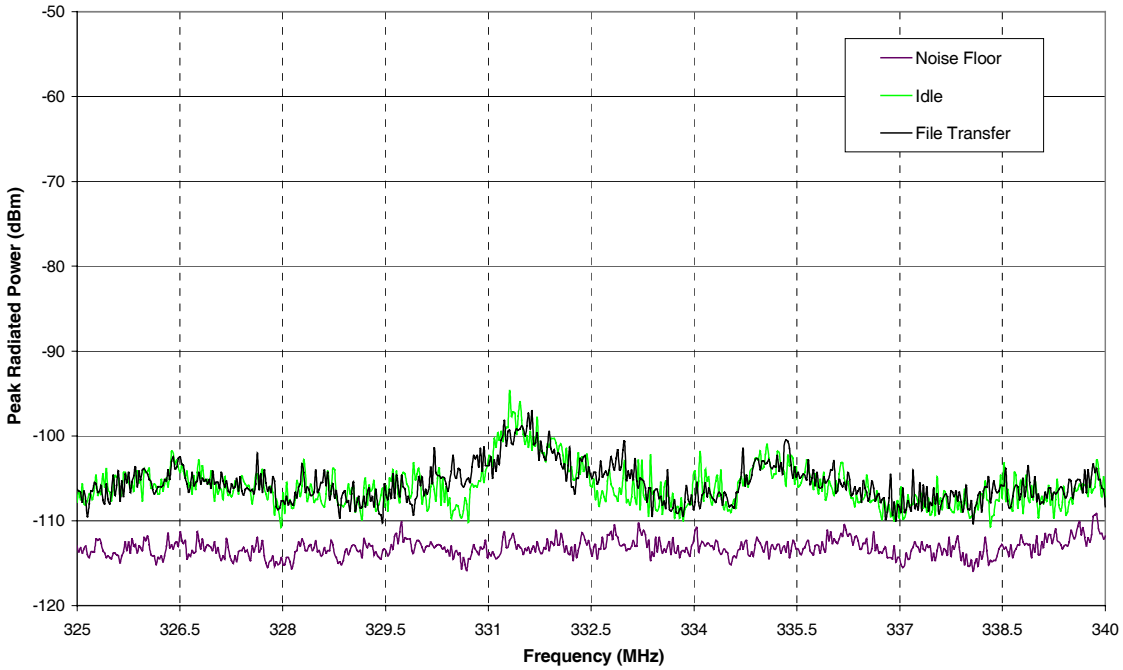

Figure B20: PDA 1, Band 2.

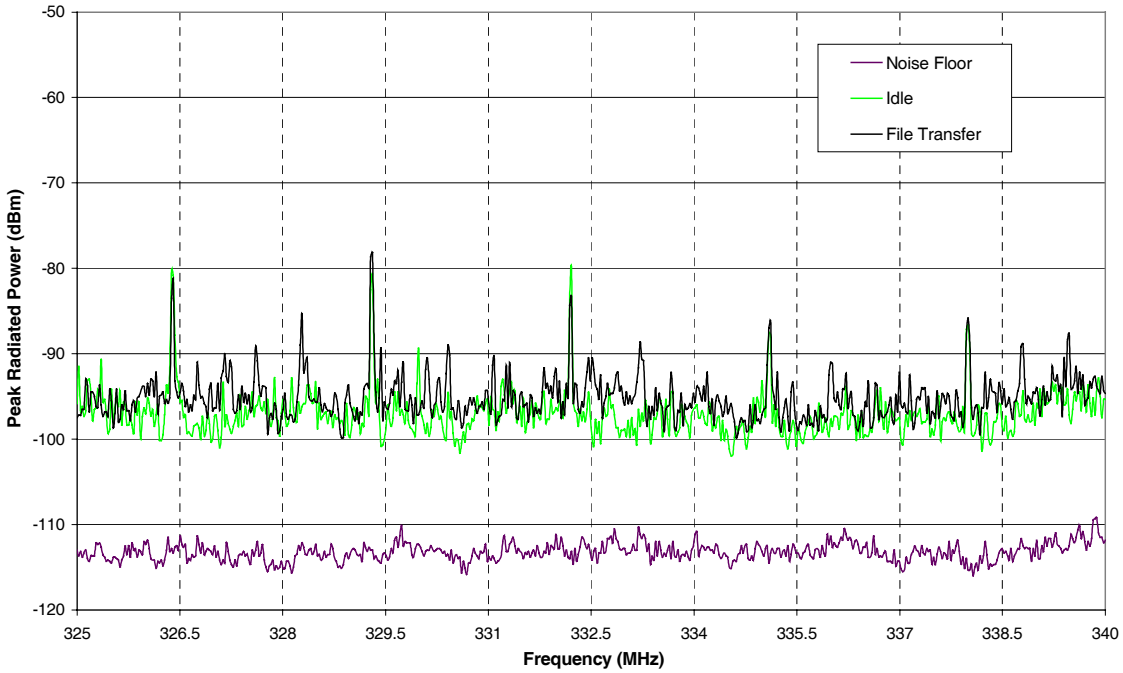

Figure B21: PDA 2, Band 2.

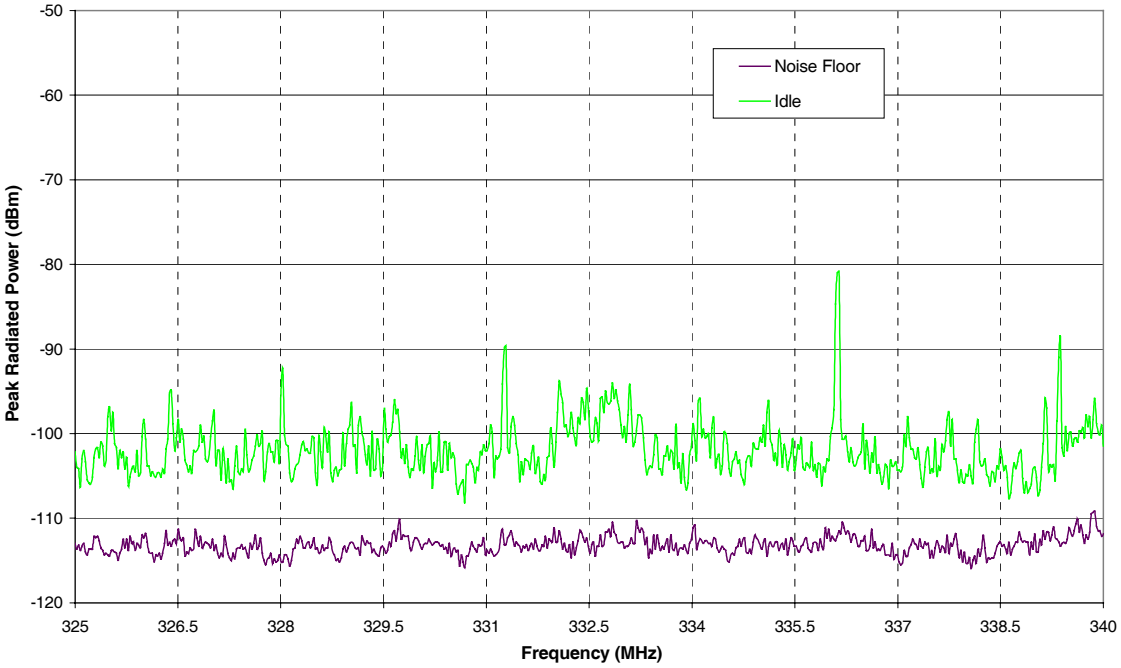

Figure B22: PRN, Band 2.

B.3 Band 3

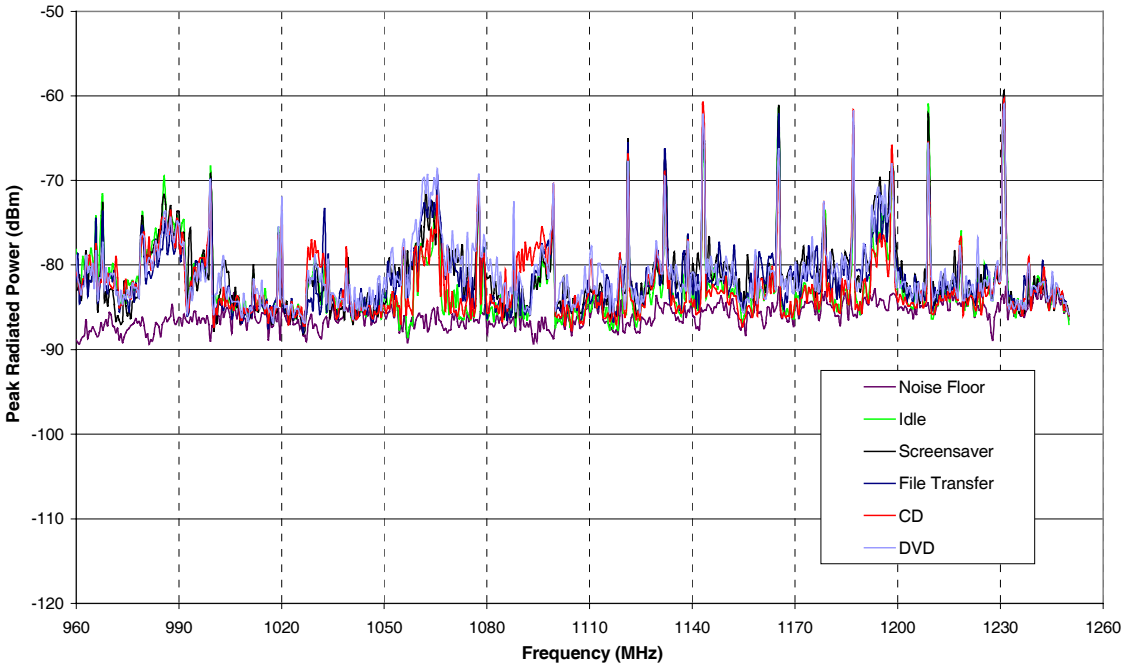

Figure B23: Laptop 1, Band 3.

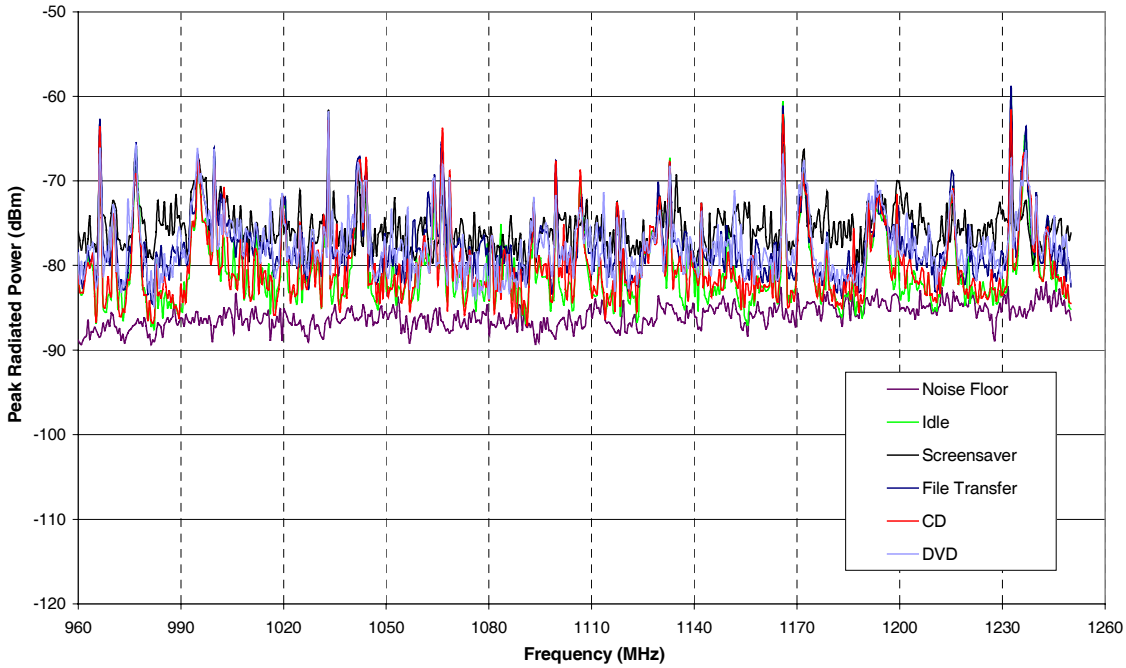

Figure B24: Laptop 2, Band 3.

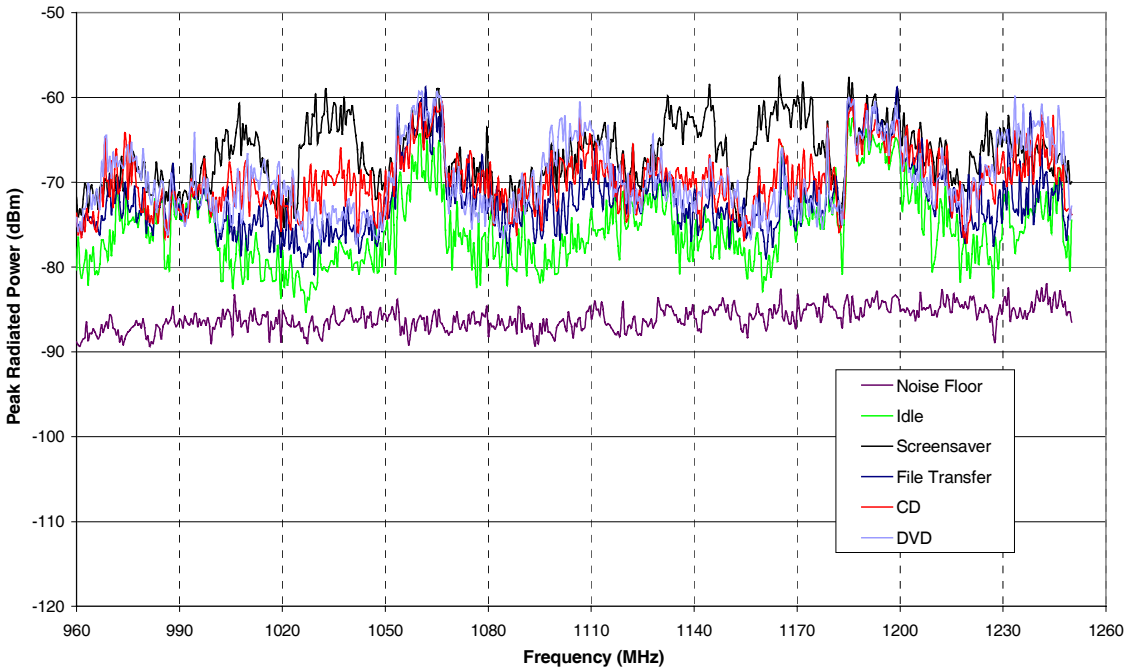

Figure B25: Laptop 3, Band 3.

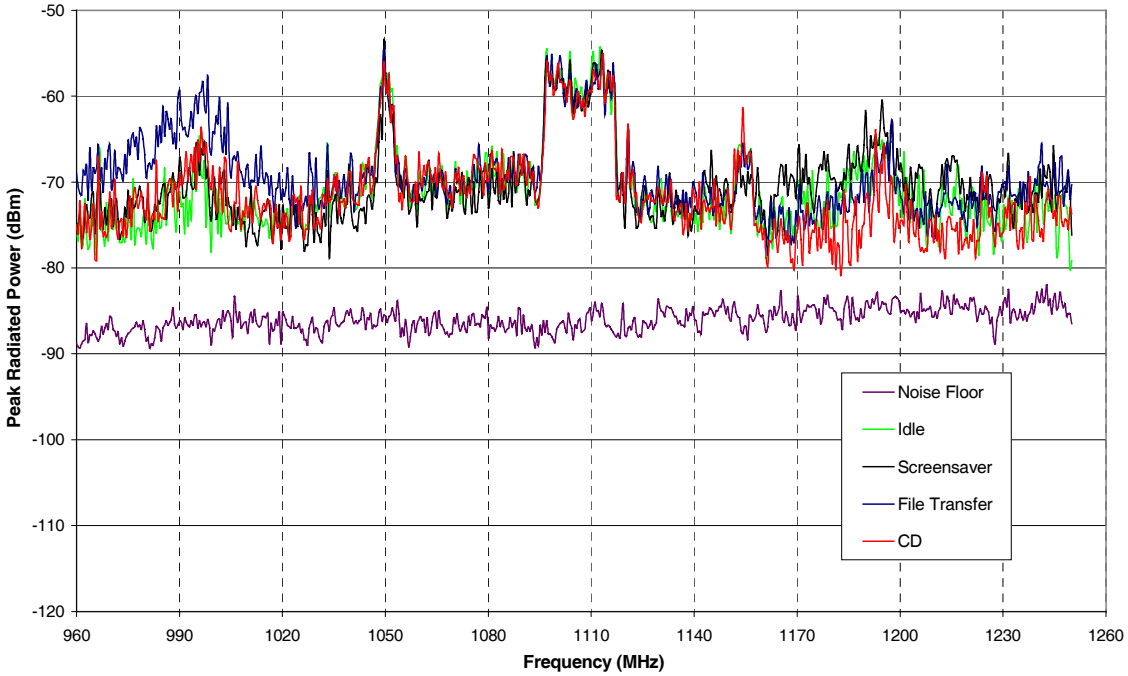

Figure B26: Laptop 4, Band 3.

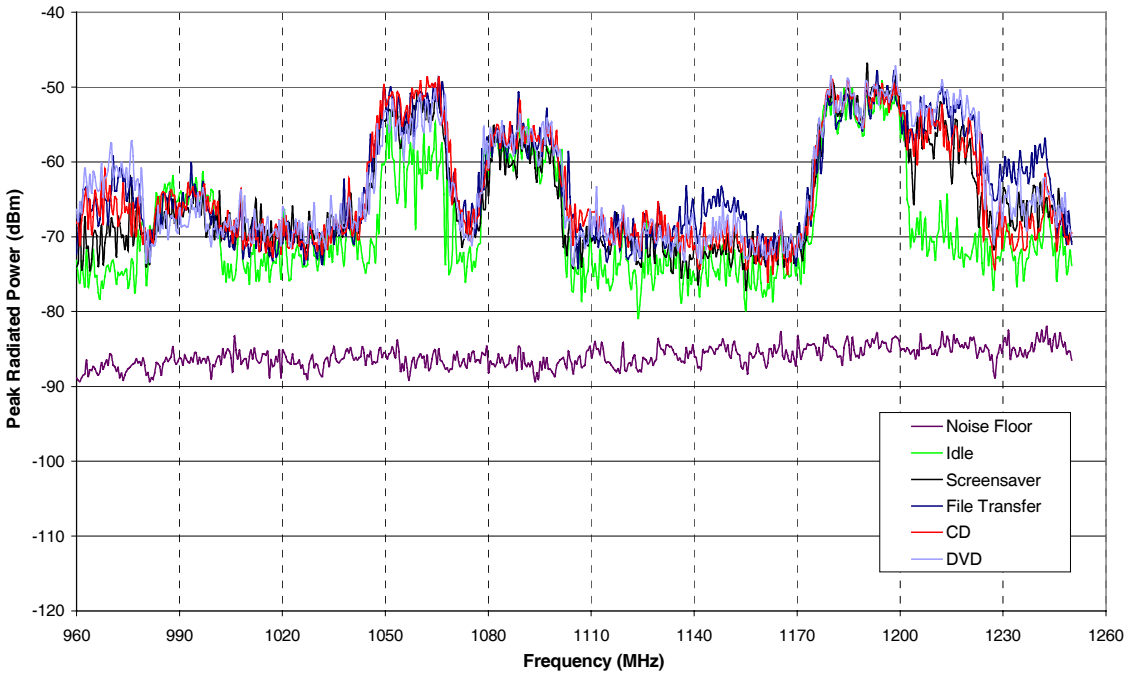

Figure B27: Laptop 5, Band 3.

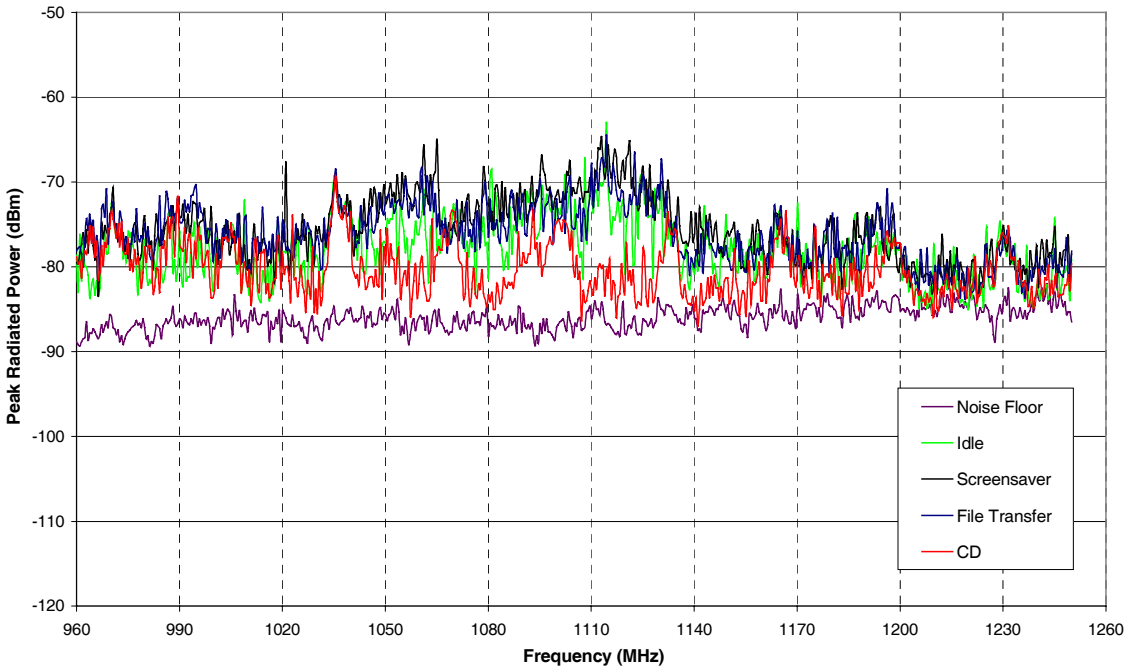

Figure B28: Laptop 6, Band 3.

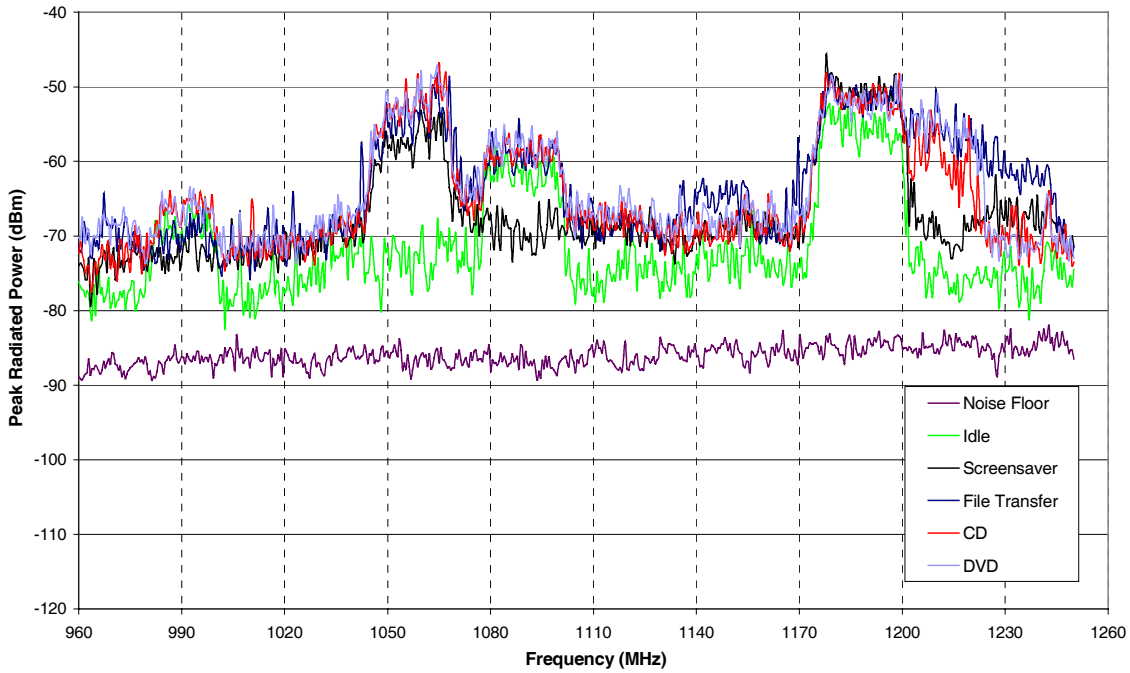

Figure B29: Laptop 7, Band 3.

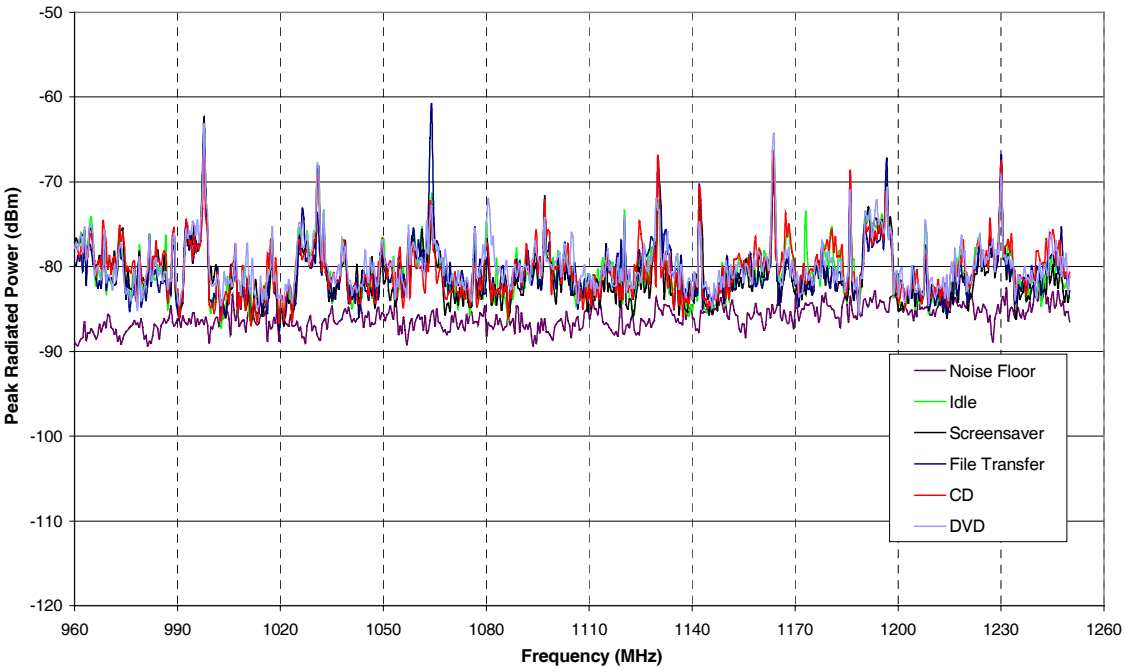

Figure B30: Laptop 8, Band 3.

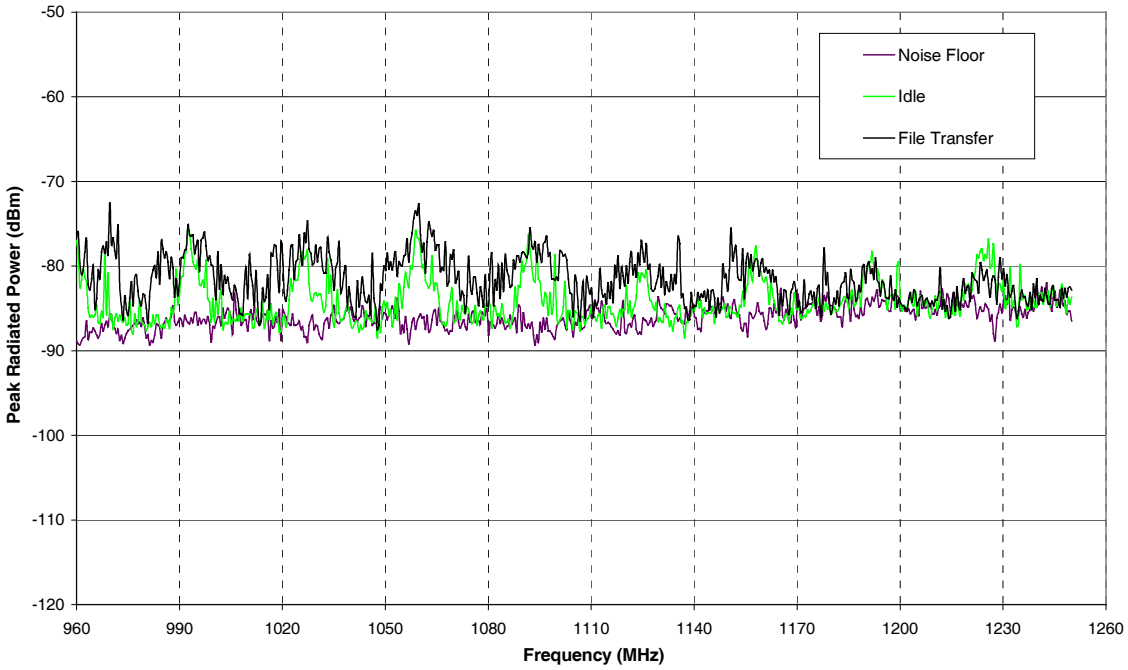

Figure B31: PDA 1, Band 3.

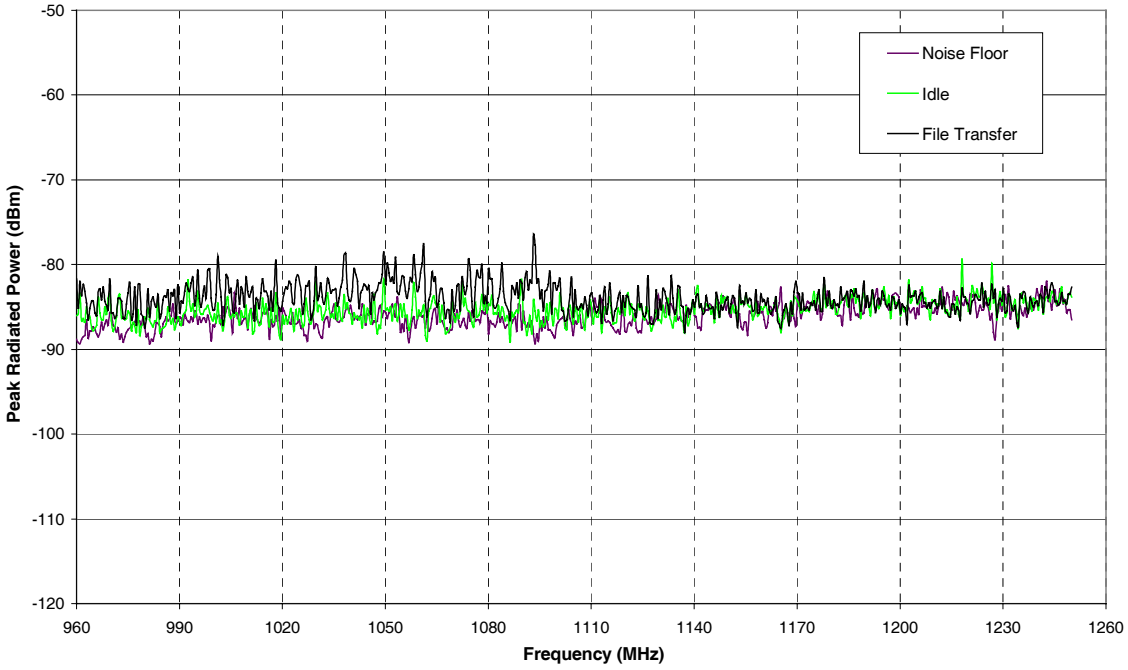

Figure B32: PDA 2, Band 3.

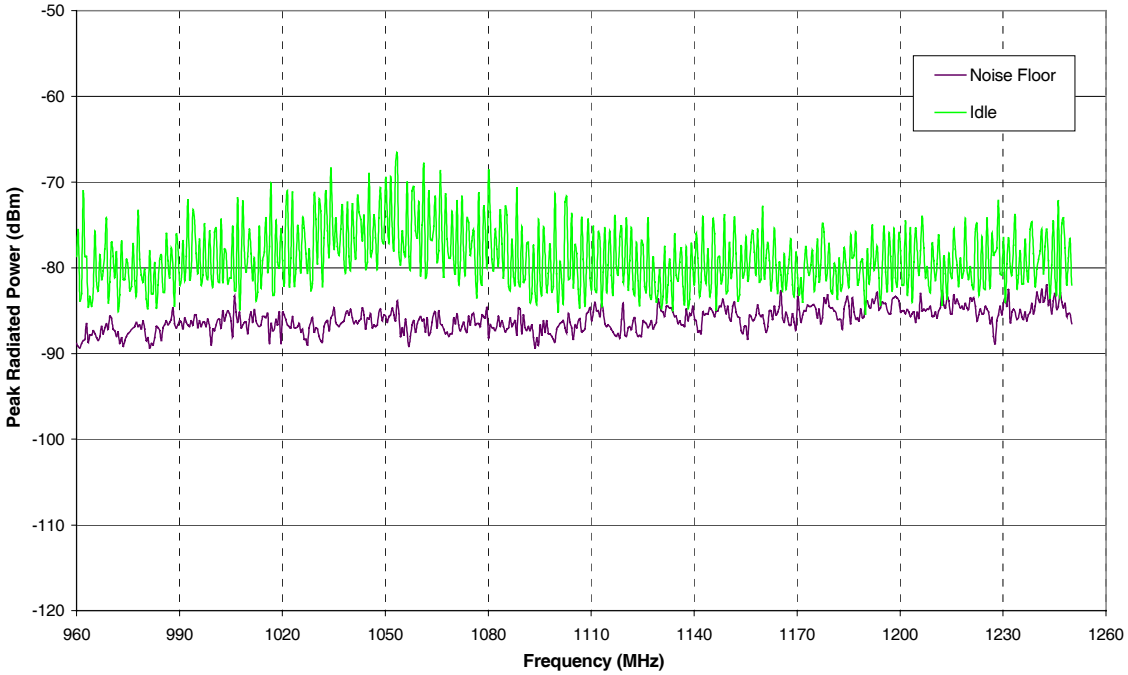

Figure B33: PRN, Band 3.

B.4 Band 4

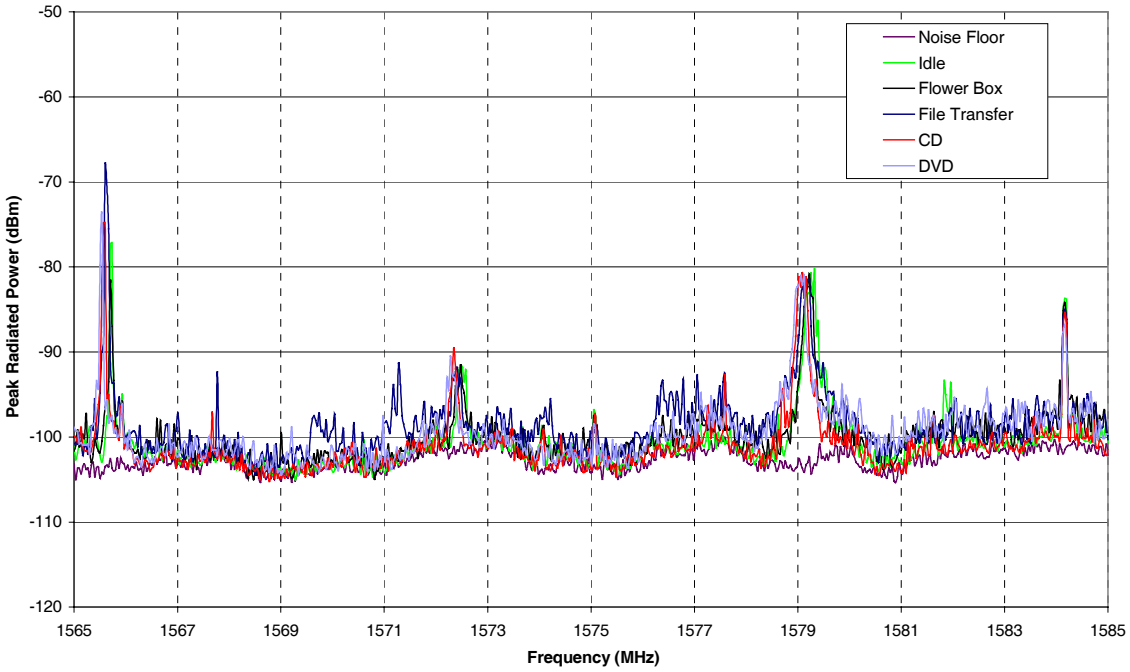

Figure B34: Laptop 1, Band 4.

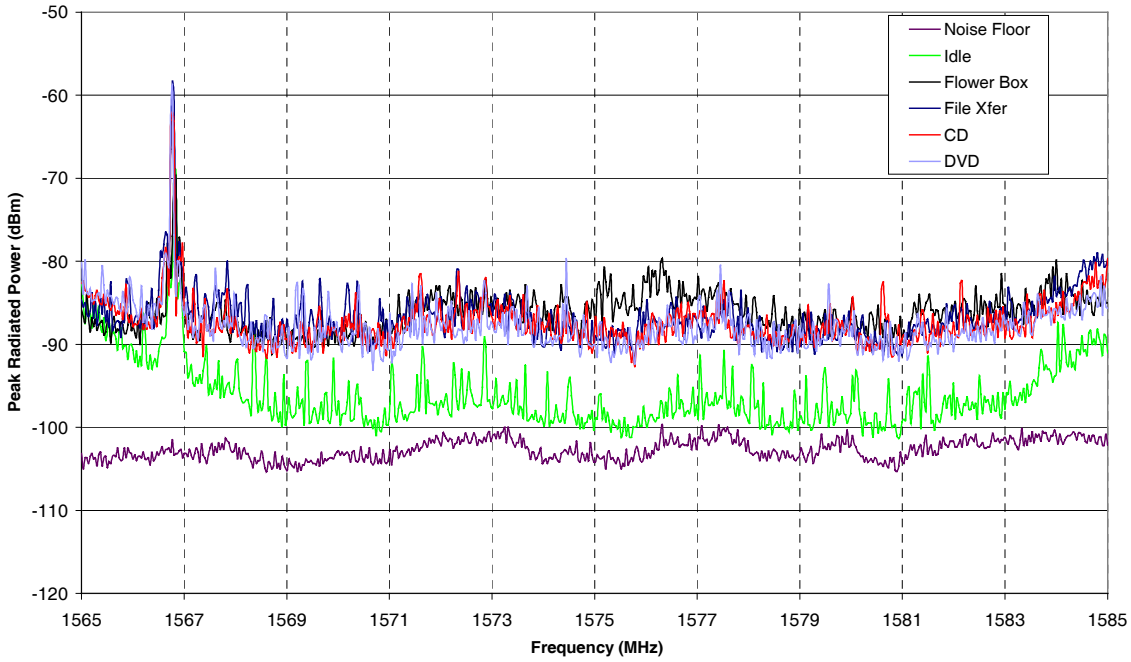

Figure B35: Laptop 2, Band 4.

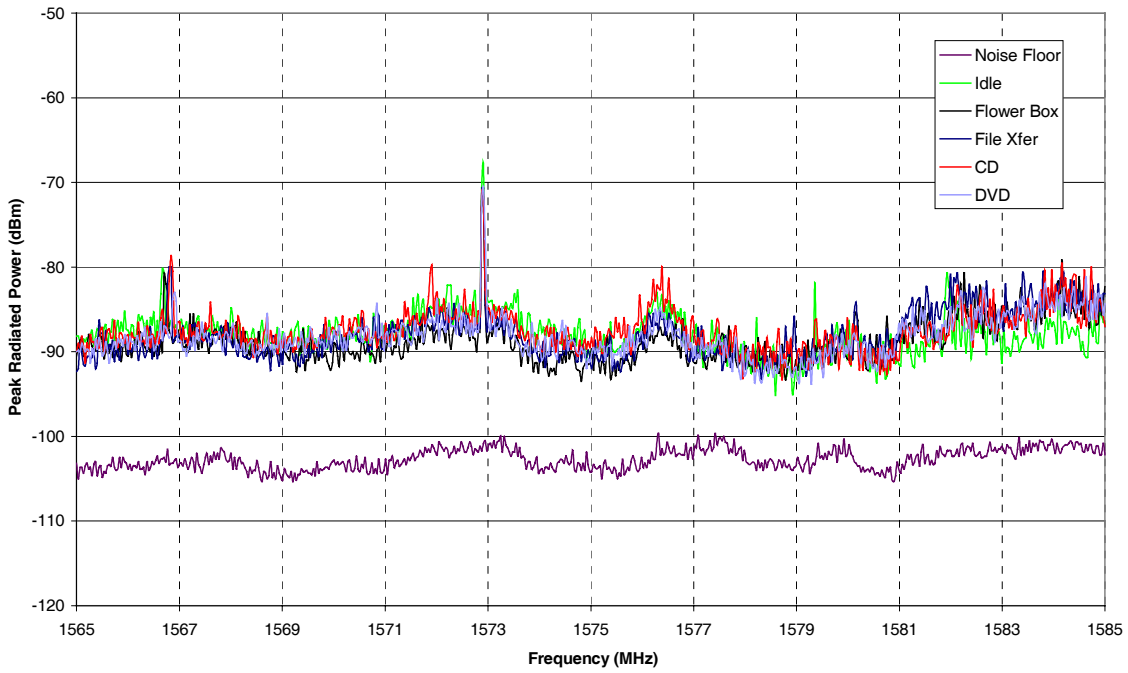

Figure B36: Laptop 3, Band 4.

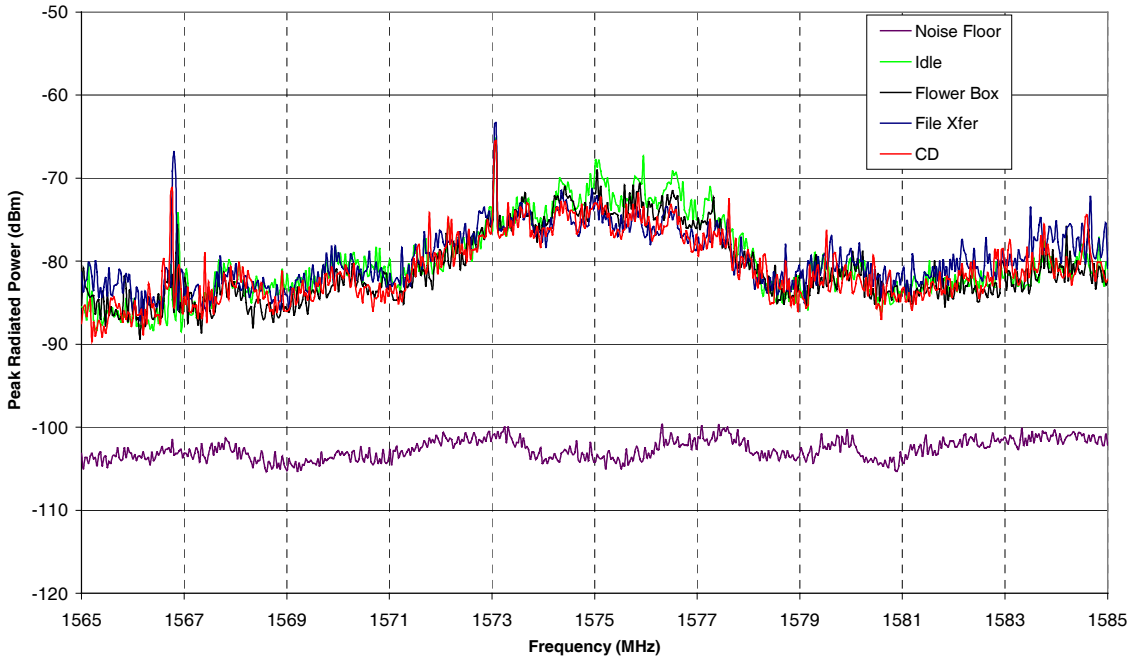

Figure B37: Laptop 4, Band 4.

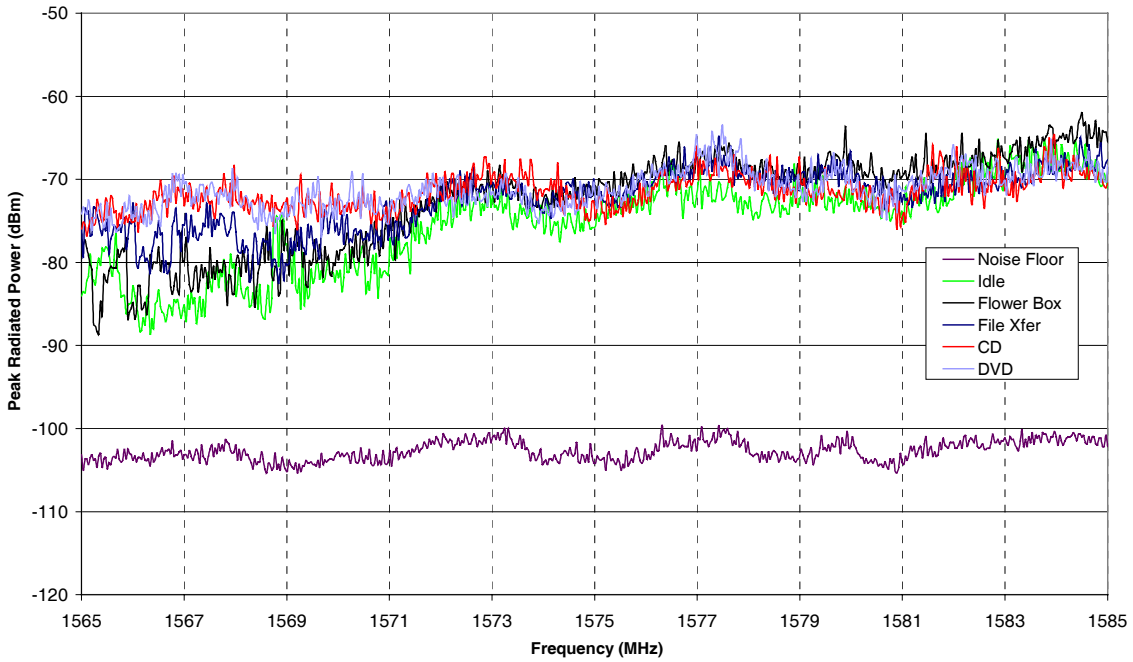

Figure B38: Laptop 5, Band 4.

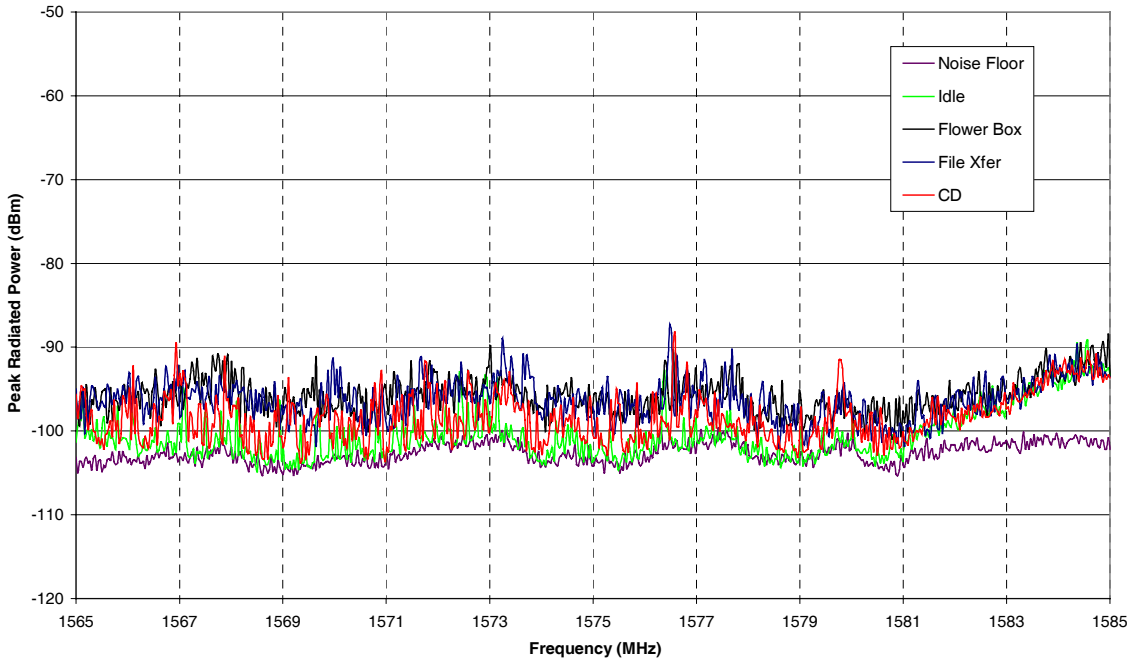

Figure B39: Laptop 6, Band 4.

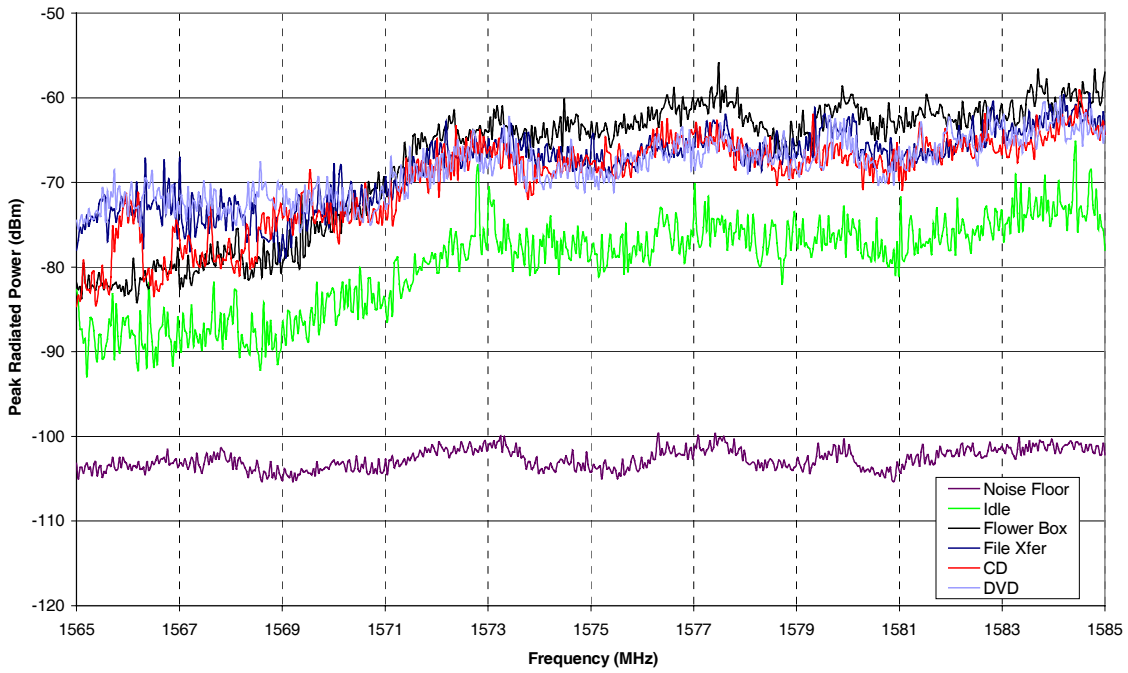

Figure B40: Laptop 7, Band 4.

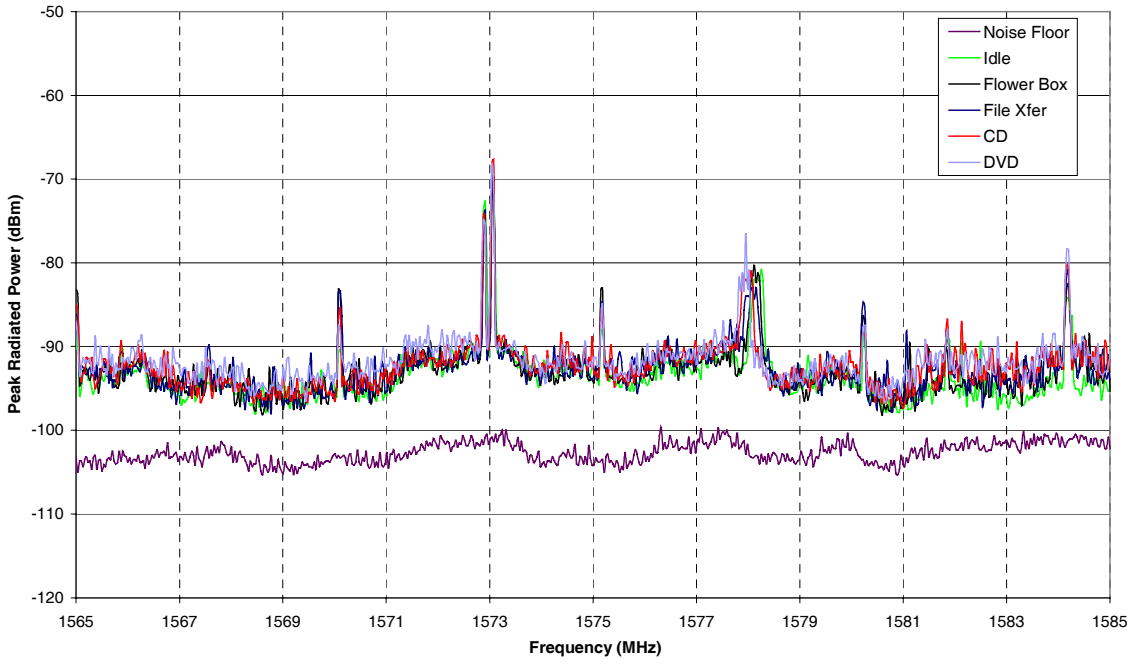

Figure B41: Laptop 8, Band 4.

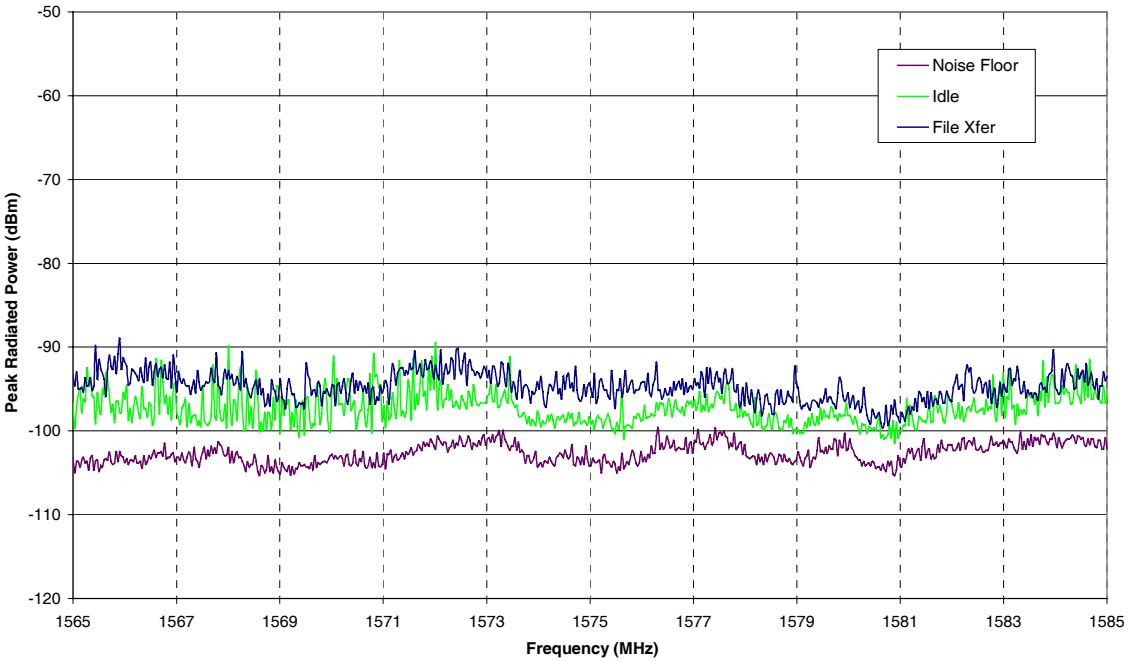

Figure B42: PDA 1, Band 4.

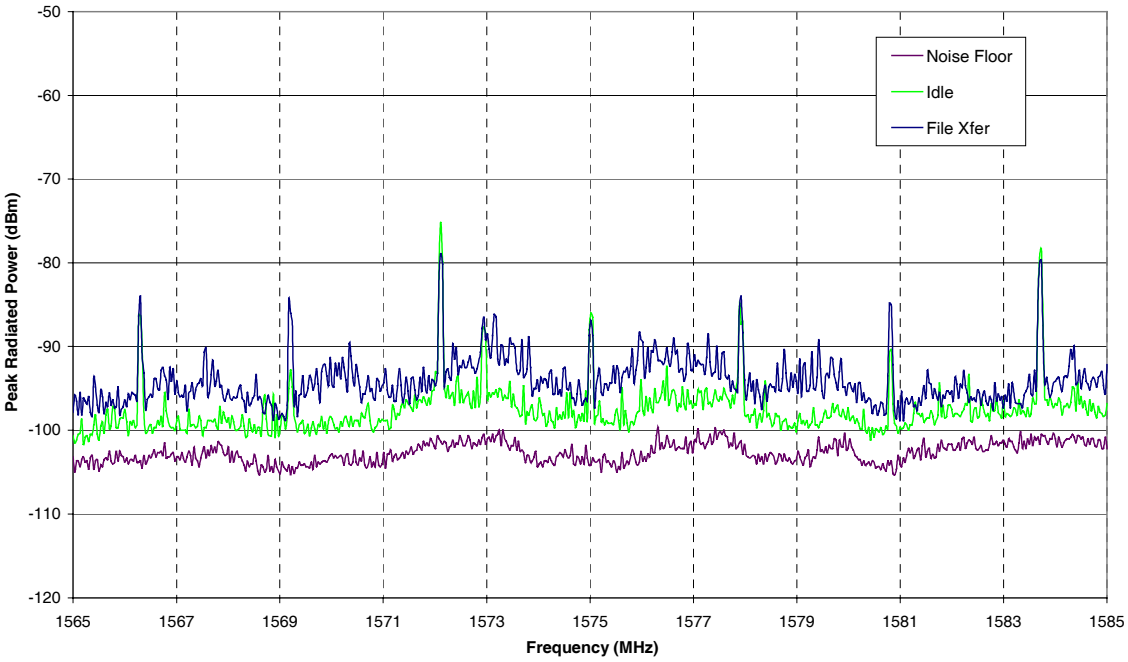

Figure B43: PDA 2, Band 4.

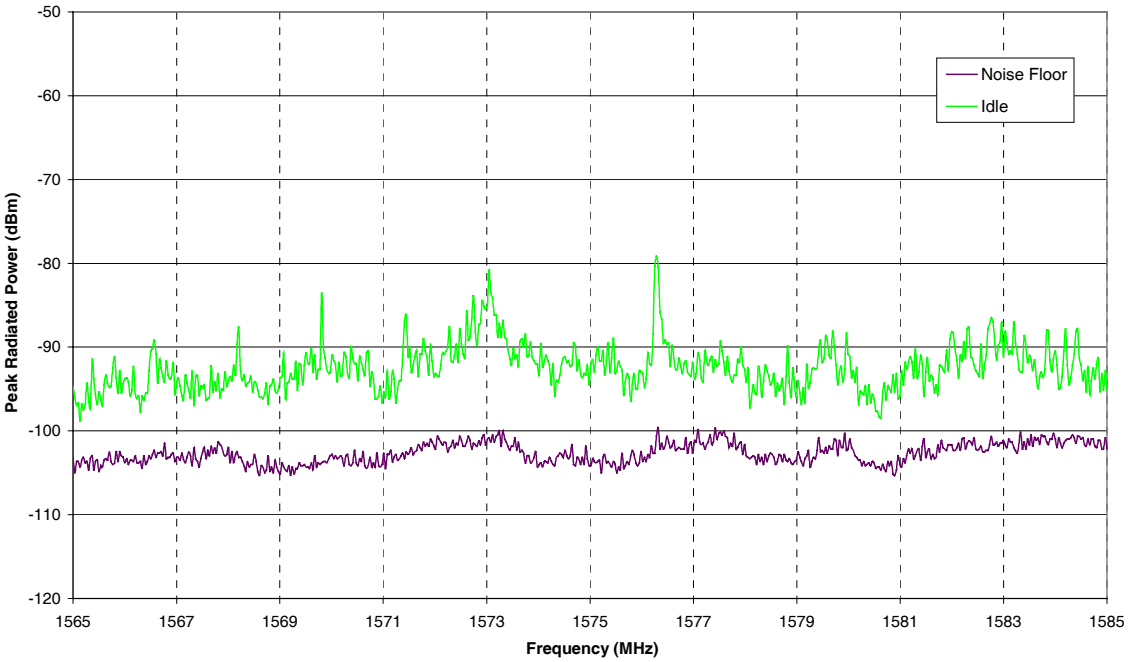

Figure B44: PRN, Band 4.

B.5 Band 5

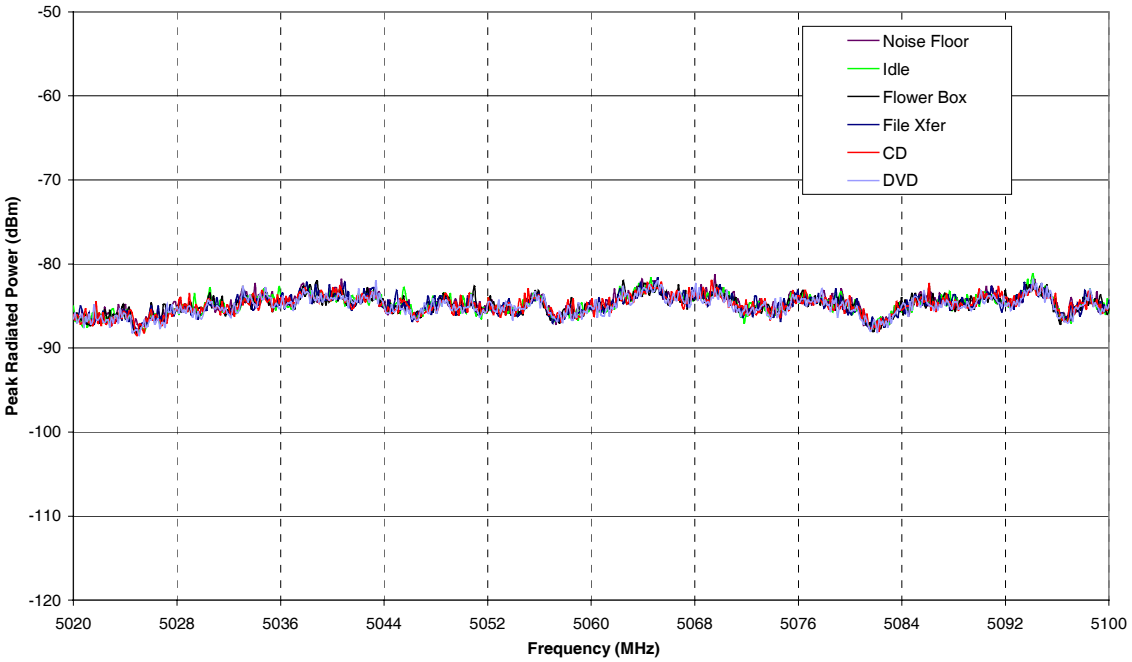

Figure B45: Laptop 1, Band 5.

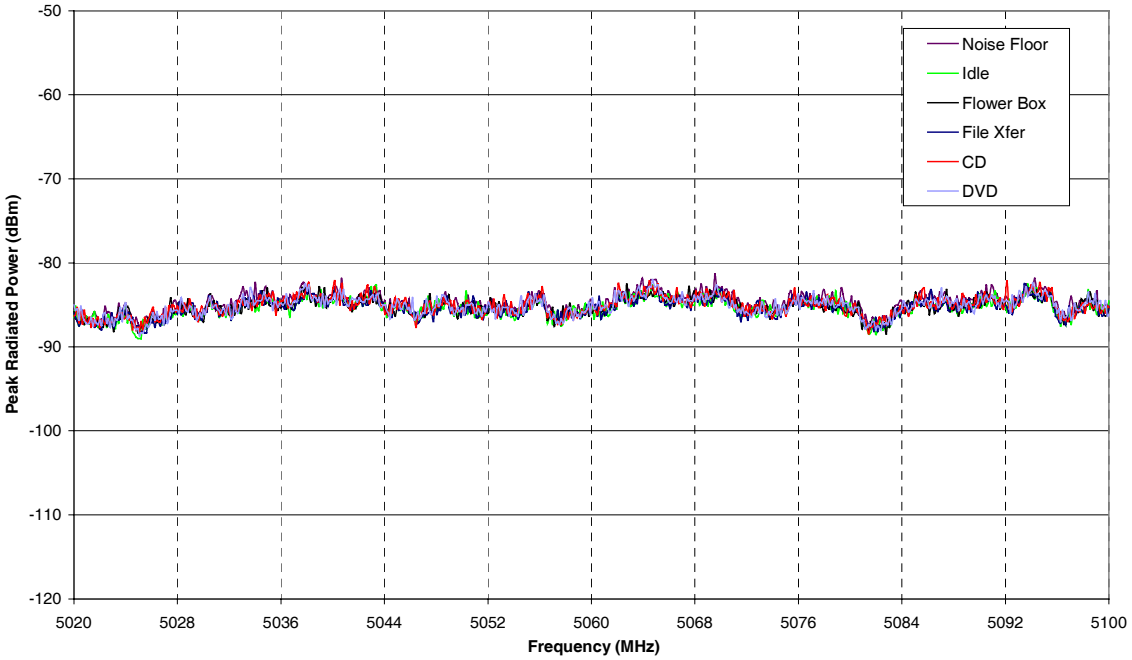

Figure B46: Laptop 2, Band 5.

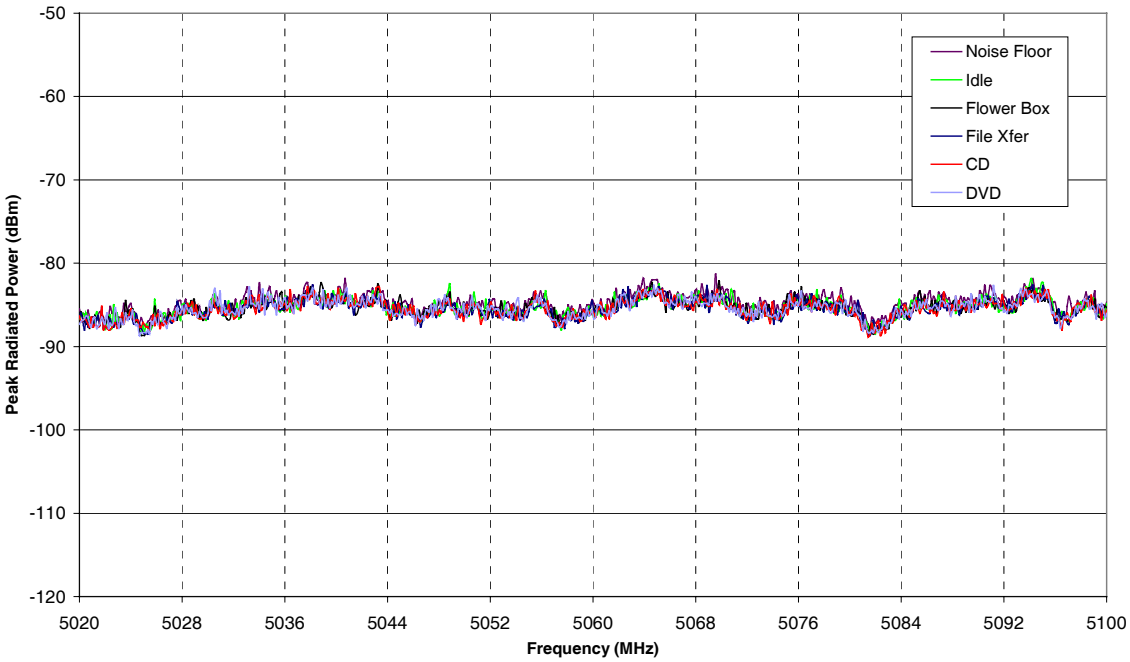

Figure B47: Laptop 3, Band 5.

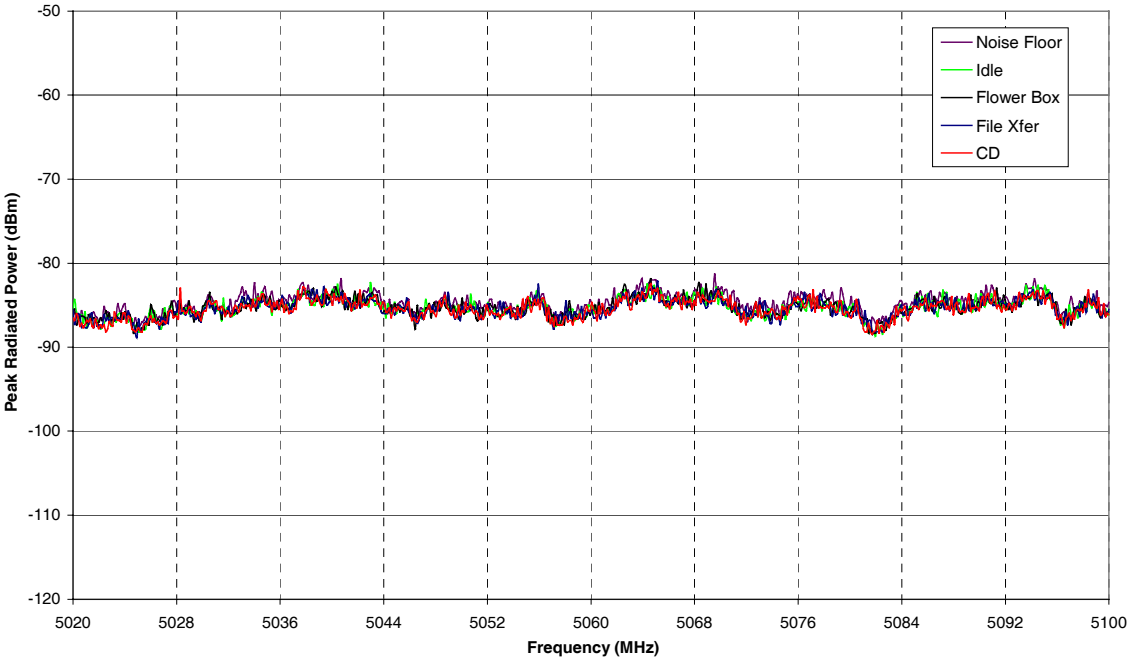

Figure B48: Laptop 4, Band 5.

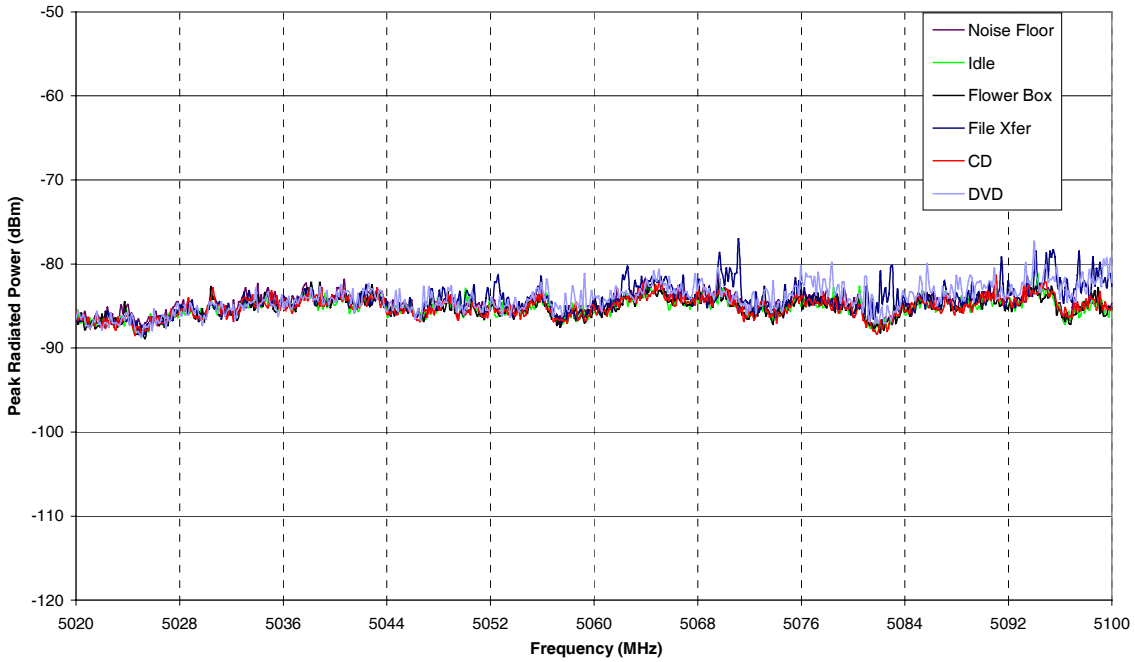

Figure B49: Laptop 5, Band 5.

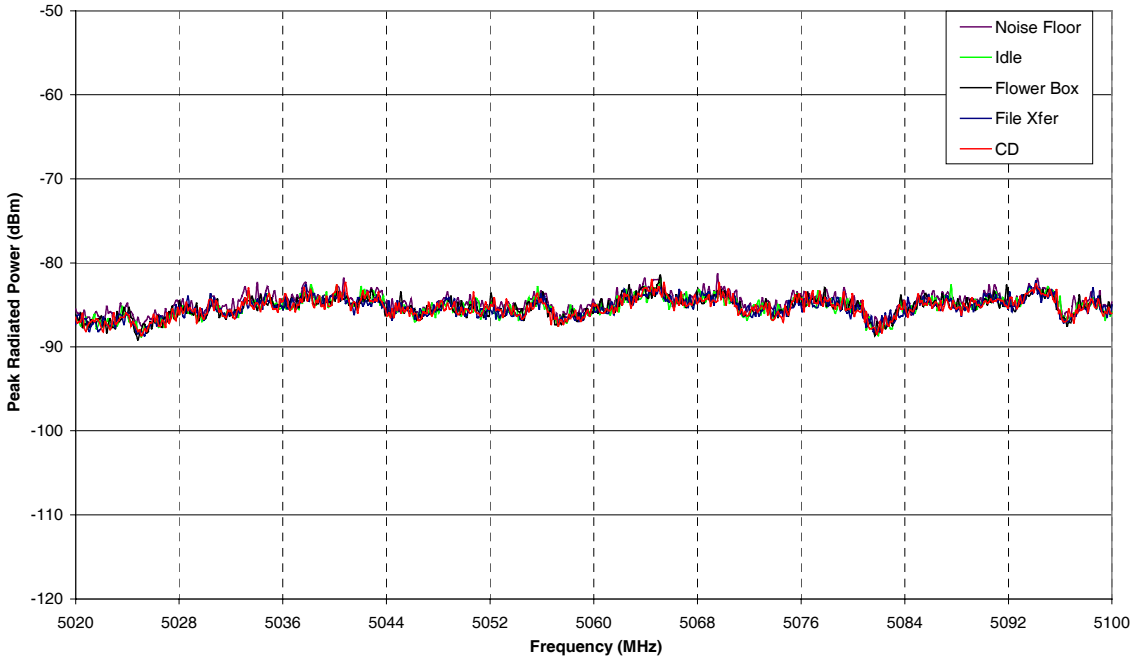

Figure B50: Laptop 6, Band 5.

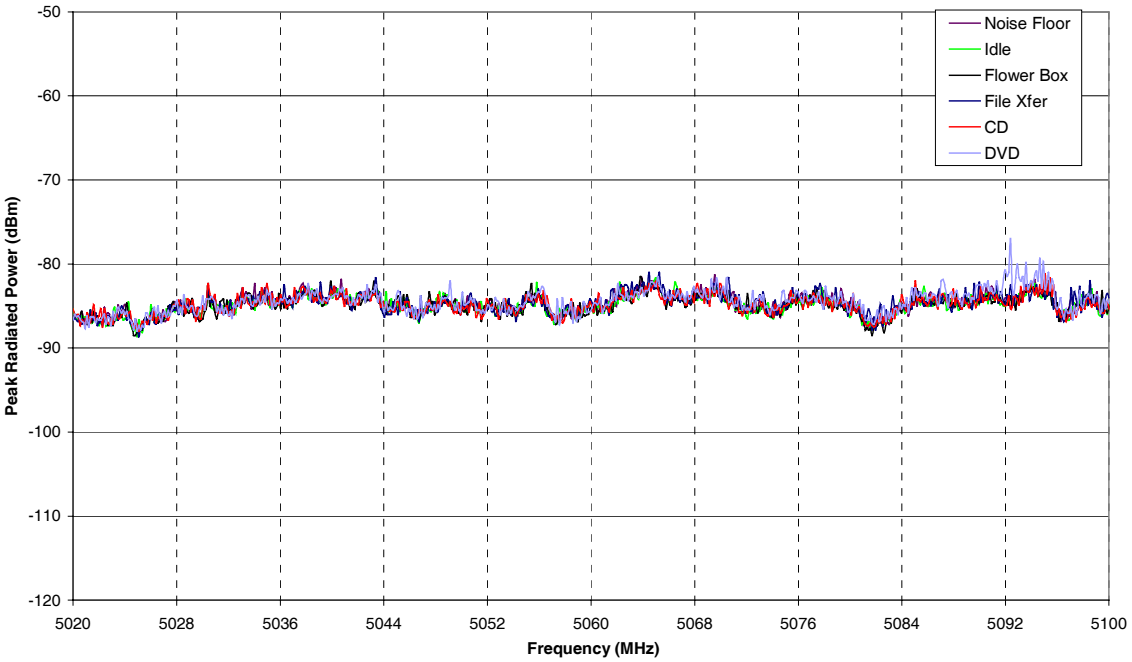

Figure B51: Laptop 7, Band 5.

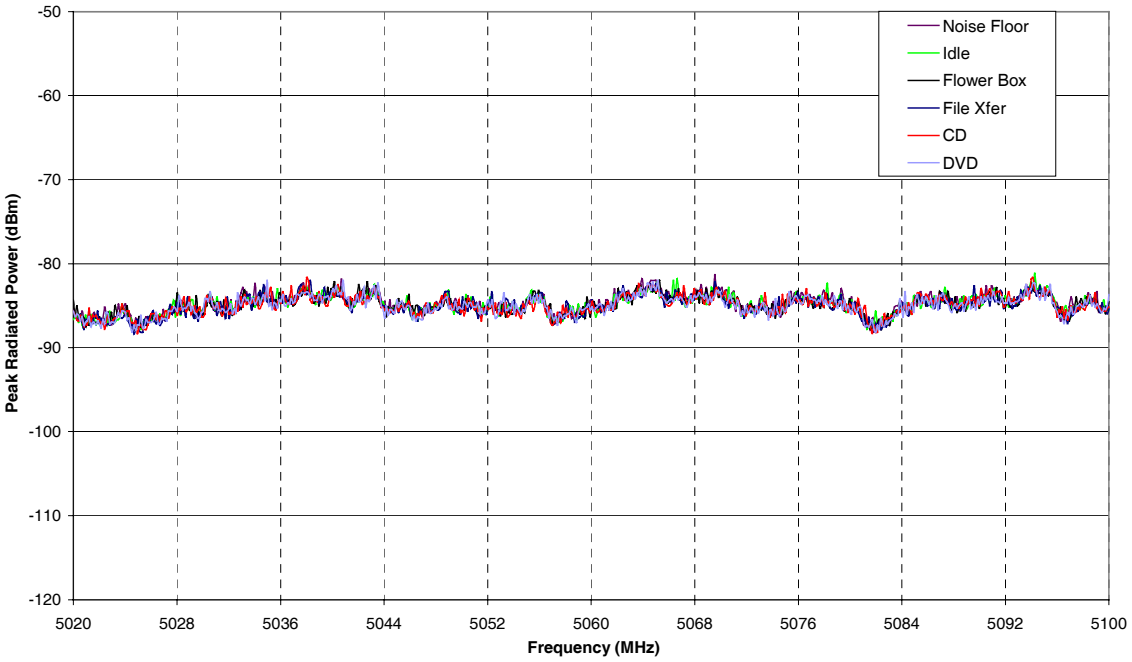

Figure B52: Laptop 8, Band 5.

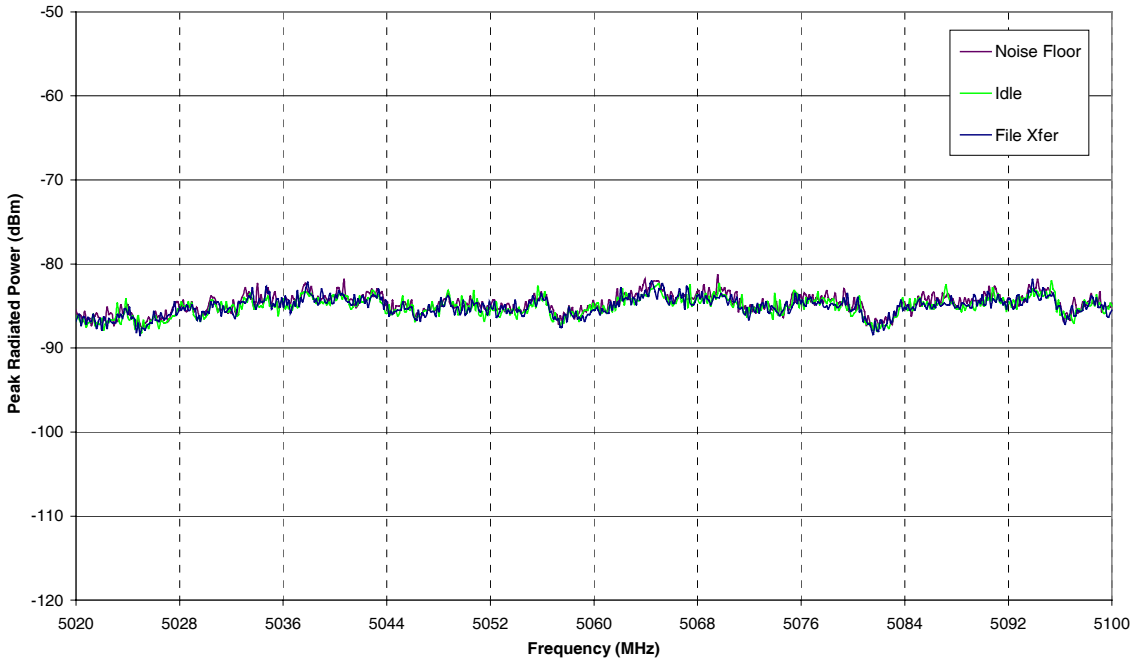

Figure B53: PDA 1, Band 5.

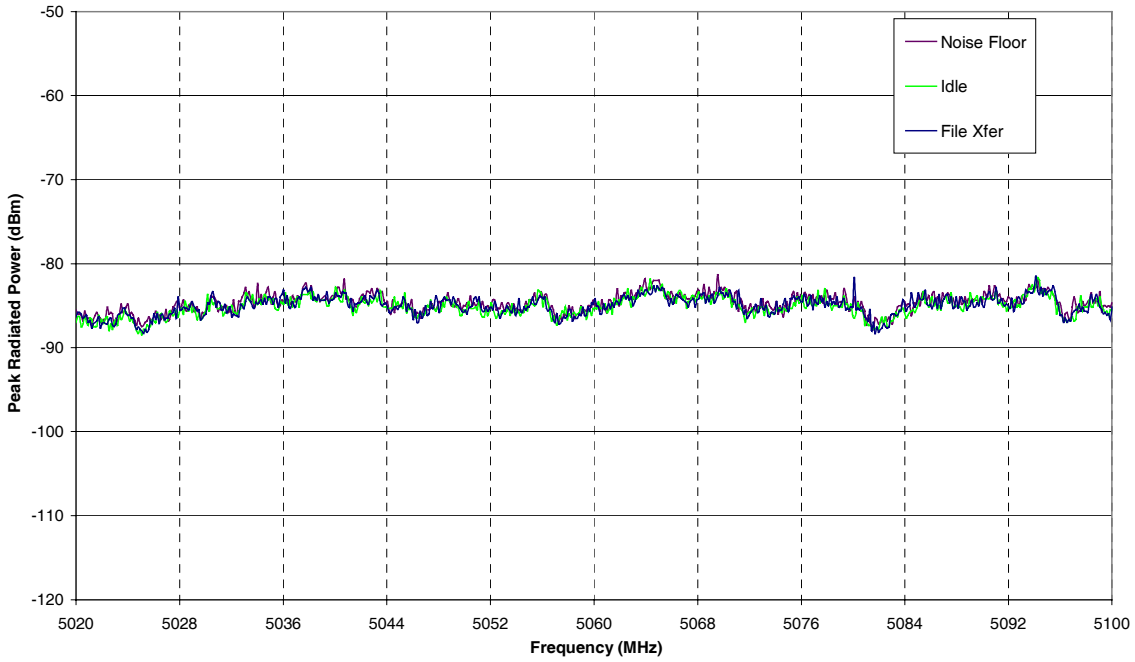

Figure B54: PDA 2, Band 5.

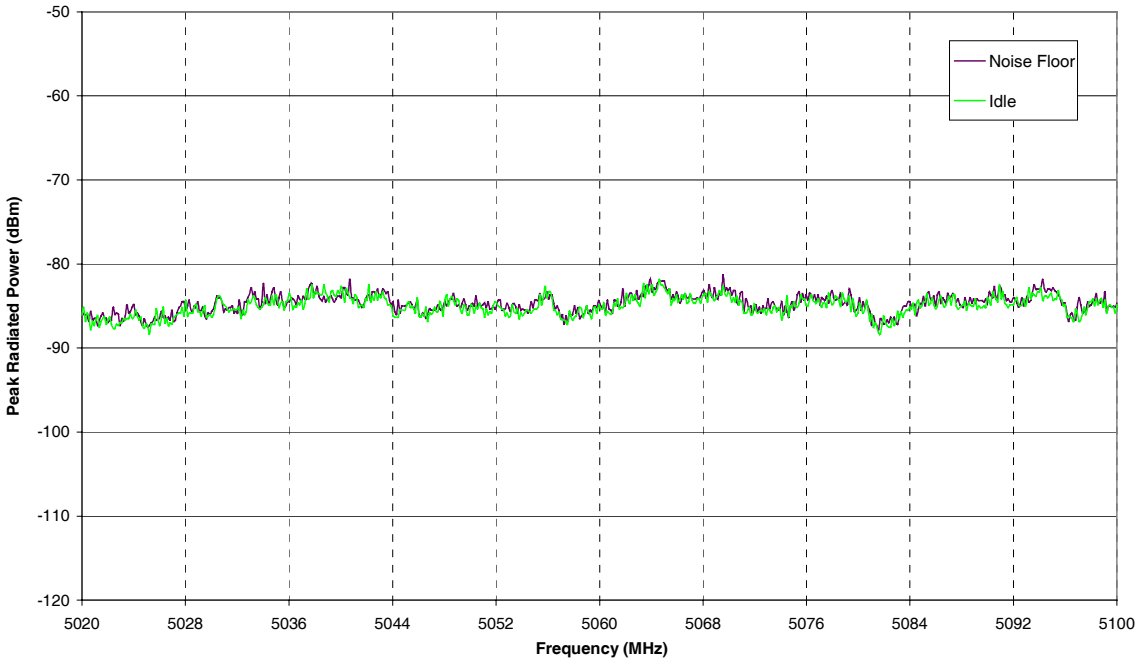

Figure B55: PRN, Band 5.

REPORT DOCUMENTATION PAGE

Form Approved
OMB No. 0704-0188

1. AGENCY USE ONLY (*Leave blank*)	2. REPORT DATE	3. REPORT TYPE AND DATES COVERED
	July 2003	Technical Publication

4. TITLE AND SUBTITLE
Portable Wireless LAN Device and Two-Way Radio Threat Assessment for Aircraft Navigation Radios

5. FUNDING NUMBERS
728-30-10-03

6. AUTHOR(S)
Truong X. Nguyen, Sandra V. Koppen,
Jay J. Ely, Reuben A. Williams,
Laura J. Smith and Maria Theresa P. Salud

7. PERFORMING ORGANIZATION NAME(S) AND ADDRESS(ES)
NASA Langley Research Center
Hampton, VA 23681-2199

8. PERFORMING ORGANIZATION REPORT NUMBER
L-18320

9. SPONSORING/MONITORING AGENCY NAME(S) AND ADDRESS(ES)
National Aeronautics and Space Administration
Washington, DC 20546-0001

10. SPONSORING/MONITORING AGENCY REPORT NUMBER
NASA/TP-2003-212438

11. SUPPLEMENTARY NOTES

12a. DISTRIBUTION/AVAILABILITY STATEMENT
Unclassified-Unlimited
Subject Category 33 Distribution: Standard
Availability: NASA CASI (301) 621-0390

12b. DISTRIBUTION CODE

13. ABSTRACT *(Maximum 200 words)*

Measurement processes, data and analysis are provided to address the concern for Wireless Local Area Network devices and two-way radios to cause electromagnetic interference to aircraft navigation radio systems. A radiated emission measurement process is developed and spurious radiated emissions from various devices are characterized using reverberation chambers. Spurious radiated emissions in aircraft radio frequency bands from several wireless network devices are compared with baseline emissions from standard computer laptops and personal digital assistants. In addition, spurious radiated emission data in aircraft radio frequency bands from seven pairs of two-way radios are provided. A description of the measurement process, device modes of operation and the measurement results are reported. Aircraft interference path loss measurements were conducted on four Boeing 747 and Boeing 737 aircraft for several aircraft radio systems. The measurement approach is described and the path loss results are compared with existing data from reference documents, standards, and NASA partnerships. In-band on-channel interference thresholds are compiled from an existing reference document. Using these data, a risk assessment is provided for interference from wireless network devices and two-way radios to aircraft systems, including Localizer, Glideslope, Very High Frequency Omnidirectional Range, Microwave Landing System and Global Positioning System.

14. SUBJECT TERMS
Electromagnetic, Compatibility, Interference, Susceptibility, Aircraft, Avionics
Path loss, Emission, PED, Wireless, WLAN, Two-Way Radio, FRS, GMRS

15. NUMBER OF PAGES
227

16. PRICE CODE

17. SECURITY CLASSIFICATION OF REPORT	18. SECURITY CLASSIFICATION OF THIS PAGE	19. SECURITY CLASSIFICATION OF ABSTRACT	20. LIMITATION OF ABSTRACT
Unclassified	Unclassified	Unclassified	UL